Imperial College London

Studies on cross presentation of antigen by human dendritic cells

Sirika Pillay

Department of Immunology
Division of Infectious Diseases
Faculty of Medicine
Imperial College London

A thesis submitted to Imperial College London for the partial fulfilment of the degree of Doctor of Philosophy
2012

Statement of Declaration

I, **Sirika Pillay**, confirm that the work presented in this thesis is my own. Where information has been derived from other sources, I confirm that it has been clearly indicated throughout the thesis.

Abstract

It is widely acknowledged that an HIV-1 vaccine requires a robust CD8+ T-cell response to effectively combat HIV-1. However, past vaccine candidates have failed to stimulate adequate cellular responses in humans, highlighting the need to explore alternative ways to induce strong cellular immunity. Animal studies have shown that if exogenous antigen can be targeted to dendritic cells (DCs), strong CD8+ T-cell responses can be generated via the cross-presentation pathway. In this study we evaluated the ability of four DC surface receptors in two different human DC subsets (monocyte-derived DCs and blood myeloid CDlc+ DCs) to efficiently target model antigens to the cross-presentation pathway to induce enhanced CD8+ T-cell responses. These receptors included DEC-205, MMR, DC-SIGN and/or CD1a. Four receptor-targeting strategies were explored, each exploiting receptor-specific antibodies in various ways to direct antigen towards the respective receptors.

Initially, selected model antigens (CMV pp65, MART-1, and streptavidin-fusion proteins) were produced in large quantities for *in vitro* experiments. Two expression systems were evaluated to produce antigens, namely, the generation of a stably-expressing cell line and a recombinant adenovirus expression system (AES). The AES emerged as a better expression system, and was used to produce the proteins of interest. These proteins were then purified using a Nickel-NTA/anti-His tag column, and yield and purity of recombinant proteins were determined. The immunogenicity of the purified antigens was assessed to confirm the integrity of the bulk-produced proteins. Additionally, TLR agonists were evaluated for their ability to augment T-cell responses. LPS (TLR4 agonist) was determined to be the favoured agonist.

The strategy utilising chemically-conjugated antigen-antibodies yielded the most significant enhancements in CD8+ T-cell proliferative responses, specifically for targeting of DEC-205, as well as MMR. Overall, this study details the successful design and production of various DC receptor targeting reagents, and goes on to assess the efficacy of novel receptor targeting strategies to enhance CD8+ T-cell responses for the eventual purpose of improving current HIV-1 vaccine strategies.

Acknowledgements

I would like to express a sincere thank you to my PhD supervisor, Dr Steven Patterson, for providing knowledgeable perspective, advice and guidance throughout this work. Steve has always had the time and patience to listen to my ideas, and make interesting suggestions, for which I am greatly appreciative.

I would like to thank Drs Adel Benlahrech, Timos Papagatsias and Sai Duraisingham for all their technical expertise and support, it was much appreciated. I would also like to thank the past and present members of the Immunology department at Chelsea and Westminster hospital, especially Karen Logan (for all her moral support), Salvinia Mletzko, Caroline Royle, Barbara Tavano, Zineb Bouzeboudjen, Philip Bergin, Adam Coleman, Anna Herasimtschuk, Adriano Boasso, Ambreen Ashraf, Rebecca Robey and Julia Hornig, for their friendship, kind encouragement and helpful discussions.

A special thank you goes to Dr Shanthi Herath. I have learnt so much from Shan's vast knowledge as a researcher, and her friendly and positive disposition has made it a pleasure to work alongside her in the laboratory. Shan provided me with invaluable guidance and moral support during the last year of my PhD. She is like a mentor to me, and I am very grateful to have met her.

I would like to thank the Commonwealth Scholarship Commission for their generous financial support, which has sustained me throughout my PhD studies. I would also like to thank the SSRC-Mellon foundation, British Society of Immunology and the Chelsea and Westminster Charity Trust for providing me with financial support to travel to international conferences during my PhD.

Finally, I would like to say a big thank you to my family and friends for all their love and support, and for being so understanding and patient during the entirety of my PhD studies. More than anyone, my parents and sisters have been a pillar of strength and kindness, and I am so appreciative to have them in my life. And lastly, thank you to my spiritual Guru for His grace and guidance throughout.

Publications/Abstracts

- **Pillay, S**., Patterson, S. Expression of a versatile DC-targeting fusion protein using an adenovirus expression system.
  (Manuscript in progress)

- **Pillay, S**., Gotch, F., Patterson, S. (Sept 2011) A novel dendritic cell-targeting strategy to potentially enhance T-cell activation.
  Poster presentation at FEBS 16th International Summer school of Immunology (Hvar, Croatia).

- **Pillay, S**., Gotch, F., Patterson, S. (Aug 2010) Design and production of novel dendritic cell-targeted antigen-antibody conjugates for their use in enhanced T-cell activation in HIV vaccine studies.
  Poster presentation at 14th International Congress of Immunology Conference (Kobe, Japan).

Table of Contents

Statement of Declaration 2
Abstract 3
Acknowledgements 4
Publications/Abstracts 5
Table of Contents 6
List of Abbreviations 11
List of Figures 13
List of Tables 16
Chapter 1 17
Introduction 17
1.1 Cellular Immunity 17
1.2 T-cell activation and differentiation 17
1.2.1 CD4+ T-cell differentiation 18
1.2.2 Th cell regulation 20
1.2.3 CD8+ T-cell differentiation 21
1.2.4 CD8+ T-cell phenotypes 24
1.3 Dendritic cells (DCs) 25
1.3.1 Blood dendritic cells 26
1.3.2 Skin dendritic cells 28
1.3.3 Monocyte-derived dendritic cells 29
1.4 Dendritic cell antigen capture 31
1.5 Antigen presentation by dendritic cells 31
1.5.1 Classical antigen presentation pathways 31
1.5.2 Cross presentation pathway 33
1.6 Dendritic cell maturation 38
1.7 Mouse versus human dendritic cells 40
1.8 DC-based vaccinations 41
1.8.1 C-type lectin receptors 44
1.9 Use of adjuvants with DC vaccinations 51

1.9.1 Toll-like receptor (TLR) family 51
1.9.2 Enhancing efficacy of adjuvants 56
1.9.3 Tolerance induction by DC-targeting 57
1.10 The importance of a cell-mediated immune response against HIV-1 58
1.11 Choice of model antigens 59
1.11.1 Cytomegalovirus pp65 60
1.11.2 Melan-A antigen 61
1.12 Hypothesis and objectives 62
Chapter 2 63
Construction of model antigen vectors and evaluation of antigen expression 63
2.1 Background and Aims 63
2.1.1 Model antigens 63
2.1.2 Mammalian expression systems 64
2.1.3 Aims of chapter 65
2.2 Materials and Methods 65
2.2.1 Immortalised cell line cultures 65
2.2.2 Genes and vectors of interest 66
2.2.3 Cloning of pcDNA6/HisC^{TM}-pp65 and pcDNA6/HisC^{TM}-MART-1 66
2.2.4 Construction of AdEasy^{TM} shuttle vectors, pShuttle.HisC-pp65 & pShuttle.HisC-MART-1 69
2.2.5 Production of streptavidin-fusion constructs 70
2.2.6 Transient transfections 73
2.2.7 Stable expression cell line generation 73
2.2.8 Recombinant adenovirus (rAd) expression system 74
2.2.9 Protein expression detection 78
2.3 Results 80
2.3.1 Construction of expression vectors to produce CMV pp65 and MART-1 80
2.3.2 Evaluation of pp65 and MART-1 production from constructed expression vectors 81
2.3.3 Generation of a stably- expressing cell line 83
2.3.4 The recombinant Adenovirus expression system (AES) 91
2.3.5 Design and production of streptavidin-fusion vectors 96

2.4 Discussion 97
Chapter 3 101
Large scale production of model antigens and creation of antigen-antibody conjugates . 101
3.1 Background and aims 101
3.1.1 Factors influencing large scale recombinant protein production in mammalian expression systems 101
3.1.2 Protein-protein conjugations 102
3.1.3 Aims of chapter 103
3.2 Materials and methods 104
3.2.1 Dose/time trial and protein production 104
3.2.2 His-tag protein purification 105
3.2.3 Protein quantification 105
3.2.4 Protein dialysis and concentration 106
3.2.5 Protein-antibody conjugates 106
3.2.6 Biotinylation of model antigen 108
3.2.7 Enzyme-linked immunosorbent assay (ELISA) 108
3.2.8 Statistical analysis 109
3.3 Results 109
3.3.1 Large scale recombinant protein production 109
3.3.2 Purification of recombinant proteins 113
3.3.3 Conjugate protein production 118
3.3.4 Confirmation of functionality of streptavidin-fusion proteins and biotinylated proteins 122
3.4 Discussion 122
Chapter 4 127
Assessment of model antigen immunogenicity 127
4.1 Background and aims 127
4.1.1 Dendritic cell subsets 127
4.1.2 Use of adjuvants 127
4.1.3 Aims of chapter 128
4.2 Materials and Methods 129

4.2.1 Cell culture media and buffers 129
4.2.2 Primary cell isolation and culture 130
4.2.3 A*02:01 Human Leukocyte Antigen (HLA) type identification 131
4.2.4 Purification of recombinant adenoviruses 132
4.2.5 *In vitro* DC-T-cell co-culture assays 132
4.2.6 Phenotypic and functional analysis of T-cells in co-culture assays 135
4.2.7 Data acquisition and gating strategy 136
4.2.8 Statistical analysis 136
4.3 Results 139
4.3.1 *In vitro* generation and phenotypic characterisation of DC subsets 139
4.3.2 Identification of A*02:01-positive individuals 143
4.3.3 Assessment of the use of agonists in moDC-T-cell co-culture assays 143
4.3.4 Immunogenicity of pp65 and MART-1 147
4.4 Discussion 159
Chapter 5 166
***In vitro* assessment of T-cell responses to specific DC-receptor targeting** 166
5.1 Background and aims 166
5.1.1 DC endocytic receptor targets 166
5.1.2 Aims of chapter 167
5.2 Materials and Methods 168
5.2.1 Assessment of targeting reagents to attach to DC surface receptors 168
5.2.2 DC-T-cell co-culture assays with the targeting reagents 169
5.2.3 Titration of reagents 171
5.2.4 Phenotypic and functional analysis of T-cells in co-culture assays 171
5.2.5 Data acquisition, gating strategy and statistical analysis 171
5.3 Results 172
5.3.1 Targeting DC receptors using biotinylated pp65 172
5.3.2 Targeting DC receptors using chemical conjugates 175
5.3.3 Targeting DC receptors using streptavidin-fusion proteins 183
5.3.4 Targeting DC receptors using a commercial pp65 dendrimer 192
5.4 Discussion 200

Chapter 6 209
Final discussion and future work 209
6.1 Production and purification of reagents 209
6.2 DC targeting strategies 210
6.3 Differences observed between DC subsets 212
6.4 Use of TLR agonists 213
6.5 Favoured receptor for cross presentation 213
References 216

List of Abbreviations

aa	Amino Acid
ab	Antibody
AB	AB Human Serum
Ad	Adenovirus
Adj.	Adjuvant
AES	Adenovirus Expression System
AIDS	Acquired Immunodeficiency Syndrome
Amp	Ampicillin
AP-1	Activator Protein 1
APC	Antigen Presenting Cell
APCC	Allophycocyanin
ATP	Adenosine Triphosphate
BDCA	Blood DC Antigen
BFA	Brefeldin A
BMDC	Blood myeloid DC
bp	Base-pair
CCR5	Chemokine (C-C) receptor 5
CD	Cluster of differentiation
CD40L	CD40 Ligand
CFSE	Carboxyfluorescein Succinimidyl Ester
CHO	Chinese Hamster Ovary
CLA	Cutaneous Lymphocyte Antigen
CLEC9A	C-type lectin domain family 9A
CLR	C-Type Lectin
CMV	Cytomegalovirus
CPE	Cytopathic Effects
CpG-ODN	C-phosphate-G Oligodeoxynucleotides
CPM	Counts Per Minute
CRD	Carbohydrate Recognition Domain
CTL	Cytotoxic T- Lymphocyte
CTLD	C-type lectin-like domain
CXCR	Chemokine (C-X-C) Receptor
DC	Dendritic Cell
DCIR	DC immunoreceptor
DCS	DC-SIGN
DC-SIGN	DC-Specific ICAM-3 Grabbing Non-Integrin
dDC	Dermal Dendritic Cell
DMEM	Dulbecco's Modified Eagle's Medium
DMSO	Dimethyl Sulphoxide
DNGR	Dendritic Cell NK Lectin Group Receptor-1
dsDNA	Double Stranded DNA
dsRNA	Double Stranded RNA
EAE	Experimental Autoimmune Encephalitis
EDTA	Ethylene-Diamine Tetra-acetic Acid
ELISA	Enzyme-Linked Immunosorbent Assay
EpCam	Epithelial Cell Adhesion Molecules
ER	Endoplasmic Reticulum
ERAD	ER-associated degradation
ERAP1	ER Aminopeptidase 1
FACS	Fluorescence Activated Cell Sorting
FcR	Fragment crystallizable receptor
FCS	Foetal Calf Serum
FITC	Fluorescein Isothiocyanate
Flt3L	FMS-Like Tyrosine kinase 3 Ligand
FOXP3	Forkhead box P3 (transcription factor)
GM-CSF	Granulocyte-Macrophage Colony-Stimulating Factor
HBV	Hepatitis B virus
HCV	Hepatitis C virus
HEK	Human Embryonic Kidney
HeLa	Henrietta Lacks
HER	Human Embryonic Retinoblastoma
HLA	Human Leukocyte Antigen
Hpi	Hours Post Infection
HPV	Human Papilloma Virus
Hrs	Hours
HSP	Heat shock protein
ICAM	Intracellular Adhesion Molecule
iDC	Immature DC
IFN	Interferon
Ig	Immunoglobulin
IL	Interleukin
ILT7	Immunoglobulin-Like Transcript 7 Receptor
IRAK	IL-1R-associated kinase
IRF	Interferon-Regulatory Factor
ITAM	Immunotyrosine Activatory Motif
ITIM	Immunotyrosine Inhibitory Motif
ITR	Inverted Terminal Repeat
Kbp	Kilo Base-pairs
kD	Kilo Dalton
LA	Luria-Bertani agar
LB	Luria-Bertani
LC	Langerhans Cell

li	Invariant Chain
Lin	Lineage
LN	Lymph Node
LPS	Lipopolysaccharide
LTNP	Long Term Non Progressor
LTR	Long Terminal Repeat
MAL	MyD88-Adaptor-Like protein
MART-strep	MART-streptavidin
MCS	Multiple Cloning Site
mDC	Myeloid dendritic cell
MFI	Mean Fluorescence Intensity
MGL	Macrophage Galactose Lectin
MHC	Major Histocompatibility Complex
MIIC	MHC class II-rich subcellular compartment
min	Minute/s
MMR	Macrophage Mannose Receptor
MoDC	Monocyte-Derived Dendritic Cells
MOI	Multiplicity Of Infection
MPL	Monophosphoryl Lipid A
mpp65	pp65 Dendrimer
mRNA	Messenger RNA
MVA	Modified Vaccinia Ankara
MyD88	Myeloid Differentiation primary response gene 88
NAb	Neutralising Antibody
Necl2	Nectin-like Protein 2
NF-kB	Nuclear Factor kappa B
NK	Natural Killer
ORF	Open Reading Frame
OVA	Ovalbumin
PALS	Periarteriolar Lymphatic Sheaths
PAMP	Pathogen-Associated Molecular Patterns
PBMC	Peripheral Blood Mononuclear Cell
PBS	Phosphate Buffer Saline
PCR	Polymerase Chain Reaction
pDC	Plasmacytoid Dendritic Cell
PE	Phycoerythrin
PerCP	Peridinin Chlorophyll Protein
PFA	Paraformaldehyde
Pfu	Plaque Forming Units
PGE2	Prostaglandin E2
PGN	Peptidoglycan
PI	Percoll Interface
PMA	Phorbol 12-myristate 13-acetate
PP	Percoll Pellet
Pp65-strep	Pp65-streptavidin
PRR	Pattern Recognition Receptor
rAd	Recombinant Adenovirus
rcf	Relative Centrifugal Force
RE	Restriction Endonuclease
ROR	Retinoid-related Orphan Receptor
rpm	Revolutions per minute
RPMI	Roswell Park Memorial Institute
RT	Reverse Transcriptase
S.D.	Standard Deviation
SATA	Succinimidylacetylthioacetate
ScFv	Single Chain Fragment Variable
SDS-PAGE	Sodium Dodecyl Sulfate Polyacrylamide Gel Electrophoresis
SEB	Staphylococcal enterotoxin B
SMCC	Succinimidyl trans-4-(maleimidylmethyl) cyclohexane-1-carboxylate
SR	Scavenger Receptor
ssDNA	Single strand DNA
ssRNA	Single strand RNA
STAT	Signal Transducer and Activator of Transcription
Strep	Streptavidin
TAP	Transporter associated with Antigen Processing
Taq	Thermophilus Aquatiqus
TC	Tissue Culture
T-cell	Thymus cell
TCR	T Cell Receptor
TEMRA	Terminally differentiated Effector Memory T-cells
Tfh	Follicular T-helper cells
TGF-β	Transforming Growth Factor beta
Th	Helper T-cell (CD4+)
TLR	Toll-Like Receptor
TNF	Tumour Necrosis Factor
TRAIL	TNF-related apoptosis-inducing ligand
TRAM	TRIF-Related Adaptor Molecule
Treg	Regulatory T-cells
TRIF	TIR-domain containing adaptor-inducing IFN-beta
VLP	Virus-Like Particle
VP	Virus particle

List of Figures

Figure 1.1 - Hypothesised regulation of Th-cell subsets 22
Figure 1.2 - Human DC development 30
Figure 1.3 – Antigen presentation via MHC class I and II molecules 34
Figure 1.4 – Possible routes of cross presentation with three potential pathways 36
Figure 1.5 – Phenotypic and functional descriptions of DCs at different stages of development 39
Figure 2.1 – A diagrammatic depiction of the two cloning strategies used 68
Figure 2.2 – A simplified illustration of overlap extension PCR 72
Figure 2.3 – Recombinant adenovirus production 76
Figure 2.4 – PCR products of the genes of interest, CMV UL83 and *mart-1* 81
Figure 2.5 – Plasmid maps and RE digests of the recombinant constructs created to express the model antigens, pp65 and MART-1 82
Figure 2.6 – A representative example of the intracellular staining flow cytometry gating strategy used to determine CMV pp65 expression from expression vectors 84
Figure 2.7 – A representative example of the intracellular staining flow cytometry gating strategy used to determine MART-1 expression from expression vectors 85
Figure 2.8 – Protein expression after transient transfection of cells with pcDNA expression vectors 86
Figure 2.9 - Protein expression after transient transfection of cells with pShuttle expression vectors 87
Figure 2.10 –Expression of CMV pp65 from blasticidin-resistant CHO and HEK293A cell clones 89
Figure 2.11 – Loss of expression of CMV pp65 in the positive stable clones 90
Figure 2.12 – Recombinant adenovirus constructs carrying the genes of interest 92
Figure 2.13 – R.E. digests of the recombinant adenovirus clones 93
Figure 2.14 - Western blots of pellet lysate samples from HeLa and A549 cells after infection with rAdpp65 and rAdMART-1 infection 94
Figure 2.15 - Recombinant *pp65-streptavidin and MART-1-streptavidin* genes 95
Figure 2.16 – Western blot from the pilot infection of HEK293A cells with rAdpp65-strep and rAdMART-strep 96
Figure 3.1 – A diagram depicting the dose-time trial set-up 104
Figure 3.2 – Chemical conjugation of two proteins in a three-step process using a protein-protein cross-linking kit 107

Figure 3.3 – The dose/time trial performed in A549 cells to determine the optimal MOI and harvesting time for bulk CMV pp65 and MART-1expression 110
Figure 3.4 – The dose/time trial performed in A549 cells to determine the optimal MOI and harvesting time for bulk pp65-streptavidin and MART-streptavidin expression 111
Figure 3.5 – Western blot analysis of His tag optimisation experiments for CMV pp65 115
Figure 3.6 – Western blots and SDS-PAGE of purified CMV pp65 extracted from A549 cells using a Nickel-NTA (anti-His-tag) column 116
Figure 3.7 – Western blots and SDS-PAGE of purified MART-1 extracted from A549 cells using a Nickel-NTA (anti-His-tag) column 117
Figure 3.8 - Western blots and SDS-PAGE of purified pp65-strepavidin or MART-streptavidin, extracted from A549 cells using a Nickel-NTA (anti-His-tag) column 118
Figure 3.9 – Western blot and SDS-PAGE analysis of pp65-antibody chemical conjugates 120
Figure 3.10 – Western blot analysis of biotinylated pp65. 121
Figure 3.11 – ELISA analysis to evaluate functionality of streptavidin core in the created fusion proteins and functionality of biotin in the biotinylated pp65 121
Figure 4.1 – Gating strategy for the flow cytometric analysis of cultured T-cells to measure proliferation and identify T-cell phenotypes 137
Figure 4.2 – Gating strategy for the flow cytometric analysis of cultured T-cells to measure proliferation and cytokine production 138
Figure 4.3 - Phenotypic analysis of in-vitro-derived moDCs and their precursors from whole blood 140
Figure 4.4 - Phenotypic analysis of cultured, immature CD1c+ mDCs and their precursors from leukocyte cone blood 141
Figure 4.5 - Gating strategy used to identify A*02:01+ individuals 142
Figure 4.6 - Evaluation of moDC activation after TLR ligand stimulation 145
Figure 4.7 – Assessment of CD4+ and CD8+ T-cell proliferation after stimulation with pp65-pulsed or rAd-infected moDC and co-stimulated with selected agonists 146
Figure 4.8 – Assessment of CD8+ T-cell proliferation after stimulation with MART-pulsed or rAd-infected moDC and co-stimulated with selected agonists 147
Figure 4.9 - Immunogenicity of pp65 as presented in the form of full-length protein or using recombinant adenovirus carrying pp65 gene 149
Figure 4.10 - Phenotypes of proliferated CD4+ and CD8+ T-cells after incubation for 7 days with LPS co-stimulated moDCs (pulsed or infected with pp65 or rAdpp65) or CD1c+ mDCs 152
Figure 4.11 – Assessment of T-cell cytokine production after co-culture with stimulated moDCs, to evaluate immunogenicity of pp65 153

Figure 4.12 – Assessment of T-cell cytokine production after co-culture with stimulated CD1c+ mDCs, to evaluate immunogenicity of pp65 154
Figure 4.13 - Immunogenicity of MART-1 as presented in the form of protein and via recombinant adenovirus 156
Figure 4.14 - Antigen-specific responses to pp65 and MART-1 stimuli, as evaluated by pentamer staining of proliferated T-cells after stimulation with antigen-pulsed or infected moDC 157
Figure 4.15 – Comparison of CD8+ T-cell proliferative responses to model antigens and streptavidin-fusion proteins as evaluated after T-cell stimulation with antigen-pulsed moDC 158
Figure 5.1 – Assessment of the binding of receptor-specific antibodies to endocytic receptors on moDC surface 173
Figure 5.2 – Assessment of the binding of receptor-specific antibodies to endocytic receptors on $CD1c^+$ mDC surface 174
Figure 5.3 – Targeting DC receptors with biotinylated pp65 using anti-biotin magnetic beads 177
Figure 5.4 – CD8+ T-cell cytokine production after targeting endocytic receptors with biotinylated pp65 using anti-biotin magnetic beads 178
Figure 5.5 – Use of chemical conjugates to target moDC receptors 180
Figure 5.6 – Proliferative CD8+ T-cell responses after targeting DCs with chemical conjugates 181
Figure 5.7 – CD8+ T-cell cytokine production (IL-2, TNF-α and IFN-γ) after targeting DCs with chemical conjugates 182
Figure 5.8 – Use of streptavidin-fusion protein to target moDC receptors 185
Figure 5.9 – Assessment of CD8+ T-cell proliferation after a 7 day co-culture with LPS-stimulated DC that underwent a receptor-targeting strategy with pp65-strep or MART-strep 186
Figure 5.10 – Troubleshooting pp65-strep targeting 187
Figure 5.11 – Optimisation of pp65-streptavidin targeting strategy 189
Figure 5.12 – CD8 T-cell cytokine production (IL-2, TNF-α and IFN-γ) after pp65-strep targeting 191
Figure 5.13 – Binding capacity of pp65-conjugated dendrimer to biotinylated receptor-specific antibodies attached to moDC 194
Figure 5.14 – Assessment of T-cell proliferation after targeting DCs with pp65 dendrimers 195
Figure 5.15 – CD8 T-cell cytokine production (IL-2, TNF-α and IFN-γ) after targeting DCs with pp65 dendrimers 196
Figure 5.16 – Evaluation of the effect of different TLR agonists on T-cell proliferation after targeting DCs with pp65 dendrimers 198
Figure 5.17 – Pilot titration experiment using ^{3}H-Thymidine incorporation assay to assess the effect of antibody concentration and pp65 dendrimer concentration on T-cell proliferation 199

List of Tables

Table 1.1 – Summary of well-characterised CLRs 50

Table 2.1 – Primers used for the PCR amplification of *pp65* and *mart-1* genes 68

Table 2.2 – Primers used for the PCR amplification of His.*pp65* and His.*mart-1* genes 70

Table 2.3 – Primers used for the PCR amplification of *His-pp65, streptavidin* and *His-mart1* genes 72

Table 3.1 – Biotinylated anti-human antibodies used in chemical conjugation reactions 107

Table 3.2 – Optimal conditions for recombinant protein production in a rAd-A549 expression system based on pilot dose-time trials 113

Table 4.1a – List of monoclonal antibodies and their isotype controls used for flow cytometry staining 134

Table 4.1b – List of pentamers for flow cytometry staining 135

Table 4.2 – Adjuvants utilised in DC-T-cell co-culture experiments 135

Table 5.1 – Antibodies used to target antigens to DC receptors and in flow cytometry staining procedures 169

Chapter 1

Introduction

1.1 Cellular Immunity

Adaptive immunity involves the induction of specific immune responses to eliminate an invading pathogen or malignant transformation. It encompasses humoral and cell-mediated responses, both of which have particular functions and work in conjunction with each other to provide a powerful defence (Janeway, 2005). In particular, cellular immunity is defined as the arm of the adaptive immune system that is involved in the active combat of pathogens and tumours, via the use of macrophages, natural killer (NK) cells, antigen-specific thymus-cells (T-cells), and the release of specific cytokines in response to an antigen. T-cells develop in the thymus and differ from other lymphocytes by the expression of a T-cell receptor (TCR) (Kindt et al., 2007). These cells are divided into two main populations based on the differential expression of CD4 and CD8 receptors. The involvement of T-cells in a multitude of functions that initiate, regulate and maintain cellular immune responses highlights their importance in immunity.

1.2 T-cell activation and differentiation

Three signals are required to initiate and maintain the activation of T-cells, and induce an adaptive immune response (Diebold, 2008). The first of these signals is the interaction of a TCR (in association with a CD3 receptor on the T-cell) with a major histocompatibility complex (MHC) molecule (on an antigen-presenting cell (APC) or a somatic cell) carrying an antigenic peptide. A synapse is formed between the TCR and MHC-peptide complex, and is only disrupted by cellular processes such as cell division, cell death or chemokine interference (Sallusto and Lanzavecchia, 2002). The duration of the synapse determines the duration of TCR stimulation, however the intensity of the signal that the T-cells receive is dependent on the number of MHC-peptide complexes, the level of co-stimulatory molecule expression (CD80, CD86, CD40) on the APC (designated as signal 2), and the amount of inflammatory cytokines (IL-12, IFN-α)

produced by the stimulated APCs or present in the microenvironment (signal 3). All three signals contribute to T-cell clonal expansion and the differentiation of naïve T-cells into effector T-cells.

1.2.1 CD4+ T-cell differentiation

The interaction of MHC class II-peptide complexes on APCs with naive CD4+ T-cells leads to CD4+ T-cell activation. Activated CD4+ T-cells develop into helper T-cells (Th cells), which play an important part in influencing the type of adaptive immune response that is elicited by providing key signals for B cell and cytolytic T-lymphocyte (CTL) activation (Kindt et al., 2007, Kaiko et al., 2008). There are a growing number of Th cell subsets involved in the adaptive immune system including Th1, Th2, Tfh, Th17 and Treg effector cells (Diebold, 2008). These are differentiated from each other based on the cytokine repertoire each subset produces and their varied functions *in vivo* (Fajardo-Moser et al., 2008). Determination of Th-cell polarisation is primarily based on the nature of the pathogen stimulus, which in turn influences DC cytokine production, co-receptor signalling and strength of antigen stimulation (Diebold, 2008). However, other factors including the local cytokine environment, presence of hormones, the dose and route of pathogen entry, and the type of APC presenting antigen, have also been shown to skew the direction of Th polarisation (Spellberg and Edwards, 2001).

Th1 cells are largely involved in the combat of intracellular pathogens such as certain bacteria and viruses (Sallusto and Lanzavecchia, 2009). They produce a combination of pro-inflammatory cytokines including interferon-gamma (IFN-γ), tumour necrosis factor-alpha or beta (TNF-α/β), and interleukin-2 (IL-2), in order to elicit CTL-specific responses, neutralising antibodies (NAb), immunoglobulin G2a (IgG2a) antibodies, and macrophage activation. Collectively, these cells eradicate pathogens through the elimination of infected tissue (Diebold, 2008). IL-12 is an essential cytokine necessary for Th1 differentiation, inducing the production of IFN-γ through signal transducer and activator of transcription 4 (STAT4) activation (Seder et al., 1993). IL-12 is predominantly produced by myeloid DCs (mDCs), and is additionally involved in the activation of CTLs and NK cells (Sallusto and Lanzavecchia, 2009). Th1 cells are also stimulated in the presence of IL-23, IL-27 and type I IFN in humans, and are dependent on the transcriptional factor, T-bet, to genetically mediate IFN-γ production (Szabo et al., 2000).

IFN-γ is one of the primary pro-inflammatory cytokines, able to stimulate phagocytosis and upregulate expression of class I and class II MHC molecules on cells, encouraging further antigen presentation to effector and Th cells (Spellberg and Edwards, 2001). Several vaccine strategies that utilise viral vectors make use of the ability of these vectors to induce Th1-biased responses through the induction of pro-inflammatory cytokines. As an example, Climent et al (Climent et al., 2011) performed *ex vivo* monocyte-derived DC-T-cell co-culture assays stimulated with a modified Vaccinia Ankara (MVA)-HIV-1 vaccine, and demonstrated the induction of high levels of Th1 cytokine production (IFN-γ and TNF-α), in addition to enhanced cross presentation and HIV-1-specific CD8+ T-cell proliferation.

On the other side of the spectrum, Th2 cells are usually induced during extracellular pathogenic infections such as those of fungi, protozoa and helminths, where they facilitate pathogen elimination through opsonisation, complement induction and toxin neutralisation (Diebold, 2008). They primarily facilitate the induction of humoral immunity, and are particularly important for the initiation of antibody class switching in B cells to IgG1, IgA and IgE production (Mazzoni and Segal, 2004). Th2 cells secrete of IL-4, IL-5, IL-9 and IL-13 cytokines, the production of which is regulated at the transcriptional level by GATA-3 (Agarwal and Rao, 1998). IL-4 is one of the driving forces behind Th2 differentiation, and is responsible for mediating IgE production along with IL-13, while IL-5 is involved in activating other immune cells such as eosinophils, mast cells and basophils that mediate humoral immunity (Spellberg and Edwards, 2001). Interestingly, foreign antigen detection at mucosal surfaces, such as the pulmonary airways, has been shown to preferentially induce Th2-mediated responses in humans and in mice (Constant et al., 2000).

The third type of Th cells, Th17 cells, was initially believed to primarily mediate inflammatory responses before adaptive immunity was fully initiated. This was supported by the short life-span of Th17 cells and their suppression by Th1 and Th2 cytokines (Harrington et al., 2005). They are now thought to mediate neutrophil-driven inflammatory responses, and have been characterised by their involvement in combating fungal and extracellular bacterial infections, and their production of the pro-inflammatory cytokine, IL-17 (Harrington et al., 2005, Acosta-Rodriguez et al., 2007). The main transcription factors involved in Th17 development are the orphan

nuclear receptors, retinoid-related orphan receptor-γt (ROR-γt) and ROR-α (Yang et al., 2008b). Tumour growth factor-β (TGF-β) and IL-6 play an important role in activating Th17 differentiation (Ivanov et al., 2006), while IFN-γ, IL-27 and IL-2 negatively regulate Th17 cells through the transcription factors, STAT1 and STAT5 (Laurence et al., 2007, Kimura and Kishimoto, 2011). In addition to a protective role, Th17 cells have been associated with a number of autoimmune diseases such as inflammatory bowel disease and experimental autoimmune encephalitis (EAE) (Kimura and Kishimoto, 2011).

In order to maintain a balance between pathogen eradication and immune-mediated damage, the fourth Th subtype, regulatory T cells (Treg), are responsible for promoting tolerance by suppressing adaptive immune responses, and are also involved in preventing autoimmunity (Chen et al., 2003). Antigen-induced Treg (iTreg) and thymus-derived, natural Treg (nTreg) are functionally alike because they are both capable of inhibiting disease *in vivo*, and can be anergic. Treg cell differentiation is controlled by the forkhead/winged helix transcription factor, forkhead box P3 (Foxp3) (Chen et al., 2003). Like Th17 cells, Treg differentiation also relies on the transcription factor, ROR-γt, although only TGF-β is required to induce Treg differentiation (Ivanov et al., 2006, Sallusto and Lanzavecchia, 2009).

Finally, the follicular helper CD4+ T cells (Tfh cells) are primarily involved in the formation, regulation and maintenance of germinal centres that are responsible for B cell differentiation into plasma cells and memory B cells (Crotty, 2011). At present, it is still unclear how Tfh cell differentiation is distinguished from, and interrelated to other CD4+ T cell differentiation subsets, and what signals in humans induce Tfh cell differentiation.

1.2.2 Th cell regulation

The relevance of inducing the correct Th response is highlighted by the differential nature of adaptive responses against different invading microorganisms. The eradication of infections require specific Th responses, and dysregulated Th responses can promote several pathological conditions, as is demonstrated in the case of allergy and asthma, which are characterized by excessive Th2 responses (Mazzoni and Segal, 2004).

Efficient CD4+ T-cell expansion and differentiation can be discerned by the cytokine repertoire that the T-cells produce. This is largely dependent on the type of foreign stimulus, and which subset of APCs is activated (Fajardo-Moser et al., 2008). Th1 and Th2 cells appear to regulate each other, mediating a fine balance between cell-mediated and humoral immunity (Figure 1.1). IFN-γ secreted by Th1 cells directly suppresses IL-4 secretion, inhibiting differentiation of naive or Th0 cells into Th2 cells (Demeure et al., 1994). In contrast, IL-4 and IL-10 suppress the secretion of IL-12 and IFN-γ, in addition to inhibition of phagocytosis and antigen presentation, blocking Th1 polarisation. This interplay between Th1 and Th2 responses allows each to regulate the other.

A similar balance has been identified between Th17 and Treg cells, for immune homeostasis, and involves mediation by IL-6 (Kimura and Kishimoto, 2010). IL-6 induces the generation of Th17 cells from naive T cells in the presence of TGF-β, however in its absence; Th cells differentiate into Treg cells (Figure 1.1).

In general, the level of plasticity of Th cells has yet to be fully elucidated, although it is believed that there is some flexibility in the cytokine repertoire that a differentiated Th cell can secrete. This suggests that perhaps Th differentiation is not terminal, as was once thought and is open to manipulation for vaccine purposes (Sallusto and Lanzavecchia, 2009).

1.2.3 CD8+ T-cell differentiation

The interaction of naïve CD8+ T-cells with MHC class I-peptide complexes results in activation of CD8+ T-cells, provided signals 2 and 3 are also present. Activated CD8+ T-cells (also referred to as CTLs or Tc cells) are predominantly involved in the elimination of infected or dysfunctional somatic cells (such as tumour cells), thus playing a vital role in adaptive immunity (Kindt et al., 2007). Upon interaction with targeted cells, CTLs induce apoptosis in one of two ways. The first involves the release of cytotoxins such as perforin and granzymes, which induce a caspase cascade that eventually leads to cell apoptosis (Vukmanovic-Stejic et al., 2000). The second apoptotic pathway is induced by Fas ligand-Fas interaction between a CTL and the

infected cell. CD8+ T-cells have long been considered a homogenous population, but in the last decade three distinct subsets (Tc0, Tc1 and Tc2) have been identified, which demonstrate functional and phenotypic differences (Vukmanovic-Stejic et al., 2000). These subsets are not as extensively defined as Th cells, but they tend to complement their Th counterparts.

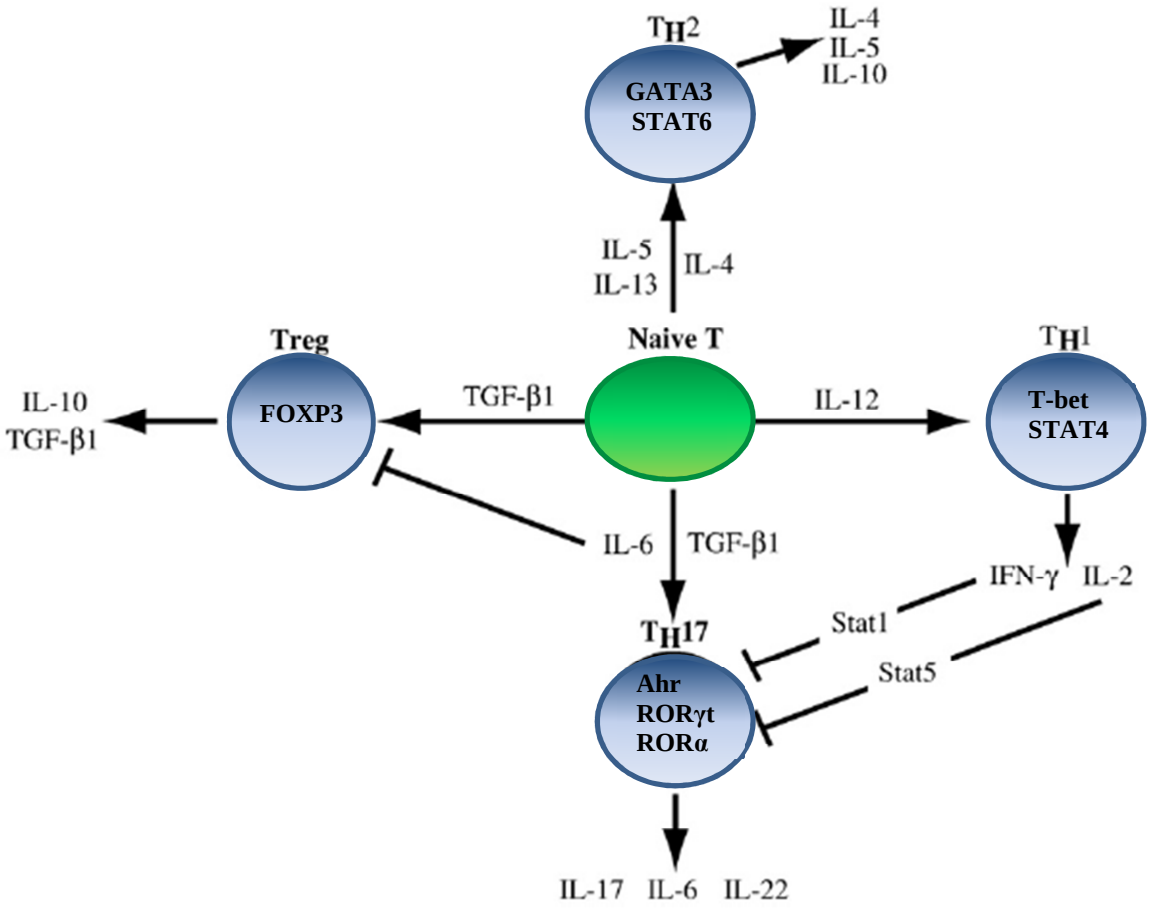


Figure 1.1 – Hypothesised regulation of Th-cell subsets. The transcription factors and cytokines involved in the differentiation and maintenance of Th cells. Derived from (Kimura and Kishimoto, 2011).

The majority of activated CD8+ T-cell clones are Tc1 cells *in vitro*, and are able to secrete IFN-γ, TNF-α, IL-2 and lymphotoxin when stimulated (Mosmann et al., 1997, Vukmanovic-Stejic et al., 2000). They produce large quantities of perforin and Fas ligand, and are involved in the rapid and efficient killing of infected cells, defining them as the classical Tc cells. Proliferation of Tc1

cells is enhanced in the presence of IL-12, as is the case with Th1 cells. On the other hand, IL-4 suppresses the proliferation of Tc1 cells, inhibiting their ability to synthesize IL-2, and downregulating proliferation, and long-term cytotoxicity (Mosmann et al., 1997). Additionally, these cells tend to be very susceptible to activated induced cell death (AICD), a process involved in T-cell homeostasis and tolerance.

On the other hand, Tc2 cells are less vulnerable to apoptosis via Fas-FasL interactions and AICD. They are distinguished from Tc1 cells by their production of IL-4 and IL-5, and lack of IFN-γ production (Mosmann et al., 1997). Tc2 cells also express high levels of CD30 and CD40. Unlike Tc1 cells, Tc2 cell growth and expansion is unaffected by IL-4, allowing them to perform cytotoxic functions in Th2 microenvironments. There is some debate as to the cytotoxic capabilities of Tc2 cells, although these cells produce similar quantities of perforin and Fas ligand compared to Tc1 (Vukmanovic-Stejic et al., 2000). Generation of Tc2 cells *in vitro* requires the additional stimulation of cells with anti-CD3 and anti-CD28 compared to Tc1 and Tc0 cells, suggesting that Tc2 CD8+ cells may only occur in significant numbers when under certain disease conditions or may only reside in specific immune compartments in humans (Vukmanovic-Stejic et al., 2000).

The final Tc subset, Tc0 cells, make up a small population (10-20 %) of activated CD8+ T-cells in peripheral blood, and possess the unique ability to produce both IFN-γ and IL-4 (Vukmanovic-Stejic et al., 2000). Tc0 cells, like Tc2 cells, express a high level of CD30 and CD40 surface receptors compared to Tc1, and their proliferation is unaffected by IL-4 and IL-12. However, they demonstrate similar cytotoxicity to Tc1 cells, producing comparable amounts of perforin and Fas ligand. The function of these cells remains to be established, although given that they possess characteristics of both Tc1 and Tc2 cells, it is possible that this is an intermediate subset that could potentially be polarised in either direction.

Unlike Th cells, Tc cells do not demonstrate a level of plasticity (Mosmann et al., 1997). However, CD8+ T-cell differentiation is polarised in the presence of certain cytokines, be it to a lesser degree than CD4+ T-cells. The subtle regulation by IL-12 and IL-4 is thought to maintain a balance in the CD8+ effector T-cell response during long periods of immune activation.

Interestingly, CD8+ T-cells play a role in regulating CD4+ T-cell differentiation, through cytokine production and cellular interactions (Vukmanovic-Stejic et al., 2000, Holmes et al., 1997). As expected, Tc1 cells encourage differentiation of Th1 cells, and Tc2 cells encourage Th2 responses.

1.2.4 CD8+ T-cell phenotypes

Naïve T-cells are commonly identified by the expression of CD45RA, CCR7 (lymph node homing marker) and CD62L (adhesion marker) (Tough and Sprent, 1994). They exist in the periphery and lymph node tissues where their interaction with matured APCs results in their development into effector T-cells, key players in the adaptive immune response. Once the detected pathogen is eradicated, the surviving antigen-specific effector T-cells develop into memory T-cells, and remain in lymphoid organs and peripheral non-lymphoid tissues as 'memory pools', to induce a rapid secondary response if they ever encounter the same antigen again (Lanzavecchia and Sallusto, 2005). Memory T-cells are able to produce the same range of cytokines upon re-stimulation with the recognized antigen, as well as 'remember' the site of initial encounter or where the response is required most. While naïve T-cells proliferate at a much lower rate under stead-state conditions, memory T-cells have a high turn-over rate and are able to act more promptly against pathogens (Lanzavecchia and Sallusto, 2005). It has been reported that naïve T cells require between 6 – 30 or more hours of TCR stimulation to commit to cell division, while memory/effector T cells respond within 0.5–2 hours (Iezzi et al., 1998). Consequently, primary immune responses require a longer time to develop compared to memory responses, which tend to occur fairly rapidly after detection.

Memory T-cells differentiate into different subsets, defined by distinct phenotypes and functions. There are three phenotypes of memory T-cells that have been prominently defined, based on their migratory capacity and effector function (Lanzavecchia and Sallusto, 2005). These include central memory T-cells (T_{CM}), effector memory T-cells (T_{EM}) and terminally differentiated effector memory T-cells (T_{EMRA} cells), and can be distinguished from one another using the naïve T-cell marker, CD45RA, and the lymph node homing marker, CCR7.

In the case of CD8+ T-cells, T_{CM} cells are mainly found in or near lymph node tissue, and are thought to be responsible for most of the recall responses, based on their high poliferative and reconstitutive abilities (Lanzavecchia and Sallusto, 2005). They are more specifically distinguished from CD8+ T_{EM} cells by the presence of CCR7 and CD62L on their surface. On the other hand, T_{EM} cells are associated with peripheral tissues, have a lower poliferative potential, and can demonstrate cytolytic properties rapidly during recall responses to provide immediate protection (Roberts et al., 2005). T_{EMRA} cells are believed to be the most differentiated T-cell phenotype, due to their low proliferative capacity, absence of CD28, CD27, and CCR7, vulnerability to apoptosis, and the high perforin levels (Masopust et al., 2006). The generation of T_{EMRA} cells is not antigen or cytokine dependent, but instead appears when a homeostatic cytokine milieu is present.

Tomiyama et al (Tomiyama et al., 2002) hypothesised that there is a natural progression from T_{CM} to T_{EM} to T_{EMRA}, defined by the presence or absence of certain co-stimulatory molecules, CD27 and CD28, and homing markers, CCR5 and CCR7, which are used to differentiate between the intermediate subsets of T_{CM} and T_{EM} cells. Furthermore, the cytokine milieu plays an important role in the differentiation and maintenance of these memory T-cells. Production of IL-7 and IL-15 by DCs induce proliferation of both T_{CM} and T_{EM} cells, however in response to certain cytokines, T_{CM} cells are able to stop CCR7 expression and attain effector functions (Spellberg and Edwards, 2001). It is hypothesised that this cytokine-driven switch between T_{CM} and T_{EM} cells allows the long-term maintenance of T_{EM} populations, which can exist for many years after the initial stimulation. In addition to the effect of cytokines, this flexibility in memory T-cell phenotype is also influenced by the cumulative history of antigen exposure (Masopust et al., 2006). A short antigenic stimulation usually leads to preferential differentiation into the T_{CM} phenotype, while prolonged exposure to antigen tends to favour differentiation into T_{EM} cells.

1.3 Dendritic cells (DCs)

DCs are the most potent of all APCs in the body, acting as the immune system's primary sensors of antigens found in the periphery and at mucosal surfaces (Banchereau and Steinman, 1998). They are considered to be important modulators of the innate and adaptive immune responses,

being dominant stimulators of CD4+ and CD8+ T-cell responses (Tacken et al., 2007, Banchereau et al., 2000, Wille-Reece et al., 2005).

Human DCs are comprised of a heterogeneous population of cells that are found in most locations in the body including the blood, lymph nodes, mucosal surfaces and skin tissue (Banchereau and Steinman, 1998). They are derived from bone marrow progenitors which differentiate into two main populations of DCs in the blood, namely the myeloid or conventional DCs (mDCs) and plasmacytoid DCs (pDCs), each of which is derived from distinct lineages (Lin et al., 2008) (Figure 1.2). Blood myeloid DCs are further divided into three populations, the blood DC antigen-1+ (BDCA-1+) DCs, the CD16+ DCs and the smaller BDCA-3+ population. In the tissues, mDCs are also divided into phenotypically distinct subsets. In the skin, interstitial or dermal DCs (dDCs) are found in the deeper dermis and tissues, while Langerhans cells (LCs) exist in the epidermis. Monocyte-derived DCs (moDCs) are commonly used as a laboratory model of DCs *in vitro*, and can be found *in vivo* in inflamed tissues and the local lymph nodes (Banchereau et al., 2000). Most DC subsets are distinguished from each other phenotypically due to their unique gene expression profiles, although they are also generally location-specific and functionally distinct.

1.3.1 Blood dendritic cells

The three blood mDC subsets express typical myeloid markers CD13, CD11c and CD33, and lack lineage (Lin)-specific markers (CD3, CD14, CD19 and CD56) (Schreibelt et al., 2010). They produce IL-12 upon activation, however, they differ in their expression of certain surface molecules, allowing them to be differentiated from one another. BDCA-1+ (CD1c+) DCs are Lin-HLA-DR+CD11c+ DCs, and express a vast range of surface receptors including DEC-205, and toll-like receptors (TLRs) 1-8, and 10 (Jarrossay et al., 2001, Ueno et al., 2010). These cells are the most extensively studied of the mDC subsets, and were initially thought to induce CD8+ T-cell responses more efficiently *in vitro* than the other blood DC subsets (MacDonald et al., 2002). However, recent research has suggested BDCA-3+ DCs are superior at antigen cross presentation (Jongbloed et al., 2010).

BDCA-3+ (CD141+ - thrombomodulin) DCs represent a much smaller mDC population (typically make up less than 5 % of blood DCs), and are Lin-HLA-DR+CD11c+ DCs that uniquely express the C-type lectin, CLEC9A (Ueno et al., 2010), along with nectin-like protein 2 (Necl2), TLR3 and TLR8 (Poulin et al., 2010). BDCA-3+ DCs exists in the blood, but have also been detected in secondary lymphoid organs, such as spleen and tonsils (Ueno et al., 2010). Their small population size makes it difficult to isolate quantities that are suitable for extensive *in vitro* experimentation, but recent research has shown that these DCs respond well to TLR3 and 8 ligands, and also display efficient cross presentation of antigens (Poulin et al., 2010, Jongbloed et al., 2010). BDCA-3+ DCs are believed to be the human equivalent of the mouse DC population CD8α+ DCs, which are the major DCs involved in cross presentation in mice. While there are some functional similarities, BDCA-3+ DCs are a minor human DC population, and differ phenotypically from CD8α+ DCs, lacking the expression of CD8α, TLR7, TLR9, or CD11b (Poulin et al., 2010). This makes it difficult to draw distinct parallels between the functions of BDCA-3+ DCs and CD8α+ DCs.

The CD16+ DC population is the largest and most variable population of DCs in the blood (40-80 %), but is the least well characterised, due to its poor viability *in vitro* (MacDonald et al., 2002). It expresses unusually high levels of CD86 and CD40, low levels of HLA-DR, CD14 and CD33, and lacks expression of cutaneous lymphocyte antigen (CLA) (common on other DC subsets). Little is currently known about this subset's functional capabilities.

The fourth blood DC subset, pDCs, circulates in the blood and enters lymphoid organs through high endothelial venules (Ueno et al., 2010). pDCs are distinguished from the other subsets by expression of CD123, BDCA-2, and immunoglobulin-like transcript 7 (ILT7) receptor. Initially, pDCs were thought to be solely of lymphoid origin, however studies have shown that pDCs can develop from myeloid precursors if cultured in the presence of Fms-like tyrosine kinase-3 ligand (Flt3L) (Pulendran et al., 2000, Valladeau and Saeland, 2005). pDCs can be subdivided into 2 subsets, namely, CD2-high and CD2-low populations (Matsui et al., 2009), where CD2-high pDCs induce better T-cell proliferation and more production of IL-12p40. Unlike mDCs, pDCs secrete large amounts of IFN-α and express the cytotoxic molecules, TNF-related apoptosis-inducing ligand (TRAIL) and Granzyme B. They are involved in viral immunity, expressing

IFN-α when activated through TLR7 or 9 by a viral stimulus (Colonna et al., 2004). pDCs also have extensive ER compartments that mediate the secretion of anti-viral factors such as type I IFNs, and appear to store pre-synthesized MHC class I and II molecules for rapid responses to viral infection (Di Pucchio et al., 2008). Cross presentation in pDCs has generally proven to be poor, although in the presence of certain TLR agonists, it can be improved (Mouries et al., 2008).

1.3.2 Skin dendritic cells

Skin-derived myeloid DCs comprise of LCs in the epidermis and dDCs in the dermis. LCs express several myeloid markers including CD11c, CD13 and CD33, in addition to CD1a, DEC-205 and the TLRs 1-3, 6 and 10 (Unger and van Kooyk, 2011). They are distinguished from other DC subsets by the unique expression of langerin (CD207), e-cadherin, and keratinocyte adhesion and epithelial cell adhesion molecules (EpCam). The development of LCs from its precursors *in vivo* and *in vitro* is heavily dependent on the presence of TGF-β (Geissmann et al., 1998). LCs can be derived from CD34+ umbilical cord stem cells as well as CD14+ monocytes *in vitro*, and these models are commonly used to study human LCs, given the difficulty of isolating adequate numbers of LCs from the skin. *In vitro*-derived LCs are able to efficiently stimulate CD4+ and CD8+ T-cell activation as demonstrated by several studies (Flacher et al., 2009, Ratzinger et al., 2004, Idoyaga et al., 2011), and have been shown to more effectively cross present antigen and induce CTL responses than dDCs *in vitro* (Ratzinger et al., 2004). In contrast, a small population of migrating LCs appear to remain in steady-state when they travel to the lymph node, and their lack of functional maturity suggests LCs tend to favour tolerogenic immune responses to self-antigens under certain circumstances (Merad et al., 2008).

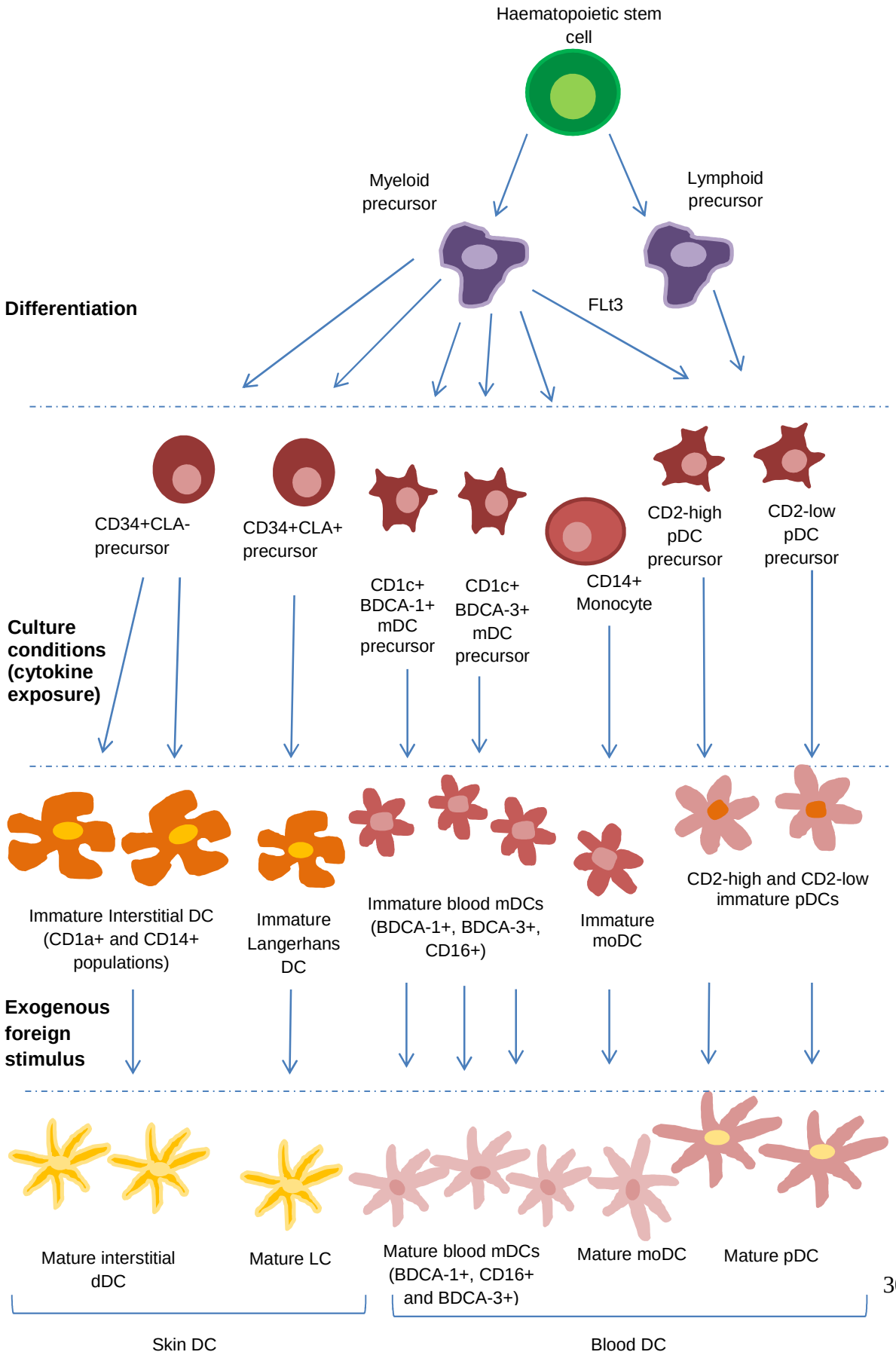
Dermal DCs are analogous to the interstitial DCs found in peripheral tissue. As with LCs, human dDCs express a number of myeloid markers including CD11c and CD1c, in addition to DEC-205, Dendritic Cell-Specific Intercellular adhesion molecule-3-Grabbing Non-integrin (DC-SIGN), and the macrophage mannose receptor (MMR) (Valladeau and Saeland, 2005). Dermal DCs are further divided into two subsets based on their differential expression of CD14 and CD1a (Nestle et al., 1993). The major dDC population, CD1a+ dDCs, express macrophage galactose lectin (MGL) and display an activated phenotype (CD40+, CD80+, CD86+) in the

steady state, demonstrating better LN-homing and T-cell priming capacity than CD1a- dDCs. These cells reside in the upper dermis near the lymphatic vessels. The CD14+ dDCs are found throughout the dermis, but only account for 10-15 % of dermal cells, and they typically express DCIR, Dectin-1 and TLR2–TLR6, TLR8 and TLR10 (Valladeau and Saeland, 2005). Once activated, these cells tend to skew immune responses towards a humoral response, inducing naïve CD4+ T-cells to develop into Tfh cells, thereby initiating B-cell differentiation and IL-21-stimulated antibody production. Dermal DCs can be generated *in vitro* from CD34+ stem cells, where CD14+ precursors are isolated and cultured with GM-CSF, TNF-α and IL-4 to develop dDCs (Caux et al., 1999). These *in vitro* cells resemble moDCs phenotypically, but are functionally different.

1.3.3 Monocyte-derived dendritic cells

Monocyte-derived DCs have been extensively studied since they were first generated by culturing peripheral blood monocytes in granulocyte-macrophage colony-stimulating factor (GM-CSF) and IL-4 (Sallusto and Lanzavecchia, 1994). They have frequently been used as an *in vitro* human DC model because of the abundance of their precursors in blood and ease of purification. MoDCs express several receptors on their surface that renders them similar to dDCs, including CD1a, CD11b, CD11c, DEC-205, and DC-SIGN. They also express a large range of TLRs from 1-8 (Schreibelt et al., 2010). MoDCs are able to secrete IL-12p70 and induce efficient $CD4^+$ and $CD8^+$ T-cell responses *in vitro*, and are therefore frequently used in clinical DC vaccination studies for this purpose. It has yet to be determined whether moDCs exist in steady state *in vivo*, as they display a much higher expression of MHC molecules and co-stimulatory molecules, and demonstrate a low migratory capacity compared to freshly isolated immature mDCs, (MacDonald et al., 2002)(Radford et al., 2006). Additionally, mouse studies have shown that monocytes appear to migrate to the LN before they differentiate into DCs (Leon et al., 2007). All these data suggest that steady-state moDCs do not exist in the periphery, and that *in vitro*-generated immature moDCs represent inflammatory DCs. In view of this, more studies are exploring the use of blood DC subsets *in vitro,* to determine to what extent moDCs resemble human mDCs, and thus verify the use of moDCs as a laboratory model.

Figure 1.2 (next page) - Human DC development. Endogenous stimulation (primarily in the form of cytokines) is necessary for the development of the respective DC precursors into immature DCs of the different lineages. Exogenous stimulus in the form of microbial products is necessary to induce DC activation/maturation (derived from Shortman & Liu, 2002 with some modifications).


Haematopoietic stem cell
Myeloid precursor
Lymphoid precursor
Differentiation
FLt3
CD34+CLA- precursor
CD34+CLA+ precursor
CD1c+ BDCA-1+ mDC precursor
CD1c+ BDCA-3+ mDC precursor
CD14+ Monocyte
CD2-high pDC precursor
CD2-low pDC precursor
Culture conditions (cytokine exposure)
Immature Interstitial DC (CD1a+ and CD14+ populations)
Immature Langerhans DC
Immature blood mDCs (BDCA-1+, BDCA-3+, CD16+)
Immature moDC
CD2-high and CD2-low immature pDCs
Exogenous foreign stimulus
Mature interstitial dDC
Mature LC
Mature blood mDCs (BDCA-1+, CD16+ and BDCA-3+)
Mature moDC
Mature pDC
Skin DC
Blood DC

1.4 Dendritic cell antigen capture

Immature DCs (iDCs) primarily reside in peripheral tissues where their function is focussed on antigen acquisition from their environment. Continual sampling of the local environments for both foreign and self-antigen, allows DCs to facilitate the induction of adaptive immunity and immune tolerance (Banchereau and Steinman, 1998).

iDCs are able to efficiently capture antigens by macropinocytosis, receptor-mediated endocytosis and phagocytosis (Dubsky et al., 2005). The process of receptor-mediated endocytosis is performed by several endocytic receptors, including pathogen recognition receptors (PRRs) such as toll-like receptors and receptors from the C-type lectin family (DEC-205, DC-SIGN, langerin). Once these receptors have bound to a recognised ligand, they endocytose the antigens into endosomal compartments, and antigens are then prepared for surface presentation to T-cells. iDCs also express complement and Fc receptors (CD32 and CD64) on their surface which facilitate the uptake of complement or antibody-opsonised pathogens via phagocytosis, all of which are also incorporated into specific cellular compartments (phagosomes) that facilitate antigen processing for presentation (Banchereau and Steinman, 1998).

1.5 Antigen presentation by dendritic cells

As previously described, DC antigen presentation via MHC molecules is the first of three signals required to activate T-cells and initiate a cell-mediated immune response. Antigen can be derived from within the cell (endogenous antigen) or can be captured from the extracellular environment (exogenous antigen). There are two classical pathways in which APCs are able to present antigen on their surfaces, and one unusual pathway that DCs primarily use (simplistically depicted in Figure 1.3)(Banchereau et al., 2000).

1.5.1 Classical antigen presentation pathways

The first classical pathway involves endogenous antigen presentation via the MHC class I pathway, which informs the immune system via CD8+ T cells of viral or intracellular pathogen

infections, or cellular transformations (Goldberg and Rock, 1992, Rock and Shen, 2005) (Figure 1.3). MHC class I molecules present peptides that are derived from a great number of cellular-synthesised proteins, including those of foreign origin. On a regular basis, one or more ubiquitin molecules are added to the N-terminus of such proteins. Ubiquitin is a small regulatory protein that is able to target intracellular antigens towards the proteasome, where they are hydrolysed into oligopeptides ranging in size from 2-20 amino acids (aa) (Bonifacino and Weissman, 1998, Rock and Shen, 2005). Most of these oligopeptides are further hydrolysed into aa that can be re-used in cellular protein synthesis processes, however, oligopeptides of more than eight residues are sometimes transported to the ER via transporter associated with antigen processing protein (TAP). In the ER, ER-aminopeptidase-1 (ERAP1) is used to further degrade the peptides into 8-9 residue-structures, which then associate with MHC class I molecules (Saric et al., 2002). MHC class I molecules are heterodimeric glycoproteins which consist of a membrane-anchored heavy chain with three α (α_1, α_2, α_3) domains and a smaller, non-covalently attached, β_2 microglobulin light chain (Silver et al., 1992). The α_1 and α_2 subunits form a peptide cleft, where the peptide is able to bind. The peptide associates with β2‑microglobulin and the heavy chains, forming a trimeric complex, and optimal folding and glycosylation occurs before MHC class I-peptide complexes are sent to DC plasma membrane for antigen display (Cresswell et al., 2005). At the cell surface, interaction of the peptide-MHC class I complex with naive CD8+ T-cells is able to trigger either CD8+ T-cell activation (leading to an immune response), or immune tolerance (in the absence of other activation stimuli).

The second pathway involves presentation of exogenous antigens via the MHC class II pathway (Banchereau et al., 2000). These antigens are commonly derived from invading pathogens, or as a result of cellular processes such as apoptosis or autophagy (Vyas et al., 2008). Only professional APCs such as DCs or macrophages express MHC class II molecules on their surface. Acquirement of foreign, soluble and particulate antigens leads to the uptake of antigen into an endocytic compartment, which interacts with a mildly acidic MHC class II–rich subcellular compartment (MIIC) (Rock and Shen, 2005, Steinman, 2001, Banchereau et al., 2000). This is a lysosome-like compartment which continually accumulates MHC class II molecules, and where the captured antigens are processed, bound to the MHC class II molecules, and sent to be displayed at the cell's surface (Banchereau et al., 2000). Within the MIICs, the

MHC class II molecules undergo a step-wise cleavage of the invariant chain (Ii) that links its α and β components (Cresswell, 1994). The Ii is a chaperone protein that assists in the assembly and transport of MHC class II molecules through the Golgi to the endosomal pathway, and is also involved in preventing the premature binding of ligands to MHC class II. Cathepsin S mediates the cleavage process of Ii, and is therefore upregulated after DC maturation to degrade Ii and allow the processed peptides to bind to MHC class II molecules. Newly-formed MHC class II-peptide complexes are trafficked to the cell membrane, where they cluster into lipid rafts in order to be presented on the surface (Vyas et al., 2008, Banchereau et al., 2000). Interaction of these complexes at the surface with CD4+ T-cells leads to the induction of T_h responses (Banchereau and Steinman, 1998). Interestingly, the cytoplasmic tail of the MHC class II β-chain is ubiquitinated in mouse DCs, to allow for the recycling of these molecules back to MIICs (Vyas et al., 2008). However, in mature DCs, ubiquitination of MHC class II is down-regulated so that loaded MHC class II complexes can accumulate at the cell surface to initiate T-cell activation.

1.5.2 Cross presentation pathway

The unique pathway for exogenous antigen presentation by DCs is known as the cross-presentation pathway. This pathway involves the display of exogenous antigen by MHC class I molecules, allowing the induction of CD8+ T-cells by DCs (Rock and Shen, 2005, Bevan, 2006, Banchereau and Steinman, 1998, Banchereau et al., 2000, Lin et al., 2008). It was first discovered in 1976 (Bevan, 1976), although the importance of its role in alerting the immune system about invading viruses (that do not replicate in DCs) and tumours was only appreciated later. Cross presentation is performed primarily in DCs because they possess the appropriate cellular machinery required for this pathway, although macrophages are also capable of cross presentation to a lesser extent (Banchereau et al., 2000). Although it has not been completely elucidated, cross presentation is thought to occur either through a phagosome-to-cytosol pathway (a TAP-dependent process), or via an endosome-ER pathway (a TAP-independent process) (Lin et al., 2008, Rock and Shen, 2005) (Figure 1.4).

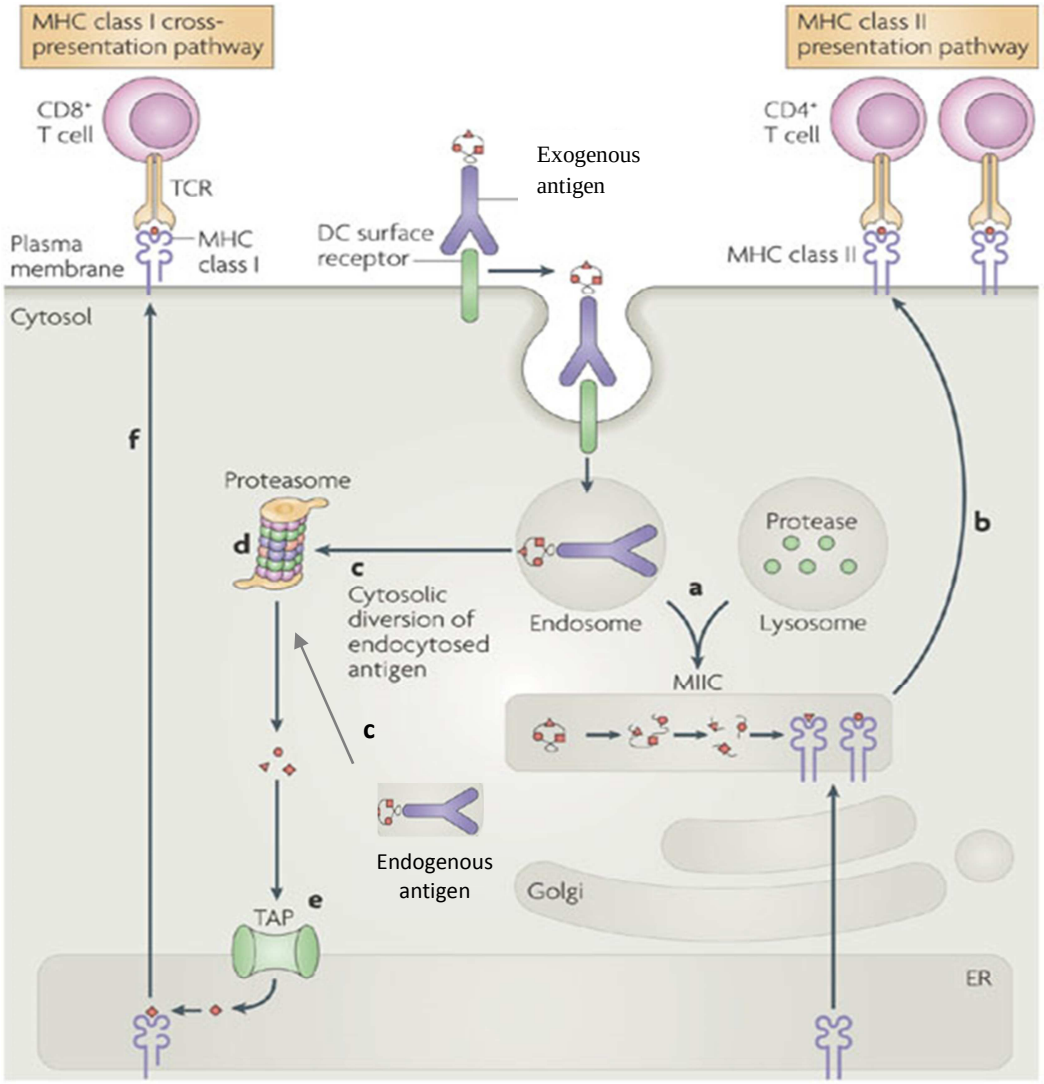


Figure 1.3 – Antigen presentation via MHC class I and II molecules. (a) Exogenous antigen is endocytosed into an endosome, which fuses with protease-containing lysosomes, resulting in degradation of the antigen into smaller peptides. (b)These peptides are loaded onto MHC class II molecules that reside in the MHC class II compartment (MIIC), and are presented at the cell surface to CD4+ T cells (MHC class II pathway), OR endocytosed antigens escape into the cytosol (One cross presentation route) and gain access to the classical MHC class I pathway which is primarily used for endogenous proteins (c). This pathway involves peptides being further degraded by the immunoproteasome (d) and then delivered to the endoplasmic reticulum (ER) in a TAP-dependent manner (e), where they are loaded onto MHC class I molecules for presentation on cell surface to CD8+ T cells (f). Adapted from (Tacken et al., 2007)

In the first pathway, soluble and particulate exogenous antigens are captured and internalized into phagosomes, micropinosomes or endosomes, where they undergo partial proteolysis by proteases within these compartments. TAP along with other ER-associated proteins such as tapasin and Sec61 function to transport captured peptides into the cytosol across the cellular membrane of the phagosome (Rock and Shen, 2005). Once in the cytosol, the proteins are processed in the same way as endogenous antigen would be via the proteosome, and are then transported to the ER via TAP and attached to MHC class I molecules to be sent for surface display. There is still some speculation as to how the ER and phagosomes are related, and to what extent ER-derived proteins participate in the transportation from phagosome to cytosol to ER, but evidence indicates that this model is the closest depiction we have of the process (Lin et al., 2008, Rock and Shen, 2005).

The second cross presentation route, called the endosome-ER pathway, is believed to be less commonly used for cross-presentation, although it can be upregulated upon DC maturation (Robson et al., 2003).This pathway involves a TAP-independent route with the fusing of ER vesicles to the endosome carrying the captured antigens (Figure 1.4). Several proteases are thought to initially break the protein down within the endosome, specifically cathepsin S. Following protein processing, it was originally thought that the endosome fused directly to the ER, forming an ERgosome, and the resulting oligopeptides were then further hydrolysed into 8-9 residues via the ER-associated degradation (ERAD) pathway (Lin et al., 2008, Ackerman et al., 2005, Imai et al., 2005). This has since been disproved, and it is now thought that the endosome fuses to an acidic ER vesicle which consists of proteins from ERAD that are necessary for antigen degradation into oligopeptides (Lin et al., 2008). Oligopeptides of the right size within this fused endosome-vesicle structure are loaded onto MHC class I molecules that have been trafficked into the endosome from the plasma membrane, or from the ER by ER-related proteins (Rock and Shen, 2005). Newly formed MHC class I-peptide complexes are sent to the surface for presentation.

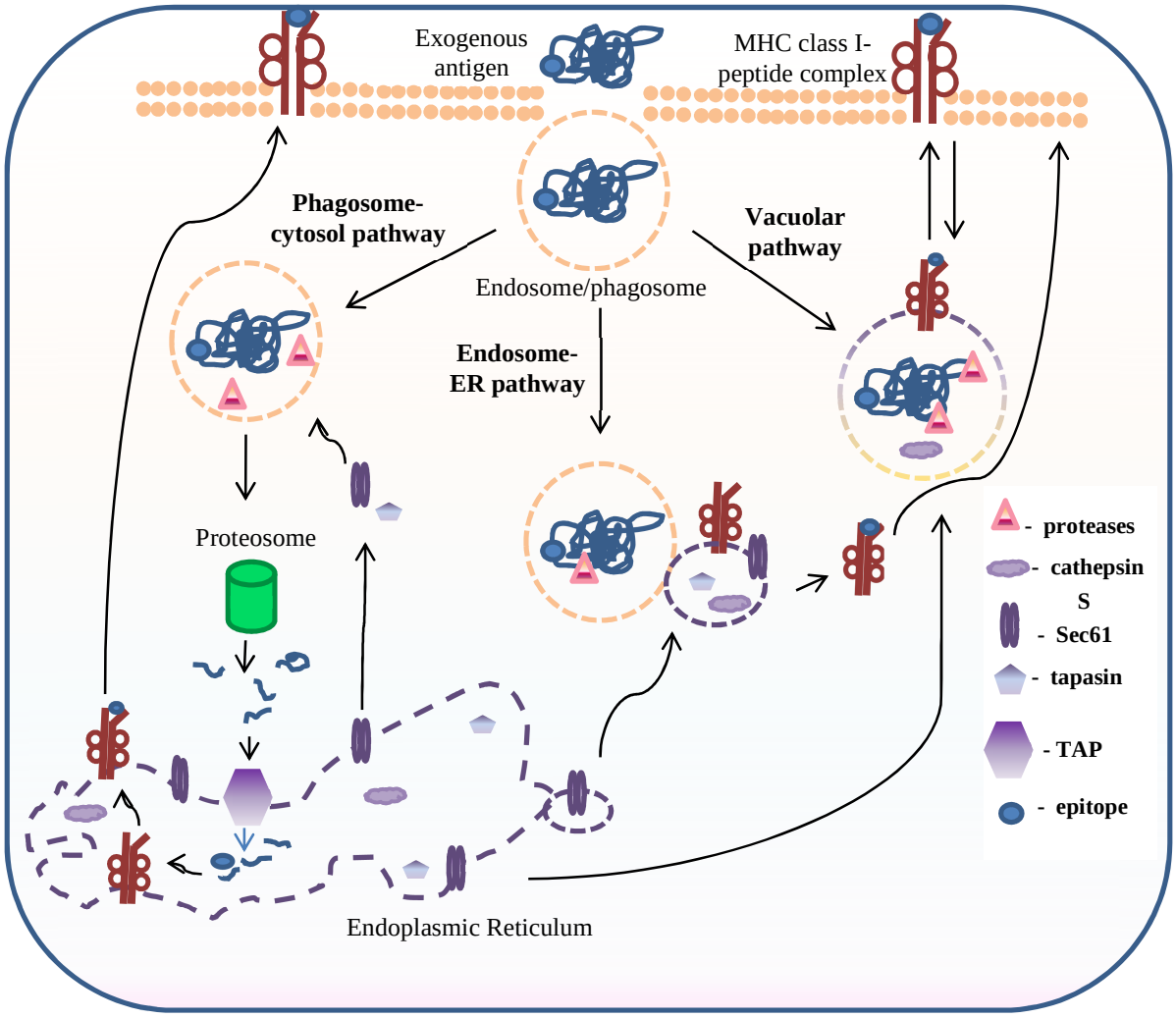


Figure 1.4 – Possible routes of cross presentation with three potential pathways. This includes phagosome-cytosol, endosome-ER and vacuolar pathways (adapted from (Lin et al., 2008, Rock and Shen, 2005)).

The final cross-presentation route is referred to as the vacuolar pathway (Rock and Shen, 2005). The mechanism of this route is unclear, but it is also TAP-independent. It is believed to involve the captured antigen being degraded by endocytic proteases and cathepsin S within the phagosome/vacuole. The resulting oligopeptides are then bound to MHC class I molecules that have been transported into the vacuole from the plasma membrane or from the ER (Rock and Shen, 2005).

The potency of the CD8+ T-cell response induced through cross presentation of a given antigen is dependent on several factors including the length of the peptide presented, nature of the

antigen, and the type of DC subset presenting the antigen (Faure et al., 2009). The length and persistence of antigen exposure have also been highlighted as important aspects of generating efficient and long lasting CD8+ T-cell priming (Jusforgues-Saklani et al., 2008, Faure et al., 2009). However, it is the nature of the antigen that seems to effect whether it will be cross presented or not. Studies have shown that particulate antigen or whole, cellular proteins are more likely to be cross presented than soluble antigen (Burgdorf et al., 2007).

This was demonstrated by the inability of soluble products to elicit CTL immunity *in vivo*, in comparison to particulate antigen (Pooley et al., 2001). Burgdorf et al (Burgdorf and Kurts, 2008) suggests that the cross presentation of particulate and soluble antigens are dependent on different factors. Particulate antigen presentation has been found to be time-dependent, whereas cross presentation of soluble antigens is localization-dependent. Phagocytosed, particulate antigen is not initially degraded in the phagosome because of an active alkalisation process that maintains a neutral pH within the phagosome. This inhibits protease activity and allows the intact antigen to be successfully transferred into the cytosol and delivered to the cross presentation processing pathway (Burgdorf and Kurts, 2008). The process of active alkalization is transient though, and once it ceases after some time, the naturally acidic nature of the phagosome activates proteases and cleavage of the antigen that is not exported. The resulting oligopeptides are then presented on MHC class II molecules. Thus, MHC-I- and II-restricted presentation of particulate antigens seems to occur sequentially (Burgdorf and Kurts, 2008). On the other hand, soluble antigens are either internalized into stable, early endosomes via endocytic receptors (which delivers them to the cross presentation pathway), or they are specifically endocytosed and routed towards lysosomal compartments (for MHC class II processing and presentation). Thus, the compartment into which soluble antigen is endocytosed determines whether it will enter the cross presentation pathway (Burgdorf and Kurts, 2008).

This data suggests that the fate of an antigen's presentation is also strongly related to the uptake process. Phagocytosis is accepted as one of the primary means by which cross presented antigen is endocytosed, however receptor-mediated endocytosis of antigens also directs antigen towards the cross presentation pathway (Lin et al., 2008). There are several APC receptors such as DEC-205, the MMR and Fc receptors, which are responsible for mediating endocytosis of exogenous

antigen, and seem to have the ability to specifically target antigens towards stable, early endosomes for processing via the cross presentation pathway (Burgdorf and Kurts, 2008). In contrast, there are receptors such as DC-SIGN and scavenger receptors, which preferably target antigen towards late, acidic endosomes/lysosomes for presentation on MHC class II molecules. Thus, the type of endocytic receptors on DCs appears to be the distinguishing factor as to why DC subsets demonstrate differences in their abilities to cross present. Dudziak et al (Dudziak et al., 2007) illustrated that in mice, CD8α− DCs specifically target antigen for presentation on MHC class II, while CD8α+ DCs (prominently expressing DEC-205) are able to cross-present antigen in addition to also contributing to MHC class II antigen presentation. Moreover, human mDCs, which harbour several endocytic receptors on its surface, are superior at cross presentation compared to pDCs, which do not appear to cross present antigen, unless in the presence of an adjuvant (Mouries et al., 2008). Thus, for the purposes of vaccine strategies that aim to enhance CD8+ T-cell responses, it is of great interest to explore the capacity of these endocytic receptors to direct antigen towards the cross presentation pathway and to determine which receptors are able to do this optimally.

1.6 Dendritic cell maturation

There are distinct phenotypic and functional differences between immature and mature DCs (Figure 1.5). Immature DCs are characterized by expression of the migratory chemokine receptors CCR1, CCR5, and low-level expression of the co-stimulatory molecules CD80, CD86 and CD40 (Banchereau et al., 2000, Steinman, 2001). While they are highly efficient at antigen capture, their ability to stimulate T-cells is poor, unlike mature DCs. Thus, once DCs have captured antigen that triggers their activation, they transition from immaturity to maturity in order to interact with T-cells and elicit an adaptive immune response. The activation stimuli are detected by DC PRRs such as TLRs, which recognise a vast range of bacterial, viral and fungal motifs. PRRs are responsible for the recognition of pathogen associated motif patterns (PAMPs) such as pathogen-derived molecules (lipopolysaccharides, bacterial DNA, dsRNA), inflammatory cytokines (IL-1, TNF) or molecules resulting from cellular trauma (heat shock proteins). Mature DCs express higher levels of the migratory marker CCR7, which is a lymph node homing receptor, and targets them towards the draining lymph node from the periphery, to

directly activate naïve T-cells. As they migrate, DCs process the captured antigens for surface display via MHC-class I or II, and antigen presentation is sustained due to the maturation of the DCs. Concurrently, there is an increased secretion of certain cytokines (IL-6, TNF-α, IL-12p70), down-regulation of immature DC receptors such as DC-SIGN, upregulation of co-stimulatory molecules (CD80, CD86) and MHC-class I and II molecules, and increased expression of CD83 (maturation marker). All these events occur to assist in the process of T-cell priming, as DCs play a vital role in directing the specificity of T-cell responses based on the cytokine repertoire that it secretes once it has arrived at the lymph node (Steinman, 2001).

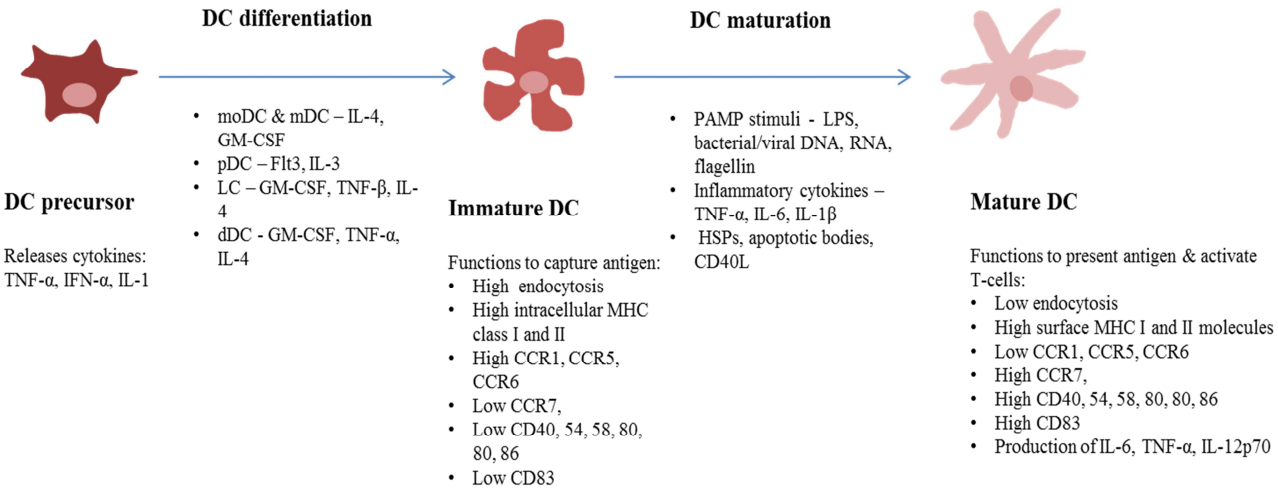


Figure 1.5 – Phenotypic and functional descriptions of DCs at different stages of development. Adapted from (Banchereau and Steinman, 1998, Tacken et al., 2007)

In vitro maturation of DCs often involves incubating cells with a cocktail of TNF-α, IL-6 (inflammatory cytokines), IL-1β (mediates inflammatory responses), and prostaglandin E2 (PGE-2 – encourages cell migration) (Schreibelt et al., 2010). However, DC activation solely by inflammatory cytokines has proven to induce less than optimal Th1 responses, with induction of CD4+ T-cell proliferation in mice but poor functional activation in terms of directing T-cell differentiation. Thus, the evidence suggests that there are different degrees and types of DC maturation (Reis e Sousa and Germain, 1995). Phenotypically mature DCs, which demonstrate an increased expression of co-stimulatory molecules and maturation markers, can occur as the result of detecting foreign stimuli or being in an inflammatory environment. However, functional

DC maturation, which is as the result of upregulated co-stimulatory molecules as well as production of pro-inflammatory cytokines (such as IL-12p70), is only stimulated by the detection of foreign stimuli. Thus, only functionally mature DCs successfully and effectively elicit T-cell functional activation, inducing differentiation into effector cells. In view of this, it appears as though vaccine antigens can only stimulate robust T-cell responses if administered with an appropriate adjuvant that can functionally mature DCs.

1.7 Mouse versus human dendritic cells

Immature DCs in both mice and humans are found in tissue and in secondary lymphoid tissue. Mouse DCs are more heterogeneous than human DC populations, with as many as five identified subsets, all expressing CD11c. Secondary lymphoid organs have two prominent DC subpopulations, namely the CD8α- (myeloid lineage) and CD8α+ (lymphoid lineage) subsets, and these can be further divided by their differential expression of CD4 (Banchereau et al., 2000). Lymphoid and myeloid murine DCs differ in their phenotype, localization, and function, however, both subsets express high levels of CD11c, MHC class II, and the co-stimulatory molecules, CD86 and CD40 (Banchereau and Steinman, 1998). CD8 α+ DCs are primarily found in the T cell–rich areas of the periarteriolar lymphatic sheaths (PALS) in the spleen and lymph nodes, and produce IL-12p70 upon activation, demonstrating better efficiency at stimulating CD8+ T-cells (Banchereau et al., 2000, Shortman et al., 2009). CD8α- cells are more commonly found in peripheral tissue, and are efficient at CD4+ T-cell induction. CD8α- cells are believed to be the mouse equivalent to the human pDC subset. In general, CD8α+ DCs are more proficient cross-presenting cells than other DC subsets including CD8α- DCs, and have recently been deemed the mouse equivalent of BDCA-3+ human mDCs (Lin et al., 2008, Shortman et al., 2009).

Similarities between mouse and human DCs with regard to basic functions and development, have allowed researchers to use preclinical mouse studies to provide a foundation *in vivo* model for DC-based vaccine strategies (Tacken et al., 2007). While this has been useful in allowing us to understand the *in vivo* cellular immune interactions induced by receptor targeting strategies, human and mouse DC subsets are phenotypically and functionally quite different, differing in

their distribution of receptors, and abilities to induce B-cell proliferation and T-cell differentiation (Banchereau et al., 2000). Murine DC subsets express a broader range of TLRs than human subsets, expressing TLR7 and 9 on almost all subsets. This allows them to recognize a wider repertoire of PAMPs than their human counterparts (Mazzoni and Segal, 2004). Furthermore, even though some human DC populations such as BDCA-3+ DCs have been identified as mouse equivalent subsets, there are still some distinct differences. The variations in cell-surface marker expression, and the fact that few studies have analysed freshly-isolated tissue human DC populations to confirm whether they react in a similar fashion to murine DC subsets, makes mouse studies difficult to rely upon, and directly translate into relevance for humans. It is therefore important to further explore *in vitro* human DC studies to gain a clearer insight as to how human DCs function, and determine whether mouse *in vivo* models are able to provide an adequate depiction of *in vivo* situations for humans.

1.8 DC-based vaccinations

The vital role that DCs play in both the innate and adaptive arms of the immune response makes them an ideal target for vaccines. DC-based vaccine designs initially explored methods to improve MHC-class I presentation (and thereby induce specific CD8+ T-cell priming), by stimulating DCs *ex vivo*. These procedures included *ex-vivo* loading of DCs with peptides/proteins, or transfecting DCs with RNA-encoding specific antigens (Tacken et al., 2007). Loading DCs *ex vivo* involves pulsing the appropriate DCs with the peptide or protein of interest, then injecting loaded DCs into the host to stimulate autologous T-cell immunity (Allard et al., 2008, Tacken et al., 2007, Benko et al., 2008). One such study by Aline et al (Aline et al., 2009), showed that DCs loaded with biodegradable nanoparticles coated with HIV-1 p24 protein resulted in efficient DC maturation, systemic CTL response induction and strong lympho-proliferative responses, as well as high serum and mucosal antibody production in mice.

Although *ex-vivo* loading allows high antigen specificity and controls maturation and activation, it is expensive, labour-intensive, and is required to be unique for each patient (Tacken et al., 2007). This makes an *ex vivo* DC vaccine inaccessible to patients in developing countries. Therefore targeting DCs *in vivo* with antigens is more favourable in terms of cost and

production. Additionally, *in vivo* targeting provides a means to allow antigen delivery to occur in the natural milieu of DCs.

The functional complexity of DCs means that several parameters need to be considered in the development of an *in vivo* DC-targeted vaccine, in order to ensure that the appropriate immune response is elicited (Ueno et al., 2010). These parameters include the DC subset targeted, the tissue distribution and biological function for the targeted DC subset, the immunogenicity of the selected antigen, the choice of adjuvant, and the surface receptor/s to be targeted.

DC subsets have been shown to influence the type of T-cell response that is induced. In mouse studies, antigen-loaded CD8α+ DCs preferentially activates CD8+ T-cell immunity, while CD8α- DCs induce CD4+ T-cell responses (Dudziak et al., 2007). Similarly, DC subsets in human studies also display a bias towards different immune responses. Activated skin-derived dDCs generally demonstrate a pro-inflammatory, migratory, and T cell-stimulatory profile, while LCs in the epidermis tend to express molecules involved in cell adhesion and DC retention in the epidermis, polarizing reactions away from a Th1 response (Santegoets et al., 2008). Further human comparative studies between moDCs and blood myeloid DCs (BMDCs) indicated that at low concentrations of stimulating antigen, BMDCs generated better antigen-specific proliferative T-cell responses, where responses were skewed towards Th1 (Osugi et al., 2002). As mentioned earlier, the distribution of endocytic receptors (specifically PRRs) among DC subsets is quite varied, and this is potentially a contributing factor to the preference a subset has to a given type of immune response. This is supported by the bias these receptors have towards a specific presentation pathway (Tacken et al., 2006). Thus, recent research has focussed on empirically determining which types of immune responses are triggered by certain DC surface receptors, and to what extent targeting these receptors is able to enhance immune responses.

Initial studies targeting DCs *in vivo* investigated the use of attaching receptor ligands to gene 'delivery vehicles' such as liposomes, polymer particles or live vectors (Tacken et al., 2006, Lisziewicz et al., 2005, Worgall et al., 2004). The vectors carrying proteins, peptides or DNA, were attached to DC receptor ligands (such as mannose, bacterial toxins and heat-shock proteins amongst others), allowing them to deliver their transgene or antigen to DCs that displayed the

complimentary surface receptor. Hattori et al (Hattori et al., 2004) compared the stimulatory effects of administering a mannosylated liposome complex carrying a DNA vaccine versus the naked DNA vaccine in mice, and found that the mannosylated liposome complex enhanced inflammatory cytokine (TNF-α, IFN-γ and IL-2) secretion and improved MHC class I-restricted antigen presentation on DCs.

Other related studies have investigated the use of antigen being directly conjugated to receptor ligands, as this eliminated the need for a delivery vehicle, while maintaining the ability to target antigen to the surface of DCs (Binder and Srivastava, 2005, Adams et al., 2008). Singh et al (Singh et al., 2009) targeted DC-SIGN using a modified version of ovalbumin (OVA) that included fucose-containing structures (a ligand that commonly binds to DC-SIGN), and showed an increase in antigen cross presentation and enhanced CD4+ and CD8+ T-cell responses. Furthermore, these authors also showed that directing natural ligands to CLRs encouraged antigen cross presentation without the required DC maturation signals.

While these DC-targeting strategies were able to elicit strong CD4+ and CD8+ T-cells, specificity of the targeting process was questionable. Many of the ligands were able to bind to multiple receptors, and most of the receptors chosen were found on more than one cell type in humans. It is preferable for vaccines to target a surface molecule that is specific to DCs, in order to avoid problematic side-effects and reduce the antigen dose required (Shortman et al., 2009). Thus, directing antigens to DCs by specifically targeting receptors that are preferentially and prominently expressed on DCs is a promising means to enhance cell-mediated immune responses.

There are currently two methods that have been utilised to target antigens specifically to endocytic DC receptors. The first method involved the production of synthetic ligands specific to the receptors of interest (Frison et al., 2003). Oligolysine-based oligosaccharide clusters that were specific for MMR or DC-SIGN were chemically conjugated to antigens, with a high affinity to the respective receptors. Further studies with such ligands have revealed that they are also able to elicit significant CD8+ T-cell responses when conjugated to antigen (Srinivas et al., 2007). Although this method shows potential, there are currently only synthetic ligands specific

to DC-SIGN and MMR, and creation of specific ligands for other receptors has yet to be explored. Also, the immunogenicity of the ligands themselves needs to be examined *in vivo* to verify safety.

Another way to specifically direct antigens to DCs is using an antibody-targeted approach, where the antigen is linked to an antibody specific to a DC endocytic receptor. Targeting an antigen to a DC endocytic receptor in this way has been shown to increase antigen-delivery efficiency by 100-1000 fold more than non-specific administration of the antigen with an adjuvant in mice (Hawiger et al., 2001).

1.8.1 C-type lectin receptors

As mentioned earlier, DCs express a plethora of PRRs on their surface and intracellularly, which are responsible for identifying characteristic pathogenic molecules and self-generated molecules (van Kooyk, 2008). PRRs encompass several receptor families, including NOD-like receptors (NLRs), RIG-like helicases (RLHs), toll-like receptors (TLRs) and C-type lectin receptors (CLRs) (Gnjatic et al., 2010).

There are 15 CLRs identified in humans to date, distributed on DCs and macrophages, with immature DCs expressing CLRs to a greater extent than mature DCs. CLRs are primarily involved in regulating immune system processes such as antigen capture, DC trafficking, and DC-T-cell interactions (Figdor et al., 2002). They form a family of lectins that are able to bind to specific self and non-self-sugar residues, usually in a calcium-dependent manner (Tacken et al., 2007). Once bound, antigens are endocytosed by CLRs and sent to endocytic compartments for MHC class I and II loading. All CLRs share a primary structural homology in their conserved carbohydrate recognition domain (CRD), although the number of domains that a given receptor consists of can vary from a single domain (found in DC-SIGN and Dectin-1) to 8-10 different CRDs (found in MMR, DEC-205) (van Kooyk, 2008). Some CRDs do not bind to calcium (Ca^{2+}) or carbohydrates, and therefore they are referred to as C-type lectin-like domains (CTLDs) (Kanazawa, 2007).

The specificity of glycan ligand recognition by CLRs is not entirely clear, but is thought to be dependent on factors such as amino acid sequence, and carbohydrate branching and multivalency (Geijtenbeek et al., 2004). Some CLRs show specificity for N-linked glycans, O-linked glycans, or monosaccharides (for example - mannose, fucose or galactose), while others recognize more complex sugar moieties (van Kooyk, 2008). Some of the most well-known and commonly investigated CLRs are described in Table 1.1. These are the receptors that have shown the most promise in vaccine-targeting experiments, and each will be explored further in sections to follow. CLRs are divided into two types (I and II) based on the position of the amino (N) terminus of the receptor (Tacken et al., 2006).

1.8.1.1 Type I CLRs

The type I CLRs are also known as the mannose receptor family and are a group of multi-lectin receptors that have their N terminus positioned extracellularly. They include DEC-205, MMR, the phospholipase A2 receptor and Endo-180 (McGreal et al., 2005). DEC-205 and MMR have been targeted in various vaccine studies, although DEC-205 is probably the best characterised.

DEC-205 (also known as CD205) is a multi-lectin protein comprising of protein motifs which allow it to target endocytosed antigen to the early and late endosomes within the cell (Badiee et al., 2007). After binding to a ligand, DEC-205-ligand complex is internalized quite rapidly via coated pits and vesicles. A triad of acidic amino acids in its carboxyl terminus targets DEC-205 to MIICs (Mahnke et al., 2000, Proudfoot et al., 2007). Murine studies revealed that antigens directed to DEC-205 increased antigen presentation efficiency to CD4+ and CD8+ T-cell by over 100-fold (Bonifaz et al., 2004). Moreover, targeting to the murine DEC-205 receptor efficiently targeted antigens to the cross-presentation pathway to elicit broad, effective CD8+ T-cell responses, provided that DC maturation stimuli were utilized in addition to the targeting strategy (Bonifaz et al., 2002). In humans, DEC-205 has been targeted on moDCs, although in these studies there was also a significant enhancement of CD4+ T-cells (Birkholz et al., 2010, Gurer et al., 2008). One of the drawbacks of using DEC-205, is that while DEC-205 has a limited distribution on immune cells in mice, it is generally quite widely distributed in humans, being found on mature DCs (and in low levels on immature DCs), thymus epithelial cells, monocytes, B cells, NK cells and T-cells (Tacken et al., 2007). Thus, despite its effective ability to enhance

T-cell induction when targeted *in vivo* in murine experiments, the specificity of a DEC-205-targeted vaccine in humans could be compromised.

The macrophage mannose receptor (MMR) (also known as CD206) has been suggested to play a role in the detection and clearance of various microorganisms, specifically identifying serum glycoproteins on microbial surfaces (McGreal et al., 2005). DCs and macrophages express a large number of MMRs, which recognize a range of carbohydrates including mannose, fucose, maltose, N-acetylglucosamine and glucose (Proudfoot et al., 2007). MMR endocytoses antigens and directs them into early endosomes which fuse with lysosomes. While MMRs are recycled back to the cell surface after delivery, the endocytosed antigens are degraded into peptides that are appropriate for MHC class II binding (Unger and van Kooyk, 2011). In some circumstances, peptides are also prepared for MHC class I binding, although this occurs to a lesser extent. Studies have shown that targeting antigens to the MMR *in vitro* and *in vivo*, stimulate both CD4+ and CD8+ T-cell immune responses (Burgdorf et al., 2007, McGreal et al., 2005, Ramakrishna et al., 2007). Furthermore, Burgdorf et al (Burgdorf et al., 2006) demonstrated that mice lacking MMR were unable to endocytose soluble antigen, and could not demonstrate antigen-specific CD8+ T-cell activation, implying a high degree of importance is designated to MMR relating to cross presentation in DCs. As with DEC-205, targeting to MMR is most efficacious when a DC maturation stimulus is co-administered.

1.8.1.2 Type II CLRs

The type II CLRs are also known as the asialoglycoprotein receptor family, and have their N terminus positioned intracellularly (Geijtenbeek and Gringhuis, 2009). They include many of the currently identified receptors such as Langerin, macrophage galactose-type C-type lectin (MGL), C-type lectin domain family 9A (CLEC9A), and DC-SIGN amongst others. These receptors are able to recognize various carbohydrate moieties, in addition to binding to pathogenic viruses such as H5N1 influenza virus and HIV-1 (Su et al., 2003, Piguet and Blauvelt, 2002). Of all the receptors being investigated for vaccine targeting, Langerin, DC-SIGN and CLEC9A are some of the most specific targets, in that they are found almost exclusively on DCs/LCs, and are thus promising vaccine options.

Langerin (also known as CD207) is a CLR-type II receptor which is a Birbeck-granule associated protein primarily found on LCs that reside in the epidermis, and is located in an endosomal recycling compartment within human LCs (Piguet and Blauvelt, 2002). Langerin binds to mannose, n-acetylglucosamine, fucose and sulphated sugars (Idoyaga et al., 2008). Despite the limited localisation of langerin on LCs, it has the potential to target antigens to the MHC class-I pathway and has shown the ability to induce cross-priming of CD8+ T-cells (Yan, 2004). *In vivo* studies revealed that anti-langerin chimeric proteins were able to induce antigen-specific CD4+ and CD8+ T cell responses when administered intravenously (Idoyaga et al., 2008). Interestingly, Flacher et al (Flacher et al., 2010) recently showed that when langerin and DEC-205 were individually targeted with antigen-antibody conjugates on skin-derived LCs *in vivo*, DEC-205 targeting elicited antigen-specific CD8+ T-cells, but langerin-targeting demonstrated poor T-cell proliferation. However, similar targeting to $CD8\alpha^+$ DCs induced CD8+ T-cell proliferation after targeting both receptors (Idoyaga et al., 2008). This indicates that both the DC subset targeted and the targeted receptor contribute significantly to determining the type of immune responses elicited (Unger and van Kooyk, 2011).

Unlike langerin, DC-SIGN (also known as CD209) is expressed on several subsets. It was initially found to interact with intercellular adhesion molecule-3 (ICAM-3), assisting in DC-T-cell interactions to initiate primary immune responses (Proudfoot et al., 2007). It also interacts with ICAM-2 on vascular endothelial cells, to mediate DC migration (McGreal et al., 2005). DC-SIGN is mainly located on immature DCs, macrophages and karyocytes, and is one of a few CLRs that are also involved in initiating signalling cascades after binding ligands (Tacken et al., 2007). The binding of DC-SIGN to its ligand results in the activation of certain kinases that regulate TLR-NF-κB interaction, specifically related to TLR4 (Geijtenbeek and Gringhuis, 2009). In this way, DC-SIGN and TLR4 collaborate to elicit amplified immune responses. As with other CLRs, DC-SIGN is also able to successfully direct foreign antigens to late endosomal/lysosomal compartments for efficient processing and presentation to T-cells, specifically CD4+ T-cells (Engering et al., 2002), and in some cases naïve and memory CD8+ T-cells too (Tacken et al., 2005). It is interesting to note that several viruses including HIV-1, Hepatitis C virus (HCV) and Dengue virus, use DC-SIGN to prevent being processed via the normal lysosomal degradation pathways, and in this way escape detection (McGreal et al., 2005).

In terms of targeting, a few *in vivo* studies have illustrated the augmentation of T-cell responses induced by directing antigen to DC-SIGN (Kretz-Rommel et al., 2007, Tacken et al., 2005). Singh et al (Singh et al., 2009) showed that DC-SIGN-antigen targeting in humanized mice can result in enhanced cross-presentation and the induction of 10-fold higher CTL and CD4+ T-cell responses, when compared to untargeted antigen. That being said, DC-SIGN is difficult to study in *in vivo* experiments due to the dissimilar structure of its homologue in mice. Thus, even with the transgenic DC-SIGN mouse models, it is still of interest to do more extensive *in vitro* human research to assess this receptor's potential use as a vaccine target.

One of the most specific DC receptors is CLEC9A (also known as dendritic cell NK lectin group receptor-1 (DNGR-1)), which is only expressed at high levels on the recently identified mDC subset, BDCA3+ DCs (Poulin et al., 2010). Its specificity to this subset, makes it a good targeting candidate, especially given the superior ability of these DCs to cross present antigen (Unger and van Kooyk, 2011). Further to this, the reason behind the favoured cross presentation by these cells can potentially be attributed to CLEC9A, which is supported by data that showed CLEC9A promoted cross presentation of antigens and potent CD8+ T-cell induction in the presence of an adjuvant when targeted *in vivo* (Caminschi et al., 2008). Without adjuvant, CD4+ T-cells and antibody production was prominently induced.

1.8.1.3 The DC immunoreceptor (DCIR) family

A new family was recently described, distinguished from the other two CLR groups based on the members sharing mutual functional features of pattern-recognition via the CRDs, and signalling through immunotyrosine inhibitory motifs (ITIMs) (Kanazawa, 2007). These receptors are CTLDs because their CRDs do not contain a Ca^{2+} dependent component. The family consists of DCIR-1, Dectin-1 and Dectin-2, BDCA-2, CLEC-1 and CLEC-2. DCIR-1 and Dectin-1 have been explored to a greater extent than the other receptors for vaccine targeting purposes, although most of the research into targeting these receptors is still fairly recent.

DCIR1 (CLEC4A) ligands have yet to be identified, but DCIR1 is expressed on DCs, monocytes, macrophages, LCs and dDCs (Kanazawa, 2007). *In vitro*, it seems to be present more prominently on CD14+ cell-derived dermal-type DCs than in CD1a+ cell-derived LC-type DCs.

Klechevsky et al (Klechevsky et al., 2010) recently demonstrated the potency of targeting DCIR-1, where a low dose of anti-DCIR-antigen induced antigen-specific naïve and memory CD8+ T-cells by all human DC subsets including *ex vivo*–generated DCs, skin-isolated LCs, BMDCs and pDCs.

Dectin-1 has a single CRD, displaying similarity to the CLRs expressed by NK cells that bind MHC class I counter-receptors (McGreal et al., 2005). It was initially believed to be a DC-specific molecule with a T-cell co-stimulatory capacity, but has recently been identified on monocytes, macrophages and neutrophils (Kanazawa, 2007). Dectin-1 recognizes β-1,3- and β-1,6-linked glucans, which are commonly found in fungal cell walls and mycobacteria components. It collaborates directly with TLR2 to mediate responses to the ligands it binds to, by interaction of its immunotyrosine activatory motif (ITAM) with the TLR2 signalling pathway (McGreal et al., 2005). It is also involved in activating certain signalling cascades that lead to secretion of cytokines such as IL-10, IL-6, TNF-α and IL-23, resulting in the activation of Th17 cell responses. Additionally, data has shown that when antigen is directly targeted to Dectin-1, it is able to elicit robust antigen-specific CD8+ T-cell responses *in vitro* (Ni et al., 2010).

Remarkably, both DCIR-1 and Dectin-1 are downregulated in the presence of LPS, indicating it is a poor choice of adjuvant for a vaccine strategy targeting these receptors (Bates et al., 1999, Brown, 2006).

1.8.1.4 Other targeted receptors

Non-CLRs like the MHC class receptors, scavenger receptors (SRs) and Fc receptors (FcRs) have also been investigated in terms of their potential as vaccine targets. SRs are primarily present on macrophages and can internalize endotoxins, oxidized low-density lipoproteins, and other negatively charged proteins (Proudfoot et al., 2007). A few of these receptors have demonstrated an ability to heighten immune responses against antigens, when they are specifically targeted. The scavenger receptor, LOX-1, has been identified as the recognition receptor for heat-shock proteins (HSPs), chaperone proteins that are well known for their ability to prominently initiate CTL-specific responses, specifically when they are derived from tumours. (Proudfoot et al., 2007). Thus, when Delneste et al (Delneste et al., 2002) immunized mice with

anti-LOX-OVA conjugates, they were able to induce strong CD8+ T-cell responses against the antigen and the mice were also protected from a fatal OVA+ tumour challenge. Similarly, FcRs, which are involved in innate and adaptive immune responses through the binding and internalization of pathogens by APCs, have also shown some potential as targeted receptors in their ability to enhance cross presentation (Kawamura et al., 2006, Wallace et al., 2001, Proudfoot et al., 2007).

Table 1.1 – Summary of well-characterised CLRs. Descriptions are provided of preferable ligands, expression, and antigen-targeting pathways. Level of presentation of bound ligands through the respective pathways in humans are depicted using +, where +++ = high; + = low and ? = unknown/requires further investigation. Adapted from (Burgdorf and Kurts, 2008, Masato Kato et al., 2006, McGreal et al., 2005)

Receptor	Family/ CLR Type	Ligand	Expression	Targeted location	Cross presentation	MHC-class II presentation
DEC-205 (CD205)	I	Mannosylated ligands	mDC, monocytes, moDCs B cells, NK cells, pDCs, T-cells	Late endosomes/ lysosomes	+++	+++
MMR (CD206)	I	Mannose, fucose, N-acetyl glucosamine and sulphated sugars	Macrophages, moDCs, dDCs, Endothelium cells	Early endosomes	++	++
DC-SIGN (CD209)	II	HIV and other pathogens; Mannose	DCs, macrophages	Lysosomes	+?	+++
Langerin (CD207)	II	Mannose, fucose, N-acetylglucosamine	LCs	Early endosomes	++	?
CLEC9A	II	Necrotic cell matter	BDCA-3+ mDCs	Early endosomes	++?	?
DCIR-1 (CLEC-4A)	DCIR	Unknown	Macrophages, DCs	Unknown	++	?
Dectin-1	DCIR	β-1,3- and β-1,6-linked glucans	Macrophages, DCs, T cells	Unknown	?	++

1.9 Use of adjuvants with DC vaccinations

Adjuvants were traditionally included in vaccine preparations because of their ability to enhance adaptive immune responses (Coffman et al., 2010). It has since been established that adjuvants provide even greater benefits to vaccine preparations in that they assist in improving the longevity of an immune response, enhance the responses in poorly responsive populations (thereby reducing the amount of a vaccine antigen required), and they can also influence the type of adaptive immune response elicited (Coffman et al., 2010, Duthie et al., 2011). Several types of adjuvants have been investigated in the past, the most successful kinds consisting of one or more components that were able to induce an innate immune response (Schwarz et al., 2003). Consequently, ligands for TLRs, one of the largest receptor families related to the innate immune system, have emerged as some of the most favourable adjuvant candidates due to their ability to initiate innate and adaptive immune responses.

1.9.1 Toll-like receptor (TLR) family

The most well characterised PRRs are the highly conserved TLR super-family, which function as the main sensors of the innate immune system (Zanoni and Granucci, 2010). This family of germ-line encoded receptors are homologues to the Toll protein that was first discovered in the fly *Drosophila*, and found to play a role in protection against fungal and bacterial pathogens (Anderson et al., 1985). TLRs in humans have a conserved membrane spanning molecules containing an ectodomain of leucine-rich repeats, a transmembrane domain and an intracellular toll-IL1-receptor (TIR) domain (Gnjatic et al., 2010). There are currently 13 TLRs that have been identified in mammals, ten of which are found in humans (Zanoni and Granucci, 2010). TLRs are distributed throughout the body, being found on DCs, macrophages, T-cells, B cells, NK cells, mast cells, and some endothelial and epithelial cells (Duthie et al., 2011). They are able to detect intra- and extracellular foreign molecules, and once activated, they initiate a cascade of signalling pathways that lead to the induction of an inflammatory response, and if need be, an adaptive immune response.

There are a few signalling pathways that can be activated by TLRs, each using a different combinations of adaptors and transcription factors to induce a complex array of genes, and trigger the appropriate responses. TLRs 2, 4, 5, 7, 8 and 9 make use of the IL-1R-associated kinase (IRAK) signalling cascade, which is controlled by the myeloid differentiation primary response gene 88 (MyD88) signalling adapter and activates transcription factors, nuclear factor-κB (NF-κB), activation protein-1 (AP-1), as well as some of the interferon-regulatory factor (IRF) family (O'Neill and Bowie, 2007). TLR2 and TLR4 also engage a second, bridging adapter called MyD88-adaptor-like protein (MAL also known as TIRAP), to effectively recruit MyD88 and initiate the cascade (O'Neill and Bowie, 2007). TLR3 utilises an alternative signalling pathway to activate the above transcription factors, making use of the TIR-domain containing adaptor-inducing IFN-beta (TRIF) and TRIF-related adaptor molecule (TRAM) adaptors, instead of MyD88. TLR4 is unique in that it can trigger signalling cascades through both the MyD88/MAL and TRIF/TRAM pathways, although it is unclear as to whether it has a preference, or if both can be triggered simultaneously.

TLR activation on DCs leads to cell maturation, co-stimulatory molecule upregulation, enhanced antigen uptake and presentation, and cytokine production (Dabbagh and Lewis, 2003). Given their role as primary sensors for the immune system, it is not surprising that DCs express all TLRs collectively between their subsets. In particular, mDCs and dDCs express all TLRs except TLR9, moDCs express TLRs 1-8, pDCs express TLR1, 6, 7 and 9, and LCs express TLRs 1-6 (Duthie et al., 2011). Their complementing TLR repertoires allow them to recognize distinct groups of foreign molecules individually, while they are able to recognize a plethora of PAMPs collectively. Several studies have shown the ability of TLR ligands to potentially affect the type of immune responses induced (Steinhagen et al., 2011, Ahonen et al., 2004, Ramakrishna et al., 2007), in addition to also demonstrating an ability to influence T-cell migration (Ueno et al., 2010).

TLRs are also integrally involved in the initiation and sustainability of immune responses, being involved in several stages of the induction and regulatory processes. Blander et al (Blander and Medzhitov, 2006) recently showed that without the correct TLR signal, MHC class molecules are not receptive to forming peptide-MHC complexes. Furthermore, TLR signalling pathways

are responsible for the induction of transcription of cytokines (IL-12, IL-18, type I IFNs) and co-stimulatory molecules, as well as regulation of the phagosome–lysosome endocytic pathway (Blander, 2008).

In general, most TLR agonists have been shown to favour Th1-type responses, although there have been exceptions to this, and some TLR agonists are more influential than others in this respect (Duthie et al., 2011). In particular, research has demonstrated a skewing of adaptive responses towards Th1 in the presence of ligands to TLR 3, 4, 7/8 and 9 (Duthie et al., 2011). These TLRs are able to initiate the activation of transcription factors that mainly regulate type-I IFN expression, and therefore promote the production of type I interferons (IFN-α and IFN-β), in addition to upregulating co-stimulatory molecules on DCs, and stimulating secretion of certain pro-inflammatory cytokines (TNF and IL-6) (Zanoni and Granucci, 2010).

TLR3 is an intracellular receptor located in endosomal compartments and is able to detect the presence of double stranded RNA (dsRNA) (a prominent viral entity) within the cell (Schulz et al., 2005). Both mDCs and pDCs express TLR3, in addition to mast cells, NK cells and epithelial cells (Gnjatic et al., 2010). TLR3 favours Th1-type responses in order to combat viral infections through the induction of IL-12 and type-I IFN production by DCs (Jongbloed et al., 2010, Duthie et al., 2011). For adjuvant purposes, a synthetic dsRNA complex known as polyribosinic:polyribocytidic acid (Poly I:C) has been used to trigger TLR3 activation, resulting in the maturation of DC *in vivo* and *in vitro* (Verdijk et al., 1999).

Another endogenous receptor, TLR9, is localized within endosomal compartments, and its distribution is somewhat restricted, mainly found on B cells, NK cells, and pDCs in humans (Duthie et al., 2011). TLR9 detects unmethylated CpG motifs on double-stranded DNA (dsDNA), and recognition of CpG DNA leads to the maturation and proliferation of T-cells, B cells and NK cells, in addition to production of Th1 cytokines (IL-1, IL-6, IFN-γ, IL-12) (Steinhagen et al., 2011). Synthetic nucleotides containing unmethylated CpG oligodinucleotide (CpG-ODN) are able to bind TLR9 and activate it in a similar way as unmethylated double-stranded DNA does, allowing their common use for adjuvant purposes in murine studies.

TLR4 is located on the surface of many cell types (DC, T-cells, neutrophils, monocytes, eosinophils, basophils, and B cells), and is able to detect bacterial lipopolysaccharide (LPS), prompting one of two possible signalling cascades as mentioned earlier (Duthie et al., 2011). As a consequence of its vast distribution, and access to two signalling pathways, TLR4 is thought to be involved in the control of various infections including *Neisseria meningitis*, *Escherichia coli*, *Klebsiella pneumoniae*, *Streptococcus pneumoniae*, and *Mycobacterium tuberculosis* (Mazzoni and Segal, 2004). Remarkably, LPS is able to elicit both Th1 and Th2 responses, based on dose and timing of LPS exposure (Eisenbarth et al., 2002). Low doses of LPS elicited an allergen-specific Th2 response in inoculated mice, while high doses induced a Th1 response with activation of neutrophils and IgG2a production. LPS in its natural form is toxic to humans; however a safe and effective derivative called Monophosphoryl lipid A (MPL) is commonly used as an adjuvant. It is currently being used as an adjuvant for the Hepatitis B virus (HBV) and human papilloma virus (HPV) licenced vaccines, with some success (Casella and Mitchell, 2008).

TLR7 and TLR8 are endogenous receptors, mainly found in endosomal compartments of mDCs, neutrophils, monocytes, eosinophils (TLR7 only), T cells (TLR8 only), B cells (TLR7 only), pDCs (TLR7 only), and endothelial cells (Duthie et al., 2011). TLR7 and TLR8 recognize single-stranded RNA segments enriched for GU or poly-U sequences, or synthetic molecules from the family of imidazoquinolines (i.e. Imiquimod (3M) and Resiquimod (R848). Imidazoquinolines are preferentially used in vaccine preparations to induce TLR7/8 activation due to the instability of RNA. They efficiently elicit Type I IFN production, and have also demonstrated an ability to enhance cross presentation in DCs (Le Bon et al., 2003).

Although not common, Th2 responses are sometime favoured by TLR stimulation, based on a number of factors. The TLR2 family (TLR 1, 2 and 6) are most prone to directing responses in this way. TLR2 can be found on the surface of many cell types including neutrophils, macrophages, monocytes, basophils, T cells, B cells, NK cells, and DCs (Duthie et al., 2011). While most TLRs form functional homodimers, TLR2 is able to form heterodimers with both TLR1 and TLR6, which allows for a unique specificity (Ozinsky et al., 2000). It has also been suggested that TLR10 dimerises with TLR2, given its similarity in sequence and structure to

TLR1, although not much is known about TLR10 at this stage (Guan et al., 2010). The TLR2 family recognise peptidoglycan (PGN) from the cell walls of Gram-positive bacteria, bacterial glycolipids, lipoproteins, amongst other lipid-related structures (Duthie et al., 2011). This allows them to participate in the combat of several bacterial infections including *Mycobacterium tuberculosis* and *Staphylococcus aureus*. TLR2/TLR1 agonists are able to induce production of high antigen-specific antibody titres and strong T-cell priming, as demonstrated by administration of tetanus toxoid with derivatives of polysaccharide from Group B Streptococcus (Gallorini et al., 2009).

The only TLR that detects a protein-only based ligand is TLR5, expressed on the plasma membrane of neutrophils, monocytes, T cells, and endothelial cells (Duthie et al., 2011). TLR 5 recognizes the conserved region of bacterial flagellin, and is able to induce mixed Th responses. Although TLR 5 also induces the MyD88 signalling pathway, it has been shown to elicit a local inflammatory response in skin, followed by a humoral response (Applequist et al., 2005).

Currently, there are other adjuvants that have also demonstrated potential for use in clinical settings. One of the more promising options includes CD40 ligand (CD40L). CD40 is a co-stimulatory molecule, mainly found on DCs, B cells, macrophages, endothelial cells and keratinocytes (Tacken et al., 2006). DC interaction with CD40L or anti-CD40 antibody leads to the up-regulation of co-stimulatory molecules and secretion of IL-12, without the need for additional stimuli (Mazouz, 2002, Miconnet, 2008). Studies have also shown that CD8+ T-cells can be activated independently of Th cells, if in the presence of CD40L, suggesting that CD40-CD40L interaction is an essential process for CD8+ T-cell enhancement. In addition, CD40 has been shown to favour cross presentation of antigens, demonstrating a preference to MHC class I-antigen complex formation (Mazouz, 2002). In view of this, recent literature has highlighted the potential benefits of including CD40L in DC-targeted vaccines to induce strong cellular responses, given its role in both DC activation and memory T-cell reactivation (Liu et al., 2008, Miconnet, 2008, Sato, 2004). As an example, Tillman et al (Tillman et al., 2000) showed that re-targeting of adenoviral vectors to CD40 resulted in DC transduction via CD40 to induce significant CD8+ T-cell responses.

1.9.2 Enhancing efficacy of adjuvants

A number of methods have been designed to further enhance the ability of TLR agonists to improve the induction of T-cell responses. Several key studies have illustrated the importance of TLR activation in the same DC presenting the antigen as being critical for CD4+ T cell activation and Th cell differentiation (Blander and Medzhitov, 2006, Reis e Sousa, 2004). Thus, one way to improve the capability of TLR agonists is to directly link the antigen of interest to the agonist so that they are able to access CLRs and TLRs on the same cell, and thereby improve efficacy of immune response induction. To illustrate this, the portion of bacterial flagellin containing the TLR5-binding region was expressed in a fusion protein with selected vaccine antigens which were delivered to APCs, and yielded immune responses (specifically antibody responses) superior to the simple mixing of antigen and agonist (Huleatt et al., 2007).

Combining certain TLR agonists could also potentially enhance the T-cell responses elicited, primarily because there is a synergy between certain TLRs, which trigger different signalling pathways that complement each other. A recent example of this was demonstrated by Napolitani et al (Napolitani et al., 2005), who showed that combining the use of TLR3 or TLR4 agonists with a TLR7/8 agonist, strongly enhanced IL-12 and IL-23 production by DCs, in addition to encouraging a potent Th1 response. The order of administration and time frame between the administrations of the TLR agonists was also deemed important, where TLR3 had to be provided before TLR7/8 and within a 4-hour window period, in order to establish a synergistic adjuvant effect. It is hypothesised that this is related to the activation of different kinases downstream, although this requires verification. Similar studies have re-iterated the benefit of synergistic TLR agonists, including studies where mice only demonstrated strong, effective T-cell responses against leishmaniasis disease when the *Leishmania* poly-protein vaccine candidate was administered with a TLR4-TLR9 fusion agonist, but not when it was administered with the individual agonists (Raman et al., 2010). In relation to these TLR synergy studies, research has also shown that the inclusion of CD40L in addition to a TLR agonist is even more promising in terms of augmenting T-cell responses (Napolitani et al., 2005) In particular, one study showed a 10–20-fold greater expansion of antigen-specific CD8+ T-cells using a TLR agonist and CD40L than using either agonist alone (Ahonen et al., 2004).

The use of CD40L and TLRs highlights the interaction of TLRs with other receptors, and their involvement in establishing adaptive immune responses. A number of studies have suggested that cross-talk between CLRs and TLRs is important for facilitating the initiation and maintenance of an adaptive immune response, suggesting that CLRs may also modulate immune reactions (Gantner et al., 2003, van Kooyk, 2008). Ramakrishna et al (Ramakrishna et al., 2007) performed an *in vitro* experiment where he targeted antigen to the MMR, and used poly I:C and R-848 as agonists. They were able to elicit good tumour antigen-specific helper and cytolytic T cells, agreeing with the premise that the augmentation of an immune response is more effective when more than one set of PRRs is involved.

1.9.3 Tolerance induction by DC-targeting

It has become increasingly clear that although not all DC targeting strategies require an adjuvant to activate DCs and elicit a robust T-cell response, the majority of them do. The absence of an adjuvant in receptor-targeting strategies demonstrates the induction of tolerance, as was depicted in the early research of Bonifaz et al (Bonifaz et al., 2002), where targeting DEC-205 in mice without an appropriate adjuvant resulted in enhanced MHC class I antigen presentation on steady-state DCs, but poor T-cell proliferation, and tolerance to the stimulating antigen. Although tolerance is not useful for vaccine strategies, its induction can be exploited in situations where autoimmune reactions occur. A type-1 Diabetes-associated peptide antigen was targeted to DEC-205 on CD8α+ DCs in disease-prone mice, and appeared to delay disease progression by inducing tolerance to the peptide and deleting reactive CD8+ T-cells (Mukhopadhaya et al., 2008). This and other similar studies demonstrate the versatility and efficacy of targeting DC receptors to influence immunological reactions. Nevertheless, for vaccines that aim to induce CD8+ T-cell responses, a suitable adjuvant is an essential component to successfully enhance cellular immune responses against a targeted antigen, and elicit sustained immunity.

1.10 The importance of a cell-mediated immune response against HIV-1

Cell-mediated immunity consists of several components that allow it to detect and combat intracellular pathogens such as viruses. As stated, cellular immunity against viral infections mostly involves the activation of CD4+ and CD8+ T-cells, which is why a number of viral vaccine strategies such as those against Human immunodeficiency virus-1 (HIV-1) and Hepatitis C virus (HCV) have identified the induction of CTL responses as a correlate of protection, and have aimed to induce stronger cellular responses against vaccine antigens (Kim et al., 2010, Rollier et al., 2005). This allows the vaccine to establish potent memory responses that will potentially eliminate the virus if the immune system is ever exposed to it.

There is an abundance of evidence to suggest that an effective, strong cellular immune response against HIV-1 can override the negative impact the virus inflicts, despite its crippling effect on CD4+ T-cell expansion (Nabel, 2002, Luciw, 1996). HIV-1-specific cellular responses are also able to decrease viral load during acute and primary HIV infections (Koup et al., 1994, Borrow et al., 1997). T_h responses play a key role in facilitating B-cell and CD8+ T cell stimulation, and maintaining long-term responses (Sadagopal et al., 2005, Proudfoot et al., 2007). Furthermore, the CTL response is mainly responsible for controlling the viral infection and suppressing viraemia in HIV-infected individuals (Pollack et al., 1997). Studies have shown that “elite controllers” (HIV-infected individuals who naturally control viral load for many years) generally display a more pronounced Gag-specific CD8+ T-cell response (Kiepiela et al., 2007), and have preserved HIV-1 specific CD4+ T cells and CD8+ T cells, all of which have been associated with control of viraemia (Sadagopal et al., 2005, Pantaleo and Koup, 2004).

In view of the importance of CD8+ T-cell responses in combating HIV-1, numerous vaccine approaches have explored ways to augment cellular responses against HIV-1 in order to control, if not eliminate the virus. Many studies have focussed on utilizing Gag-based antigens because the *gag* gene is highly conserved in the viral genome, and Gag proteins possess many CTL epitopes (Doan et al., 2005, Nabel, 2002). In addition, the inclusion of accessory and regulatory HIV-1 proteins (such as Tat and Nef) in vaccines has demonstrated the ability to improve the magnitude and breadth of CTL responses (Pillay et al., 2010, Hel et al., 2002).

Strategic approaches such as prime-boost vaccine regimens have also emerged as successful means to enhance cellular responses. These regimens involve an initial prime of the immune response against one or more target antigens using one vector (usually DNA-based), and then a boost inoculation with a second vector (viral vector- or protein-based) to enhance the specificity of the initial response (Woodland, 2004). While this approach has been very effective in animal studies, the use of viral vectors raises safety concerns in addition to issues of pre-existing immunity (Duerr et al., 2006). These problems became more prominent after the disappointing results of the STEP HIV vaccine clinical trial in 2008, where vaccinating individuals with three recombinant, replication-defective serotype-5 adenovirus vectors containing the *gag*, *pol*, and *nef* genes, failed to elicit protection against HIV-1 infection, in addition to causing some subjects to become more susceptible to infection (Buchbinder et al., 2008, Sekaly, 2008). Although it is not entirely clear, research suggested that use of adenoviral vectors may have contributed to the enhanced susceptibility (Benlahrech et al., 2009).

Thus, vaccine approaches that avoid the use of viral vectors are currently being favoured. Novel approaches such as the targeting of vaccine antigens to DCs have shown great promise, and have been described to effectively stimulate the induction of CD8+ T-cells. Several mouse studies have demonstrated the efficacy of this strategy, and recently human studies too. Bozzacco et al (Bozzacco et al., 2007) targeted the DEC-205 receptor on DCs of HIV-1 infected individuals with an HIV-1 Gag antigen, and showed the induction of antigen-specific CD8+ T-cell proliferation and high IFN-γ production. In view of the promising nature of this approach, targeting vaccine components to receptors on DCs are being explored to a greater extent.

1.11 Choice of model antigens

Model antigens are typically characterised as antigens that are highly immunogenic, able to induce strong immune responses. This makes them useful for experimental studies exploring how the immune system functions. Previous research has employed a number of different foreign antigens as models for immunogenicity studies. They are able to elicit strong immune responses in the general population, and include Concanavalin A (a lectin protein and plant

mitogen) (Currier et al., 2010), keyhole limpet haemocyanin (an oxygen-carrying metalloprotein) (Tacken et al., 2005), and influenza haemoggluttin and neuraminadase (Koshiol et al., 2006). The most commonly used antigen in mouse studies is ovalbumin, while in human studies, tetanus toxoid, influenza, and CMV antigens are favoured. For our study, we focussed on using the CMV antigen, pp65, to study secondary immune responses and a tumour antigen, Melan-A, to study primary immune responses.

1.11.1 Cytomegalovirus pp65

Cytomegalovirus (CMV) is a 230 kb double-stranded DNA human herpesvirus (also known as human herpesvirus-5) consisting of more than 200 proteins (Harari et al., 2004). These proteins include structural components that make up the CMV virion (viral tegument positioned between the nucleocapsid and viral envelope), as well as regulatory proteins associated with the progression of CMV infection (Rasmussen, 1999). The viral life cycle is approximately 48-72 hours, in which time three overlapping phases (immediate early, early, and late) occur.

Healthy, immunocompetent individuals appear to be unaffected by CMV infection, demonstrating no adverse symptoms however, CMV infections cause severe complications and sometimes morbidity in immunocompromised patients and congenitally infected newborns (Spaete et al., 1994, Harari et al., 2004). *In vivo*, CMV cell tropism during acute infection suggests its distribution is wide spread, with detection of the virus in epithelial cells, fibroblasts, endothelial cells, smooth muscle cells, hepatocytes, trophoblasts, myeloid DCs and macrophages in the blood (Jahn et al., 1999). Like many herpesviruses, CMV has an ability to remain latent in certain cells, particularly CD33+ cells, which are precursors of myeloid DCs (Mendelson et al., 1996). Evidence suggests that myeloid DCs and macrophages in healthy HCMV-seropositive individuals are therefore important reservoirs of latent CMV (Abate et al., 2004).

Of the many CMV proteins, two have proven to be highly immunogenic, comprising of a number of immunodominant CTL epitopes. These proteins are the immediate early 1 (IE1) and the lower matrix protein, pp65 (encoded for by the UL83 gene). In particular, 14 CTL epitopes have been identified in pp65 (Kondo et al., 2004). Pp65 is a major constituent of the CMV virion

and CMV dense bodies (non-infectious particles generated during replication), consisting of 18 % of the viral mass (Abate et al., 2004, Bennekov et al., 2004). It localizes predominantly to the nucleus after virus entry and accumulates in the nucleus and cytoplasm as CMV matures. The role of pp65 in the viral cycle is related to preventing the activation of the transcription factor, IRF-3, during the early phase of infection. This leads to dampening of the host antiviral response, specifically interferon cytokine production (Abate et al., 2004). Despite this negative effect on the anti-CMV immune response, pp65 is able to generate humoral and cellular (CD4+ and CD8+ T-cell) immune responses, with high levels of pp65-specific CTLs being maintained for up to 20 months. In addition, the expanded IFN-γ secreting virus-specific CD4+ T cells are primarily effector memory cells that demonstrate longevity (Harari et al., 2004). Given the prominent induction of pp65-specific memory T-cell responses from seropositive donors, pp65 has proven to be a good model antigen in previous research (Yuan et al., 2006).

1.11.2 Melan-A antigen

Melan-A or melanoma antigen recognized by T cells (MART-1) is an 18-kD transmembrane protein of unknown function that is expressed in primary and metastatic melanomas (Romero et al., 2002, Pittet et al., 2002). It is a self-antigen which gained recognition because of the immunogenicity of its immunodominant peptide, (E)AAGIGILTV (Butterfield et al., 2008). Most antigens that the immune system is newly exposed to, generate low T-cell responses which are difficult to detect and measure. This makes the study of primary immune responses complicated, with most data relying on allogeneic immune interactions. This is not the case for MART-1 though, because HLA-A*02:01 positive individuals express an unusually high frequency of naïve CD8+ T-cells (1:2500) that recognise the immunodominant epitope of this antigen (Pittet et al., 1999). As many as 10^8 MART-1-specific $CD8^+$ naïve T cells have been detected per A*02:01+ individual, which is approximately the average pool size of single epitope-specific memory CD8+ T cells. Thus, the use of MART-1 as a model antigen of choice, allows the unique autologous analysis of primary immune responses (Butterfield et al., 2008).

1.12 Hypothesis and objectives

HIV protein vaccines that target the cross-presentation pathway to induce effective CD8+ T-cell responses may avoid concerns with increased susceptibility to infection associated with viral vector vaccines. DCs are able to stimulate an antigen-specific CD8+ T-cell response by cross-presentation but it is currently unknown which endocytic receptors on different DCs subsets would best facilitate transportation to the cross-presentation pathway. Thus, the hypothesis of this study is that different DC surface receptors vary in their ability to target exogenous antigens to the MHC-class I pathway, and thus elicit CTL responses. Additionally, we hypothesise that the induced CTL responses can vary greatly depending on factors such as the nature of the antigen, DC subset targeted, method by which DC receptor is targeted, and use of TLR agonist.

Thus, this study aims to use *in vitro* experiments to investigate the magnitude and functional capacity of CD8+ T-cell responses induced by directing antigen to specific DC receptors from different DC subsets, with the use of an optimal TLR agonist. Specific aims include:

(i) To produce large quantities of model antigens (CMV pp65 and MART-1) and streptavidin-fusion proteins, for use in *in vitro* experiments

(ii) To briefly characterise the immunogenicity of these antigens so to confirm their viability in *in vitro* experiments

(iii) To investigate which TLR agonist would be most suitable in DC targeting experiments in terms of its ability to enhance CD8+ T-cell responses

(iv) To determine which endocytic receptors on immature human DCs would most efficiently direct antigen of interest towards the cross-presentation pathway (specifically targeting DEC-205, MMR, DC-SIGN, and/or CD1a) using different targeting strategies

(v) To compare the elicited CD8+ T-cell responses (proliferation and cytokines) after targeting antigens to two different human DC subsets, namely monocyte-derived DCs and blood BDCA1+ (CD1c+) DCs

Chapter 2

Construction of model antigen vectors and evaluation of antigen expression

2.1 Background and Aims

2.1.1 Model antigens

The model antigen of choice in mouse studies is OVA because of the ease of availability of transgenic mice expressing high levels of the OVA-specific T-cell receptors (i.e. OT-1, OT-2 and DO11.10 mice), thus allowing the generation of large, detectable quantities of antigen-specific T-cells (Singh et al., 2009, Burgdorf et al., 2006). As mentioned in Chapter 1, the present *in vitro* human study makes use of CMV pp65 protein and MART-1 protein as model antigens based on their high immunogenicity in specific human populations.

CMV pp65 has been widely used for this purpose in the past due to its highly immunogenic nature. As an example, Yuan et al (Yuan et al., 2006) used pp65 as a model antigen to demonstrate that LCs transduced with a retroviral vector encoding a full-length antigen could stimulate strong CTL responses directed against multiple epitopes compared to using one immunogenic peptide epitope. Similarly, the second selected model antigen, MART-1, also demonstrates an ability to stimulate CD8+ T-cell expansion in A*02:01 individuals. Amongst others, Schumacher et al (Schumacher et al., 2004) illustrated this well when they induced strong CTL-specific responses for the melanoma-associated MART-1 epitope, and further enhanced these responses using reconstituted influenza virosomes as an adjuvant.

In addition to the above two model antigens, this study also explores the use of streptavidin-fused proteins as stimulatory antigens, where a core-streptavidin unit is genetically fused to both pp65 and MART-1. These fusion proteins contribute to a novel DC targeting strategy (see Chapter 5), which is a potentially more flexible method for directing antigens towards DC

endocytic receptors, compared to using the model antigens alone. Streptavidin is a 52-kD tetrameric protein produced by *Streptomyces avidini* (Gonzalez et al., 1997). It is a very robust protein, demonstrating stability at high temperatures and extreme pH, and is particularly useful in molecular biology applications because of its high affinity for biotin ($K_D = 10^{-15}$ M). Many studies have highlighted the versatility of streptavidin-fusion proteins in terms of directing biotinylated molecules to specific locations *in vitro* and *in vivo*. Recently, Fahrer et al (Fahrer et al., 2010) fused streptavidin to a cytosol-bound protein component which allowed the transportation of biotinylated molecules into the cytosol of cancer cells, thereby demonstrating a simple and effective means to transport drugs or vaccines into cancer cells. Consequently, the use of streptavidin-fusion proteins as a means to target DC receptors provides an interesting approach to effectively direct antigens to the selected receptors.

2.1.2 Mammalian expression systems

There are several types of expression systems available for the production of recombinant proteins, many of which are bacterial-, insect cell- or plant cell-based. While each has its advantages, mammalian cell expression approaches provide a production platform which is able to generate complex recombinant molecules that are processed and folded in the correct manner, and are not contaminated by toxic cellular components of the host expression system (a frequent occurrence in prokaryotic expression systems) (Geisse et al., 1996, Demain and Vaishnav, 2009).

Two mammalian expression systems were explored in this chapter, namely a stably-expressing cell line, and an adenovirus expression system (AES). The first system evaluated the generation of stably-expressing cell lines using Chinese hamster ovary (CHO) and human embryonic kidney adhesive (HEK293A) cells. This method was selected because it involved a relatively straight-forward procedure for protein production, and offered the opportunity to obtain a continuous source of the recombinant proteins, once the system was established and optimized. An AES was also assessed, given that several heterologous proteins have been highly expressed in adenovirus-HEK293 expression systems, with recombinant protein accounting for as much as 4-5 % of the total cellular proteins in cells (Wurm and Bernard, 1999). Given the advantages of both systems,

each was critically evaluated in order to determine the optimal system for the expression of the chosen model antigens.

2.1.3 Aims of chapter

(i) To design and produce expression vectors carrying the genes of the selected model antigens.
(ii) To design and produce expression vectors carrying novel fusion genes, which express the model antigens attached to a core streptavidin component.
(iii) To evaluate two mammalian expression systems in terms of antigen production, (assessing both quality and quantity), allowing the identification of the optimal system for large scale recombinant protein production.

2.2 Materials and Methods

2.2.1 Immortalised cell line cultures

CHO-K1 cell line was a kind gift from Dr James Pease (Leukocyte biology, Imperial College London). Cells were maintained in F-12+ Glut medium (Gibco), supplemented with 10 % foetal calf serum (FCS) (Sigma-Aldrich, UK), 100 IU/ml penicillin and 100 μg/ml streptomycin (Sigma-Aldrich, UK). The human alveolar epithelial cell line (A549) and Henrietta Lacks (HeLa) cell lines were grown and maintained in Dulbecco's essential modified medium (DMEM) (PAA Laboratories GmPH, Austria), supplemented with 10 % FCS (Sigma-Aldrich, UK), 1 % glutamate (Lonza), 100 IU/ml penicillin and 100 μg/ml streptomycin (Sigma-Aldrich, UK). HEK293A cells and modified 911 human embryonic retinoblastoma cells (HER) were cultured in DMEM and supplemented in the same way as described above. These two cell lines are packaging cell lines for recombinant adenovirus (rAd). They contain the E1A and E1B adenovirus 5 (Ad5) viral replication genes, which complement the deletion of these essential replication regions in recombinant replication-deficient adenoviruses.

All cells were split once they reached ~90 % confluency using trypsinisation. Briefly, trypsinisation involved cells being washed with 1 x PBS before 0.05 % trypsin-EDTA (Gibco) was added (enough to coat cell layer). Cells were left at room temperature until they began to detach, then 10 ml of supplemented medium was added, and cells were split 1 in 5 or 1 in 10. All cells were incubated at 37 °C in 5 % CO_2.

All cell lines were assessed for mycoplasma contamination using the MycoProbe® mycoplasma detection kit (R&D systems®, UK), as described in the manufacturer's instructions.

2.2.2 Genes and vectors of interest

The genes used in this study encoded for the CMV matrix protein pp65 (UL83 gene product) (1.662 kb) (kindly provided by Dr Rebecca Robey (University College London, UK) in a recombinant adenovirus 5 (rAd5) vector), and human MART-1 protein (0.374 kb) (generously provided by Dr Lisa Butterfield (University of Pittsburgh, USA) in a VR1012 vector (Ribas et al. 1997)). In addition, the gene for a single unit streptavidin (derived from *S. avidinii*) was kindly provided by Prof. M. Suresh (University of Alberta, Canada) (Wang et al., 2007), and was used to create streptavidin-fusion proteins with the above antigens.

The cloning strategy to produce the necessary expression vectors for this study is illustrated in Figure 2.1. PCR and subcloning techniques were utilised to insert the UL83 and *mart-1* genes into a pcDNA6/HisC™ expression vector (Invitrogen), a vector used primarily for mammalian cell transfection and generation of stably-expressing cell lines. The genes were also inserted into the AdEasy™-based pShuttle-CMV expression vector (Q-biogene), for the generation of rAds (see section 2.2.4). Details of these procedures are provided below.

2.2.3 Cloning of pcDNA6/HisC™-pp65 and pcDNA6/HisC™-MART-1

The genes of interest were initially cloned into the pcDNA6/HisC™ vector such that they would be expressed in frame with the His tag. Details are provided below.

2.2.3.1 Polymerase chain reaction (PCR)

Polymerase chain reaction (PCR) was used to amplify the respective genes from the original vectors in order to insert the genes of interest into the pcDNA6/HisC^{TM} vector. To facilitate directional cloning, restriction enzyme (RE) sites were incorporated into the 5' and 3' ends of the PCR products. The forward and reverse primers are detailed in Table 2.1. Each experimental PCR reaction of 50 µl contained 50 or 100 ng template DNA, 10 pmol of the primers (AD1/AD2 pair for CMV UL83, and MRT1/MRT2 pair for *mart-1*), 10X Pfu polymerase buffer (includes $MgCl_2$), 40 mM dNTPs (Stratagene), 1 unit Pfu proof-reading polymerase (Stratagene) and sterile distilled H_2O. A mastermix of the above reagents (excluding the polymerase and template DNA) was made based on the number of PCR reactions that were run in one experiment, and this was aliquoted into each reaction tube before the addition of template DNA and polymerase. The PCR amplification cycle profile for CMV UL83 amplification consisted of 1 cycle of 94 °C (1 min), 30 cycles of 94 °C (45 sec each), 62 °C (45 sec each), 72 °C (150 sec each), and 1 cycle of 72 °C (5 min). The amplification for the *mart-1* gene consisted of 1 cycle of 94 °C (1 min), 30 cycles of 94 °C (45 sec each), 60 °C (45 sec each), 72 °C (60 sec each), and 1 cycle of 72 °C (5 min). The negative controls included a reaction using sterile water in place of the template DNA, and a reaction with no primers.

2.2.3.2 Restriction enzyme digestion

Overnight RE digestion of the pcDNA6/HisC vectors and the resulting PCR products were performed with the compatible enzymes (Table 2.1) (all REs were from New England Biolabs, UK). Once digested, the products were run on an agarose gel (0.8 % agarose dissolved in 1 x Tris-borate-EDTA (TBE – 10.8 g Tris, 5.5 g Boric acid, 4 ml 0.5 M EDTA made up to 1L with dH_2O), and supplemented with SYBR Safe DNA gel stain (1:10 000) (Invitrogen). Running conditions were 85 V for 40 min in 1 x TBE buffer. Visualization was done on a long-wavelength UV trans-illuminator. Depending on the size of the DNA fragment, either a 1 kb or a 500 bp DNA ladder (Promega) was used as a marker.

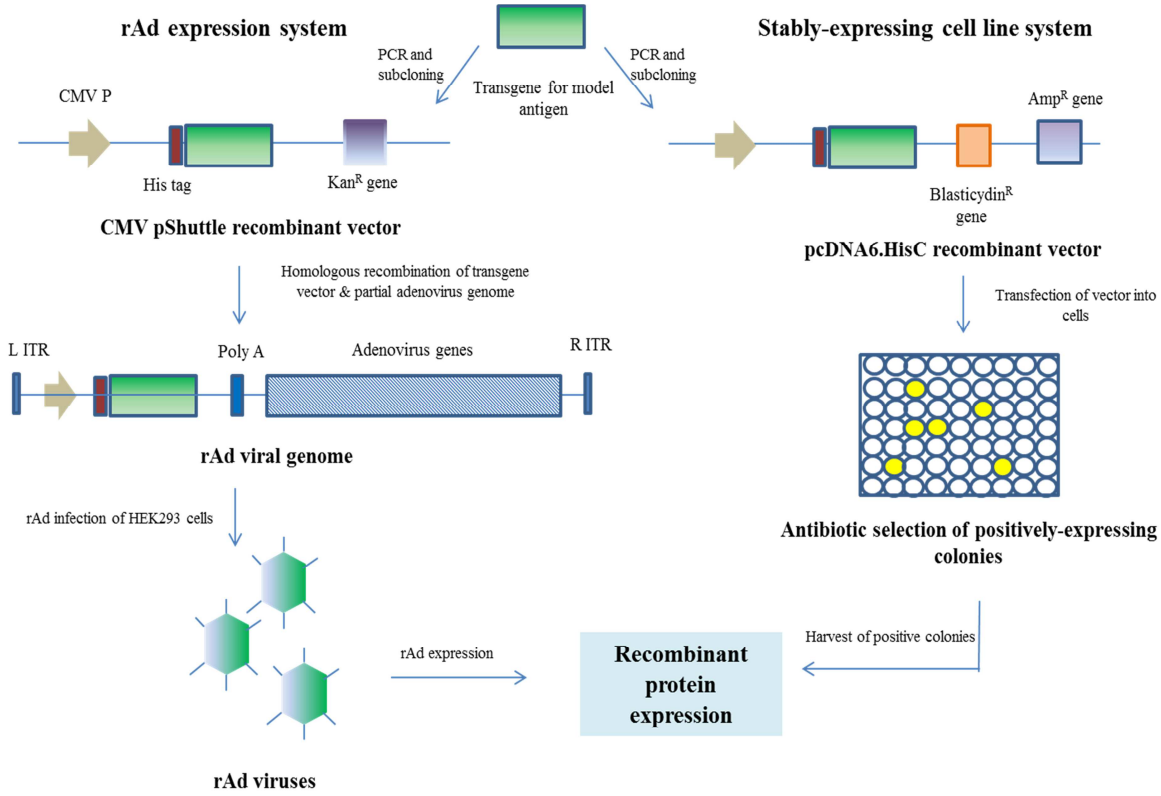


Figure 2.1 – A diagrammatic depiction of the two cloning strategies used. Two expression systems were evaluated to express the transgene of the respective model antigens/fused antigens, namely the rAd expression system and generation of a stably-expressing cell line.

Table 2.1 – Primers used for the PCR amplification of UL83 and *mart-1* genes. Primers used to clone the respective genes into pcDNA6/HisC vector.

Name of primer	Sequence*	Restriction enzyme site	Orientation
AD1	5' A**GAATTC***ATG*ATATCCGTACTGGGTCCC 3'	*Eco*RI	Forward
AD2	5' C**CTCGAG**TCAACCTCGGTGCTTTTTGG 3'	*Xho*I	Reverse
MRT1	5' CAA**GGTACC**T*ATG*CCAAGAGAAGATGCT 3'	*Kpn*I	Forward
MRT2	5' CAGC**CTCGAG**AGGTGAATAAGGTGGTG 3'	*Xho*I	Reverse

* R.E. sites are in bold, and start codons are italicised

2.2.3.3 Ligation and transformation

The digested gene bands and vector DNA were extracted and purified from agarose gel using the Geneclean® Spin Kit (Q-Biogene), as per the manufacturer's instructions. A rapid DNA ligation kit (Roche) was used to ligate the gene and vector DNA, performed as per the manufacturer's instructions. Competent TOP10F' *E.coli* cells (Invitrogen) were then transformed with the ligated products and were subsequently plated on Luria-Bertani agar (LA) plates supplemented with 100 µg/ml ampicillin (Sigma-Aldrich, UK), and incubated overnight at 37 °C and 5 % CO_2.

Colony PCR was performed on 20-40 of the resulting transformed colonies to identify clones that were positive for the gene of interest. The conditions of the colony PCR were the same as the PCR procedure described above, with the following modifications: (i) the total volume of the colony PCR reactions was 20 µl, (ii) Template DNA was supplied by inoculating the PCR reaction with the colony of interest (using a sterile pipette tip), (iii) GoTaq® Flexi DNA Polymerase Kit (Promega) and its buffers were used according to manufacturer instructions. DNA from positively identified colonies was then extracted using a Qiaprep spin mini-prep kit (Qiagen), and underwent RE digestion to confirm the sizes of both gene and vector. Further characterisation of the clones included sequencing of the gene insert to verify that the gene's integrity remained intact (Eurofins MWG Operon UK services). Two positive clones were selected and the plasmid DNA was amplified and purified using a HiSpeed Maxi-prep Kit (Qiagen). The DNA concentrations were determined using the NanoDrop 1000 spectrophotometer (Thermo-Scientific), according to manufacturer's instructions.

2.2.4 Construction of AdEasy^{TM} shuttle vectors, pShuttle.HisC-pp65 & pShuttle.HisC-MART-1

PCR was used to amplify the respective genes from the recombinant pcDNA6/HisC clones in order to insert the genes of interest with the His tag into the pShuttle-CMV vector (Figure 2.1). Again, to facilitate directional cloning into the pShuttle-CMV vector, restriction sites were incorporated into the 5' and 3' ends of the PCR products. The forward and reverse primers are detailed in Table 2.2. The PCR reaction was performed as described in section 2.2.3.1 for the respective genes, with the AD3/AD2 pair for CMV UL83, and MA1/MA2 pair for *mart-1*.

Table 2.2 – Primers used for the PCR amplification of His.*UL83* and His.*mart-1* genes. Primers used to clone the respective genes into the pShuttle-CMV^{TM} vector.

Name of primer	Sequence	Restriction enzyme site	Orientation
AD3	5' GATT**GTCGAC**A*ATG*GGGGGTTCTCATCATC 3'	*Sal*I	Forward
AD2	5' C**CTCGAG**TCAACCTCGGTGCTTTTTGG 3'	*Xho*I	Reverse
MA1	5' ATT**GCGGCCGC**AT*ATG*GGGGGTTCTCATC 3'	*Not*I	Forward
MA2	5' GGC**GATATC**TTAAGGTGAATAAGGTG 3'	*Eco*RV	Reverse

* R.E. sites are in bold, and start codons are italicised

The positive PCR products and AdEasy^{TM} pShuttle-CMV vectors underwent overnight RE digestion with the respective enzymes, and were ligated and transformed in a similar manner as described in 2.2.3.3. Positive clones were identified using colony PCR, RE digestion and sequencing analysis, as described above.

2.2.5 Production of streptavidin-fusion constructs

Fusion genes were designed to consist of a core *streptavidin* gene joined to the C-terminal of the UL83 and *mart-1* genes in-frame. Overlap extension PCR (Horton et al., 1989) was used to create the pp65-streptavidin gene as shown in Figure 2.2. Briefly, this method consists of three consecutive PCR reactions which allow two genes to be fused to one another. Initially, each gene is amplified separately with sticky-ended primers (PCR 1). The products of PCR 1 then act as both primer and template in the second PCR reaction, allowing them to form a fused gene product. Finally, PCR 3 amplifies the fused product using two primers from PCR 1.

PCR 1 consisted of *His*-UL83 and *streptavidin* genes being amplified separately using AD3/pp65R and ST2F/STR primer pairs respectively (Table 2.3). The *His*-UL83 gene was amplified using the same mastermix contents and cycle protocol as described section 2.2.3.1, while the *streptavidin* gene amplification consisted of a single cycle at 94 °C (1 min), followed by 30 cycles of 94 °C (45 sec each), 65 °C (45 sec each), 72 °C (60 sec each), and 1 cycle of 72 °C (5 min).

It is important to note here that the pp65 reverse primer was specifically designed to eliminate the stop codon of UL83 so that the reading frame remained open and continued into the *streptavidin* gene. In addition, the reverse primer of UL83 and forward primer of *streptavidin* contained "sticky ends" that were complimentary to each other. This allowed the UL83 and *streptavidin* PCR products to anneal to form a fusion product under the correct conditions. Thus, once the single gene products were purified, PCR 2 was performed, whereby the single gene products were used as template and primer DNA (Figure 2.2). This involved a single cycle at 94 °C (5 min), followed by 5 cycles of 94 °C (45 sec each), 55 °C (3 min each), 72 °C (4 min each), and 1 cycle of 72 °C (5 min). The PCR2 amplification allowed the two products to fuse and produce a small number of copies of the fusion gene, *His-UL83-streptavidin*. An extra unit of Pfu polymerase, 40 mM dNTPs and the AD3/STR primer pair, were added to the PCR reaction after the 5 cycles, and a final PCR amplification, PCR 3, was performed to amplify the fused product. The cycle for this final PCR included a single cycle of 94 °C (5 min), 30 cycles of 94 °C (45 sec each), 60 °C (45 sec each), 72 °C (150 sec each), and 1 cycle of 72 °C (5 min).

The positive fusion PCR product underwent dATP tailing (as described in pGem-T-Easy manual (Promega, 1996-1999)) in order to incorporate adenine (A) bases on the termini of the DNA product. The resulting product was then cloned into a pGEM T-Easy vector as per manufacturer's instructions, to facilitate sub-cloning strategies to follow. Positive recombinant pGEM T-Easy clones were identified and confirmed using colony PCR, RE digestion and sequencing analysis. The fusion gene was then sub-cloned into the AdEasy^{TM} pShuttle-CMV vector in a similar manner as described in section 2.2.2.3, and positive recombinant clones were identified and confirmed using colony PCR, RE digestion and sequencing analysis.

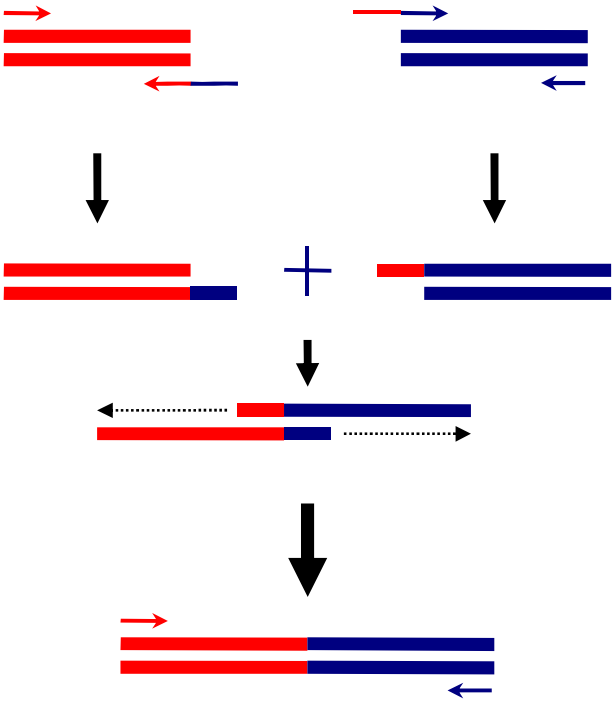


Figure 2.2 – A simplified illustration of overlap extension PCR.

Table 2.3 – Primers used for the PCR amplification of *His*-UL83, *streptavidin* and *His-mart1* genes. Primers used to produce streptavidin-fusion genes.

Name of primer	Sequence*	Restriction enzyme site	Orientation
Pp65 R	5' ACCTCC**GCGGCCGC**TACCTCGGTGCTTTTTGGG 3'	*Not*I	Reverse
ST2 F	5' CGAGGTA**GCGGCCGC**GGAGGTGGCGGATCAGAG 3'	*Not*I	Forward
ST R	5' CA**CTCGAG**TCAGGAGGCGGCGGACGGCTTC 3'	*Xho*I	Reverse
MA2 F	5' ATT**GTCGAC**AT*ATG*GGGGGTTCTCATCATC 3'	*SalI*	Forward
MA2 R	5' ATA**GCGGCCGC**TAGGTGAATAAGGTGGTGG 3'	*Not*I	Reverse

* R.E. sites are in bold, and start codons are italicised

2.2.6 Transient transfections

Transient transfection was used to test gene expression from the recombinant constructs. CHO cells or HEK293A cells were seeded into tissue culture (TC) 6-well plates using media that was not supplemented with antibiotics, and incubated for 18-24 hrs until they were 70-80% confluent. Cell lines were then transiently transfected with the respective recombinant constructs, employing one of two transfection agents (Lipofectamine™ 2000 (Invitrogen) and TransIT® (Mirrus)), which were used according to the manufacturer's instructions. Briefly, 1:1 (µl transfection agent: µg DNA) reactions were set up, using approximately 2-4 µg of plasmid DNA per reaction (found to be the optimal ratios for the respective agents). Negative controls included untransfected cells, and cells transfected with pcDNA6/HisC™-lacZ plasmid or empty pShuttle-CMV™ plasmid. Once transfection reactions had been added to the seeded cells, plates were incubated at 37 °C for 48 hrs. Cells were then detached from wells using trypsinisation. To measure protein expression, intracellular staining was performed on cell samples (see section 2.2.9 for protein expression detection).

2.2.7 Stable expression cell line generation

The following sections describe in detail the generation of stably-expressing cell lines expressing CMV pp65 (from UL83 gene).

2.2.7.1 Blasticidin dose sensitivity assay

The minimum concentration of Blasticidin S-HCl (Invitrogen) to use for stably-expressing cell line generation was determined by performing a dose sensitivity assay. Briefly, CHO or HEK293A cells were seeded at approximately 30 % confluency into a TC 96-well flat-bottomed plate, and left overnight at 37 °C and 5 % CO_2. After 20 hrs, the respective culture medium was removed from adherent cells, and replaced with medium containing increasing concentrations of blasticidin from 0-10 µg/ml. After incubation for 4-5 days, wells were examined and those in which 80-100 % cells were dead were considered positive (granular appearance, rounding and detachment of cells). The minimum concentration of blasticidin that was able to kill all infected

wells was used as the selected concentration for production of the stably-expressing cell line. The assay was repeated three times for reproducibility purposes.

2.2.7.2 Production and selection of stable integrants

The stably-expressing cell line expressing CMV pp65 was created as described by the pcDNA6.HisC™ manual. Briefly, CHO or HEK293A cells were transiently transfected with the pcDNA6/HisC™ recombinant constructs as described in section 2.2.6 using Lipofectamine 2000 or TransIT® as the transfection agent. After 48 hrs, cells from each 6-well plate were trypsinised and these cells were diluted in 10 ml of the appropriate growth media supplemented with blasticidin (dose determined for the individual cell lines as outlined in section 2.2.7.1), and plated into a 96-well plate. Cells were then incubated at 37 °C and 5 % CO_2 until wells with positive clones showed confluent growth. During the time taken to reach confluency, blasticidin-selective media was replenished every 3-4 days. Once potential positive clones were identified, they were expanded gradually into larger wells, and finally into TC flasks. Further growth was maintained in blasticidin-selective media. After expansion, samples of cells were removed and underwent intracellular staining (see section 2.2.9.1) to identify which clones were expressing pp65.

2.2.8 Recombinant adenovirus (rAd) expression system

The following sections describe in detail the generation of replication-incompetent rAds expressing CMV pp65, MART-1 or the streptavidin fusion proteins, pp65-streptavidin (pp65-strep) and MART-streptavidin (MART-strep).

2.2.8.1 Production of recombinant adenovirus vectors

Production of the rAds was performed as described in the AdEasy™ Instruction manual (Stratagene) (Figure 2.3). Transient transfection experiments (section 2.2.6) were used to confirm expression of the respective genes from the pShuttle-CMV recombinant vectors. Once verified, 1-3 μg of the respective recombinant pShuttle-CMV vectors (section 2.2.3.1) were digested with *Pme*I restriction enzyme under the appropriate conditions. The digested DNA was

purified and concentrated to 1 μg/ml by ethanol precipitation. Briefly, this involved adding sodium acetate (3 M, pH 5.2) to the sample (1/10 of sample volume), followed by the addition of 95 % ethanol (2-3 times of sample volume). Samples were incubated on ice for 15 min, then centrifuged at 13 000 rpm for 10 minutes at 4 °C, and supernatant was discarded. Pellet containing DNA was rinsed with 70 % ethanol, centrifuged again and finally, the resulting pellet was resuspended in the appropriate volume of water.

The purified DNA was subsequently electroporated into electrocompetent BJ5183-AD1 *E.coli* cells (Stratagene) under manufacturer's conditions. Transformed cells were plated onto LA plates (supplemented with 100 μg/ml kanamycin) and grown overnight at 37 °C and 5 % CO_2. The resulting clones containing the DNA of the rAd were identified as positive clones by *Pac*I and *Bst*XI RE digests of mini-prepped plasmid DNA. Once a positive clone was identified, its plasmid DNA was transformed into TOP10F' *E.coli* cells (Invitrogen), to avoid the mutagenic problems that occur with recombination-prone BJ1583 clones. Positively-transformed TOP10F' clones were again identified with respective RE digests, followed by maxi-preparation of DNA using a HiSpeed Maxi-prep Kit (Qiagen).

Recombinant adenoviruses were generated by transfecting HEK293A or 911 cells with 4-8 μg of the respective rAd vector DNA (digested overnight with *Pac*I), using Lipofectamine 2000 transfection reagent. The transfected cells were incubated at 37 °C and 5 % CO_2 for 7-10 days. During this time, cytopathic effects (CPE) were not always identifiable.

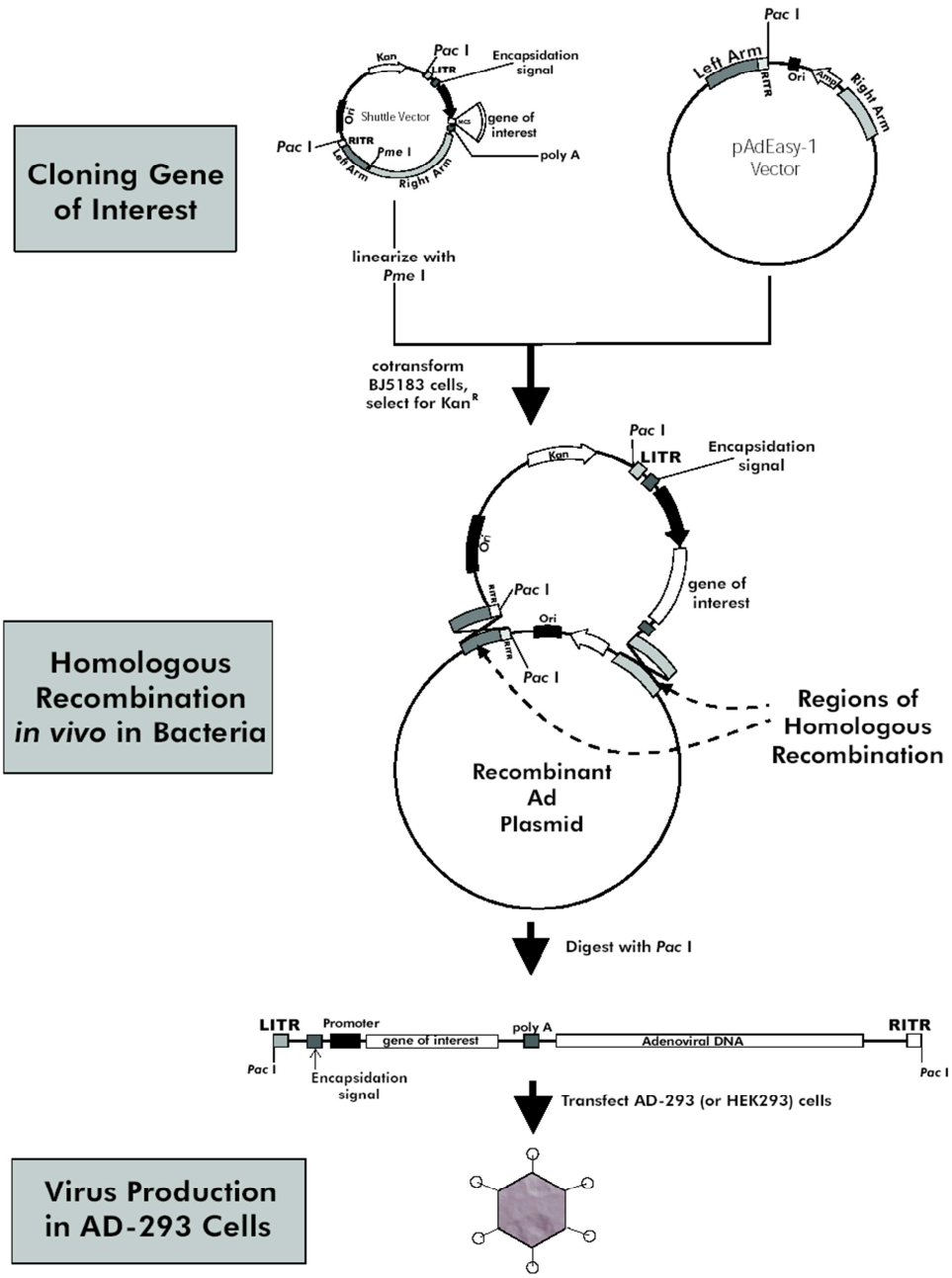


Figure 2.3 – Recombinant adenovirus production. Derived from the Stratagene AdEasy^{TM} instruction manual (Stratagene, 2008).

Once cells detached from the well, the virus was ready to harvest. Cells were removed, and underwent 4 freeze-thaw cycles, before being centrifuged at 1580 rpm for 5 min. Supernatant (also known as the seed stock) was removed and stored at -80 °C for further use. The generation of final viral stock involved several rounds of infection of expanding cell cultures.

Initially, cells were incubated with a concentrated volume of infectant in a minimum amount of serum-free medium at 37 °C for 1 hr. Infectant was then diluted in 10 % FCS-supplemented high-glucose DMEM medium, and cells were further incubated for 5-7 days, or until cells had completely detached from the surface of flask. Virus stock was harvested as described above, and the infection process was repeated with the newly harvested infectant (which was more potent than the previous stock) until a sufficient amount of viral stock had been generated for recombinant protein production. The final viral stock was the sixth harvested infectant, where 30 T175 flasks were infected to generate 750 ml of supernatant.

2.2.8.2 Tissue Culture Infectious Dose 50 ($TCID_{50}$) assays

Viral titre of recombinant adenoviral stocks were measured using $TCID_{50}$ assays. Under sterile conditions, HEK293A cells (cell density: $1.5x10^6$ cells/ml) were seeded in each well of a flat-bottomed 96 well TC plate, and were left to settle for 24 hrs. A log dilution series of rAd supernatant 6 (10^{-2} – 10^{-12}) was prepared using DMEM, and each dilution was designated a row (8 wells) of the TC plate. Fifty µl of the appropriate dilution was then added to each well in the respective row. One row was used as a negative control (DMEM added instead of infectant). After 10 days, each well was studied to determine if it was infected or not. The $TCID_{50}$ of the assay was calculated using the Karber formula (O'Reilly, 1994, Wold, 1999), and infectivity of the viral stock was calculated using the following equation:

$$\text{Infectivity (pfu/ml)} = 0.69 \times TCID_{50}$$ (Dee and Shuler, 1997)

2.2.8.3 Expression of model antigens in non-packaging cell lines

Under sterile conditions, A549 and HeLa cells (cell density: $1.5x10^6$ cells/ml) were seeded in T125 flasks, and were left to settle for 24 hrs at 37 °C. Cells were then incubated for 1 hr with

rAdpp65 or rAdMART-1 infectant using 3 MOI (50, 100 and 150), in a volume of 2 ml. A volume of 8 ml of supplemented RPMI media was added, and cells were incubated for a further 48 hrs, before being harvested. Harvested cells were lysed and pelleted. The resulting supernatant was assessed for the presence of pp65 or MART-1 released from cells, using western blot analysis (see 2.2.9.2).

2.2.9 Protein expression detection

2.2.9.1 Intracellular staining

After transfection/infection, cells were washed and trypsinised in a similar way as described in section 2.2.1. Approximately 2-10 $x10^5$ cells were transferred into labelled flow cytometry tubes. Cells were centrifuged at 1580 rpm for 5 min to sediment cells. Media were aspirated and 3 ml FACS buffer (PBS, 2 % FCS, 2 mM EDTA, 0.1 % sodium azide) was used to resuspend the pellet, followed by another centrifugation step, as described above. FACS buffer was removed, and pellets were resuspended in 200 µl 4 % paraformaldehyde (PFA) solution. Samples were incubated for 10 min at room temperature before being washed with FACS buffer and re-centrifuged. Pelleted cells were resuspended in 100 µl of primary antibody solution (1:20 dilution of CMV pp65 mouse monoclonal primary antibody (AbD) or MART-1 mouse monoclonal primary antibody (AbCam) in FACS buffer containing 0.1 % saponin). After 45 min incubation at room temperature, samples were washed with FACS buffer containing 0.1 % saponin and centrifuged. Cell pellets were resuspended in 100 µl of secondary antibody solution (1:100 dilution of PE-labelled goat anti-mouse secondary (Ig) antibody for CMV pp65 (BD Bioscience) or 1:20 PE-labelled goat anti-mouse secondary antibody for MART-1 (AbCam) in FACS buffer containing 0.1 % saponin). Cells were incubated in the dark at room temperature for 45 min, before being washed again with FACS buffer containing 0.1 % saponin and re-centrifuged. Cell pellets were resuspended in 200 µl 2 % PFA/PBS solution and stored at 4 °C until analysis. As negative controls, untransfected cells, as well as cells transfected with an empty vector, were used. Cells were acquired on a FACS Calibur and analysed using CellQuest Pro (Becton Dickinson, UK) or WinMDI software.

2.2.9.2 Coomassie-stained SDS-PAGE and Western blotting

The NuPage western blotting apparatus and buffers (Invitrogen) were used for all sodium dodecyl sulphate polyacrylamide gel electrophoresis (SDS-PAGE) gels and western blots. Samples were prepared by incubating cells in cell lysis buffer (Invitrogen) for 15 min under shaking conditions, and then centrifuged at 13000 rpm for 15 min at 4 °C. Loading buffer (4X) and reducing agent (10X) was added to a sample of the supernatant. The samples were then incubated at 70 °C for 10 min, after which they underwent SDS-PAGE (at constant current) on a 4-12 % Bis-acrylamide SDS gel (Invitrogen), in order to separate proteins on the basis of molecular weight. A standard protein marker was used to identify migration distance of proteins with molecular weights of between 20 – 260 kD (Promega). Conditions for running the SDS-PAGE were as follows: 200 V, 120 mA, for 35 min.

Once proteins were separated, Coomassie staining or western blotting was performed. For Coomassie-stained SDS-PAGEs, the SDS polyacrylamide gels were incubated overnight in 10 ml Coomassie blue stain (0.1 % (w/v) Coomassie blue R350, 20 % (v/v) methanol, and 10 % (v/v) glacial acetic acid) under shaking conditions (50 rpm) at room temperature. The gels were then destained the next day by incubation in Coomassie destain (50 % (v/v) methanol in water with 10 % (v/v) glacial acetic acid) for 3-5 hrs, or until protein bands were visible.

For western blotting, proteins from the respective samples were transferred from the SDS-polyacrylamide gel onto Hybond-ECL membrane (Amersham) using wet blotting NuPage equipment. The conditions used for wet-blot transfer were as follows: 125 mA, 25 V, for 90 min. The membrane was then incubated in blocking buffer (5 % dried milk powder, 0.1 % Tween 20 in 1 x PBS) for 30 min, followed by incubation overnight at 4 °C in blocking buffer containing the respective primary antibodies (1:2000 dilution of CMV pp65 mouse monoclonal antibody (AbD) or Melan-A mouse monoclonal primary antibody (AbCam)). The membrane was subsequently washed three times for 15 min using wash buffer (0.1 % Tween 20 in 1 x PBS), then incubated for 1 hr in a 1:5000 dilution of goat anti-mouse IgG secondary antibody (Sigma-Aldrich, UK) (conjugated to alkaline phosphatase) in blocking buffer. This incubation was followed by a second set of washes, and protein bands were visualized using Nitro blue tetrazolium chloride/5-bromo-4-chloro-3-indolyl phosphate tablets (NBT/BCIP, Roche). The

membrane was rinsed with water after protein bands were visible, to stop visual development reaction. In the initial western blots, a commercially available CMV antigen preparation (AbD serotec) was used as a positive control to confirm binding functionality of the primary CMV pp65 antibody.

2.3 Results

2.3.1 Construction of expression vectors to produce CMV pp65 and MART-1

To produce the antigens of interest (CMV pp65 and MART-1), two expression systems were evaluated, namely, a stably-expressing cell line system and a recombinant adenovirus expression system (AES) (Figure 2.1). Both systems utilized mammalian cells for protein expression, and required the antigen genes to be cloned into specific expression vectors. PCR was used to amplify the genes of the respective proteins, and to insert the appropriate RE sites at the genes' termini, to facilitate directional cloning of the genes into the expression vectors. The amplified PCR products were of the expected sizes (approximately 1.7 kb for UL83 gene, and 0.4 kb for the *mart-1* gene), and no products were detected in the negative controls (Figure 2.4). The PCR-purified genes were cloned into the pcDNA6/HisC^{TM} vector (used for the stably-expressing cell line expression system), such that they were in-frame with the 6xHis tag (Figure 2.5a and b). Positively-transformed clones carrying the genes of interest, UL83 and *mart-1*, were confirmed using colony PCR. RE digests were then used to verify the gene and vector sizes (Figure 2.5c and d). Following verification, the genes were sequenced to validate their integrity.

The recombinant pShuttle-CMV^{TM}-based plasmids (necessary for rAd generation) were created in a similar way. Briefly, the *hisC*-UL83 and *hisC-mart-1* genes were PCR-amplified using the respective recombinant pcDNA6/HisC^{TM} plasmids as template DNA. The transgenes were then cloned into the multiple cloning site of the pShuttle-CMV^{TM} vector (Figure 2.5e and f), and potential positive clones were isolated, cultured and screened using colony PCR, RE digestion (Figure 2.5g and h) and gene sequencing. Selected, positive recombinant expression plasmids were then amplified, purified and concentrated.

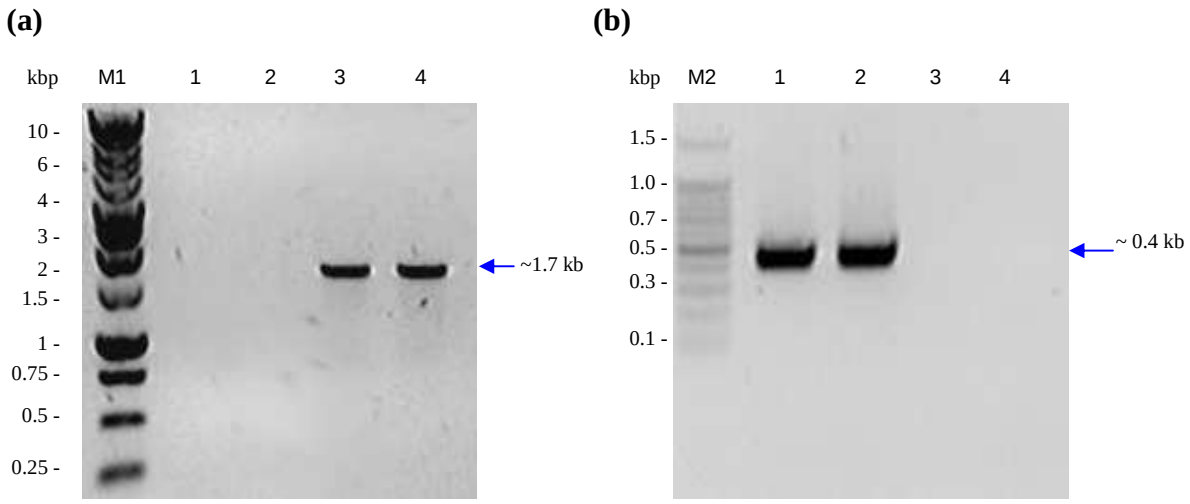


Figure 2.4 – PCR products of the genes of interest, (a) *CMV* UL83 and (b) *mart-1*. (a) Lanes: 1-water negative control (no DNA template), 2-template control (no primers), 3-PCR product from 50 ng of the provided rAdpp65 DNA template, 4- PCR product from 100 ng rAdpp65 DNA template. (b) Lanes: 1-PCR product from 50 ng of the provided rAd-MART-1 DNA template, 2-PCR product from 100 ng rAd-MART-1 DNA template, 3-water negative control (no DNA template), 4-template control (no primers). M1 = 1 kb DNA ladder; M2 = 100bp DNA ladder. Blue arrows indicate the respective genes and molecular weight of genes.

2.3.2 Evaluation of pp65 and MART-1 production from constructed expression vectors

Protein expression from the resulting recombinant constructs was confirmed using transient transfection of mammalian cells. CHO and/or HEK293A cells were transfected with the respective plasmids, and recombinant protein expression was evaluated using intracellular staining flow cytometry (Figures 2.6 for pp65 and Figure 2.7 for MART-1). The negative controls included untransfected cells, and cells that were transfected with an empty expression vector or an expression vector carrying a different gene. As illustrated (Figure 2.6 and 2.7), all four recombinant plasmids demonstrated expression of the respective proteins of interest compared to the negative controls. In general, higher recombinant protein expression was observed in 293A cells compared to CHO cells, with a difference between cell lines of as much as 24.7 % for pp65 expression (Figure 2.8a and c), and 8.75 % for MART-1 expression (Figure 2.8b and d).

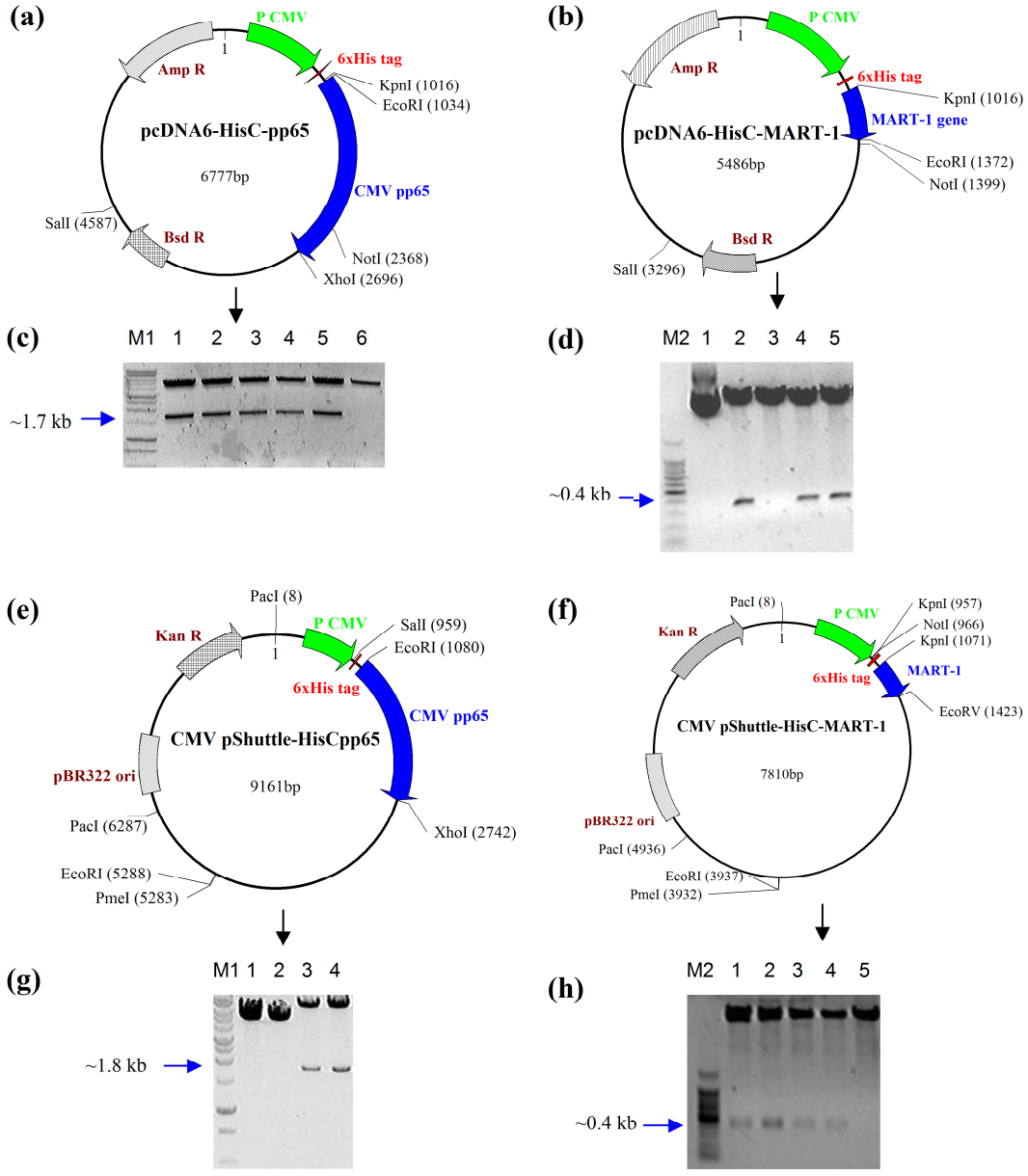


Figure 2.5 – Plasmid maps and RE digests of the recombinant constructs created to express the model antigens, pp65 and MART-1. (a) pcDNA6 expression vector carrying the CMV UL83 gene, pcDNA6.HisC-pp65; (b) pcDNA6 expression vector carrying the human *mart-1* gene, pcDNA6.HisC-MART-1; (c) *Eco*RI-*Xho*I RE digests of selected pcDNA6.HisC-pp65 clones, where clones in lanes 1-5 carry the *CMV* UL83 gene (±1.7 kb) and vector (5.1 kb); (d) *Kpn*I-*Xho*I RE digests of selected pcDNA6.HisC-MART-1 clones, where clones in lanes 2, 4 and 5 carry the *mart-1* gene (±0.4 kb) and vector (5.1 kb). (e) AdEasy system's pShuttle vector carrying UL83 gene, pShuttle.HisC-pp65; (f) AdEasy system's pShuttle vector carrying the human *mart-1* gene, pShuttle.HisC-MART-1; (g) *Sal*I-*Xho*I RE digests of selected pShuttle.HisC-pp65 clones, where clones in lanes 3 and 4 carry the *HisC*-UL83 gene (1.8 kb) and vector (7.4 kb); (h) *Not*I-*Eco*RV RE digests of selected pShuttle.HisC-MART-1 clones, where clones in lanes 1-4 carry the *HisC-mart-1* gene (±0.4 kb) and vector (7.4 kb). M1 = 1 kb DNA ladder; M2 = 100bp DNA ladder. Blue arrows indicate the gene of interest in the respective

The transfection agents, TransIT and Lipofectamine, displayed similar levels of transfection efficiency for pp65 expression, although Lipofectamine appeared to be more effective for transfection of the pcDNA/HisC-MART-1 plasmid. MART-1 expression levels were found to be more than 2 fold greater in both CHO and HEK293A Lipofectamine transfections compared to TransIT transfections (Figure 2.8b and d).

Similar results were obtained with pShuttle.HisC-MART-1 transfections, where MART-1 expression was higher when Lipofectamine was used for transfection (Figure 2.9b). As with the pcDNA6/HisC plasmids, there was a detectable production of the both proteins of interest by the pShuttle-CMV plasmids in HEK293A cells (Figure 2.9a and b), illustrating that these expression plasmids were functional, and could be used for rAd production.

In general, higher levels of pp65 were produced in both cell lines, compared to MART-1. The differences observed in transgene expression between pp65 and MART-1 are not unusual though, given the number of factors that affect recombinant protein expression. These factors include efficiency of transfection, localization of the protein, expression plasmid stability, and nature of the protein, and should be taken into account when comparing expression levels.

2.3.3 Generation of a stably- expressing cell line

The development of a stably-expressing cell line involves the incorporation of an expression plasmid carrying the gene of interest into cells of a selected cell line. Once cells are transfected, the DNA plasmid randomly integrates into the cell's genome and both the transgene and an antibiotic resistance gene (acting as a selection marker) are expressed within the cell. Transfected cells are grown in selective medium (containing the chosen antibiotic agent), and only those cells (and their progeny) that express the antibiotic resistance gene at sufficient levels survive and proliferate.

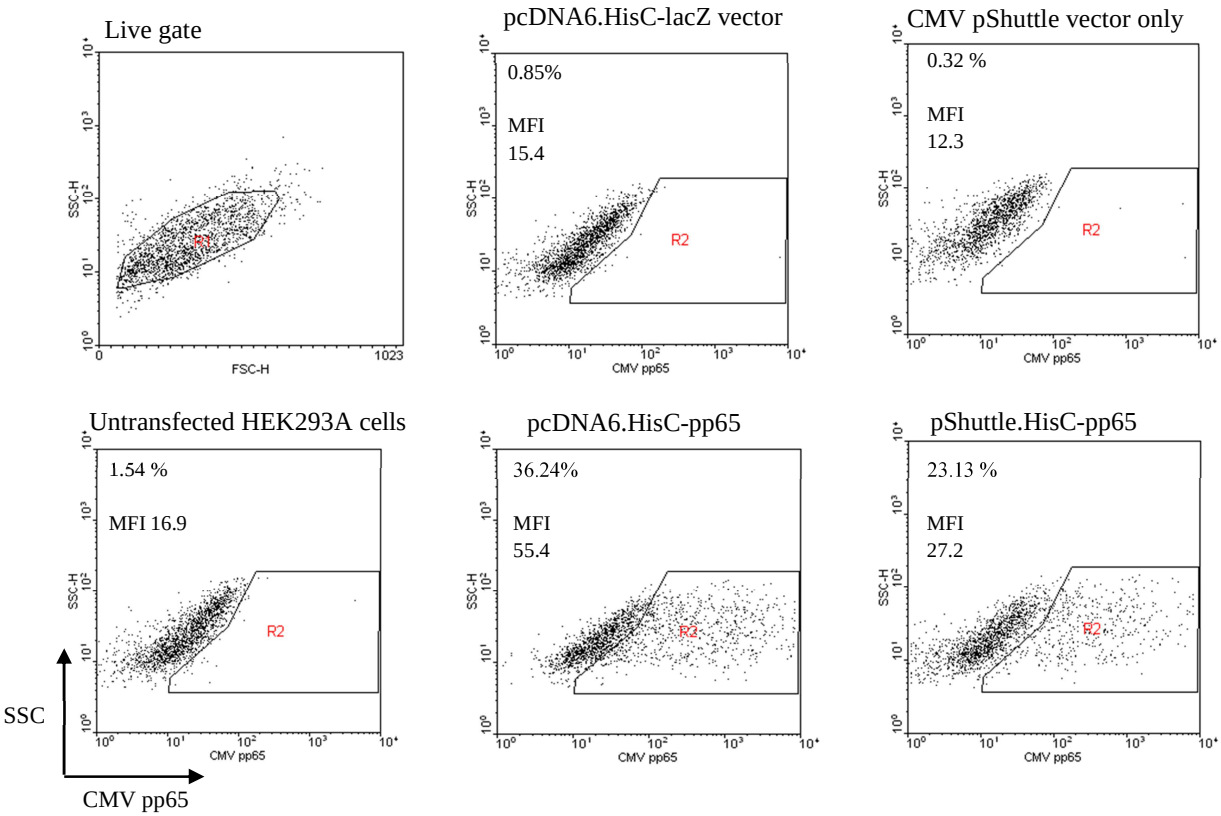


Figure 2.6 – A representative example of the intracellular staining flow cytometry gating strategy used to determine CMV pp65 expression from expression vectors. pcDNA6.HisC-pp65 and pShuttle.HisC.pp65 constructs were transfected into HEK293A cells. Transfections were performed using Lipofectamine 2000 in a 1:1 transfection reaction. Negative controls included untransfected HEK293A cells, as well as transfections with pcDNA6.HisC-LacZ vector or empty pShuttle vector. Percentage of positively-expressing pp65 cells is given in the top left corner of each panel, in addition to the mean fluorescence intensity (MFI) of these cells.

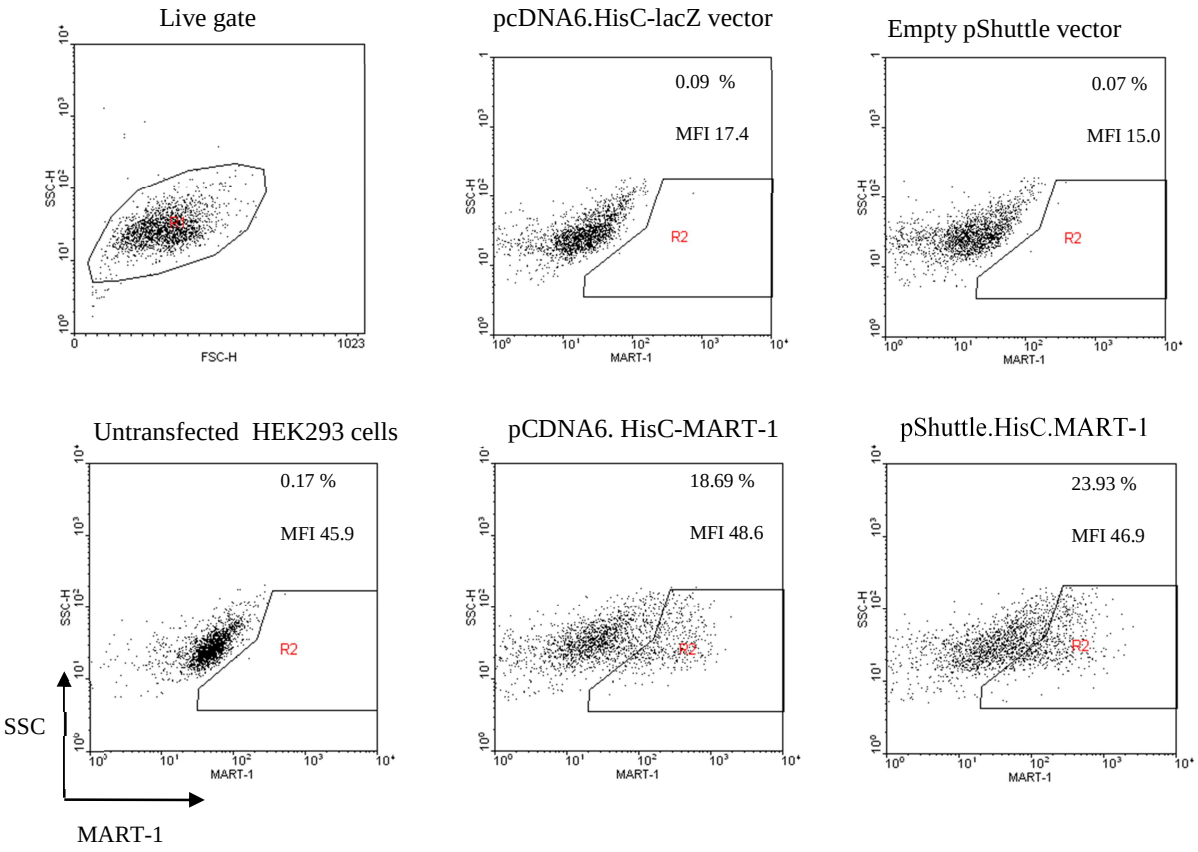


Figure 2.7 – A representative example of the intracellular staining flow cytometry gating strategy used to determine MART-1 expression from expression vectors. pcDNA6.HisC-MART-1 and pShuttle.HisC.MART-1 constructs were transfected into in HEK293A cells. Transfections were performed using Lipofectamine 2000 in a 1:1 transfection reaction. Negative controls included untransfected HEK293A cells, as well as transfections with pcDNA6.HisC-lacZ vector or empty pShuttle vector. Percentage of positively-expressing MART-1 cells is given in the top right corner of each panel, in addition to the mean fluorescence intensity (MFI) of these cells.

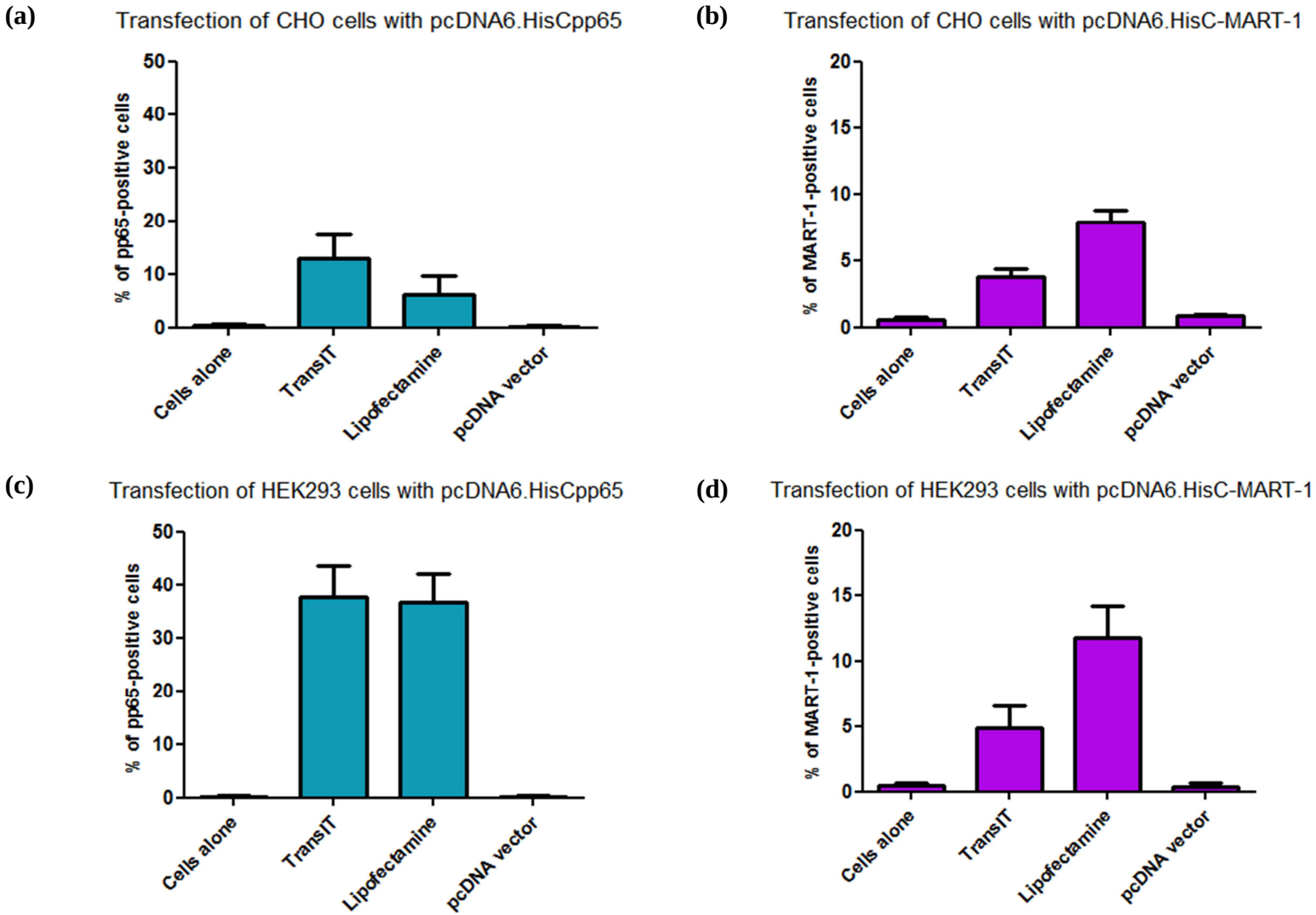
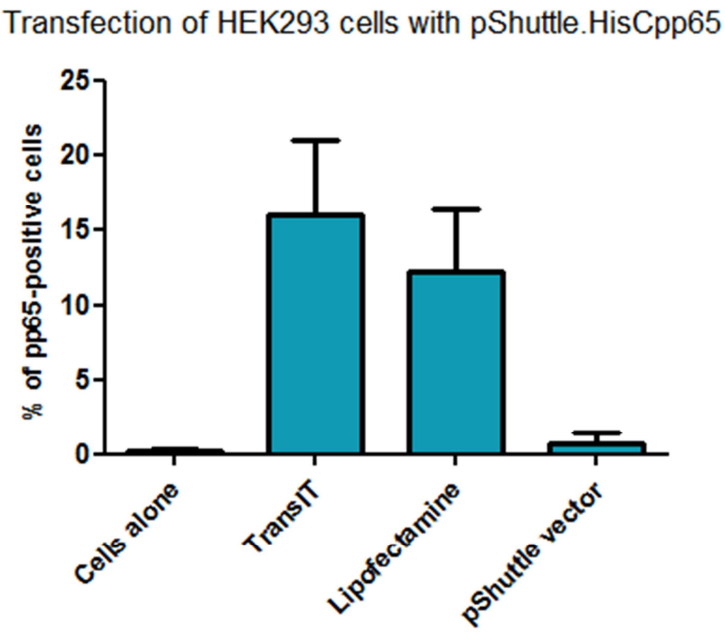


Figure 2.8 – Protein expression after transient transfection of cells with pcDNA expression vectors. CHO (a and b) and HEK293A cells (c and d) were transfected with recombinant pcDNA6.HisC^{TM} constructs to test expression of respective insert proteins and transfection efficiency. (a) and (c) depicts pp65 expression, (b) and (d) depicts MART-1 expression.

(a)



(b)

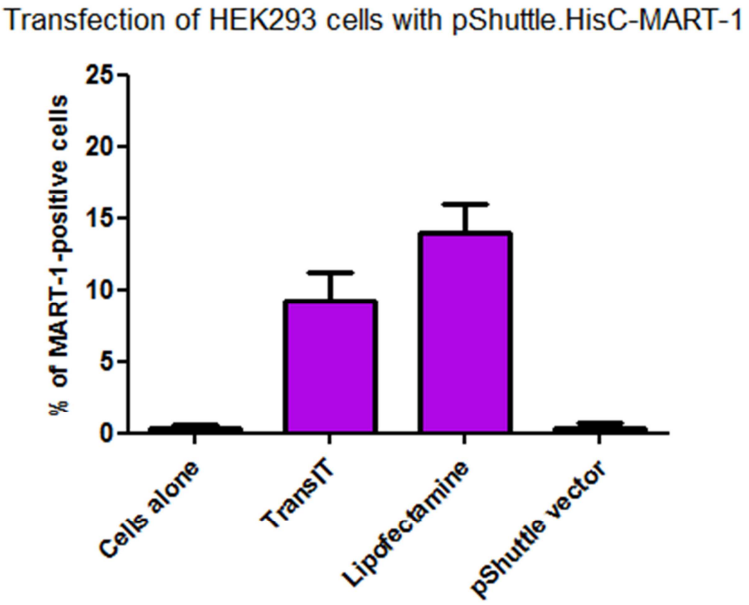


Figure 2.9 - Protein expression after transient transfection of cells with recombinant pShuttle expression vectors. pShuttle™ constructs were transfected into HEK293A cells to test expression of respective insert proteins and transfection efficiency. (a) pp65 expression; (b) MART-1 expression.

Over time, these cells continue to express the transgene and the protein can be harvested periodically, while keeping cells in culture. In this way, a continuous expression system is established, where protein can be harvested at any time.

In this study, production of a stably-transfected cell line expressing pp65 was evaluated. The recombinant pcDNA expression plasmid carrying the *pp65* gene was transfected into both CHO and HEK293A cells using Lipofectamine (in a 1:1 ratio). Transfected cells were initially incubated without antibiotics for 48 hrs before being moved into a 96-well plate, and incubated for a further 2 weeks in selective TC medium containing blasticidin antibiotic at a concentration of 6 μg/ml (CHO cells) or 8 μg/ml (HEK293A cells). These concentrations were previously determined using dose sensitivity assays to find the lowest concentration of blasticidin that would kill the respective cells in 4-6 days (Data not shown). Potentially positive, stable clones were expanded until they confluently occupied wells in a 6-well plate. At this stage they were tested for expression of pp65 using intracellular staining. In total, 29 CHO-cell clones and 12 HEK293A-cell clones were isolated.

Unexpectedly, several of the blasticidin-resistant clones tested did not express detectable amounts of pp65, as determined by intracellular staining and western blots (Figure 2.10). Of the selected clones, only 5 CHO clones (9, 10, 11, 16 and 23) (Figure 2.10a) and 6 HEK293A clones (1-4, 7, 9 and 10) (Figure 2.10c) displayed over 5 % of live pp65-expressing cells. Expression was also quite low, as confirmed using western blots, where pp65 production was barely detectable (Figure 2.10b and d). The highest expressing clones demonstrated less than 35 % of live-expressing cells in both cell lines, and their levels of pp65 expression decreased over time from early to later passages by as much as 25-fold for CHO clone 10, and 2.5 fold for HEK293A clone 3 (Figure 2.11a and 2.11b respectively). Some optimisation of this expression system was attempted in the hope of eliminating resistant, non-transfected cells. Higher initial blasticidin concentrations were utilized and cells were passaged fewer times, however, similar results were obtained.

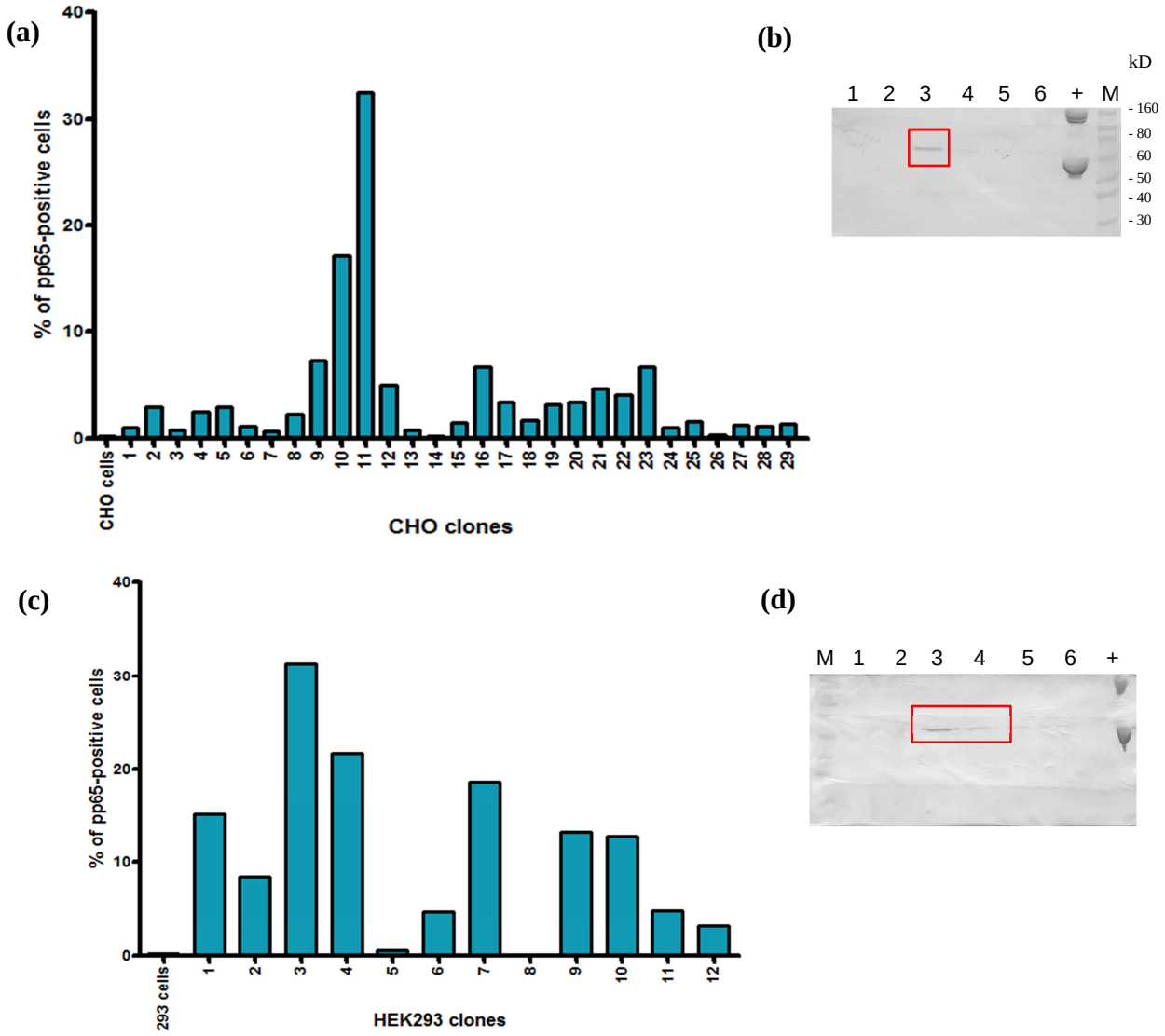


Figure 2.10 –Expression of CMV pp65 from blasticidin-resistant CHO cell clones (a and b) and HEK293A cell clones (c and d). Expression was measured using intracellular staining flow cytometry (a and c) or western blots (b and d). Lanes: (b) 1-6 = isolated CHO clones 9, 10, 11, 16 and 23; (d) 1- 6 – isolated HEK293A clones 1-4, 9, and 10. + = commercially available CMV antigen (positive control for CMV to confirm primary antibody was functional); - = negative cell lysate control. Red boxes highlight detectable pp65 protein on western blots.

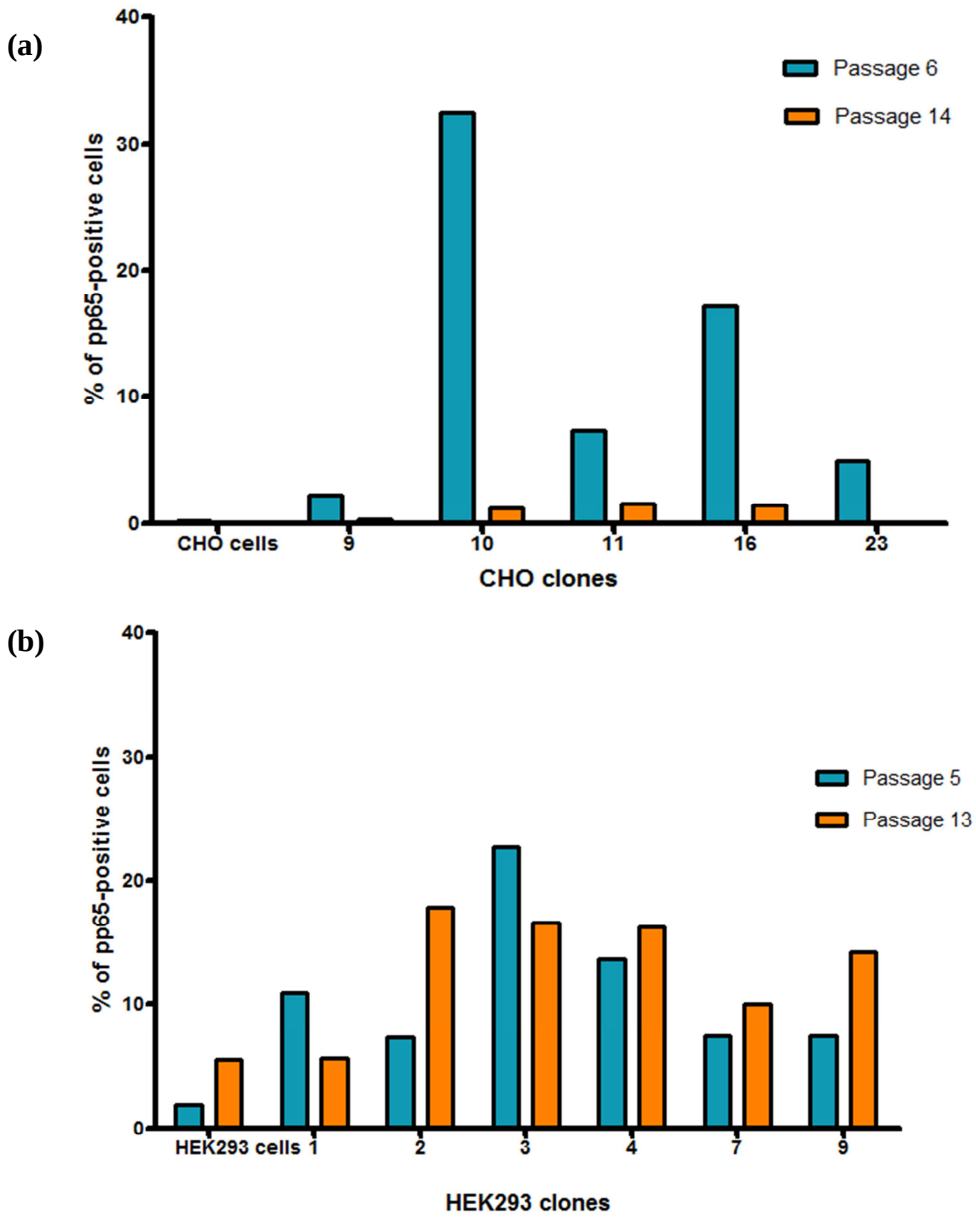


Figure 2.11 – Loss of expression of CMV pp65 in the positive stable clones. CHO cell clones (a), and HEK293A cell clones (b), as measured using intracellular staining (over 8 cell passages).

The quantity of pp65 produced from stably-expressing clones was inadequate for the required amount of protein needed in the *in vitro* tissue culture experiments to follow, and therefore this expression system could not be used for CMV pp65 production, without substantial optimisation. Additionally, the poor results for pp65 expression and the low transfection rates of the pcDNA-

MART-1 clone, suggested that this would not be an advantageous system for MART-1 production either, and therefore no stably-expressing cell line generation was attempted for MART-1 production.

2.3.4 The recombinant Adenovirus expression system (AES)

Recombinant adenovirus production involved integrating the genes of interest, *pp65* and *mart-1*, into replication-incompetent rAd DNA. This was achieved using the AdEasy^{TM} rAd expression system (Figure 2.3). Briefly, this involved transformation of BJ1583 *E.coli* bacteria with the recombinant pShuttle-CMV plasmid carrying the transgene (transfer vector). These bacteria harbour the pAdEasy plasmid which contain the adenovirus 5 backbone without the replication E1 genes (Stratagene, 2008). Thus, homologous recombination of the recombinant pShuttle-CMV plasmid with the resident pAdEasy plasmid in these bacterial cells yielded replication-incompetent rAd DNA, carrying either pp65 (Figure 2.12a) or MART-1 (Figure 2.12b). Positive bacterial clones were identified using *Pac*I and *Bst*XI RE digests, where 2 bands of approximately 33kB and 4.5 kb were expected following a *Pac*I digest, and 8 (for rAdpp65) or 7 (for rAdMART-1) bands from a *Bst*XI digest. As is seen in Figure 2.13a and b, only one positive clone was detected for both RE digests of the rAdpp65 plasmid clones tested. In the case of the rAd plasmid carrying MART-1, however, there were 4 positive clones that displayed the expected banding pattern, as compared to the negative controls (rAd backbone control and recombinant pShuttle-CMV control) (Figure 2.13c and d).

After another transformation procedure into a stable strain of *E.coli*, the rAd DNA from positive clones was isolated and used to transfect HEK293A or HER 911 cell lines. Both these cell lines were previously modified to specifically produce replication incompetent rAd. Thus, they contained a copy of stably-integrated E1 replication genes (E1a and E1b) that allowed for rAd particle production (Schaack, 2005).

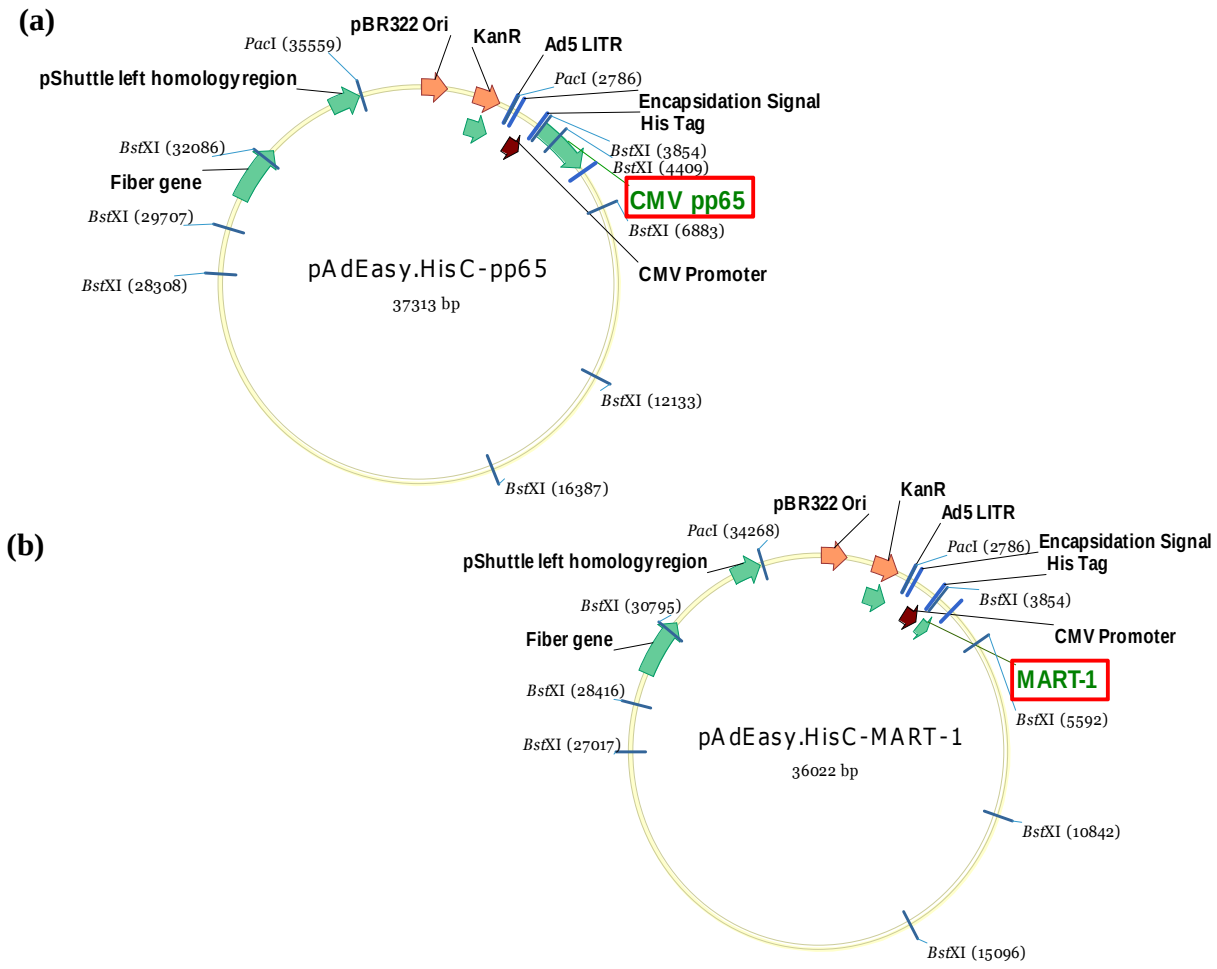


Figure 2.12 – Recombinant adenovirus constructs carrying the genes of interest, CMV pp65 (a) and MART-1 (b).

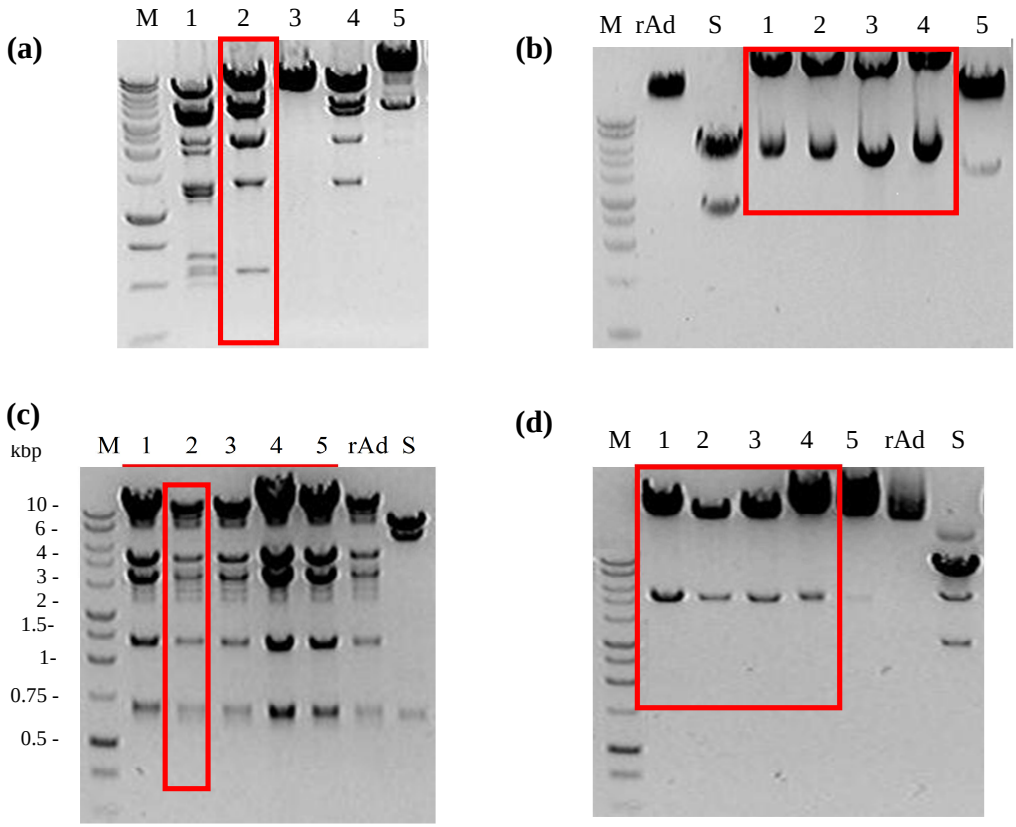


Figure 2.13 – R.E. digests of the recombinant adenovirus clones, rAd.HisC-pp65 clones (a and b) or rAd.HisC-MART-1 (c and d) isolated after transformation of the respective recombinant pShuttle-CMV plasmids into BJ5183 *E.coli* cells. (a) and (c) illustrate *Bst*XI digests; (b) and (d) illustrate *PacI* digests. M = benchtop 1 kb DNA ladder; S = recombinant pShuttle-CMV vector, pShuttle.HisC-MART-1; rAd = recombinant adenovirus backbone. All other lanes were occupied by the selected clones. Red boxes highlight those clones that were identified as positive.

The rAds isolated from HEK293A or HER911 infections were amplified over a series of passages, and the virus titre of unpurified infectious stock was determined using a $TCID_{50}$ (or end-point dilution) assay, which was done in duplicate. The pp65 rAd viral titre was approximately 2.43 x 10^9 plaque-forming units/ml (pfu/ml), while the MART-1 rAd was almost 10 fold lower at 3.11 x 10^8 pfu/ml.

Two cell lines were selected to evaluate recombinant protein expression for bulk protein production purposes, namely HeLa cells and A549 cells. A preliminary infection of these cell lines was performed using the final passage of the respective rAds. Cells were grown to confluency (approximately 1.5 x 10^6 cells/ml), and infected using three MOI values (MOI 50, 100, 150). These values were relatively high, given that the virus was unable to replicate in the chosen cell lines. Expression of the respective proteins was assessed using western blot analysis. While A549 cells produced large quantities of pp65 (Figure 2.14a) and detectable amounts of MART-1 protein (Figure 2.14b), there was no production of protein in HeLa cells. This was surprising, given the common use of this cell line for recombinant protein production, but was possibly due to the use of a high passage number of HeLa cells. This could potentially affect its ability to produce the recombinant protein.

Overall, the rAd expression system produced better recombinant protein yields than the stably-expressing cell line system, making it a more adequate expression system for our purposes.

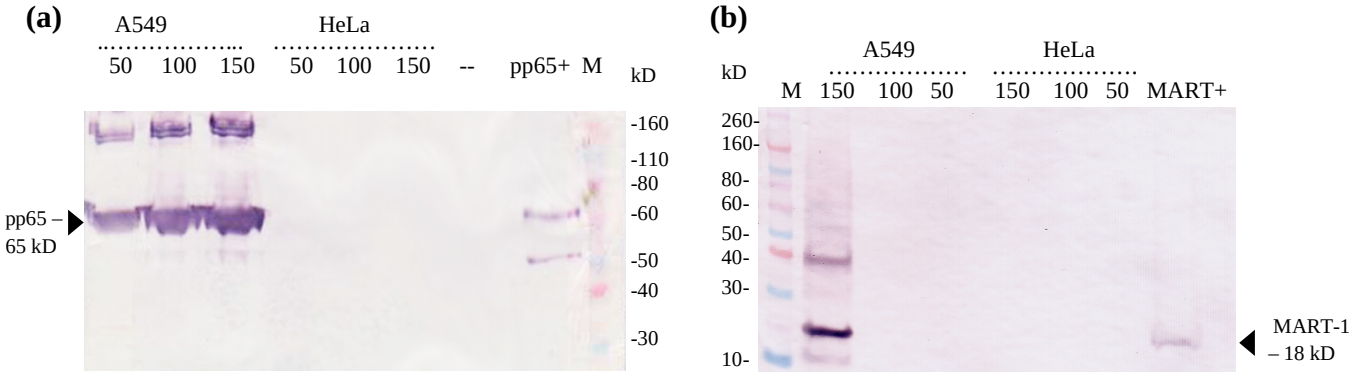


Figure 2.14 - Western blots of pellet lysate samples from HeLa and A549 cells after infection with rAdpp65 (a) and rAdMART-1 (b) for 48 hrs. Black arrow heads indicate the expressed proteins of interest being detected; CMV pp65 (65 kD) (a) and MART-1 (18 kD) (b). Monoclonal mouse anti-pp65 (a) or anti-MART antibody (b) (1:2000) and polyclonal goat anti-mouse antibody (1:5000) were used as primary and secondary antibodies respectively for western blots. M = standard protein marker. Positive control (designated with +) for pp65 and MART antigens were taken from samples isolated from transfections of HEK293A cells with pShuttle recombinant DNA.

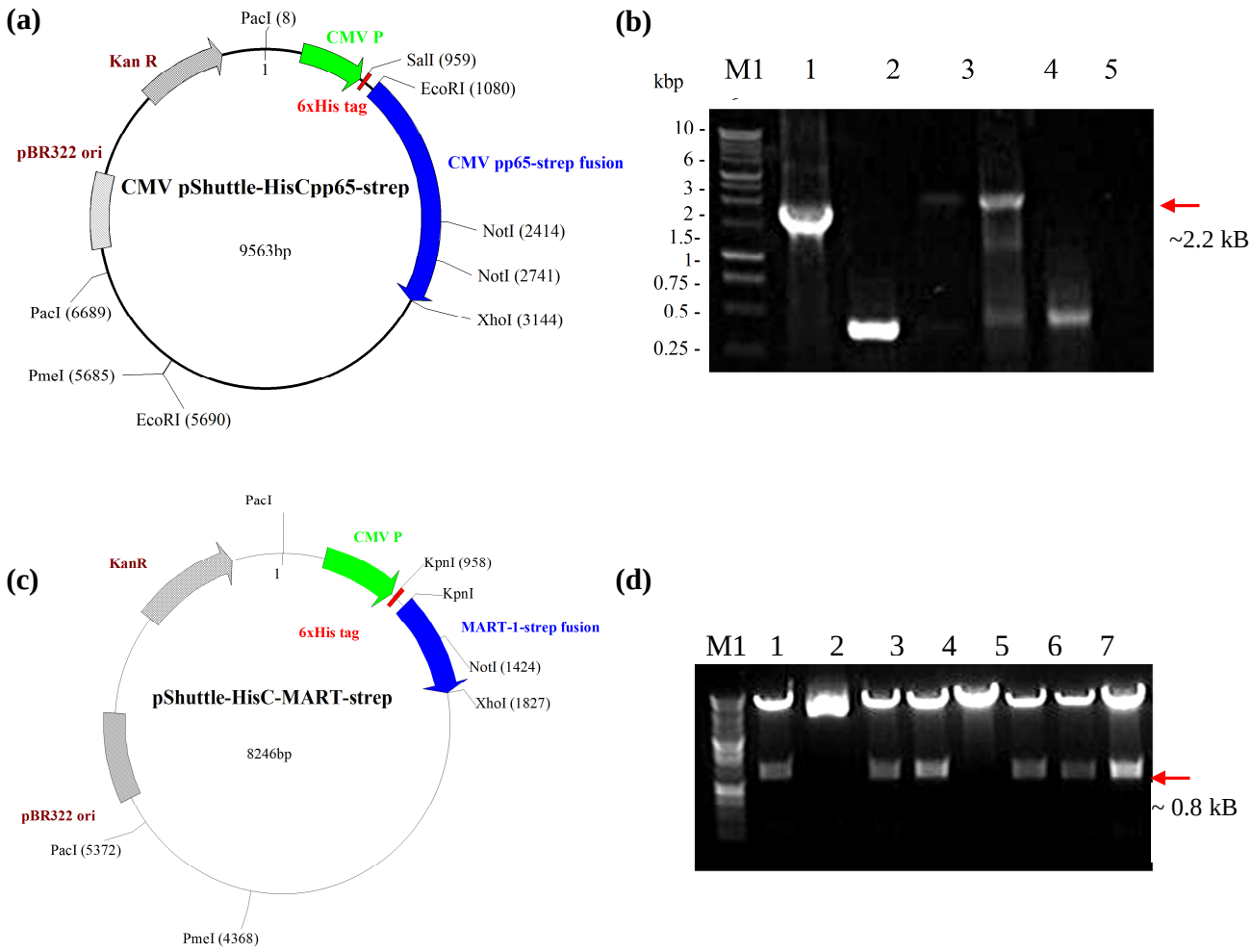


Figure 2.15 - Recombinant *pp65-streptavidin and MART-1-streptavidin* genes. (a) CMV pShuttle expression vector carrying the *Hispp65-streptavidin* fusion gene; (b) PCR products of the three OE-PCR reactions performed to produce fusion gene; Lanes: 1 - *Hispp65* gene (±1.7 kb) from PCR 1, 2 – *streptavidin* gene (±0.42 kb) from PCR 1, 3 –fusion gene product (±2.2 kb) of PCR 2, 4 – amplified fusion product from PCR 3 using 55 °C, 5 - amplified fusion product from PCR 3 using 65 °C, 6 – negative control for PCR 3 reaction. (c) Plasmid map of CMV pShuttle-HisC-MART-1, created by sub-cloning MART-1 into the plasmid in (a). (d) RE digestion using recombinant plasmid. Red arrows denote the fusion genes.

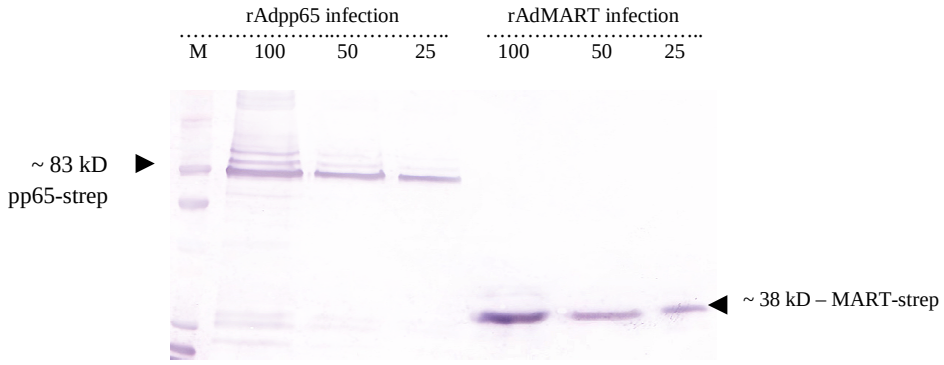


Figure 2.16 – Western blot from the pilot infection of HEK293A cells with rAdpp65-strep and rAdMART-strep (48 hr infection). Cell lysates expressing pp65-streptavidin (83 kD) and MART-streptavidin (38 kD) were detected with a primary anti-streptavidin antibody (1:5000) and a secondary goat-anti-mouse antibody (1:5000). Black arrow-heads indicate the expressed fusion proteins at their respective molecular weights.

2.3.5 Design and production of streptavidin-fusion vectors

The strong affinity of streptavidin for biotin makes it an excellent protein to exploit for the attachment of the respective antigens to biotinylated receptor antibodies. Hence, a fusion gene was designed to link His.pp65 to a single streptavidin unit in a similar method as utilized by Wang et al (Wang et al., 2007). An overlap extension PCR (OE-PCR) strategy (Figure 2.2) was employed to fuse the two genes together, which consisted of three PCR reactions. OE-PCR reaction 1 was designed to eliminate the stop codon in the first gene (*His.pp65*), and PCR 2 facilitated the fusion of the two genes so that the second gene (core streptavidin) could be read in-frame with the first gene. The final PCR reaction then amplified the fused product (Horton et al., 1989). As seen in Figure 2.15a and b, the *His.pp65-streptavidin (His.pp65-strep)* fusion gene was successfully produced and amplified. The conditions for PCR3 of the OE-PCR strategy required some initial optimisation to obtain the desired fusion product of 2.2 kb. At a high annealing temperature of 65 °C, a product of approximately 0.5 kb was produced, however by decreasing this temperature by 10 °C, the correct fusion product was obtained (lanes 4 and 5 in Figure 2.15b). The *His.mart-1-strep* fusion gene was created by a sub-cloning procedure using

the *His.pp65-strep* gene to join the *His.mart-1* and *streptavidin* genes. It was detected in several clones after restriction enzyme digestion of extracted recombinant plasmids (Figure 2.15c and d).

The *His.pp65-strep* and *His.mart1-strep* fusion genes were cloned into the pShuttle-CMV^{TM} vectors for production of recombinant adenoviruses. Intracellular staining was used to confirm expression of the respective fusion genes from recombinant pShuttle vectors, although results appeared to be ambiguous and therefore unreliable (data not shown). This was suspected to be a structural folding problem with the fusion proteins, rendering the detectable epitope difficult to access. Thus, we continued to produce recombinant adenoviruses as done with the model antigens. Infection of A549 cells using rAdpp65-strep and rAdMART-strep was performed, and expression of the respective proteins was investigated using western blot analysis (Figure 2.16). The production of both pp65-strep and MART-strep was detectable in infected A549 cells after three days of infection, at the expected molecular weights of 85 and 38 kD respectively. This confirmed the successful generation of rAd carrying the fusion genes, as well as that these genes expressed fusion proteins with a streptavidin core and antigen of interest, as detected with the primary anti-streptavidin and anti-antigen antibodies on the western blots. Recombinant adenoviruses carrying the fusion genes were propagated in HEK293 cells, and the virus titre of the unpurified infectious stocks were determined to be approximately 1.23×10^9 plaque-forming units/ml (pfu/ml) for rAdpp65-strep, and 2.4×10^8 pfu/ml for rAdMART-1-strep. All virus stocks were aliquoted and stored at -20 °C for future use.

2.4 Discussion

The antigens chosen for the *in vitro* DC stimulation experiments were CMV pp65 and MART-1. The full-length forms of these proteins were produced so that they could be used as model antigens to evaluate CD8+ T-cell induction via the cross-presentation pathway. Research has shown that while peptides are more efficiently presented to CD8+ T-cells in the short term, proteins or long peptides are potentially better vaccine candidates because they demonstrate persistent presentation over a longer period of time, and are not limited by MHC restrictions (Faure et al., 2009, van Montfoort et al., 2009).

As mentioned previously, mammalian expression systems were chosen to produce the respective proteins. Generation of a stably-expressing cell line was the first system explored. Research has shown that protein yields in mammalian stably-expressing cell lines are quite high, although lower than some of the other eukaryotic expression systems (Soares et al., 2000, Demain and Vaishnav, 2009). However, the levels of pp65 expression detected in the stable CHO and HEK293A clones generated in this study were inadequate for the bulk production of CMV pp65. Expression levels were poor, with amounts of expressed recombinant protein barely detectable via western blot, and not quantifiable. Research in the area of stably-expressing cell line production has suggested that the transgene integration site and copy number are some of the main influencing factors for the yields obtained from recombinant protein expression in stably-expressing cell lines (Chusainow et al., 2009, Kwaks et al., 2003). The point of transgene integration in the chromatin determines recombinant protein expression levels, where integration into heterochromatin (tightly packed areas/ chromatin) leads to poor expression, and integration into euchromatin (loosely packed chromatin) leads to high expression levels (Chusainow et al., 2009). This so-called 'position' effect (which can also result in gene silencing) could possibly account for the poor pp65 yields that were obtained here, as chromatin integration was assumed to occur randomly with the chosen pcDNA vector, according to the manufacturer. If this is the case, it may be of interest in future work in our laboratory to explore the use of cis-acting DNA elements such as anti-repressors or scaffold matrix associated regions (S/MAR), as these have been suggested as adequate tools to improve yield and stability of recombinant protein expression (Barnes and Dickson, 2006, Kwaks et al., 2003).

The clones isolated from both generated stably-expressing cell lines demonstrated loss of pp65 production over time, and despite some optimisation of the system, clones were unable to continuously produce pp65. This could be attributed to transgene instability, or stunted transcription of the recombinant gene due to silencing. Lack of stability of a transgene in a stably-expressing cell line expression system has been described before, and is mainly due to the heterogeneity of cell lines (such as CHO and HEK293) which results in the development of populations of transfected cells that produce varying amounts of transgenic protein (Kromenaker and Srienc, 1994, Browne and Al-Rubeai, 2007). High-producing cells have a lower growth rate owing to their greater levels of protein expression, and are therefore easily outgrown by the low-

or non-producing cells. This suggests that low- or non-producing pp65-cells may have been isolated with the high-producing cells, and outgrew the latter as the clones were passaged. This agrees with the data obtained, where the non-expressing clones demonstrated antibiotic resistance, despite negligible protein levels.

Past studies documenting stably-expressing cell line clones have involved monitoring hundreds of clones to identify those which appear to be expressing well and are healthy (Soares et al., 2000). Consequently, it is possible that if more clones were screened, a high-expressing clone could have been identified. However, given the laborious nature of screening clones, and the low-level pp65 expression from the clones that were tested, it was of interest to explore other expression systems.

The second expression system, using recombinant adenovirus production, was a much more promising means to produce the proteins of choice. The production of the recombinant adenovirus carrying the genes of interest was a less time-consuming task than generating a stably-expressing cell line, in addition to producing higher protein yields. Previous research showed that a number of mammalian cell lines have been utilized for recombinant protein expression using rAds, including the packaging lines themselves (Garnier et al., 1994, Zhong et al., 2006). Thus, initially the packaging cell lines, HEK293A and HER 911 cells, were considered for protein expression. These cells were eventually decided against, due to the risk of purifying replication-competent adenovirus with the protein of interest (Havenga et al., 2008). Furthermore, because of the lytic life cycle of adenovirus in the packaging cell lines, protein expression can be fairly limited in these cells. This was not a problem in other cell lines because the virus was not able to replicate after infection, but it did mean having to use a larger amount of infectious virus. HeLa and A549 cell lines were evaluated as non-packaging expression lines for pp65 and MART-1 production. A549 cells were able to successfully produce adequate quantities of pp65 and MART-1 post rAd infection, but no recombinant protein was detected in HeLa cells. This has been attributed to the high passage number of cells that were used for the pilot experiment. Although we could have evaluated a lower passage number of HeLa cells, this was unnecessary given the high levels of expression in A549 cells. Thus, we went on to use A549 cells to produce the recombinant proteins.

Differences in protein yield between pp65 and MART-1 were significant, but this is to be expected given the variety of factors that influence protein expression, specifically relating to the recombinant virus clone, the infected cells and the protein itself.

Consequent to the successful use of the recombinant AES to express the model antigens, it was also used to generate the streptavidin-fusion proteins. These proteins were produced in order to explore an alternative means of targeting antigens to DCs, taking advantage of the strong affinity between streptavidin and biotin. The initial difficulty in detecting the fusion proteins using intracellular staining could be attributed to inaccessibility of the epitope targeted by the primary staining monoclonal antibody due to unusual folding, or perhaps due to the processed antigen accumulating in the endoplasmic reticulum (ER), as has been shown with other fusion proteins (Mascola et al., 1996). Despite the initial difficulty to detect the fusion proteins, the recombinant adenovirus infections demonstrated detectable production levels of both fusion proteins, and potentially good yields in A549 cells for future large-scale production of the fusion proteins.

Overall, the production of both the model antigens and fusion proteins were produced intact and in detectable amounts using the AdEasy expression system. This system was therefore used for large scale production of all the respective proteins.

Chapter 3

Large scale production of model antigens and creation of antigen-antibody conjugates

3.1 Background and aims

3.1.1 Factors influencing large scale recombinant protein production in mammalian expression systems

The expression of recombinant proteins can be affected by several factors. Some of the major external factors that have been identified when using a mammalian-based cell expression system include the cell line employed, cell density, multiplicity of infection (MOI), infection time, medium contents, temperature, osmolarity and pH (Nadeau et al., 1996, Garnier et al., 1994). In general, pilot expression studies are performed before bulk production of recombinant proteins, so as to identify the influencing factors on protein production, and determine the optimal conditions for production in the chosen expression system. Every expression system has varying factors that appear to primarily affect protein production, and these are the factors that are focussed on in optimising production, while other conditions are kept constant. As an example, Nadeau et al (Nadeau et al., 1996) assessed the effect of a few factors on recombinant protein expression in mammalian cell systems, and found that pH and osmolarity had pronounced effects on expression levels. Specifically, acidification of the growth medium, led to significantly decreased protein production, while increased osmolarity resulted in the recombinant protein production peak shifting from 48 to 72 hours post infection (hpi). Previous work in our laboratory identified MOI, time post infection, and selected cell line as major determinants in influencing recombinant protein production using the rAd expression system (pers. comm.: Dr Timos Papagatsias, Imperial College London). Therefore these factors were further investigated for the large scale production of recombinant proteins in this study.

As others have shown, a high MOI generally demonstrates a high recombinant protein production, although once the expression system becomes saturated, the level of production

remains fairly constant, even as MOI increases (Hu et al., 2008). This saturation point has to be determined empirically as it differs from protein to protein. Similarly with infection time, its effects on recombinant protein production can vary quite substantially, depending on the efficiency of the transduction process and stability of the cell line used. While a minimum of 6 hours is necessary before any detectable protein production under the CMV promoter is observed, recombinant protein expression levels only peak around 48-72 hours in rAd packaging cell lines (Massie et al., 1998b). Given that non-packaging cell lines are able to continue to produce recombinant protein until they are limited by other factors, they can potentially produce better expression levels at later times, although this needs to be further investigated. Finally, cell lines also differ in their capacities to express recombinant proteins, specifically in a rAd expression system, where a number of cell lines can be utilised, including the rAd packaging cell lines (293A and HER 911 cells), or non-packaging mammalian cell lines such as HeLa, CHO or A549 cells (Gaillet et al., 2007, Shiver et al., 2002, Vieira et al., 2009).

Thus, to produce high yields of the model antigens for immunogenicity work in this study, it was necessary to look at the most favourable conditions for production of the model antigens and fusion proteins, based on the above factors.

3.1.2 Protein-protein conjugations

The biopharmaceutical industry has highlighted a growing need to simply and accurately conjugate proteins to secondary components for their use in medical and biological processes, such as increasing the immunogenicity of peptides for vaccine purposes (by linking them to carrier proteins), or labelling antibodies with fluorescent markers/other molecules, for diagnostic/research purposes. There are currently several cross-linking agents available that can be used to chemically conjugate proteins to each other, many of which are bifunctional (contain two reactive groups), and therefore allow the cross-linking of one protein to another via the side chains of particular amino acids (Carlsson et al., 1978). Some of these agents include glutaraldehyde (links proteins at their N-termini non-specifically, and involved in polymerisation of proteins), succinimide esters (links the free amino group of one protein to a cysteine residue of another protein), periodate (allows attachment to carbohydrate groups of proteins), and

isothiocyanate (used to label antibodies with fluorochromes) (Kluger et al., 2010). Heterobifunctional agents, which have reactive groups that interact with two different functional groups on the proteins, allow for a more controlled inter-cross linking reaction, and are consequently preferred (Carlsson et al., 1978). Succinimide esters are some of the most commonly used heterobifunctional reagents, primarily based on the stability of the resulting conjugates and the ability to control conjugation formation (Carlsson et al., 1978, Kluger et al., 2010). The production of such chemical conjugates has been shown in many recent studies, including that of Sancho et al (Sancho et al., 2008), where tumour antigens were covalently coupled with a DC receptor-specific antibody using a succinimide ester, and used to elicit strong tumour-specific CTL responses in mice.

In addition to chemical conjugations, the use of genetically fused proteins has emerged as another successful means to couple proteins. Idoyaga et al (Idoyaga et al., 2008) genetically fused OVA to the heavy-chain of a langerin-specific antibody in order to target the protein to Langerhans cells, and successfully did so, inducing CD4+ and CD8+ specific T-cell responses. Furthermore, as mentioned in Chapter 2, researchers have also looked at the genetic fusion of molecules such as streptavidin to proteins, as a means to direct biotinylated molecules to specific sites *in vivo* (Lin et al., 2006, Wang et al., 2007).

In view of these and several other methods to direct various molecules towards specific cells *in vivo* and *in vitro*, the work here explores a few approaches to target certain receptors on the surface of DCs. In particular, this chapter describes the production of the reagents needed for these receptor-targeting approaches, including the necessary optimisation and purification procedures of their production.

3.1.3 Aims of chapter

(i) To investigate which conditions are most suitable for the production of the model antigens and fusion proteins, specifically evaluating four MOI and infection time conditions.

(ii) To produce and purify large quantities of these proteins.

(iii) To conjugate purified pp65 protein to certain DC-receptor-specific antibodies and their isotypes.

(iv) To produce a biotinylated pp65 protein and confirm its functionality.

3.2 Materials and methods

3.2.1 Dose/time trial and protein production

A549 cells were seeded into TC 6-well plates and incubated at 37 °C in 5 % CO_2 until 80-90 % confluent. They were then infected in a volume of 2.5 ml and incubated using specific doses of recombinant virus infectant and incubation times (Figure 3.1), so as to determine the optimal dose (as measured by MOI) of rAd to use, and the time post infection to incubate the cells before harvesting the proteins of interest. It is important to note here that the MOI values used were particularly high, given that the cell line chosen was not a packaging cell line. Also, efficiency of adenovirus infection can be markedly influenced by the concentration of the virus in the inoculum. At the designated time point for the respective wells, cells were harvested using trypsinisation and stained intracellularly for pp65 or MART-1 to evaluate recombinant protein expression (see section 2.2.9.1 for primary and secondary antibodies used). The dose/time trial was repeated three times for reproducibility purposes.

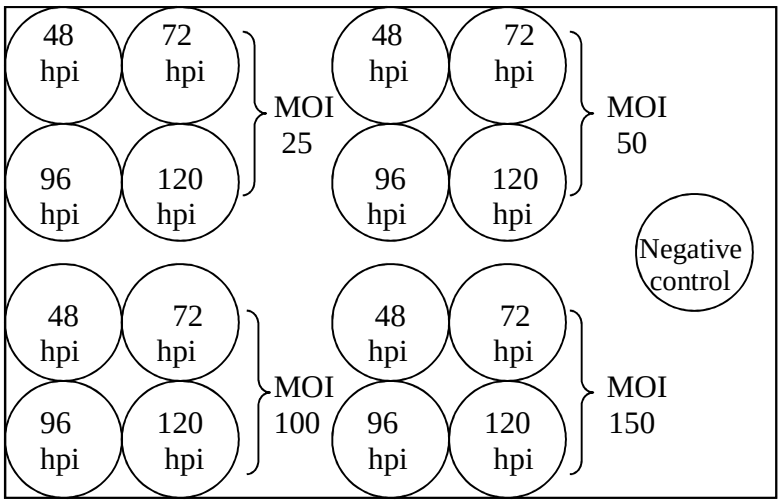


Figure 3.1 – A diagram depicting the dose-time trial set-up for pp65 as an example. Four wells of each 6-well plate were infected with respective rAd using the MOI shown, and two were designated as negative controls/uninfected wells. The trial experiments were done to investigate the optimal conditions for recombinant protein production via rAd infections. Hpi: hours post infection (incubation time); MOI: multiplicity of infection.

Once the optimum dose and incubation time were determined, 50 T175 cm^2 TC flasks (containing cells of 75-90 % confluency) were infected with the recombinant adenovirus in a volume of 8 ml, and incubated at 37 °C in 5 % CO_2. At the determined harvest time, cells were trypsinised and pelleted by centrifugation. Cell pellets were stored at -80 °C for further processing.

3.2.2 His-tag protein purification

The respective recombinant proteins were purified using a Nickel-nitrilotriacetic acid (Ni-NTA) purification kit (Invitrogen). Three purification conditions (native, denatured and hybridisation) were described in the manufacturer's instructions, and all were tested to find the optimum conditions to use for the respective recombinant proteins. Briefly, each process involved incubation of the cell pellet lysate and Ni-NTA-conjugated agarose beads in a column for approximately 30-40 min at room temperature under shaking conditions. The beads were then washed several times with buffers of varying pH and imidazole concentration (to elute attached protein off the beads), where the final buffer was the elution buffer and contained the highest concentration of imidazole. The procedures were performed according to the manufacturer's instructions with a few exceptions: (i) denatured cell lysate was centrifuged at 4000 rpm for 20 min, not 3000 x g for 15 min, (ii) the native buffer wash before elution was only repeated twice and not three times, and (iii) beads were always recharged before each purification to maximize recombinant protein isolation. All steps were performed under sterile conditions. The isolated protein fractions were stored (short-term) at 4 °C for further use. Samples were taken for western blots, SDS-PAGE (see section 2.2.9) and protein quantitation assays, to quantitate and verify purity of the isolated protein.

3.2.3 Protein quantification

To quantify the purified protein, standard bicinchoninic acid (BCA) assays (Pierce) were performed as described in the manufacturer's instructions. The NanoDrop 1000

spectrophotometer was used to measure the absorbance of samples at 562 nm. A standard curve was plotted based on BSA standards of 0.025 – 2.0 mg/ml. The percentage of total soluble protein (% TSP) was also determined using BCA assay as follows:

$$\% \text{ TSP} = \frac{\text{(Total amount of purified protein from all fractions)}}{\text{(Amount of protein in cell lysate before purification)}} \times 100$$

3.2.4 Protein dialysis and concentration

Protein dialysis and concentration was performed using a 20-30 U-tube concentrator (Merck) according to the manufacturer's instructions. Briefly, the U-tube concentrator was washed once with 70 % ethanol (to sterilise) and twice with native purification buffer (from the Ni-NTA purification kit), by centrifugation at 4000 rpm for 15 min each time. Fractions containing the recombinant protein were then pooled, placed in the top compartment of the concentrator, and centrifuged at 4000 rpm for 20 min. Filtrate was removed, native purification buffer was added to the top compartment to dilute the concentrated protein and sample was re-centrifuged at 4000 rpm for 20 min. This step was repeated twice to eliminate the salts and unwanted smaller molecules (such as imidazole). Glycerol was added to the concentrated sample (approximately 500 µl) to a final concentration of 20 %, and samples were snap-frozen using dry ice and stored at -80 °C.

3.2.5 Protein-antibody conjugates

Receptor-specific antibodies and CMV pp65 were conjugated using a protein-protein cross-linking kit (Pierce), following manufacturer's instructions. Briefly, the procedure involved modifying the lysine residues to thiols on the antibody molecule of interest, using succinimidylacetylthioacetate (SATA), and adding thiol-reactive maleimide groups to the model antigen using succinimidyl trans-4-(maleimidylmethyl) cyclohexane-1-carboxylate (SMCC). Once the two proteins were activated in this way, they were purified separately, and then allowed to react with each other to form a stable thioether bond between them (Figure 3.2).

Approximately 0.5-1 mg of each protein was added to the initial activation reactions, and they were combined in a 20:1 ratio of antigen to antibody. Utilised receptor-specific antibodies are shown in Table 3.1. The final conjugated product was stored in 15 % glycerol at -80 °C.

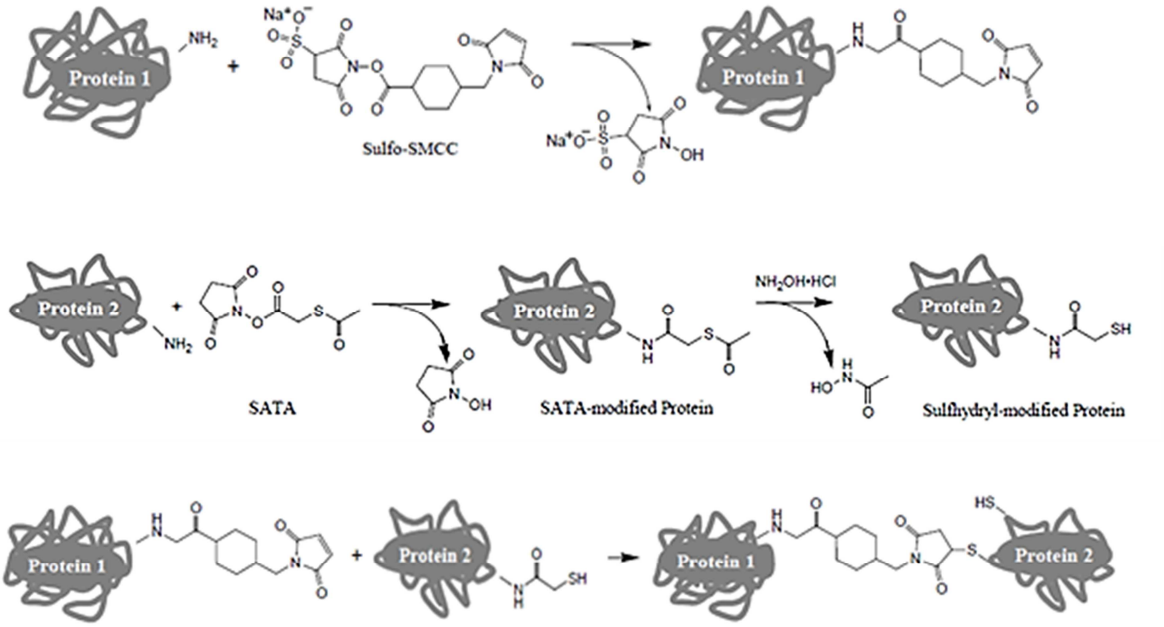


Figure 3.2 – Chemical conjugation of two proteins in a three-step process using a protein-protein cross-linking kit (derived from Pierce datasheet).

Table 3.1 – Biotinylated anti-human antibodies used in chemical conjugation reactions

Antibody	Clone	Isotype	Supplier
DEC205	MG38	Mouse IgG2b	eBioscience, UK
MMR	15-2	Mouse IgG1	Cambridge Biosciences, UK
DC-SIGN	eB-h209	Rat IgG2a	eBioscience, UK

3.2.6 Biotinylation of model antigen

CMV pp65 was biotinylated using an EZ-Link Sulfo-NHS-biotinylation kit (Pierce). A calculated amount of 10 mM Sulfo-NHS-Biotin was added to CMV pp65 (0.5 mg) and incubated for 60 minutes at room temperature. The mixture was then passed through a pre-supplied desalting column to recover the biotinylated protein and remove any existing reactants. Biotinylated samples were stored at 4 °C.

3.2.7 Enzyme-linked immunosorbent assay (ELISA)

Enzyme-linked immunosorbent assays (ELISA) were used to confirm the functionality of the core streptavidin in the fusion proteins produced, as well as to verify that the biotinylation of pp65 had occurred. Flat-bottomed 96-well plates (NUNC) were used to prepare samples. When testing the streptavidin functionality, diluted samples of purified pp65-streptavidin and MART-streptavidin (1:10) were added to wells in triplicate (100 µl per well). Three sets of wells were allocated for each test sample, so that 3 biotinylated-antibody concentrations could be tested (10, 5 and 1 µg/ml). The plate was incubated at 4 °C overnight then washed six times with 0.05 % Tween-PBS the next day. This was followed by and incubation for 2 hrs in blocking buffer (Sigma-Aldrich, UK), before another six washes with 0.05 % Tween-PBS. The antibody was then added to the respective wells at the above mentioned concentrations for 1 hr. The antibody used was a biotinylated mouse anti-human IgG1 antibody (eBioscience). Plates were washed again with 0.05 % Tween-PBS six times, followed by the addition of streptavidin-horse radish peroxidase (streptavidin-HRP) (Pierce) at a dilution of 1:5000 (in blocking buffer), for 30 min. There was a final 6-time wash with 0.05 % Tween-PBS, before the addition of 100 µl TMB substrate (Sigma-Aldrich, UK). The plate was stored at room temperature in the dark for approximately 5-10 min before 50 µl of 10 % H_2SO_4 was added to stop the reaction. An Anthos 2020 ELISA plate reader (Anthos Labtec) was used to detect the results at a wavelength of 450 nm within 10 min of adding the stopping solution.

3.2.8 Statistical analysis

GraphPad Prism V5 software was used to perform two-way ANOVA on the dose-time trial data, applying a Bonferroni post-test to correct for the number of comparisons made.

3.3 Results

3.3.1 Large scale recombinant protein production

After confirming the expression of all recombinant proteins using western blot analysis, factors affecting large scale production of these proteins were considered. Although a number of different factors influence recombinant protein expression, previous work in our laboratory determined cell line, multiplicity of infection (MOI) and infection/incubation time to be primary influencing factors. From the pilot expression experiments (section 2.3) A549 cells were chosen as an adequate expression cell line. Dose/time trials were therefore performed to determine the most suitable conditions for pp65, MART-1, and the fusion proteins' production in A549 cells. Four MOI values and four incubation times were selected, in order to evaluate the concentration of virus needed and the incubation time necessary for optimal protein production. MOI values were determined using previous $TCID_{50}$ data (see section 2.3). All other factors were kept constant, and confluent A549 cells were infected accordingly. A lower set of MOI values were evaluated for MART-1 and fusion gene expression compared to pp65 expression, due to the lower titre of these recombinant viruses. At the appropriate times, cells were harvested and intracellular staining analysis was used to determine the levels of pp65 or MART-1 production. The experiment was then repeated twice.

As can be seen in Figure 3.3, pp65 and MART-1 expression was detected in all samples tested, although expression levels varied substantially among replicates. In general, the results of the pp65 trial showed a positive correlation between MOI and pp65 expression. Expression levels seemed to plateau at the highest MOI, with similar levels measured for MOI 100 and 150, and with significant differences observed in pp65 expression between 48 and 96 hpi at MOI of 100 (13.5 % and 35.8 %; MFI of 8.7 and 40.1) (Figure 3.3a and b).

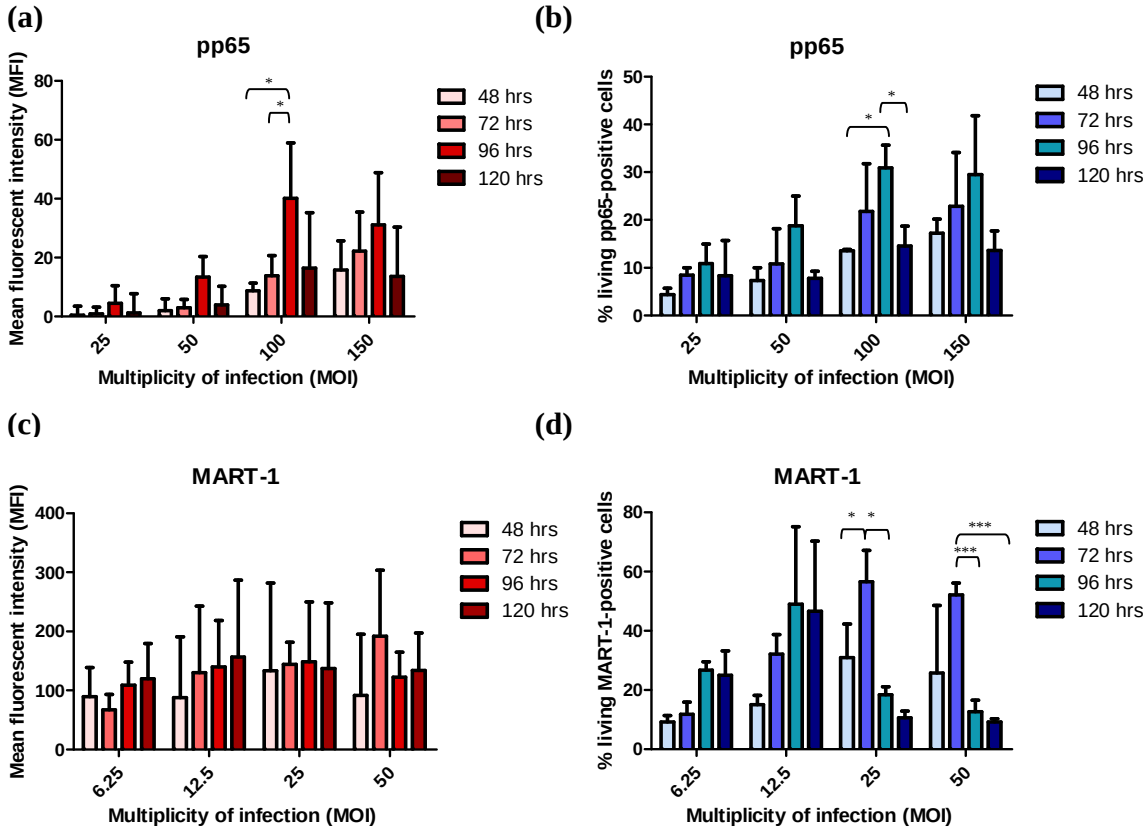


Figure 3.3 – The dose/time trial performed in A549 cells to determine the optimal MOI and harvesting time for bulk CMV pp65 and MART-1expression. Intracellular staining was used to evaluate the expression of pp65 (a and b) and MART-1 (c and d) in the rAd-infected cells. (a) Percentage expression of CMV pp65 by infected A549 cells; (b) Mean fluorescence intensity (MFI) of CMV pp65-expressing cells displayed by infected A549 cells; (c) Percentage expression of MART-1 by infected A549 cells; (d) MFI of MART-1-expressing cells displayed by infected A549 cells. The data was normalised by subtracting background levels of expression (from A549 cells alone) from all data points. All values displayed are mean values (n=3) ± S.D. * , ** , *** , denotes $p < 0.05$, $p < 0.01$ and $p < 0.001$ respectively, as analysed by two-way ANOVA and Bonferroni post-test.

*

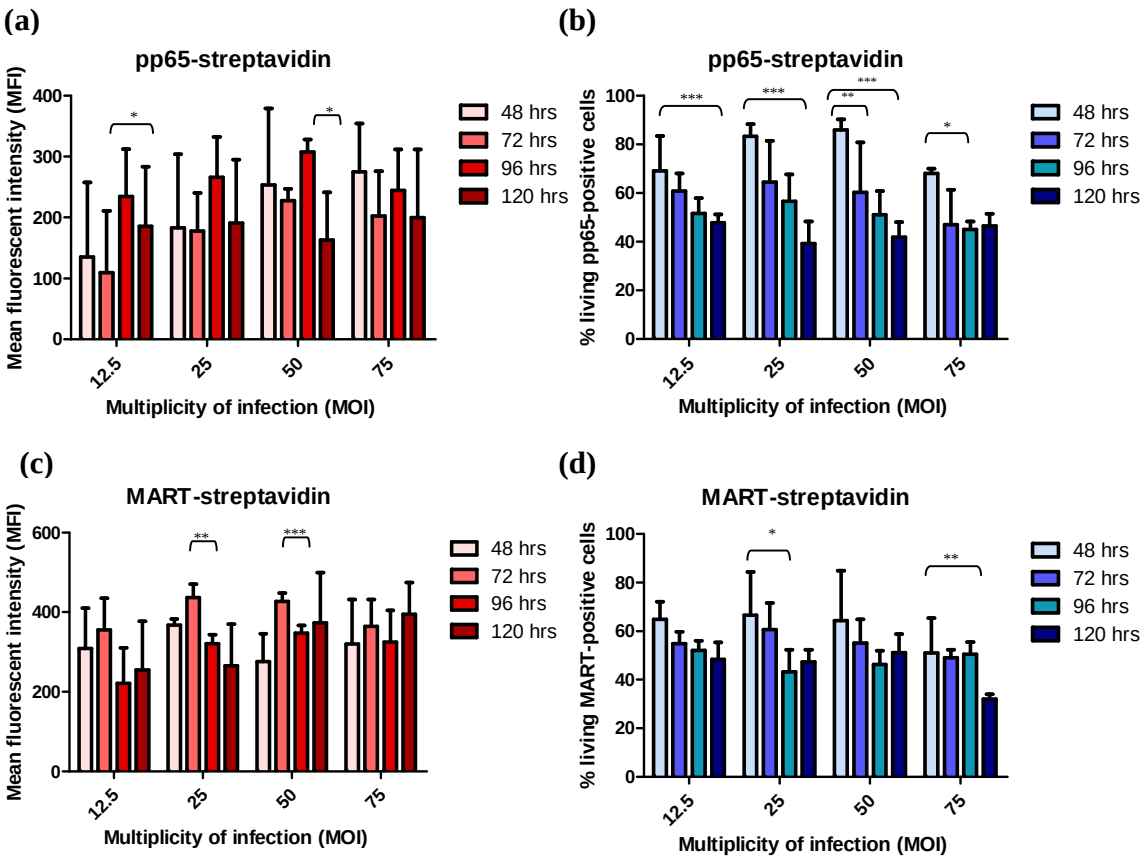


Figure 3.4 – The dose/time trial performed in A549 cells to determine the optimal MOI and harvesting time for bulk pp65-streptavidin and MART-streptavidin expression. Intracellular staining was used to evaluate the expression of pp65 (a and b) and MART-1 (c and d) in the rAd-infected cells. (a) Percentage expression of pp65-streptavidin by infected A549 cells; (b) Mean fluorescence intensity (MFI) of pp65-expressing cells displayed by infected A549 cells; (c) Percentage expression of MART-streptavidin by infected A549 cells; (d) MFI of MART-1-expressing cells displayed by infected A549 cells. The data was normalised by subtracting background levels of expression (from A549 cells alone) from all data points. All values displayed are mean values (n=3) ± S.D. * , ** , *** , denotes $p < 0.05$, $p < 0.01$ and $p < 0.001$ respectively, as analysed by two-way ANOVA and Bonferroni post-test.

An incubation time of 96 hours post infection (hpi) was most favoured at all MOI values, specifically at MOI 100, while in some cases, 72 hpi was also adequate in terms of levels of protein produced (21.8 %). Unexpectedly, the expression levels at 120 hpi were almost as low as the results of 48 hpi (7.8 % and 7.3 % respectively at MOI 50), suggesting that either protein degradation within cells was occurring after 96 hours, or infected cells had died. The percentage of cells expressing pp65 and the expression level of pp65 in cells on average (as indicated by the MFI) seemed to be highest at 96 hpi for MOI of 100 or 150 (Figure 3.3a). Conditions of 96 hpi and MOI 100 were thus selected as the conditions for bulk pp65 production (Table 3.2).

Similarly, MART-1 expression was also low at 120 hpi and high MOI values, although the drop in MART-1 expression occurred as early as 96 hpi at high MOI values (12.7 % compared to 25.4 % at 48 hpi). MART-1 expression significantly peaked at 72 hpi using a MOI of 25, with an average of 56.9 % of live-expressing MART-1 cells being detected. The MFI data did not indicate significant differences between the conditions tested for MART-1 expression, and thus the conditions chosen for bulk MART-1 expression (Table 3.2) were determined by the percentage of MART-1-positive cells (Figure 3.3d).

Relatively high variability in protein expression was observed for pp65-streptavidin and MART-streptavidin production as well (Figure 3.4). In general, there were greater percentages of cells positively expressing the fusion proteins than the pure antigens, indicating the fusion proteins were well expressed. However, unlike the pure antigens, the MFI and percentage of positive-expressing cells did not correspond in the dose-time trials of the fusion proteins. In the case of pp65-streptavidin, the percentage of positively-expressing cells decreased as hpi increased, although MFI values were generally high, and not significantly different as time increased (Figure 3.4 a and b). This suggested that, even though percentages of positively-expressing cells were between 40 and 60%, the higher hpi values were either resulting in cell death or malfunction. The significantly lower number of positively-expressing cells as MOI and time post infection increased (Figure 3.4b), indicated that the favoured conditions for expression was to use a relatively low MOI value and hpi to produce the protein (Table 3.2).

Similar to pp65-streptavidin, infection with recombinant adenovirus carrying MART-streptavidin displayed comparably high MFI values for all conditions, as well as a reduction

in the percentage of positively-expressing cells as time and MOI increased (although this appeared to be less pronounced than was observed for pp65-streptavidin) (Figure 3.4c and d). Thus, a low MOI and infection time point seemed appropriate for MART-streptavidin expression as well (Table 3.2).

The MOI values used in the fusion protein trials were considerably lower than what was used for pp65 expression, and yet cell viability seemed to have been negatively affected with the fusion virus infections. That being said, the chosen conditions seemed adequate to produce good yields of the recombinant proteins, and were therefore used for large scale production of the proteins.

Table 3.2 – Optimal conditions for recombinant protein production in a rAd-A549 expression system, based on pilot dose-time trials

Recombinant proteins	**Conditions for protein production**	
	MOI	**Infection time (hpi)**
pp65	100	96
MART-1	25	72
pp65-streptavidin	50	48
MART-streptavidin	25	72

3.3.2 Purification of recombinant proteins

A Ni-NTA (anti-His tag) column kit was used to purify the proteins of interest. Before the bulk production of the proteins, the purification procedure was optimized so that the yield and purity of the isolated proteins would be as high as possible. Three purification protocols were tested to establish the most suitable method to isolate the respective proteins. The protocols described a native (the protein maintains its native conformation throughout purification), denaturation (the protein is denatured before purification, and is eluted in denatured form) and hybridisation purification (the protein is denatured before purification, and is eluted in native form). These protocols mainly differed in salt concentrations and pH conditions, as these factors were used to manipulate the conformation of the protein for purposes of exposing the His tag and encouraging protein attachment to the column agarose beads.

Figure 3.5a depicts the resulting fractions from a native purification of pp65 (isolated from 293A cells). While the purity seemed to be adequate, the yield seemed poor compared to what was seen in cell lysate samples before purification. This was possibly because the His tag may not have been entirely accessible with the protein folded in its native conformation, and this is supported by the results of the denaturation purification (Figure 3.5b) where pp65 was detected in all fractions and more pp65 appeared to be eluted. Unfortunately, denaturing the protein also resulted in pp65 cleavage products occurring (detected at approximately 50 kD), suggesting denaturing the protein was not ideal, despite the better yields. The hybridisation purification seemed to provide a good balance between obtaining a good yield and high level of purity, without destroying the integrity of pp65 (Figure 3.5c). Consequently, this seemed to be the best purification procedure for pp65. Purification optimisations for the other proteins revealed the same procedure was sufficient for the other proteins, and was therefore used for all purifications.

Once the dose-time trial and purification optimisation was complete, large scale production of the proteins of interest were carried out. A549 cells were grown in bulk (50 T175 TC flasks per virus, with cells at a confluency of 80-90 %), and were infected using the chosen conditions for the respective recombinant adenoviruses. Harvested cells were pelleted and stored at -80 °C for further processing. Purification of the harvested, infected cell-pellets was carried out in two sets (approximately $4x10^7$ cells). Samples underwent chemical cell lysis and were then added to a Ni-NTA (anti-His tag) column.

For pp65 purification, large quantities were isolated at a relatively high level of purity in the eluted fractions 2-7 (Figure 3.6a). Although there was some aggregated pp65 and smaller pp65 bi-products detected, the majority of the protein detected was whole, intact pp65. The quantity of pp65 in the fractions compared to the lysate suggested a large percentage of the expressed protein was successfully purified, but a small amount of the protein was lost in the wash buffers (Figure 3.6b). Additionally, the Coomassie-stained SDS-PAGE data indicated a high purity of the fractions compared to the wash buffers, with pp65 at 65 kD being the only protein detected (Figure 3.6c).

MART-1 purification did not yield high protein production, with only fractions 2 and 3 of the purification providing detectable amounts of MART-1 (Figure 3.7a and b), but these were

relatively pure according to the Coomassie-stained SDS-PAGE data (Figure 3.7c). There were noticeable amounts of MART-1 in lysate and wash buffers, indicating that either the purification required additional optimisation, or that smaller proteins such as MART-1 are not purified as effectively as larger proteins (Figures 3.7b and c). Further optimisation did not appear to improve the yields, implying that the latter explanation was more likely.

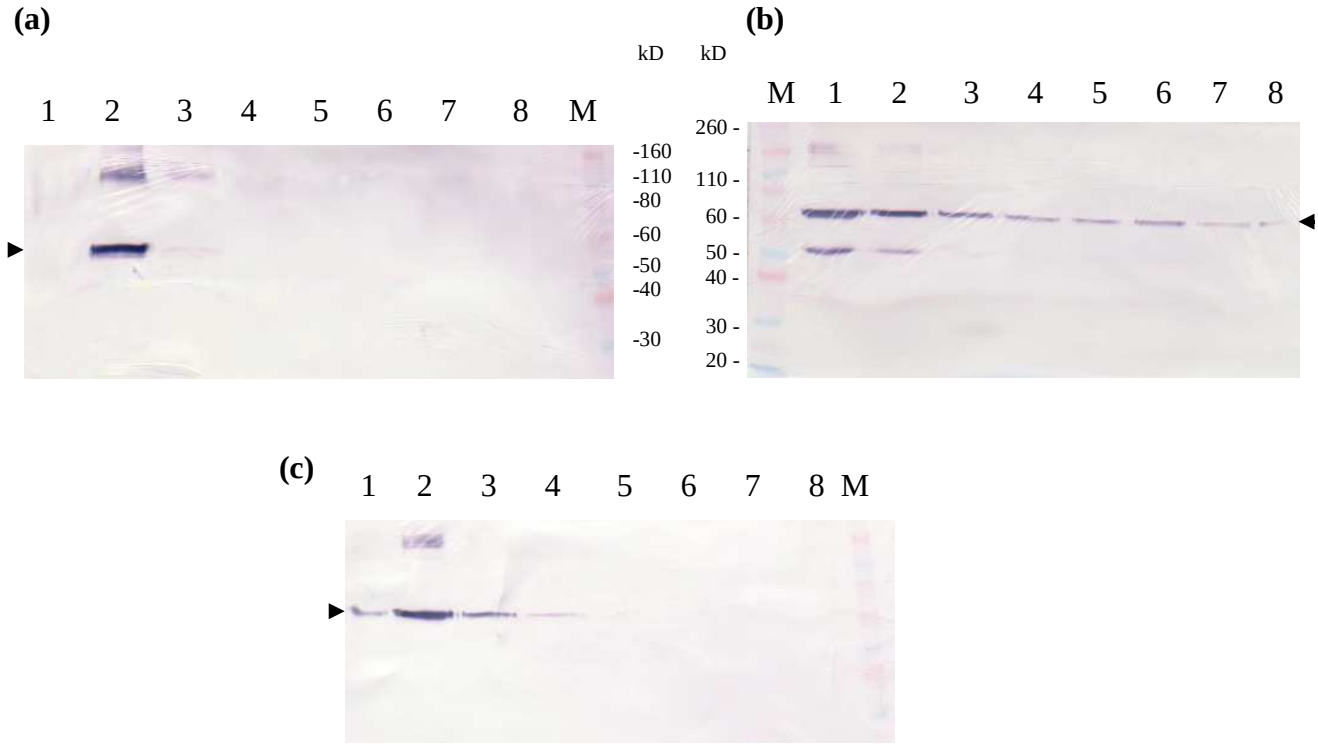


Figure 3.5 – Western blot analysis of His tag optimisation experiments for CMV pp65 using (a) native, (b) denaturation or (c) hybridisation purification conditions. Lanes: 1-8 = fractions 1-8 that were eluted from the Ni-NTA column under the respective conditions. Monoclonal mouse anti-pp65 antibody (1:2000) and polyclonal goat anti-mouse antibody (1:5000) were used as primary and secondary antibodies respectively for western blots. M = molecular weight protein marker used for all blots (weight markings are depicted for (a) and (c), but also applicable to (b)). Black arrow heads indicate pp65 detected at a molecular weight of approximately 65 kDa.

In the case of the fusion proteins, recombinant protein was detected in all fractions, but most prominently in the first four (Figure 3.8a and b). Purity of fusion proteins were relatively high, with the fusion protein band prominently detected on the Coomassie-stained SDS-PAGEs (Figure 3.8c and d). There were small quantities of cellular protein detected at approximately 65 kD in both pp65-strepavidin and MART-streptavidin purified samples, but in negligible quantities compared to the proteins of interest.

To quantify protein in the fractions isolated after dialysis and concentration, a standard BCA assay was used. Approximately 3-7 µg/ml pp65 protein (a total of 8.2 mg) and 1.6-2 µg/ml MART-1 protein (a total of 2.9 mg) were detected per purification. For pp65 samples, this accounted for approximately 6-20 % of the cell lysate's total soluble protein (TSP), while for MART-1, it only accounted for 3-12 % TSP.

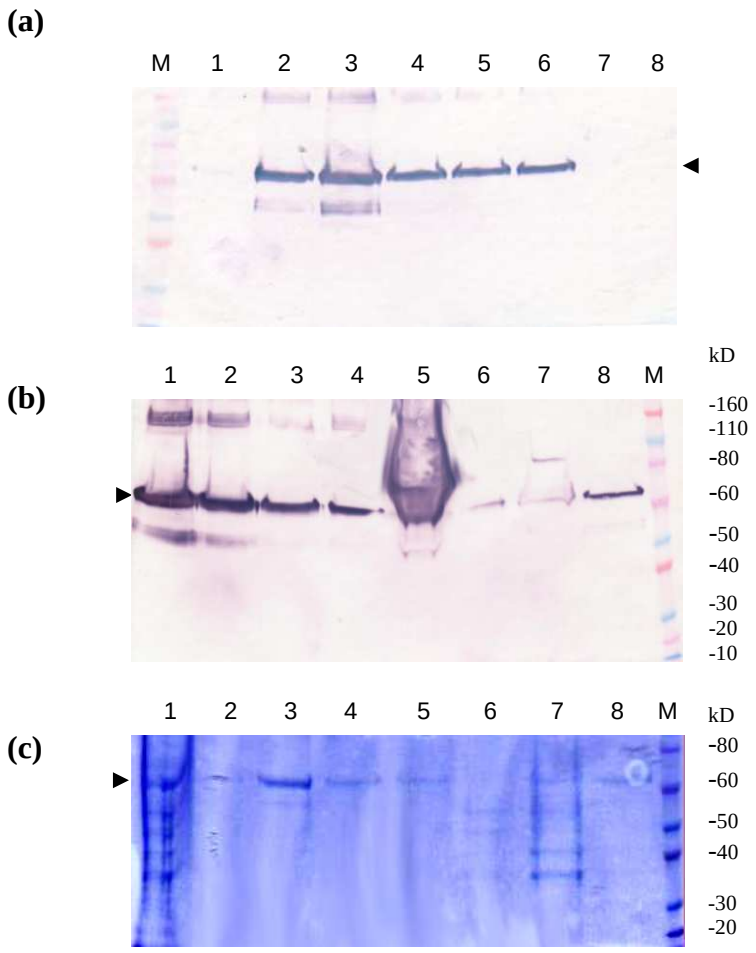


Figure 3.6 – Western blots (a and b) and Coomassie-stained SDS-PAGE (c) of purified CMV pp65 extracted from A549 cells (5 x 10^7 cells) using a Nickel-NTA (anti-His-tag) column. Lanes: (a) 1-8 – collected fractions 1-8. (b) 1-4- fractions 2-5, 5 - cell lysate before purification, 6- first wash of Nickel column after protein binding, 7- second wash of column, 8- final wash (before elution). (c) 1- cell lysate before purification, 2-5- fractions 1-4, 6- first wash of Nickel column after protein binding, 7- second wash of column, 8- final wash (before elution). Monoclonal mouse anti-pp65 antibody (1:2000), and polyclonal goat anti-mouse antibody (1:5000) were used as primary and secondary antibodies respectively for western blots. M = protein molecular weight marker (weight markings are depicted for (b) and (c), but are also applicable to (a)). Black arrowheads indicate pp65 at 65 kD.

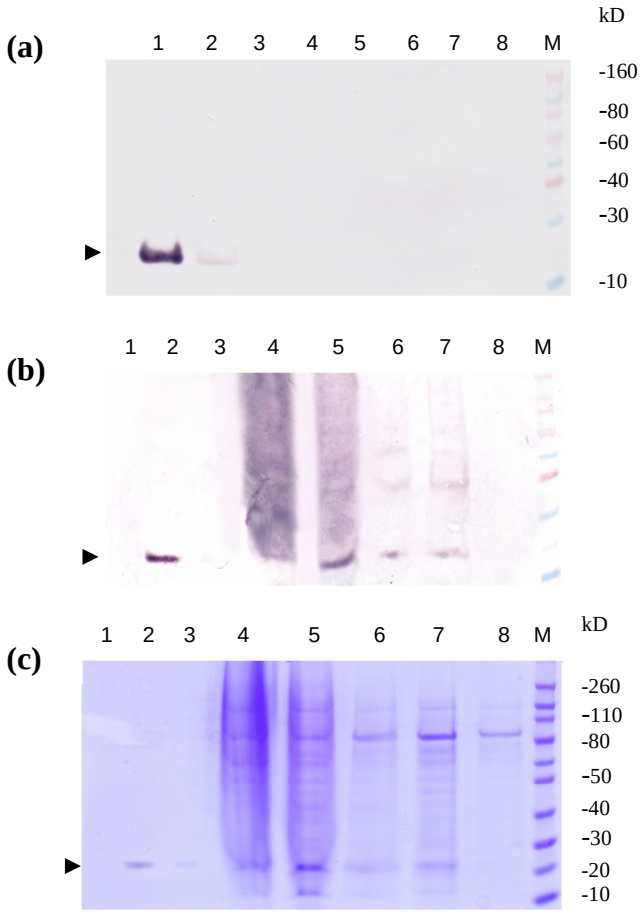


Figure 3.7 – Western blots (a and b) and SDS-PAGE (c) of purified MART-1 extracted from A549 cells (5 x 10^7 cells) using a Nickel-NTA (anti-His-tag) column. Lanes: (a) 1-8 – collected fractions 1-8. (b) 1-3- fractions 1-3, 4 - cell lysate before purification, 5- lysate after protein-agarose binding, 6 – first wash of Nickel column after protein binding, 7 – second wash of column, 8 - final wash (before elution). (c)1-3 - fractions 1-3, 4 - cell lysate before purification, 5 – lysate after protein-agarose binding, 6 - first wash of Nickel column after protein binding, 7 – second wash of column, 8 - final wash (before elution). Monoclonal mouse anti-MART-1 antibody (1:1000), and polyclonal goat anti-mouse antibody (1:5000) were used as primary and secondary antibodies respectively for western blots. M = protein molecular weight marker marker (weight markings are depicted for (a) and (c), but are also applicable to (b)). Black arrow heads indicate MART-1 band at approximately 18 kD.

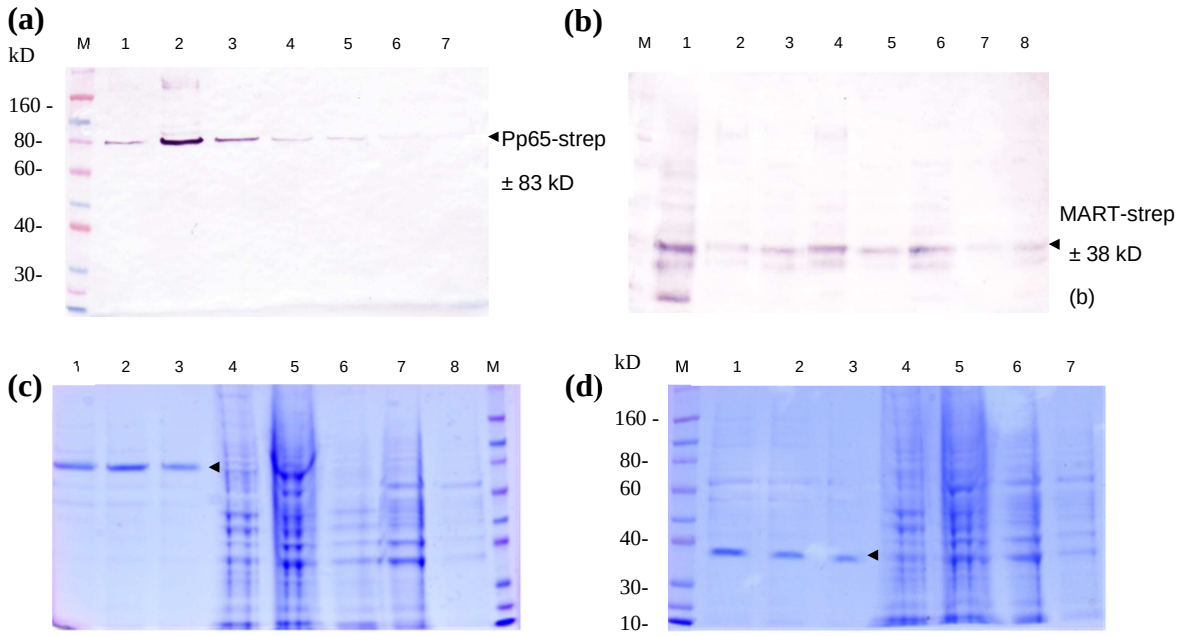


Figure 3.8 - Western blots (a and b) and Coomassie-stained SDS-PAGE (c) of purified pp65-strepavidin (a and c) or MART-streptavidin (b and d), extracted from A549 cells (5 x 10^7 cells) using a Nickel-NTA (anti-His-tag) column. Lanes: (a) 1-7 – collected fractions 1-7. (b) 1-8 – collected fractions 1-8. (c)1-3 - fractions 1-3, 4 - lysate after protein-agarose binding, 5 - cell lysate before purification, 6 - first wash of Nickel column after protein binding, 7 – second wash of column, 8 - final wash (before elution). M = protein molecular weight marker (Invitrogen). (d) 1-3 - fractions 1-3, 4 - lysate after protein-agarose binding, 5 - cell lysate before purification, 6 - first wash of Nickel column after protein binding, 7 – second wash of column. Monoclonal mouse anti-streptavidin antibody (1:2000) and polyclonal goat anti-mouse antibody (1:5000) were used as primary and secondary antibodies respectively for western blots. M = protein molecular weight marker used (weight markings are depicted for (a) and (d), but are also applicable to (b) and (c)). Black arrow heads indicate protein bands, pp65-streptavidin (± 83 kD) and MART-streptavidin (± 38 kD) respectively.

The fusion protein yields were similar to MART-1, with a total amount of approximately 5.1 mg and 3.2 mg of pp65-streptavidin and MART-streptavidin being purified respectively, and an average of 8 % TSP. Once purified, 15 % glycerol was added to the protein samples and they were subsequently stored at -80 °C.

3.3.3 Conjugate protein production

Chemical conjugations between purified pp65 protein and the receptor-specific antibodies (or their isotype controls) was performed using a cross-linking kit that formed a thiol-ester bond between the heterologous proteins. Initially, optimisation of this chemical process was required, exploring the effect of changing molar ratios of the respective proteins, removing a desalting step, as well as changing the order in which the proteins were activated before

conjugation. After initial failure to detect a conjugate, optimisation of the procedure resulted in conjugation of biotinylated antibodies specific for DEC-205 (CD205), MMR (CD206) and DC-SIGN (CD209) to pp65 protein. Proteins of approximately 215 kD were detected on a western blot following conjugation in the unreduced samples (Figure 3.9a). Reduced samples displayed prominent bands at 25 kD (molecular weight of V_L chain of antibody) and 52 kD (molecular weight of V_H chain of antibody) due to dissociation of the antibody chains. Bands detected in the IgG negative control appeared to be because the IgG antibody was mouse-derived, and therefore reacted with the goat anti-mouse secondary antibody. After the successful conjugations with these antibodies, their respective isotype control conjugates were also produced, and all conjugates were purified via a His-tag column, using the native purification protocol (Figure 3.9b). After purification and concentration of the conjugates, there did appear to be a significant loss of yield of the conjugated proteins, with approximately 200-280 µg/ml detected in BCA assay analysis (20-28 % of initial pp65 used, and approximately 300 µg in total). This was a significant loss in conjugate yields; however, enough protein was produced for use in later experiments. The resulting conjugates appeared to be the prominent product detected in the conjugation reaction as seen in the Coomassie-stained SDS-PAGE data with fairly high purity (Figure 3.9c). All conjugates were stored at 4 °C to prevent degradation of antibody component.

3.3.3 Production of biotinylated pp65

Purified pp65 protein was biotinylated using a standard kit. It was then desalted and concentrated. Biotinylation of pp65 was confirmed using a western blot with an anti-biotin primary antibody (Figure 3.10). BCA analysis revealed that approximately 220 µg/ml biotinylated pp65 was purified (total of approximately 500 µg), which accounted for 44 % of the original pp65 used initially.

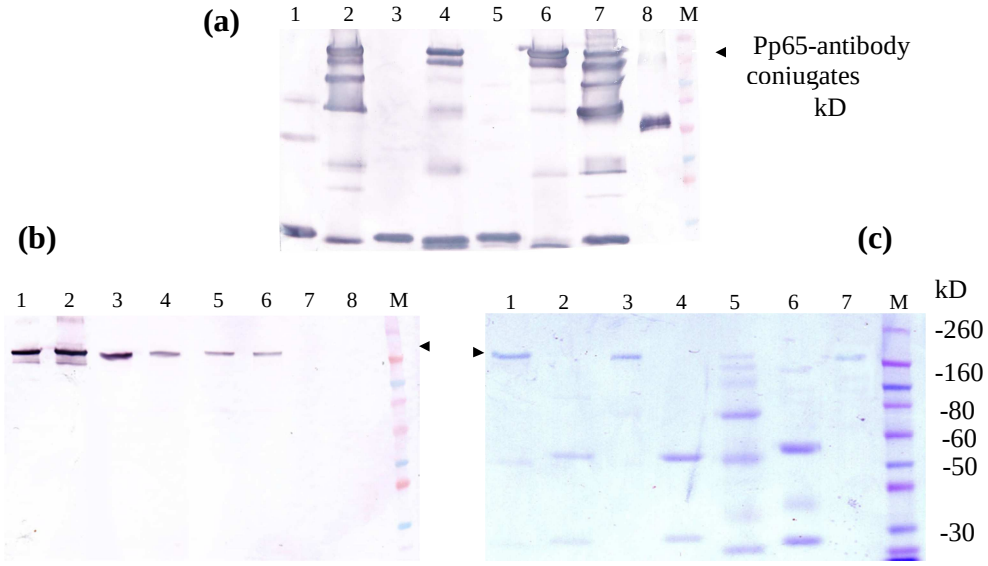


Figure 3.9 – Western blot (a and b) and Coomassie-stained SDS-PAGE (c) analysis of pp65-antibody chemical conjugates. (a) Detection of conjugates after production. Lanes: 1 – reduced DC-SIGN-pp65 conjugate, 2 – unreduced DC-SIGN-pp65 conjugate, 3 – reduced MMR-pp65 conjugate, 4 – unreduced MMR-pp65 conjugate, 5 - reduced DEC205-pp65 conjugate, 6 - unreduced DEC205-pp65 conjugate, 7 – reduced IgG antibody (control), 8 – pp65 protein (+ive control). (b) Conjugates after a His-tag purification. Lanes: 1 – unreduced DEC205-pp65 conjugate, 2 - unreduced MMR-pp65 conjugate, 3 - unreduced DC-SIGN-pp65 conjugate, 4 – unreduced IgG1-pp65 conjugate, 5 – unreduced IgG2a-pp65 conjugate, 6 – unreduced IgG2b conjugate, 7 and 8 = blank. (c) Conjugates after His tag purification. Lanes: 1 – unreduced DEC205-pp65 conjugate, 2 – reduced DEC205 -pp65 conjugate, 3 – unreduced MMR-pp65 conjugate, 4 – reduced MMR-pp65 conjugate, 5 - reduced IgG antibody (control), 6 – reduced DC-SIGN-pp65 conjugate, 7 - unreduced DC-SIGN-pp65 conjugate. Monoclonal mouse anti-pp65 antibody (1:2000) and polyclonal goat anti-mouse antibody (1:5000) were used as primary and secondary antibodies respectively for western blots. Reduced samples included β-mercaptoethanol reducing agent in loading buffer compared to the unreduced samples, which did not. M = protein molecular weight marker (weight markings are depicted for (c), but are also applicable to (a) and (b)). Black arrow heads indicate respective proteins.

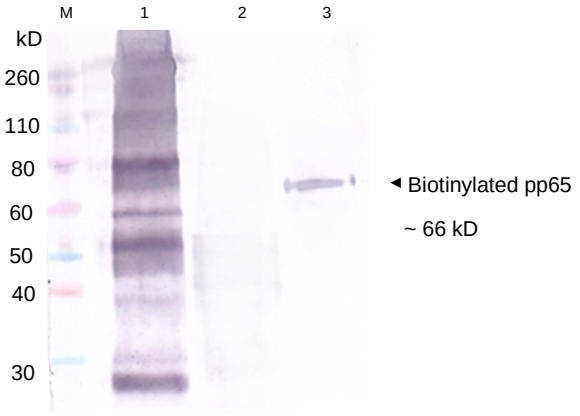


Figure 3.10 – Western blot analysis of biotinylated pp65. Lanes: 1 – biotinylated CD5 antibody (positive control), 2 – flow-through from de-salting column after protein desalting, 3 – desalted, purified biotinylated pp65. Monoclonal mouse anti-biotin antibody (1:2000) and polyclonal goat anti-mouse antibody (1:5000) were used as primary and secondary antibodies respectively for western blots. M = protein molecular weight marker. Black arrow heads indicates biotinylated pp65 protein.

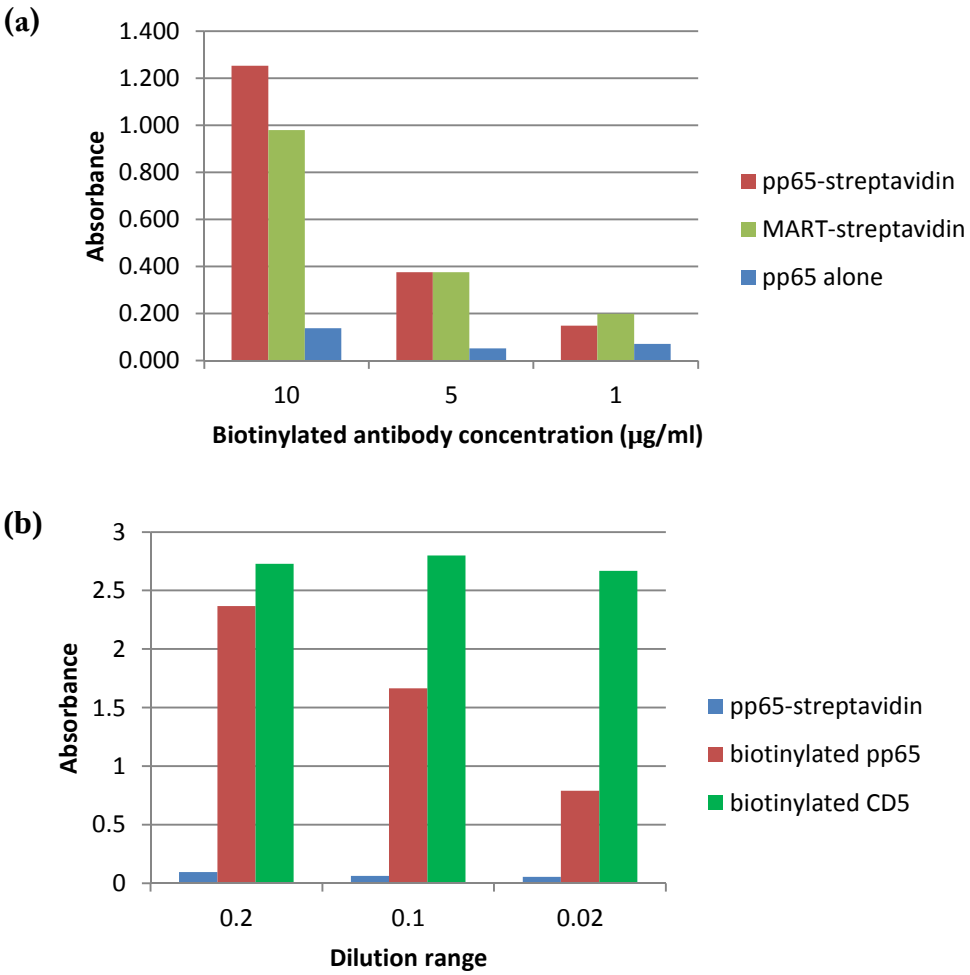


Figure 3.11 – ELISA analysis to evaluate functionality of streptavidin core in the created fusion proteins (a) and functionality of biotin in the biotinylated pp65 (b). All samples in (a) were 1 in 10 dilutions of stock protein samples, and the biotinylated antibody used was an IgG1 isotype antibody. (b) Positive control = biotinylated CD5 antibody; negative control = pp65-streptavidin.

3.3.4 Confirmation of functionality of streptavidin-fusion proteins and biotinylated proteins

To verify the functionality of streptavidin core and biotin on the respective, produced proteins, an ELISA analysis was carried out. With regard to the streptavidin fusion proteins, pp65-streptavidin and MART-streptavidin, both appeared to have a high affinity to the biotinylated antibody at all tested concentrations compared to pp65 alone, as would be expected (Figure 3.11a). Lower dilutions of the proteins of 1 in 50, and 1 in 100, were tested with the same result (not shown), confirming that the streptavidin core in the fusion proteins was able to attach to biotin. The biotinylated pp65 sample similarly demonstrated its affinity to streptavidin in the ELISA analysis compared to pp65-streptavidin (negative control) (Figure 3.11b), verifying that the biotinylation process was a success.

3.4 Discussion

Before bulk production of the proteins of interest, the optimal conditions for expression were evaluated in a number of small scale experiments, so as to produce the maximum yield in the most efficacious manner. As with other expression systems, the production of a given recombinant protein using a recombinant adenovirus expression system is dependent on several variables that affect quality and quantity of the resulting protein. In particular, cell line, MOI, and infection or incubation time were the determining factors for the production of the model antigens and fusion proteins in this study.

Research has shown that significant yields of recombinant protein can be obtained when using AES and the packaging cell line 293A, for expression purposes (Vieira et al., 2009, Nadeau et al., 1996). However, the lytic nature of the rAd infection limits long term (more than 24 hrs) recombinant protein production post infection in packaging cell lines, and there is the danger of generating replication-competent virus. Additionally, purified protein preparations are also more likely to be contaminated with virus proteins if produced in the packaging cell lines. These disadvantages are avoided by use of a different cell line, while still maintaining a good recombinant protein yield. Massie et al (Massie et al., 1998a) demonstrated this, obtaining recombinant protein production of as much as 15-20 % of total cellular protein in A549 and HeLa cells, both of which are non-packaging cell lines. Given

the high levels of expression of pp65 detected in A549 cells compared to HeLa cells in the pilot infection experiment in Chapter 2 of this study, this cell line was selected for large scale protein production.

We show here that the optimal MOI and infection time for recombinant protein production varied between the different proteins expressed. In general, the MOI provides the means to control a rAd infection, as the higher the MOI (within reason), the more viral particles there are available to infect one cell (Flint et al., 1999), and therefore the better the infection and recombinant protein production efficiency. However, while high MOI values theoretically mean a potentially high yield of recombinant protein, they can be problematic for two reasons. Firstly, using high MOI values requires greater quantities of infectant to be used, especially if the infection is done on a large scale. Secondly, even though the virus is unable to replicate in A549 cells, rAd infection is still able to stunt growth and productivity of the cells. This means that a MOI that is too high could be potentially detrimental to the system, hindering the ability of the cell to efficiently produce protein. This seemed to be particularly true for the MART-1, MART-streptavidin and pp65-streptavidin expression levels, where all three proteins were preferentially expressed at one of the lower MOI values tested, an MOI of 250. In particular, the MOI values used in the fusion protein trials were considerably lower than what was used for pp65 expression, and yet cell viability seemed to have been negatively affected with the fusion virus infections. These data suggests that the addition of streptavidin to the proteins induced higher expression levels, but also hindered cellular processes to some extent, perhaps by the fusion protein aggregating in ER (Mascola et al., 1996). In hindsight, it would therefore have been of interest to have assessed cell viability before harvest, and perhaps explored lower MOI values, to be able to obtain the expected sigmoidal expression curve that can be seen with the pp65 expression.

Unusually, pp65 production did not appear to decrease as MOI increased, even though much higher MOI values were assessed. It is possible that this is related to a low infectivity ability of the virus expressing pp65, and this is supported by the lower MFI values observed in this dose-time trial compared to that of the other proteins. It is important to note that the efficacy of the viral infections is related to the concentration of virus surrounding the cells, and therefore the high MOI values used here may not have been entirely necessary, had lower infection volumes been used, or more concentrated virus. However, given that unpurified virus was used for all infections, the final concentration of virus was relatively low, and may

have accounted for why such high MOI values could be used for pp65 infection, without adversely affecting cells. In addition, MOI for all viruses was calculated using 293A cells, as these cells lyse during the $TCID_{50}$ assay, allowing the evaluation of infectious viral titre to be easily calculated. It is possible that MOI differs from cell to cell, and thus what appears to be a high MOI for 293A cells (for example, MOI 150), may not have necessarily been the true MOI for A549 cells. This means that the MOI values chosen here were more of a point of reference to decide on an appropriate amount of virus to use for bulk production, rather than an accurate evaluation of MOI.

The infection/incubation period seemed to affect protein expression quite dramatically, with a consistent drop in recombinant protein detection at 120 hpi, except for MART-1 expression, which began falling as early as 96 hpi. All recombinant genes were controlled by the CMV promoter, and were transiently expressed independently of the viral infection. Even though this was the case, the expression profiles were quite different for the four recombinant proteins in terms of the effect that infection time had on expression. There was a clear decrease in expression of pp65-streptavidin as hpi increased, but an increase up to 96 hours for pp65 expression, and no significant differences for MART-streptavidin production at different time points. There are several possibilities why such variations were observed, related to virus potency, protein size, protein degradation, stunted cell productivity, or premature cell death. The early decrease in MART-1 expression and the unusually high MFI of rAd-MART-1-infected cells suggests that the latter two arguments may be valid for rAd-MART-1 infection, as large quantities of MART-1 protein production possibly affected cell growth and metabolism. This also seems to be true in the case of pp65-streptavidin, where high MFI values were observed despite the negative correlation between the percentage of positively-expressing cells and hpi. This indicated that, even though percentages of positively-expressing cells were between 40 and 60%, the prolonged infection time was either resulting in cell death or malfunction. More data is required to determine what factors are primarily affecting expression of the other proteins, but collectively, the varying expression profiles observed goes further to reiterate the need for empirical data to assess influencing factors on recombinant protein expression for individual proteins.

Once expressed in bulk using the optimal conditions, recombinant protein purification was optimized successfully to maximize final protein yields. There was a fair amount of recombinant protein loss after purification, but the yields and level of purity of the

recombinant proteins were relatively good, and sufficient for future experiments. While large scale batch (bioreactor) cultures can produce up to 90 μg/ml of recombinant protein using an AES, most small laboratory large-scale protein production systems provide between 5-7 μg/ml (Garnier et al., 1994), indicating that the expression levels of MART-1 (1.6-2 μg/ml) were average, but that of pp65 (3-7 μg/ml) was relatively high. The fusion protein yields were unexpectedly low compared to pp65, given the data of the dose /time trials. This was perhaps because the exposure of the His tag to agarose beads was limited, possibly due to a steric interference from the additional streptavidin core on these proteins. The fusion proteins could also have been aggregating due to the ability of streptavidin to form tetramers. This could have masked the His tag, and prevented attachment to the column. Lichty et al (Lichty et al., 2005) hypothesised such a problem for small, soluble aggregates that form in protein lysates, and showed decreased yields of isolated protein because the His tag was inaccessible. Alternatively, the poorer purification of the fusion proteins was perhaps related to the denaturation and renaturation of the protein in the hybridisation purification protocol. Matsumato et al (Matsumoto et al., 2011) suggested something similar in their study, describing lower than expected yields of a streptavidin-fusion protein because of problematic re-folding of the protein. Despite the lower purified yields, the quantities of the fusion proteins that were purified here were adequate for the purposes of this study.

After purification, the proteins were used to create the targeting reagents needed for this study. Chemically conjugated proteins/peptides to receptor-specific antibodies are commonly used as a reagent to target particular cell types *in vivo* (Ramakrishna et al., 2007, Sancho et al., 2008, Bonifaz et al., 2002). While there appear to be many types of conjugations, the most adaptable method is via succinimide esters, which allows the coupling of two unrelated proteins, regardless of their side groups. This method was thus employed to create the chemical conjugates here, for one of the four DC targeting strategies to be explored. The chemical conjugates were successfully created by a fairly simple procedure, and detected at the correct molecular weights. However, there was a significant decrease in yield after purification. The extensive loss of pp65-antibody conjugates is possibly explained by the large size of the conjugates, and potential partial His-tag concealment because of the size. In addition, the poorer yields generally obtained from the native purification protocol may have contributed to this loss (as shown in Figure 3.5). The presence of several other bands (including those of the reactants) detected faintly in the final product, suggested that there was perhaps a heterologous mix of protein species, as has been noted in other studies (Pagel

et al., 2006). These species were difficult to separate from the required products, and it is something to bear in mind for future experiments in terms of interference involving the targeting of receptors.

As mentioned earlier, one of the targeting strategies included the use of genetically fused proteins with a slight variation on the genetic fusion approach. A versatile targeting reagent was created in the form of a genetic fusion of streptavidin to the antigen of interest. This offers a means to attach various biotinylated receptor-specific antibodies or biotinylated TLR agonists to the antigen in a simple process. Recent literature documenting the exploitation of such streptavidin-fusion proteins to target certain cells within the body has shown great promise. Wang et al (Wang et al., 2007) produced and characterized a bifunctional fusion protein that consisted of an antibody variable domain (recognizing the CA125 antigen of ovarian cancer cells) and core-streptavidin. *In vitro* testing of the fusion protein showed an ability to target biotinylated antigens and biotinylated liposomes to ovarian cancer cells very efficiently. In view of this, use of the streptavidin-fusion proteins created in this study, could open up many more DC targeting possibilities than originally planned, making it a potentially more beneficial system to use than the chemical conjugates.

Another approach to target DC receptors in this study makes use of biotinylated pp65. This method is one that is less straight forward than the two previously described. It also exploits the strong affinity between biotin and streptavidin, and involves the use of biotinylated antigen and biotinylated antibodies mixed in equimolar amounts, and added to anti-biotin magnetic beads. The idea behind this strategy is that the mixture containing the biotinylated antibodies, biotinylated antigen and anti-biotin beads allows the majority of beads to attach to both the antigen and antibody. The resulting antibody-antigen complexes would then be added to cells, and should theoretically allow the antigen to be targeted to specific receptors. This method has potential to be useful for *in vivo* applications, and is therefore worthy of exploration.

Overall, all reagents created were produced in satisfactory quantities and were determined to be functionally competent. The methods outlined above for targeting the produced antigens to surface DC receptors will be assessed individually and comparatively in experiments to come in Chapter 5 using these reagents. In view of the mix of advantages and disadvantages attached to the targeting schemes, it will be necessary to evaluate each method based on ease of production, efficacy, and versatility.

Chapter 4

Assessment of model antigen immunogenicity

4.1 Background and aims

4.1.1 Dendritic cell subsets

Monocyte-derived DCs (moDCs) were initially identified and described in 1994 (Sallusto and Lanzavecchia, 1994), and have since been the most commonly used human DC model, extensively studied with regard to phenotype and function. The ease of moDC generation and the abundance of their precursors in blood make them the ideal laboratory model. However, studies have suggested that moDCs may not be entirely reflective of the functionality of human myeloid DCs (mDCs) as previously thought (Proudfoot et al., 2007, Osugi et al., 2002, Patterson et al., 2005). These DCs are considered to be inflammatory DCs that are recruited to sites of inflammation rather than resident immature tissue DCs which would be the target of a HIV-1 vaccine (Naik et al., 2006). Thus, while moDCs are a useful means to understand the interactions of DCs with other immune cells, it is important to explore other human DC subsets, and determine whether they differ significantly from moDCs. Functional differences between DC subsets' have been highlighted in the literature (Duraisingham et al., 2009, Osugi et al., 2002), and could be in part a result of differences in the type of stimulation used, or the experimental protocol or criteria, amongst other factors. Due to limited current literature exploring DC targeting strategies in blood mDCs (CD1c+ mDCs), it is of interest to investigate the potential of these cells and moDCs to induce enhanced CD8+ T-cell responses, when stimulated by targeted foreign antigens.

4.1.2 Use of adjuvants

Adjuvants are able to enhance an immune response to a specific antigen through activation of antigen-presenting cells (APCs), and via induction of prolonged antigen presentation (Schwarz et al., 2003). Some studies have shown that without the presence of an adjuvant in addition to a foreign antigen, DCs can remain in steady state, and elicit tolerance to the

antigen, through the activation of T_{reg} cells (Bonifaz et al., 2002, Reis e Sousa, 2004). Thus, for vaccine purposes, it is important to include an adjuvant in order to fully activate DCs, and induce the appropriate T-cell responses.

Research has shown toll-like receptors (TLRs) to be particularly useful in this respect, given their responsiveness to pathogen-associated molecular patterns (PAMPs), and their ability to influence the type of immune response elicited (Th1 or Th2) based on the stimulatory molecules initiating the responses. Even with the similarities in signalling pathways induced by different TLR ligands, there are prominent differences in their adjuvant properties (Schwarz et al., 2003). In humans, it has been noted in several studies that TLRs 3,4,7 and 9 appear to be most effective in inducing Th1 responses, while TLR1, 2 and 6 are more capable of inducing Th2 responses (Mazzoni and Segal, 2004, Ramakrishna et al., 2007).

4.1.3 Aims of chapter

The general aim of this chapter was to verify that the purified CMV pp65 and MART-1 antigens were immunogenic and adequate for use *in vitro*. The capacity of different TLR ligands to influence antigens-specific T cell responses was also addressed. The specific aims of this chapter are as follows:

(i) To briefly characterise the DC subsets used in this study, looking specifically at purity and phenotype of cells.
(ii) To compare several adjuvants, and select the one best able to enhance T-cell responses.
(iii) To evaluate the immunogenic properties of pp65 and MART-1 via their ability to induce T-cell proliferation and cytokine production in DC-T-cell co-culture assays.
(iv) To characterise the phenotype and function of T-cells expanded using the model antigens as stimuli.

4.2 Materials and Methods

4.2.1 Cell culture media and buffers

For the maintenance of T-cells after DC-stimulation, RPMI-1640 supplemented with 10 % human AB serum (Sigma-Aldrich, UK), 2 mM L-glutamine, 100 IU/ml penicillin and 0.1 mg/ml streptomycin was used (all from PAA Laboratories GmPH, Austria). DC precursors were differentiated in culture medium consisting of RPMI-1640 supplemented with 10 % foetal calf serum (FCS) (PAA Laboratories GmPH, Austria), 2 mM L-glutamine, 100 IU/ml penicillin and 0.1 mg/ml streptomycin, 100 ng/ml GM-CSF (Granulocyte-Macrophage Colony Stimulating Factor), and 1000 U/ml IL-4. FCS was purchased heat-inactivated, however human AB serum was incubated at 56 °C for 30 min in order to inactivate it. For washing steps, RPMI-1640 Hepes modification (RPMI-Hepes) supplemented with 2 % FBS, 2 mM L-glutamine, 100 IU/ml penicillin and 0.1 mg/ml streptomycin was used. The percoll solution utilised in the separation of lymphocytes and monocytes was a 50 % percoll solution. Three percoll solutions were used in the blood cell separation protocol, and were made up as follows:

50 % percoll = 107 ml 70 % percoll solution + 43 ml Hanks balanced salt solution (HBSS) (Sigma-Aldrich, UK)
70 % percoll = 145 ml percoll (Sigma-Aldrich, UK) + 85 ml percoll mix
Percoll mix = 60 ml 10× PBS + 176 ml H_20

The freeze-mix solution utilised for long term cell-storage in liquid nitrogen was made up of 10 % dimethyl sulfoxide (DMSO) (Sigma-Aldrich, UK) in FCS.

For the incubation of cells with magnetic beads, magnetic-associated cell sorting (MACS) buffer was used, and consisted of sterile PBS supplemented with 2 % FCS and 2 mM ethylenediamine tetra-acetic acid (EDTA) (Roche Diagnostics, UK). The buffer required for washing and resuspension of cells to be used for flow cytometry was fluorescence-activated cell sorting (FACS) buffer, and consisted of sterile PBS supplemented with 2 % FCS, 2 mM EDTA and 0.1 % sodium azide. To fix cells after fluorescent staining, 2 % paraformaldehyde

(PFA - made up in 1 x PBS) was used. BD stabilizing fixative (BD biosciences, UK) was preferentially used for less stable fluorochromes.

4.2.2 Primary cell isolation and culture

4.2.2.1 Isolation of mononuclear leukocytes from whole adult blood

Leukocyte cones from healthy individuals were obtained from the National Blood Services (Colindale, UK). Each cone (approximately 20 ml) was equally divided into two 50-ml Falcon conical tubes. Blood sample was diluted 1:1 with 10 % FCS HEPES-RPMI modified medium. The diluted blood was underlaid with 15 ml lymphocyte separation medium (PAA Laboratories GmPH, Austria) and spun for 25 min at 2000 rpm (ROTINA 46, Hettich Zentrifugen) with no brake. Peripheral blood mononuclear cells (PBMCs) were subsequently harvested from the interface and washed twice with 50 ml of 2 % FCS HEPES-RPMI modified medium for 10 min at 1580 rpm. PBMCs were then either frozen for long-term storage or used for the separation of lymphocytes from non-lymphocytic cells.

4.2.2.2 Separation of PBMCs into lymphocyte and monocyte-enriched fractions

Percoll (50 %) was overlaid with isolated PBMCs and spun for 30 min at 300 rcf with no brake. The percoll interface (PI) (monocyte / DC-enriched fraction) and percoll pellet (PP) (lymphocyte enriched fraction) were harvested. Both PI and PP cells were washed twice with 50 ml of 2 % FCS-RPMI to remove any residual percoll. Cell viability was determined by trypan blue exclusion, prior to the cells being frozen and stored in liquid nitrogen. Briefly, cell count was determined by diluting cells 1:40 in trypan blue, loading 10 µl of the resulting dilution onto a disposable haemocytometer (Biostat, UK), and counting the number of total cells within nine of the smaller squares. Total cell count was calculated using the formula below:

$$\text{Total no. of cells} = \text{average cell count} \times 10^4 \times \text{dilution factor} \times \text{volume}$$

Fresh PI cells underwent further separation into CD14+ monocytes and/or CD1c+ mDC precursors (see below), before freezing. If not, PI and PP cells were resuspended in freeze mix at a cell density of approximately $10\text{-}50\times10^6$ cells/ml, and frozen overnight at -80 ˚C.

Samples were then transferred to liquid nitrogen storage, if they were not used directly after separation.

4.2.2.3 Generation of monocyte-derived dendritic cells (MoDCs)

Fresh PI cells were washed once in MACS buffer, while frozen PI cells were thawed at 37 °C and washed twice in 10 %-FCS RPMI media, and once in MACS buffer. Cell pellets were resuspended in MACS buffer and CD14+ cells were isolated using immunomagnetic anti-CD14 microbeads and MACS separation columns as per the manufacturer's instructions (Miltenyi Biotec, Germany). The purified CD14+ monocytes were cultured in 10 % FCS-RPMI with 100 ng/ml GM-CSF and 1000 U/ml IL-4 for 5-7 days at 37 °C and 5 % CO_2 to generate immature moDCs. Fresh cytokines were added after 2-3 days. Immature moDCs were phenotypically characterised and their purity was assessed based on a number of surface markers, detected using flow cytometry (Table 4.1a).

4.2.2.4 Isolation of $CD1c^+$ blood dendritic cells (myeloid blood DCs)

Blood myeloid DC precursors were isolated from fresh PI cells, which were washed once in MACS buffer upon isolation. Cell pellets were resuspended in MACS buffer and the human CD1c+ (BDCA-1+) DC isolation kit (Miltenyi Biotec, Germany) was used to purify myeloid DC precursors. Briefly, this involved a two-step isolation procedure of CD1c+ CD19- cells using immunomagnetic anti-CD19 beads, biotinylated anti-CD1c beads, FcR blocking reagent, anti-biotin beads and MACS LD and LS separation columns as per the manufacturer's instructions. The purified BDCA-1+ DCs were counted and 10^4 cells/well were added to 96-well U-bottomed plates. Cells were cultured in 10 % FCS-RPMI with 100 ng/ml GM-CSF and 1000 U/ml IL-4 for 2 days to allow differentiation into immature blood myeloid DCs (CD1c+ mDCs). These cells have the phenotype expected of immature tissue DCs. Immature CD1c+ mDCs were phenotypically characterised and assessed on purity based on a number of surface markers, detected using flow cytometry (Table 4.1a).

4.2.3 A*02:01 Human Leukocyte Antigen (HLA) type identification

A sample of PBMCs was taken from each cone before it underwent percoll separation, and cells were surface stained with HLA-A2 antibody (Table 4.1a) and analysed by flow

cytometry. Once a cone showed positive staining for HLA-A2, further tests were needed to determine if it exhibited an HLA-A*02:01 phenotype. In brief, approximately 1-5 × 10^6 PBMCs from the positive samples were stained with the CMV pp65 and MART-1 pentamers (ProImmune Ltd, UK). These pentamers bind to T cell receptors of a particular specificity, determined by the major histocompatibility complex (MHC) allele, which in this case is A*02:01 (see Table 4.1b). Pentamer staining was followed by a wash step and second step of staining with anti-CD19, CD3 and CD8 antibodies (Table 4.1a) as per manufacturer's instructions (ProImmune Ltd, UK). Cells were then fixed and analysed by flow cytometry. Samples displaying a population of pentamer-positive cells for both pentamers were deemed A*02:01-positive.

4.2.4 Purification of recombinant adenoviruses

Viruses were purified for use in cell culture assays using an Adenopure LS Adenovirus Purification Kit (Puresyn Inc, USA) as per manufacturer's instructions. Briefly, this involved passing the viral infectious supernatant through a series of clarification and virus-binding filters in a low-pressurised column in order to isolate adenovirus particles in a minimum elution volume in the final stage of the procedure. Once isolated, purified virus samples were quantified using ultraviolet (UV) light spectrometry (Maizel et al., 1968). This allowed us to obtain virus particles (VP) per ml values for the purified virus samples, which was preferred over pfu/ml in the case of cell culture experiments, as it more accurately depicted the amount of viral antigen that the DCs were to be exposed to.

4.2.5 *In vitro* DC-T-cell co-culture assays

4.2.5.1 DC pulsing

Cells were counted and 10^4 cells/well were added to 96-well U-bottomed plates. They were then pulsed for 18-20 hrs with three concentrations of pp65 (1, 5 and 10 μg/ml), or infected with three concentrations of rAdpp65 (1000, 2500 and 5000 virus particles (VP)) at 37 °C. Similar pulsing/infections were carried out for MART-1 stimulations using A*02:01 cell samples, although the concentrations of MART-1 assessed were 0.1, 0.5 and 1 μg/ml. Staphylococcal enterotoxin B (SEB) (500 ng/ml) stimulation was used as a positive control. To account for any proliferation due to adenovirus, rAdGag (carrying a full-length Gag

sequence from a Chinese Clade B/C chimaeric strain CN54) was used to infect cells at 5000 VP. This rAd was created in the same way as rAdpp65. A comparative experiment evaluating immunogenicity of the model antigens compared to the respective fusion antigens was also performed. Cells were pulsed with three concentrations of protein as described above (0.1, 1 and 10 μg/ml for pp65 and pp65-strep; 0.1, 1 and 5 μg/ml for MART-1 and MART-strep), and incubated overnight, to be used in a DC-T-cell co-culture assay the next day.

4.2.5.2 Adjuvant stimulation of DCs

This experiment was to evaluate which agonist would be best suited for enhancing T-cell proliferation after stimulations with pp65/MART-1. Once this was assessed, the agonist that stimulated the highest proliferative T-cell responses was used in all further work. Initially, DCs were pulsed with 1 protein concentration or infected with 2500 VP of rAd (as described above) followed by an overnight incubation. Adjuvants were added the next day to stimulated cells (only one protein and one virus concentration was evaluated) using the concentrations shown in Table 4.2, and cells were further incubated for 3-4 hrs at 37 °C and 5 % CO_2. CFSE-stained autologous T-cells (see 4.2.4.3) were then added to DCs, and a further incubation of 7 days occurred before harvesting cells.

4.2.5.3 Carboxyfluorescein succinimidyl ester (CFSE) staining of T-cells

CFSE staining of T-cells interacting with stimulated DCs was used to measure antigen-induced CD4+ and CD8+ T-cell proliferation. Frozen PP lymphocytes were thawed and washed twice in 10 % FCS-RPMI and incubated with 1 μg/ml DNaseI (Roche Diagnostics) for 3-4 hrs. These cells underwent two PBS-washes, were counted and diluted in PBS to approximately 10-20 × 10^6 cells/ml. Human AB serum (1 %) was added to the cells, and they were kept suspended on the vortex as a 4 μM CFSE-PBS solution was added to them (final concentration of 2 μM). Samples were then left under shaking conditions for 5 min, followed by two washes with 10 % FCS-RPMI and one final wash with 10 % AB-RPMI. They were resuspended in 10 % AB-RPMI, and added to stimulated DCs at 10^5 cells/well (DC: T ratio of 1:10). As a control, some wells contained CFSE-stained and unstained T-cells only. All CFSE procedures were performed under low-level illumination. Proliferation assays were cultured at 37 °C for 7 days, after which the cells were either surface stained alone (for proliferation and phenotypic data), or underwent both surface and intracellular staining (to evaluate proliferation and cytokine production).

Table 4.1a – List of monoclonal antibodies and their isotype controls used for flow cytometry staining

Antibody	Fluorochrome	Clone	Isotype	Supplier
Dendritic cell markers				
CD11b	PE	ICRF44	IgG1	BD Pharmingen™, UK
CD11b	APCC	ICRF44	IgG1	BD Pharmingen™, UK
CD11c	PE	B-ly6	IgG1	BD Pharmingen™, UK
CD11c	APCC	3.9	IgG1	eBioscience Ltd, UK
CD1a	APCC	HI 149	IgG1	BD Pharmingen™, UK
CD14	PE	M5E2	IgG2a	BD Pharmingen™, UK
CD19	FITC	HIB19	IgG1	BD Pharmingen™, UK
DC-SIGN (CD209)	FITC	DCN46	IgG2b	BD Pharmingen™, UK
CD80	PE	2D10	IgG1	eBioscience Ltd, UK
CD83	PE	HB15e	IgG1	BD Pharmingen™, UK
CD83	FITC	HB15e	IgG1	BD Pharmingen™, UK
CD86	FITC	FUN-1	IgG1	BD Pharmingen™, UK
CD86	APCC	FUN-1	IgG1	BD Pharmingen™, UK
CD123	PE	9F5	IgG1	BD Pharmingen™, UK
HLA-DR	Pe-Cy5	L243 (G46-6)	IgG2a	BD Pharmingen™, UK
HLA-A2	FITC	BB7.2	IgG2b	BioLegend UK, Ltd
Lineage cocktail (consists of CD3, CD14, CD16, CD19, CD20, CD56)	FITC	NCAM16.2, MφP9, L27, SJ25C1, 3G8, SK7	IgG1 IgG2b	BD Pharmingen™, UK
T-cell markers				
CD3	Pe-Cy5	UCHT1	IgG1	BD Biosciences™, UK
CD4	APCC	OKT4	IgG2b	eBioscience Ltd, UK
CD8	PE	37006	IgG2b	R&D Systems Europe Ltd
CD8	APCC-H7	SK1	IgG1	BD Biosciences, UK
CCR7	PE	3D12	IgG2a	eBioscience Ltd, UK
CCR7	APCC	FAB197A	IgG2a	R&D Systems Europe Ltd
CD45RA	Pe-Cy7	HI100	IgG2b	eBioscience Ltd, UK
T-cell cytokines				
IFN-γ	Pe-Cy7	4S.B3	IgG1	eBioscience Ltd, UK
TNF-α	APCC	MAb11	IgG1	BioLegend UK, Ltd
IL-2	PE	MQ1-17H12	IgG2a	eBioscience Ltd, UK

Table 4.1b – List of pentamers for flow cytometry staining

Pentamer origin	Pentamer origin	Peptide Sequence	Allele	Fluorochrome	Supplier
Human cytomegalovirus	pp65 495-504	NLVPMVATV	A*02:01	APC	ProImmune Ltd (UK)
Human	Melan A/ MART 26-35	ELAGIGILTV	A*02:01	APC	ProImmune Ltd (UK)

Table 4.2 – Adjuvants utilised in DC-T-cell co-culture experiments

Agonists	Receptor	Concentration	Supplier
Poly (I:C)	TLR 3	50 µg/ml	Sigma-Aldrich (UK)
Lipopolysaccharide (LPS) (Escherichia coli 0111:B4)	TLR 4	1 µg/ml	Sigma-Aldrich (UK)
Flagellin	TLR 5	1 µg/ml	Invivogen (France)
PAM2CSK4	TLR 2/6	1 µg/ml	Invivogen (France)
CLO97 (Imidazoquinoline)	TLR 7 and TLR 8	5 µg/ml	Invivogen (France)
CD40 Ligand (CD40L)	CD40	5 µg/ml	Invitrogen (UK)

4.2.6 Phenotypic and functional analysis of T-cells in co-culture assays

4.2.6.1 Surface staining of cultured T-cells to detect specific TCRs

After culturing, cells were harvested and stained with antibodies against CD3, CD4, CD8, CCR7 and CD45RA (all in FACS buffer) for 20 min on ice (see Table 4.1a). Cells were then washed with FACS buffer, fixed with stabilizing fixative (BD Biosciences, UK) and stored at 4 °C until they were acquired on a 3-laser-configuration LSR II flow cytometer (BD Biosciences, UK).

4.2.6.2 Intracellular staining of cultured T-cells to detect cytokines

Cytokine production by stimulated T-cells was assessed by re-stimulating the 7-day cultured cells for 5 hrs with Phorbol 12-myristate 13-acetate (PMA) (0.1 µg/ml) and ionomycin (1 µM) (both from Sigma-Aldrich, UK). Brefeldin A (BFA) (10 µg/ml) (Sigma-Aldrich, UK) was added for the last 4 hrs. For each set of experiments, a set of samples did not receive

PMA and ionomycin stimulations, but did receive BFA. These samples were used as controls to set flow cytometry gates for cytokine production analysis. After re-stimulation, cells were harvested and intracellularly stained in FACS buffer on ice for 20 min with anti-CD3, CD4, and CD8 antibodies (Table 4.1a). Cells were then washed, and fixed in 2 % PFA for 10 min at room temperature. Following washing, cells were stained with antibodies against IFN-γ, IL-2 and TNF-α in 0.1 % saponin buffer for 40 min at room temperature. Cells were finally washed, fixed and stored at 4 °C before acquirement.

*4.2.6.3 Pentamer staining of A*02:01 cultured T-cells*

T-cells (non-CFSE-stained) were harvested from co-culture assays after seven-day incubation, and were incubated with the respective conjugated pentamer (see Table 4.1b) at 25 °C for 10 min to surface stain antigen-specific T-cell receptors, as per manufacturer's instructions (ProImmune, UK). Cells were then washed using FACS buffer, and surface staining was performed as described in section 4.2.6.1 with the addition of an anti-CD19 antibody.

4.2.7 Data acquisition and gating strategy

Data from co-culture assays were acquired on an LSRII 3-laser flow cytometer and analysed using FACS Diva software (BD Biosciences, UK) or FlowJo 7.6.5 software (Tree Star, Inc, USA). The gating strategy used to evaluate T-cell phenotypes and cytokine production is shown in Figures 4.1 and 4.2 respectively.

4.2.8 Statistical analysis

Statistical analysis was carried out using GraphPad Prism 5.0 software (San Diego, USA). The paired Wilcoxon signed rank test was applied to all paired, non-parametric data, as recommended by a professional statistician (Mr Joseph Eliahoo, Imperial College London). A Bonferroni post-test correction was used to correct for multiple comparisons, and $p < 0.05$ was considered statistically significant.

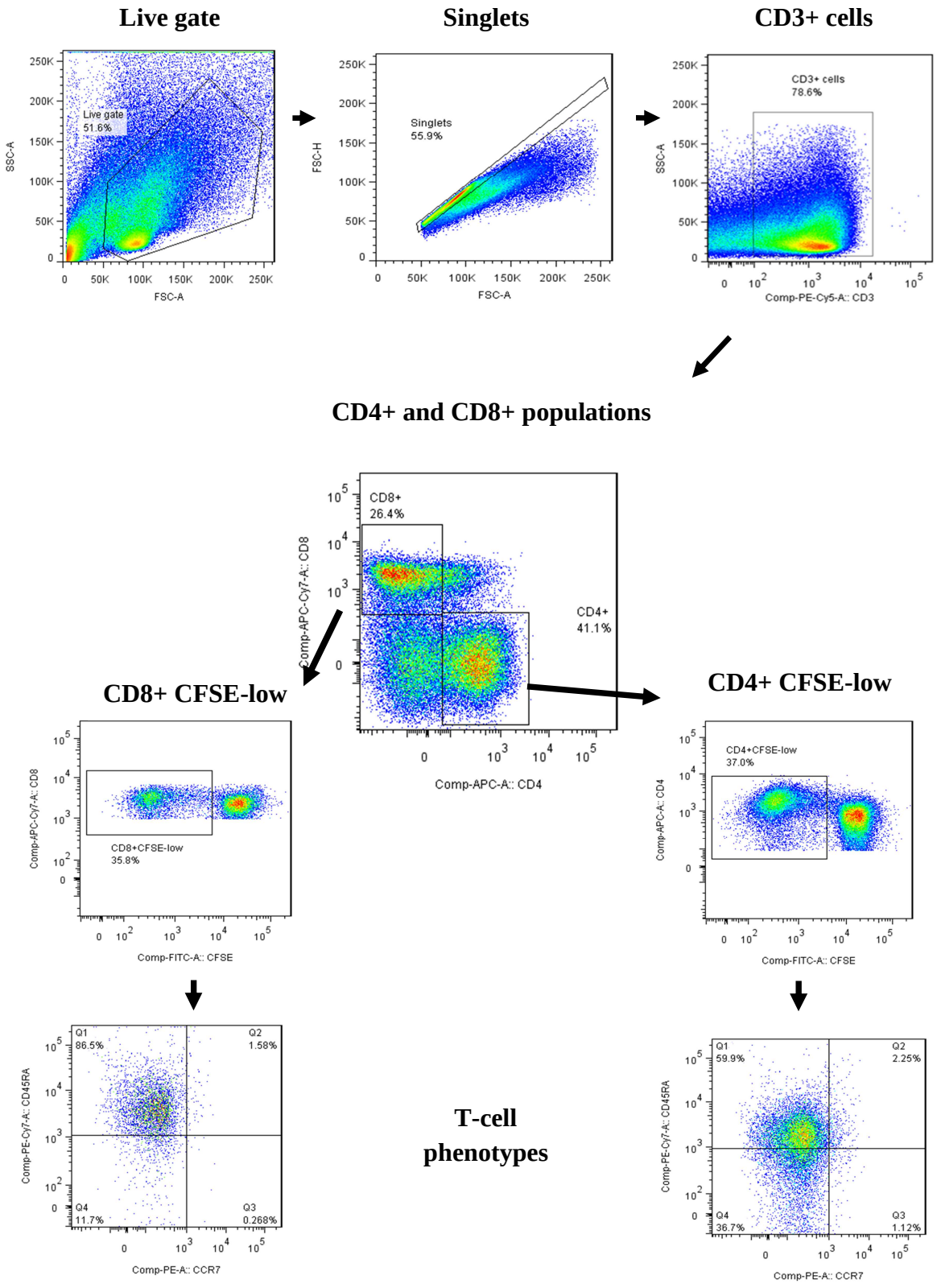


Figure 4.1 – Gating strategy for the flow cytometric analysis of cultured T-cells to measure proliferation and identify T-cell phenotypes. T-cell proliferation is shown after 7-day incubation with LPS-stimulated pp65-pulsed moDCs. First, live cells were gated on, followed by gating on CD3+ T-cells. Second, CD4+ and CD8+ T-cell populations were identified, and further gated on to identify proliferating cells (i.e. CFSE-low cells). Phenotypes of the proliferated populations were determined using CCR7 and CD45RA markers. Position of gates (CD3, CD4, CD8, CCR7, CD45RA) was based on isotype controls.

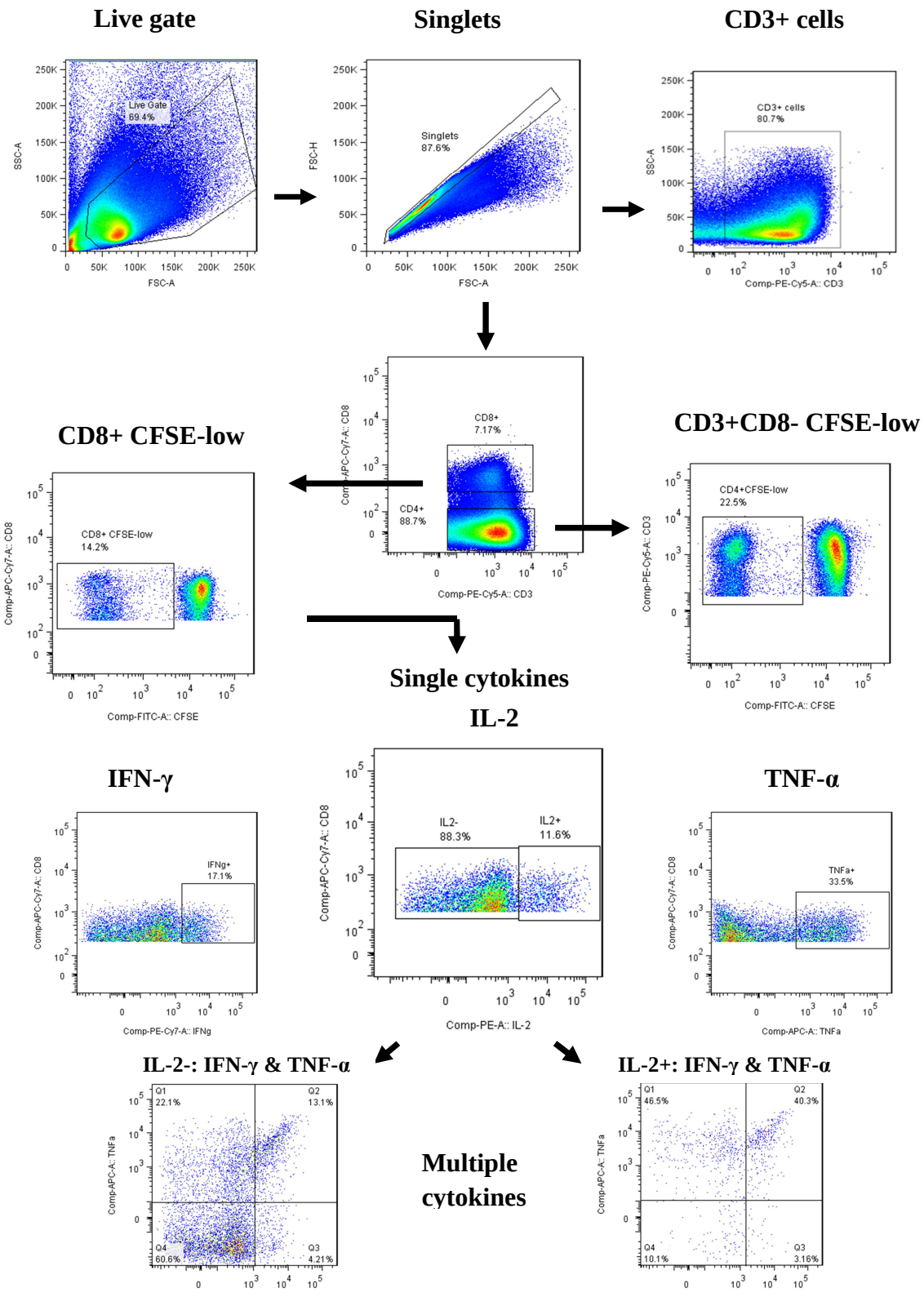


Figure 4.2 – Gating strategy for the flow cytometric analysis of cultured T-cells to measure proliferation and cytokine production. T-cell proliferation is shown after 7-day incubation with LPS-stimulated pp65-pulsed moDCs. First, live cells were gated on, followed by gating on CD3+ T-cells (slightly down-regulated due to PMA and ionomycin stimulation). Second, CD8+ and CD3+CD8- T-cell populations were identified and further gated on to identify proliferating cells (i.e. CFSE-low cells). Cytokine production of proliferated populations was determined after re-stimulation of cells with PMA and ionomycin, specifically measuring IL-2, IFN-γ, and TNF-α production. Position of gates (CD3, CD4, CD8) was based on isotype controls. Position of cytokine gates was based on control cells that were not re-stimulated with PMA and ionomycin, but were exposed to Brefeldin-A.

4.3 Results

4.3.1 *In vitro* generation and phenotypic characterisation of DC subsets

Monocyte-derived dendritic cells (moDCs) and blood myeloid dendritic cells (CD1c+ mDCs) were generated from monocytes and CD1c+ mDC precursors respectively, isolated from leukocyte cones of healthy individuals. For moDCs, CD14+ monocytes were purified from the monocyte-rich interface layer after a percoll separation, using magnetic beads. Approximately 15-30 million monocytes were isolated, and the purity of the resulting cells was evaluated using flow cytometry. Cells were found to be of a high purity, characterised as CD14+ HLA-DR+ (Figure 4.3a). These cells were then cultured for 5-7 days in medium containing GM-CSF and IL-4 to generate immature moDCs. Phenotypic characterization of immature moDC was assessed by flow cytometric analysis of the expression of a C-type lectin (DC-SIGN), MHC class II marker (HLA-DR), myeloid markers (CD1a, CD11b, CD11c), maturation marker (CD83) and co-stimulatory molecules (CD80 and CD86) (Figure 4.3b). Cells were shown to express high levels of HLA-DR, DC-SIGN, and all myeloid markers. They were deemed immature due to negligible expression levels of CD80, CD83 and CD86.

The CD1c+ mDCs were also purified from the interface layer after a percoll separation using two magnetic separation steps. A negative selection was initially done to exclude CD19+ cells (as a proportion of CD1c+ cells also express CD19), followed by a positive selection of CD1c+ cells. Between 0.8-3.5 million cells were isolated on average, and evaluated for purity by flow cytometry using CD123 (pDC marker) and CD11c (myeloid marker). As expected, cells were CD123- CD11c+ (Figure 4.4a). Purified cells were cultured for two days with GM-CSF and IL-4 to generate immature CD1c+ mDCs. Phenotypic characterization of cultured immature mDCs was assessed using antibodies against lineage (Lin) markers (cell surface antigens that are commonly found on lymphocytes), CD123, HLA-DR, co-stimulatory molecules (CD80, CD86), CD83 (maturation marker) and DC-associated markers including CD1a, CD11c, CD11b, and DC-SIGN (Figure 4.4b). Cells were shown to express high levels of HLA-DR and all myeloid markers, while not expressing any of the lineage cocktail markers and CD123, and only expressing intermediate levels of DC-SIGN.

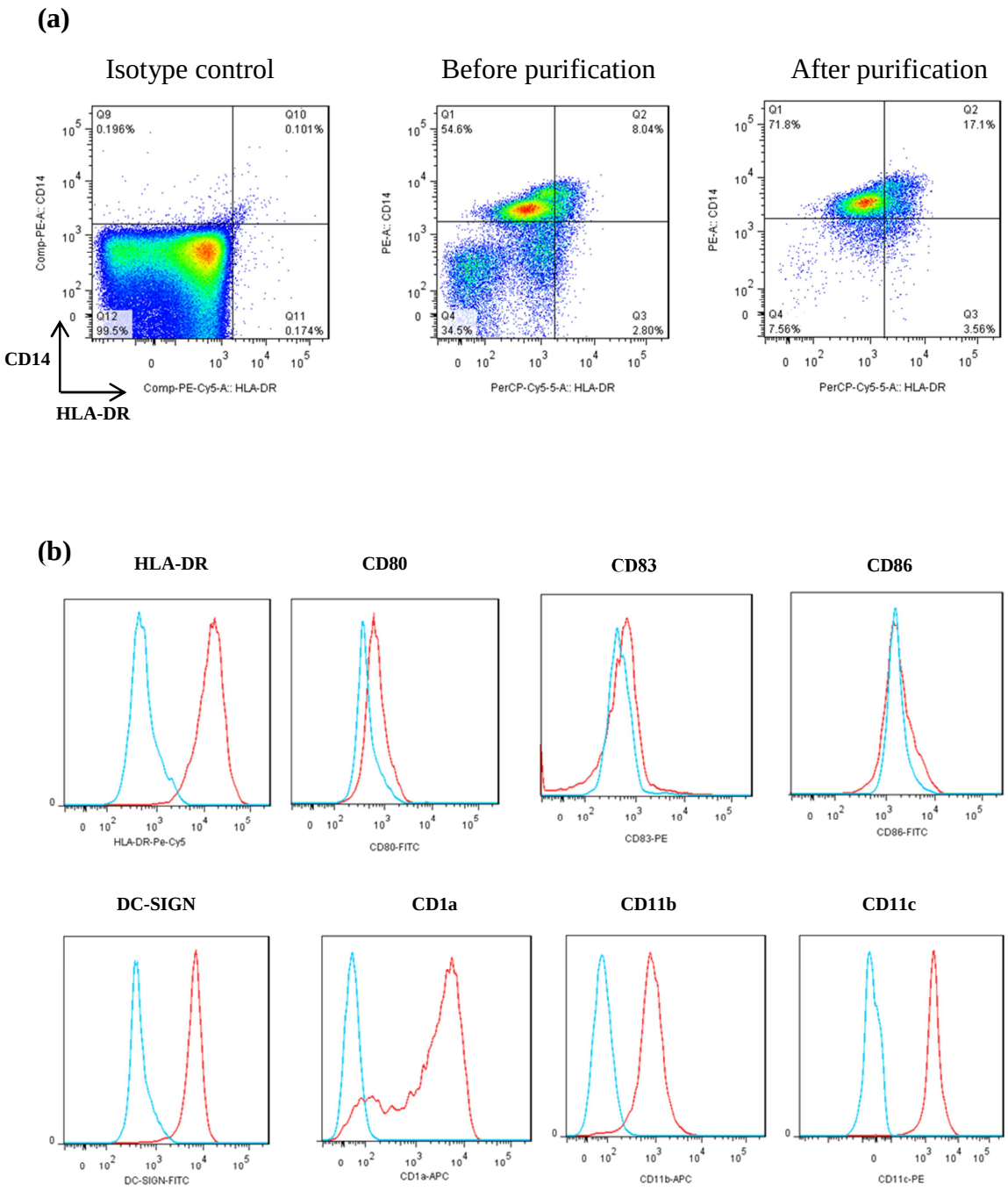


Figure 4.3 - Phenotypic analysis of in-vitro-derived moDCs and their precursors from leukocyte cone blood. (a) Purity of isolated monocytes before and after CD14+ bead separation was evaluated based on CD14 and HLA-DR. (b) Expression of myeloid markers, co-stimulatory markers, and DC-associated markers are shown for immature (5-day cultured) moDCs. Blue histograms show non-specific isotype staining whereas red histograms show marker-specific staining. Data shown are representative of three independent experiments.

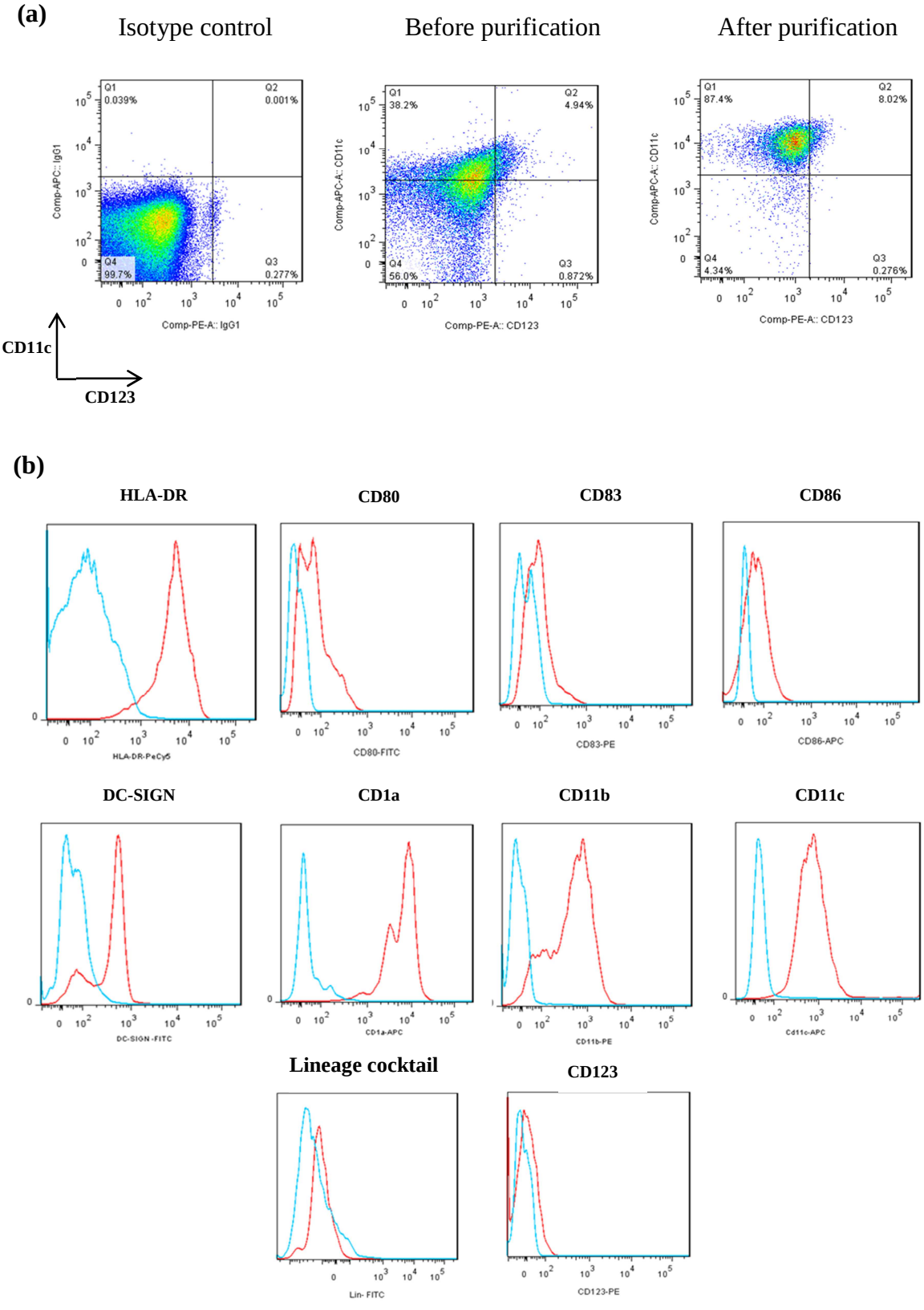


Figure 4.4 - Phenotypic analysis of cultured, immature CD1c+ mDCs and their precursors from leukocyte cone blood. (a) Purity of isolated CD1c+ mDC precursors was evaluated before and after CD1c+ separation based on CD123 and CD11c. (b) The expression of myeloid markers and co-stimulatory markers (amongst others) is shown for immature (2-day cultured) CD1c+ mDCs. Blue histograms show non-specific isotype staining whereas red histograms show marker-specific staining. Data shown are representative of three independent experiments.

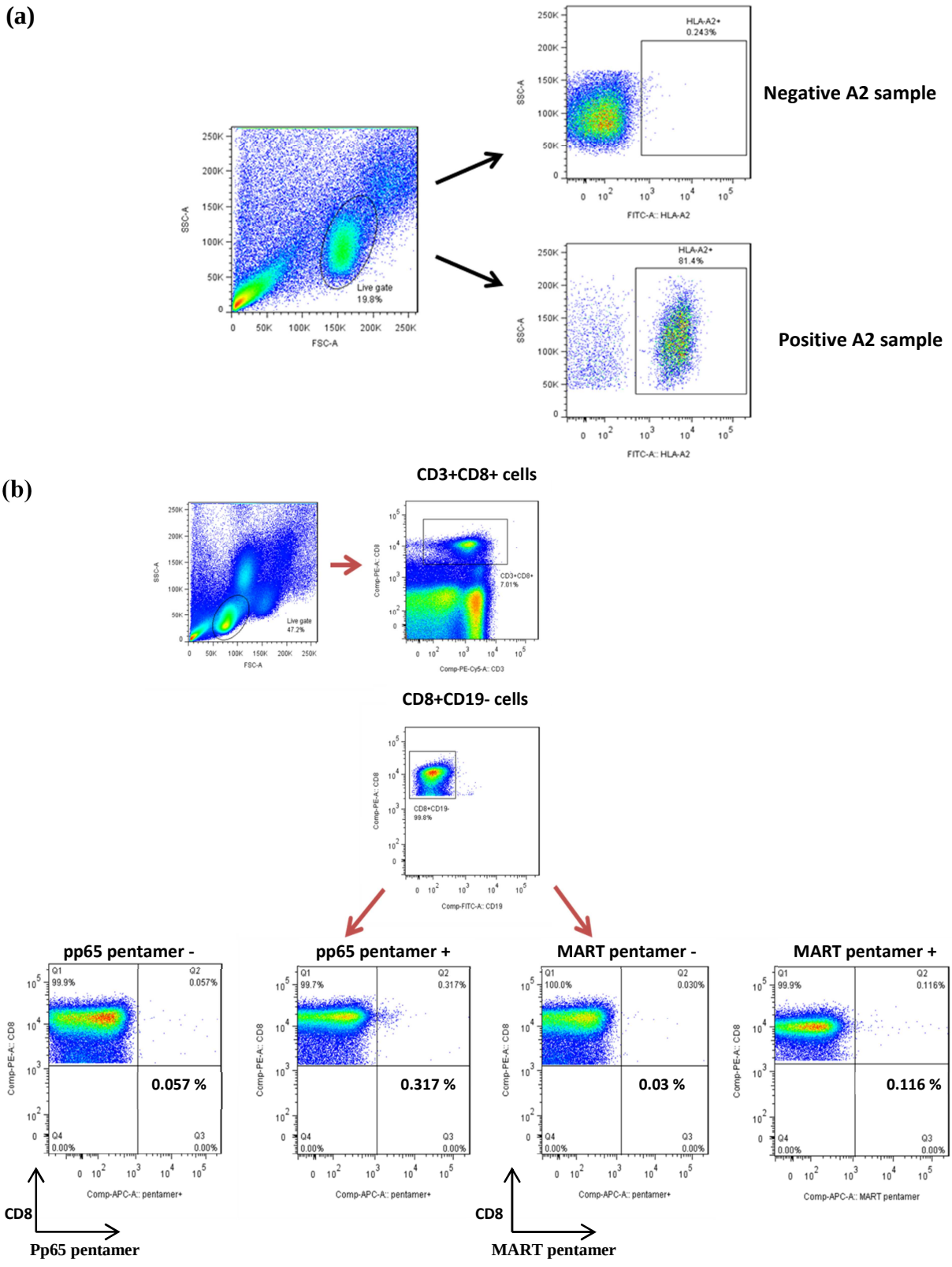


Figure 4.5 - Gating strategy used to identify A*02:01+ individuals. Initially HLA-A2 positive samples were identified (a), and further stained with CMV pp65 or MART-1 pentamers to identify A*02:01+ individuals (b). Positive cells were CD3+CD8+CD19- pentamer+.

Interestingly, immature mDCs expressed low levels of co-stimulatory and maturation markers (CD80, CD86 and CD83), while moDCs demonstrated a negligible expression of these markers. This has been seen before (Osugi et al., 2002) and suggests mDCs are slightly phenotypically activated, even in the immature state. Overall, the generated immature moDCs and CD1c+ mDCs demonstrated the presence of all expected markers, and purity of samples was accepted as adequate for experiments to follow.

4.3.2 Identification of A*02:01-positive individuals

Donors with the HLA-type A*02:01 were identified using flow cytometric analysis. Initially, individuals were determined to be A2-positive using an HLA-A2-specific antibody (Figure 4.5a). The presence of CD3+ CD8+ CD19- T-cells that were CMV-positive (memory) and MART-1 positive (naïve) was then assessed in these A2-positive donors, using A*02:01-specific CMV pp65 or MART-1 pentamers (Figure 4.5b). The pentamers were designed to bind directly to specific T cell receptors, based on the MHC allele and peptide combination, and therefore allow the detection of antigen-specific populations (ProImmune, 2011). In general, the detection of A*02:01-positive donors was not as high as expected (40-60 % of Caucasian population), with only about 1 positive individual per 9 donors. We were able to identify at least 7 individuals for this study who were A*02:01-positive.

4.3.3 Assessment of the use of agonists in moDC-T-cell co-culture assays

To evaluate the ability of chosen adjuvants to mature DCs, moDCs were stimulated overnight with TLR agonists that bound to TLRs 3-8 and CD40. These adjuvants were chosen given their success in inducing DC maturation in previous work within our laboratory (pers. comm.: Dr Sai Duraisingham). Samples were analysed by assessing the level of expression of CD83, CD80, CD86 and HLA-DR on stimulated DCs (Figure 4.6). There was a notable increase in the number of cells positively expressing CD83 and CD86 in samples stimulated with agonists for TLR3, 4 and 7/8 (poly I:C, LPS and CLO97 respectively), compared to unstimulated moDCs and the isotype control (Figure 4.6a). The percentage of cells expressing CD80 did not appear to increase after adjuvant stimulations. This was also observed after stimulation with TLR 5 and 6 agonists (flagellin and PAM2CSK4), in addition to a low percentage of cells expressing CD86. However, these agonists did induce an increase

in the number of cells expressing CD83 (Figure 4.6b). The mean fluorescence intensity (MFI) data, which indicated the mean expression of the respective receptors per cell, showed a marginal increase in levels of CD80, CD83 and HLA-DR expression between unstimulated DCs and stimulated DCs (Figure 4.6c). However, CD86 expression levels were greater for samples stimulated with LPS and poly I:C than the other samples. Thus, these agonists were able to fully activate DC maturation, while the other agonists were perhaps only partially inducing phenotypic maturation.

Further analysis of the stimulatory effects of these adjuvants was assessed using preliminary moDC-T-cell co-culture assays. T cell proliferation experiments using CFSE-stained responders were conducted, in which immature DCs were pulsed with model antigens or infected with rAds, incubated overnight and then matured using selected adjuvants. Autologous CFSE-stained T-cells were later added to the stimulated, mature DCs at a ratio of 1:10 (DC: T-cell), and samples were incubated for 7 days before T-cell proliferation was analysed.

Stimulations with CMV pp65 protein and rAdpp65 in addition to any of the agonists demonstrated higher proliferative responses than using stimulus or agonist alone (Figure 4.7). This confirms that all the agonists were able to mature DCs sufficiently to activate T-cells. Noticeably, while samples exhibited variation, LPS increased proliferation of both CD4+ and CD8+ T-cells to a greater extent than the other agonists, particularly for the rAdpp65 virus-infected samples, where there was a significantly higher proliferation compared to samples stimulated with flagellin and CD40L ($p < 0.05$). This was in agreement with the maturation data illustrated in Figure 4.6, where flagellin and PAM2CSK4 only partially matured DCs, and therefore enhanced T-cell proliferation to a lesser extent. Surprisingly, CD40L did not demonstrate an ability to enhance T-cell responses for most samples, except CD4+ T-cell samples stimulated with pp65.

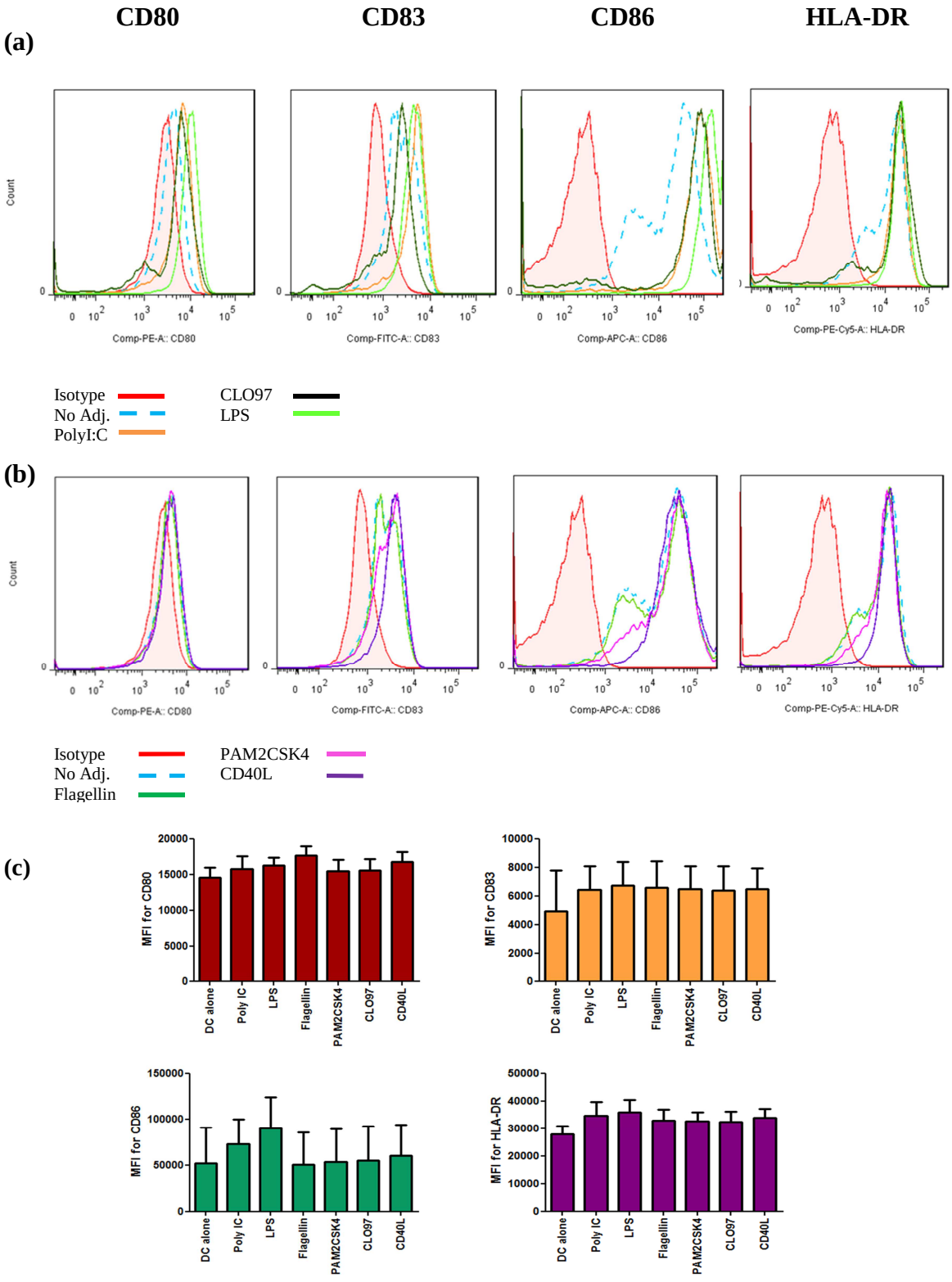


Figure 4.6 - Evaluation of moDC activation after TLR ligand stimulation using surface receptor staining and flow cytometry. (a) and (b) Representative expression of activation markers, CD80, CD83, CD86 and the MHC class II cell surface receptor, HLA-DR are shown after cells were incubated overnight with the respective agonists. (a) Comparison of isotype and DC only (designated none) to agonists activating TLR 3, 4 and 7/8 (PolyI:C, LPS and CLO97 respectively). (b) Comparison of isotype and DC only (designated no adj.) to agonists activating TLR 5 and 6 (flagellin and PAM2CSK4), and CD40L. (c) The mean fluorescence intensity (MFI) of the respective receptors on positively expressing cells is shown using data from three independent experiments. Adj. = adjuvant

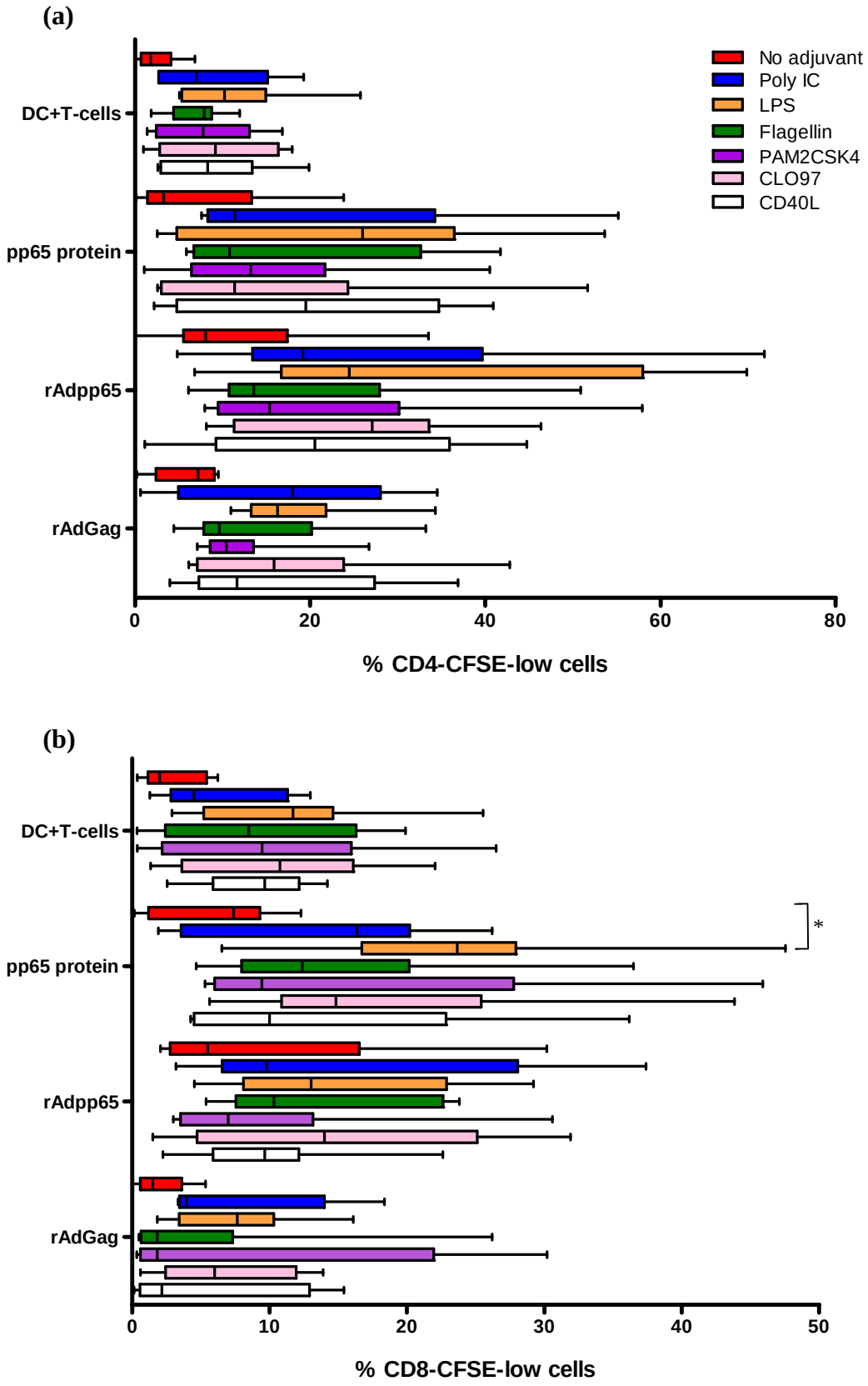


Figure 4.7 – Assessment of (a) CD4+ and (b) CD8+ T-cell proliferation after stimulation with pp65-pulsed or rAd-infected moDCs and co-stimulated with selected agonists. The cumulative data from 9 independent experiments are shown. Data depicts the median with the range. * - denotes $p < 0.05$; as analysed by the non-parametric, paired Wilcoxon signed rank test, with a Bonferroni post-test.

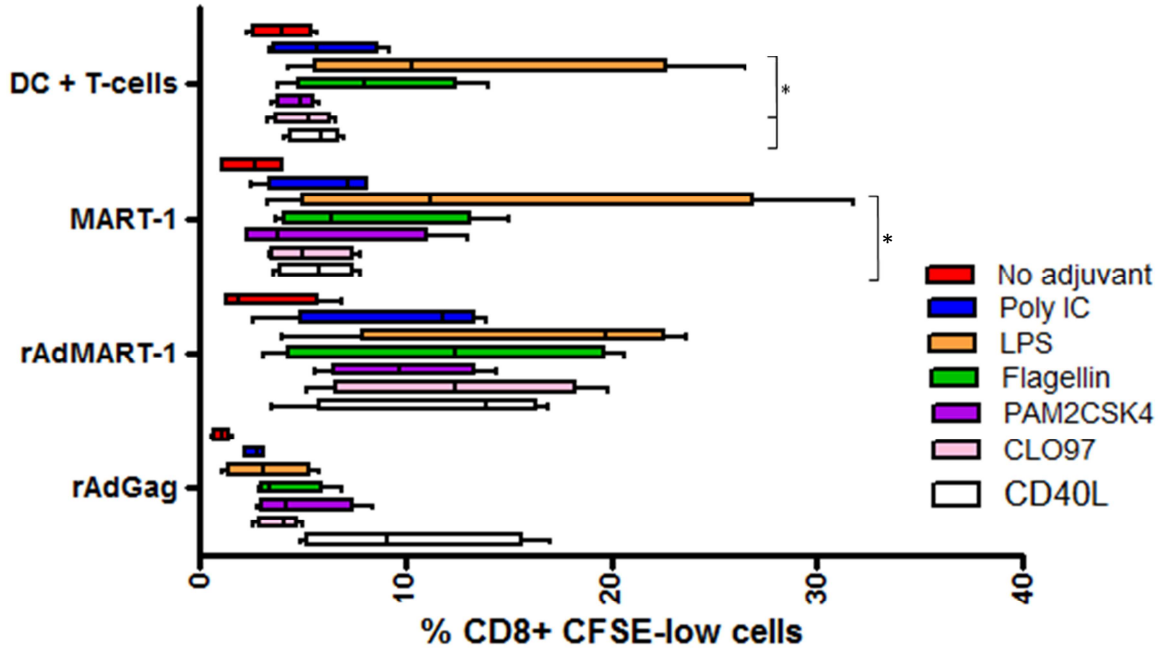


Figure 4.8 – Assessment of CD8+ T-cell proliferation after stimulation with MART-1-pulsed or rAd-infected moDCs and co-stimulated with selected agonists. The cumulative data from 4 independent experiments are shown. Data depicts the median with the range. * - denotes $p < 0.05$; as analysed by the non-parametric, paired Wilcoxon signed rank test, with a Bonferroni post-test.

MART-1 stimulated samples also demonstrated the best responses when LPS was used as an agonist (Figure 4.8). While CD40L induced some high responses here, these were mainly for virus-infected samples. Despite other studies highlighting the use of CD40L to improve cross presentation of antigen (Bozzacco et al., 2007), the responses observed here rendered the use of CD40L as a less attractive adjuvant option. LPS was favoured because of its ability to stimulate consistent, enhanced T-cell proliferative responses for protein samples. It was therefore chosen as an adequate adjuvant for all co-culture experiments.

4.3.4 Immunogenicity of pp65 and MART-1

The stimulatory capacity of purified pp65 and MART-1 proteins was evaluated to confirm their immunogenicity. Immunogenicity of the recombinant adenoviruses carrying model antigens was also included to provide a positive proliferative control, as well as to make qualitative comparisons between protein- and virus-stimulated responses.

Co-culture experiments were set up as described above using both moDCs and CD1c+ mDCs. Three concentrations of pp65 (1, 5 and 10 μg/ml), MART-1 (0.1, 0.5, 1 μg/ml), rAdpp65 or rAdMART-1 (1000, 2500 and 5000 VP) were evaluated, and all samples included a SEB stimulation as a positive control for the autologous reaction. Examples of the gating strategies used to identify T-cell proliferation via CFSE-staining, T-cell phenotypes and cytokine production is illustrated in Figures 4.1 and 4.2.

4.3.4.1 CMV pp65

Monocyte-derived DC samples stimulated with pp65 and rAdpp65 (Figure 4.9a) displayed widely varied responses, suggesting that although the general population have memory responses against CMV, the magnitude of these responses varies substantially. The T-cell responses against SEB were much higher than all other responses (as much as 80-95 % proliferation), confirming reactions to be autologous (data not shown). There were strong proliferative responses detected for all rAdpp65-infected samples, with the highest responses demonstrated by 5000 VP of rAdpp65, showing median values as high as 23.8 % and 18.5 % of CD4+ and CD8+ T-cell responses respectively. The rAdGag responses were indicative of the adenovirus-stimulated responses and were found to be significantly detectable, accounting for approximately half of the responses induced by rAdpp65 of the same concentration (5000 VP). Proliferation as a result of pp65 protein stimulation was less pronounced, although still strong, with 5 μg/ml stimulating better responses than the other two concentrations (median* values of 16.2 % and 10.1 % for CD4+ and CD8+ T-cell responses respectively).

* Quantitative data quoted in the text can be assumed to be median values unless otherwise stated.

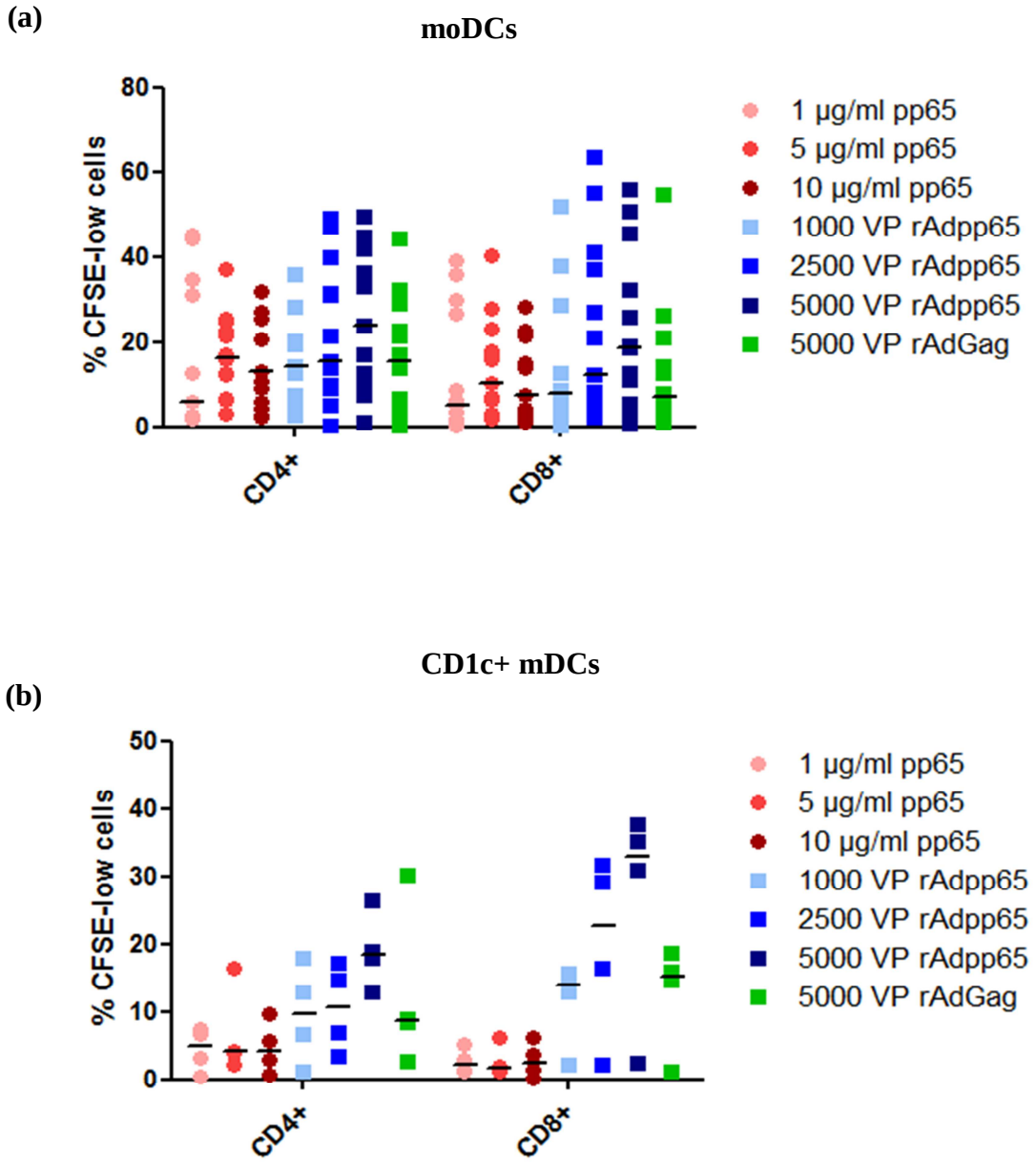


Figure 4.9 - Immunogenicity of pp65 as presented in the form of full-length protein or using recombinant adenovirus carrying pp65 gene. T-cell proliferation is shown after incubation for 7 days with LPS-stimulated antigen-pulsed moDCs (a) and CD1c+ mDCs (b). The cumulative data from 12 (a) and 4(b) independent experiments are shown after correction for background responses to DCs alone (DC background median and range: 1.4 % and 0.2-3.1 % for (a); 1.0 % and 0.3-1.9 % for (b). Horizontal lines depict median values, and circles/squares represent individual donor responses.

Stimulations of CD1c+ mDCs demonstrated less variation in responses and showed a robust response to virus stimulations, with 5000 VP rAdpp65 inducing as much as 33.03 % CD8+ T-cell proliferation, less than half of which was due to Ad (Figure 4.9b). This is not entirely surprising, given that the recombinant adenoviruses would have had access to the classical MHC class-I and cross presentation pathways. The responses to pp65 protein did not seem to differ noticeably with an increase in concentration, and were more than two-fold lower than what was obtained when moDCs were stimulated, specifically the CD8+ T-cell proliferative responses. This suggests that moDCs were able to process and present pp65 protein epitopes via the cross presentation pathway more efficiently than CD1c+ mDCs.

Proliferating T-cells stimulated by both moDCs and CD1c+ mDCs were primarily characteristic of terminally differentiated effector memory T-cells (TEMRA) (CCR7-CD45RA+) or effector memory T-cells (EM) (CCR7-CD45RA-) (Figure 4.10). The ratio of TEMRA: EM for induced CD4+ and CD8+ T-cells showed no marked differences between stimulating moDCs with protein or virus. CD1c+ mDC CD8+ T-cell phenotypes demonstrated higher percentages of TEMRA cells for all samples (especially protein-stimulated samples), compared to moDC-activated T-cells.

Cytokine production by samples co-cultured with moDCs induced IFN-γ production by CD4+ T-cell for all samples, although 10 µg/ml pp65 seemed to stimulate a marginally greater percentage of cells producing IFN-γ (Figure 4.11a). No IL-2 was produced, but 1 µg/ml pp65 was able to induce reasonable levels of TNF-α-producing cells (2.01 %). There were high percentages of CD8+ T-cells producing TNF-α when stimulated with 10 µg/ml pp65 (10.2 %), and CD8+ T-cell-mediated IFN-γ production elicited by both protein and virus stimulations were generally better than CD4+ T-cell production (Figure 4.11b). With regard to multi-functional T-cells, 5 and 10 µg/ml pp65 induced the most prominent responses, with a large proportion of CD4+ T cells producing IL-2 and IFN-γ (16.18 and 24.28 % respectively) (Figure 4.11c). IL-2+ IFN-γ+ TNF-α production from CD8+ T-cells was also high for 10 µg/ml pp65-stimulated samples (32.32 %), with low levels of IL-2+IFN-γ+ production for the virus-infected samples (Figure 4.11d).

As seen with moDC samples, CD4+ and CD8+ T-cell stimulated by CD1c+ mDCs mainly produced IFN-γ, although lower percentages of positive cells were detected in these samples compared to moDC samples (Figure 4.12). Virus-infected samples generally demonstrated

better IFN-γ production by CD8+ T-cells, except in the case of 1 µg/ml pp65, which induced a percentage of cells expressing IFN-γ (7.2 %) (Figure 4.12b). A high percentage of CD4+ T-cells expressing IL-2 and IFN-γ was observed when mDCs were stimulated with pp65 protein and rAdpp65 (Figure 4.12c). The percentages of CD8+ T cells producing multiple cytokines were overall higher compared to that produced by CD4+ T-cells, especially when cells were stimulated with 1 ug/ml pp65, producing IL-2+ IFN-γ+, IFN-γ+ TNF-α+, and IL-2+ IFN-γ+ TNF-α+ (3.78, 6.18 and 15.07 % respectively) (Figure 4.12d). Hence, CD1c+ mDCs activated greater percentages of polyfunctional T-cells when stimulated with lower concentrations of pp65.

4.3.4.2 Melan-A/MART-1

For MART-1-stimulated samples, only the CD8+ T-cell responses from HLA-A2 positive individuals were analysed, as these individuals express an unusually high frequency of naïve CD8+ T-cells (and not CD4+ T-cells) that recognise an immunodominant epitope of MART-1 (Pittet et al., 1999). In general, there seemed to be little difference in the stimulated responses obtained for different concentrations of MART-1 protein, with only a two-fold increase in proliferative response between 0.1 and 1 µg/ml MART-1 (Figure 4.13a). The rAdMART-stimulated samples demonstrated an increase in proliferation as the number of VP increased, with 5000 VP displaying better responses (32.8 %) than the other two concentrations of virus (16.8 and 19.6 % respectively).

The ratio of TEMRA: EM CD8+ T-cells from MART-1 stimulated samples was approximately 60:40 for most samples, with TEMRA cells again demonstrating more prominence than what was seen for T-cells co-cultured with pp65-stimulated moDCs (Figure 4.13b).

With regard to cytokine production, 0.5 µg/ml MART-1 protein stimulated detectable amounts of cytokine production from CD8+ T-cells, especially at the lower concentrations as was seen with pp65-mDC samples (1.65 % IFN-γ, 2.1 % TNF-α, and 1.8 % IL-2). As shown with pp65, IFN-γ was prominently produced by all samples, with the highest percentage of IFN-γ-producing cells detected when cells were stimulated with 5000 VP rAdMART (2.75 %). Polyfunctional T-cells were not activated well by rAdMART, although IFN-γ+ TNF-α+ cells were elicited by MART-1 protein, with a median percentage of 16.2 % for 1 µg/ml MART-1 stimulation.

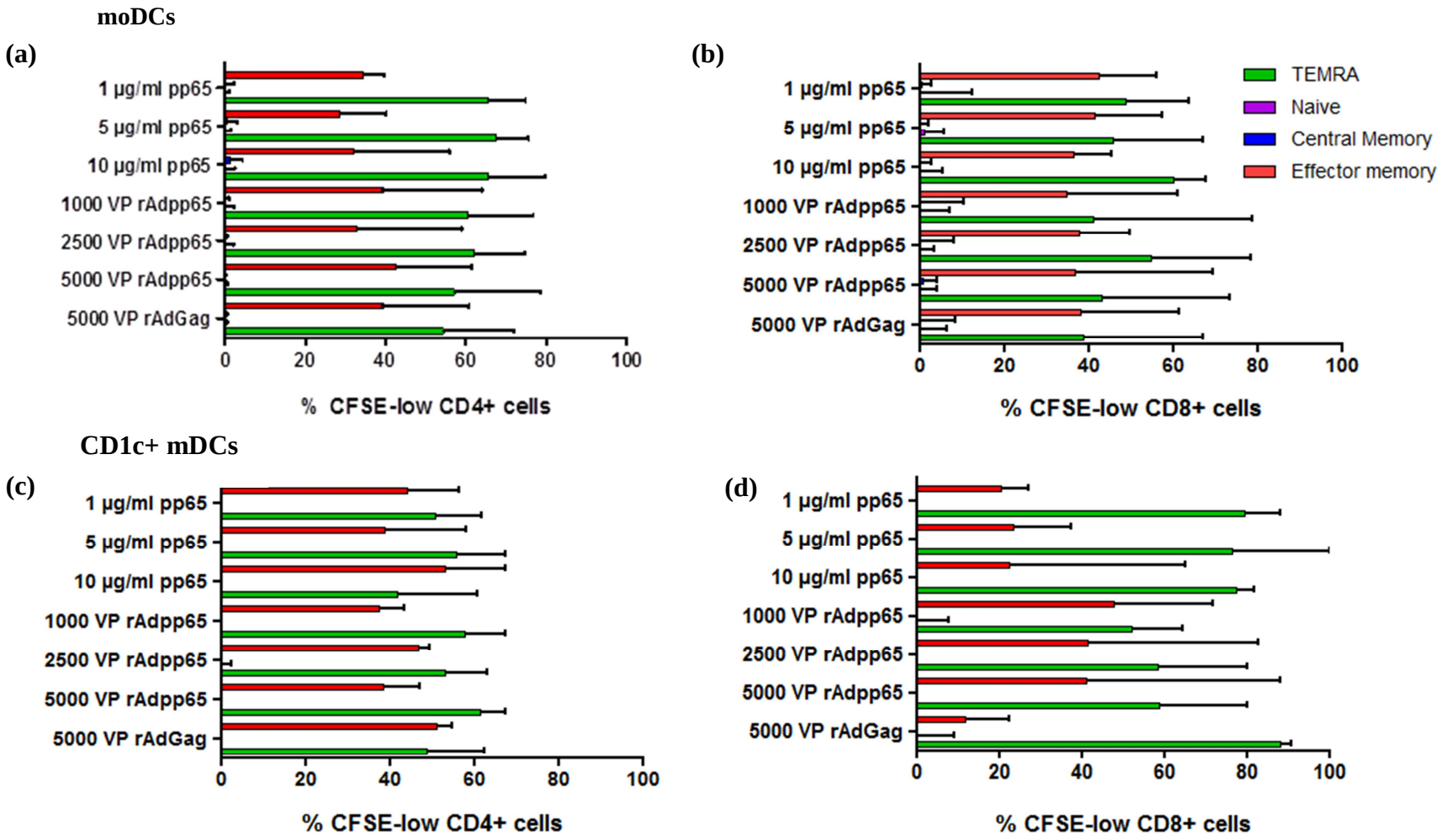


Figure 4.10 - Phenotypes of proliferated CD4+ (a and c) and CD8+ (b and d) T-cells after incubation for 7 days with LPS co-stimulated moDCs (pulsed or infected with pp65 or rAdpp65 respectively) (a and b) or CD1c+ mDCs (c and d). The cumulative data from 5 (a and b) and 3(c and d) independent experiments are shown, where bars represent the median, and error bars represent the maximum values.

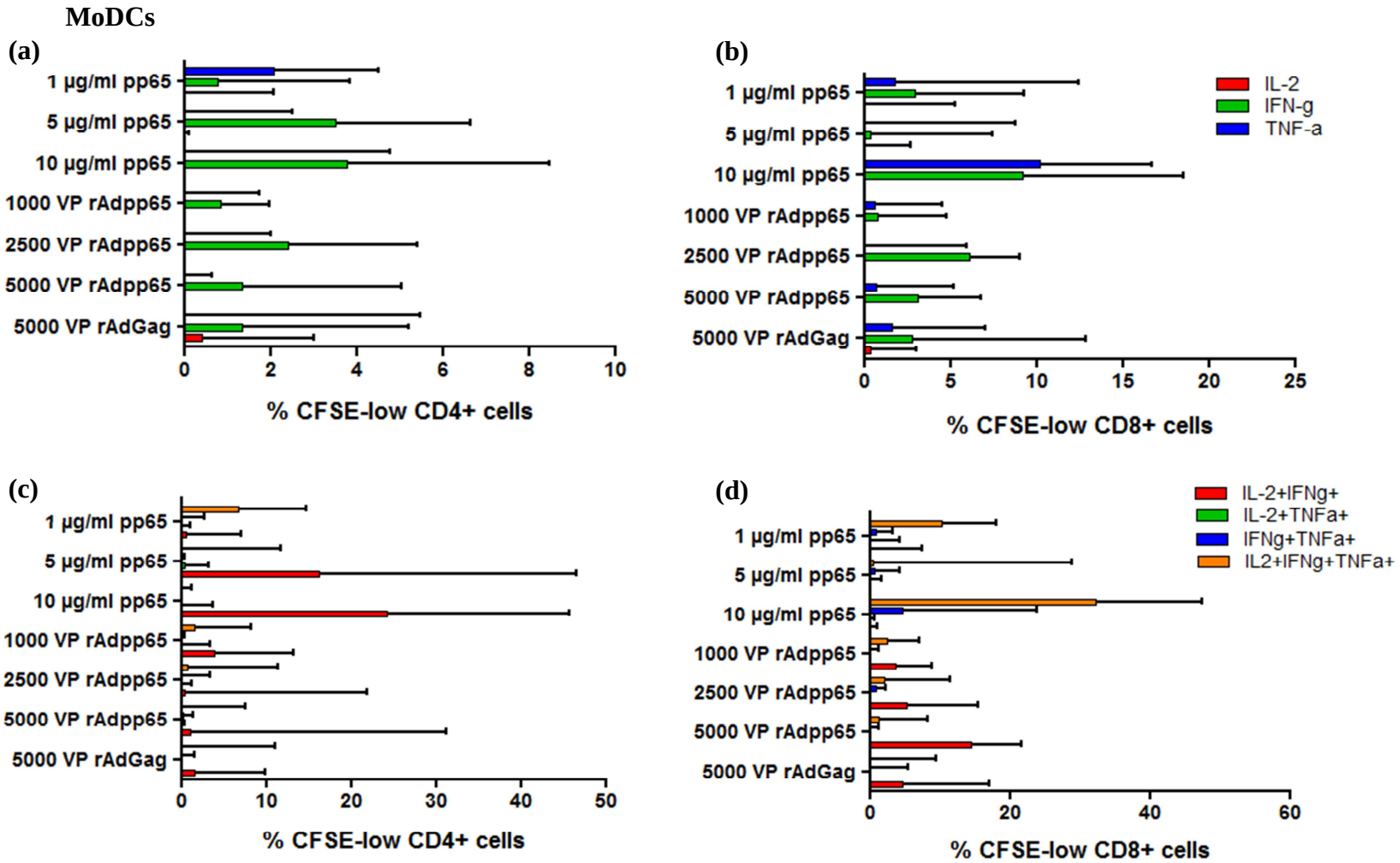


Figure 4.11 – Assessment of T-cell cytokine production after co-culture with stimulated moDCs, to evaluate immunogenicity of pp65 (in the form of full-length protein or via recombinant Adenovirus carrying pp65 gene). CD4+ (a and c) and CD8+ (b and d) T-cell cytokine production (IL-2, TNF-α and IFN-γ) is shown after incubation for 7 days with LPS co-stimulated moDCs (previously incubated with respective protein/virus for 24 hrs), followed by re-stimulation with PMA, ionomycin and BFA. (a) and (b) depict single cytokine production, while (c) and (d) depict multiple cytokine production by individual cells. The cumulative data from 6 independent experiments are shown after correction for background responses to DCs alone (negative values were designated 0). Bars depict the medians whereas error bars represent the maximum values.

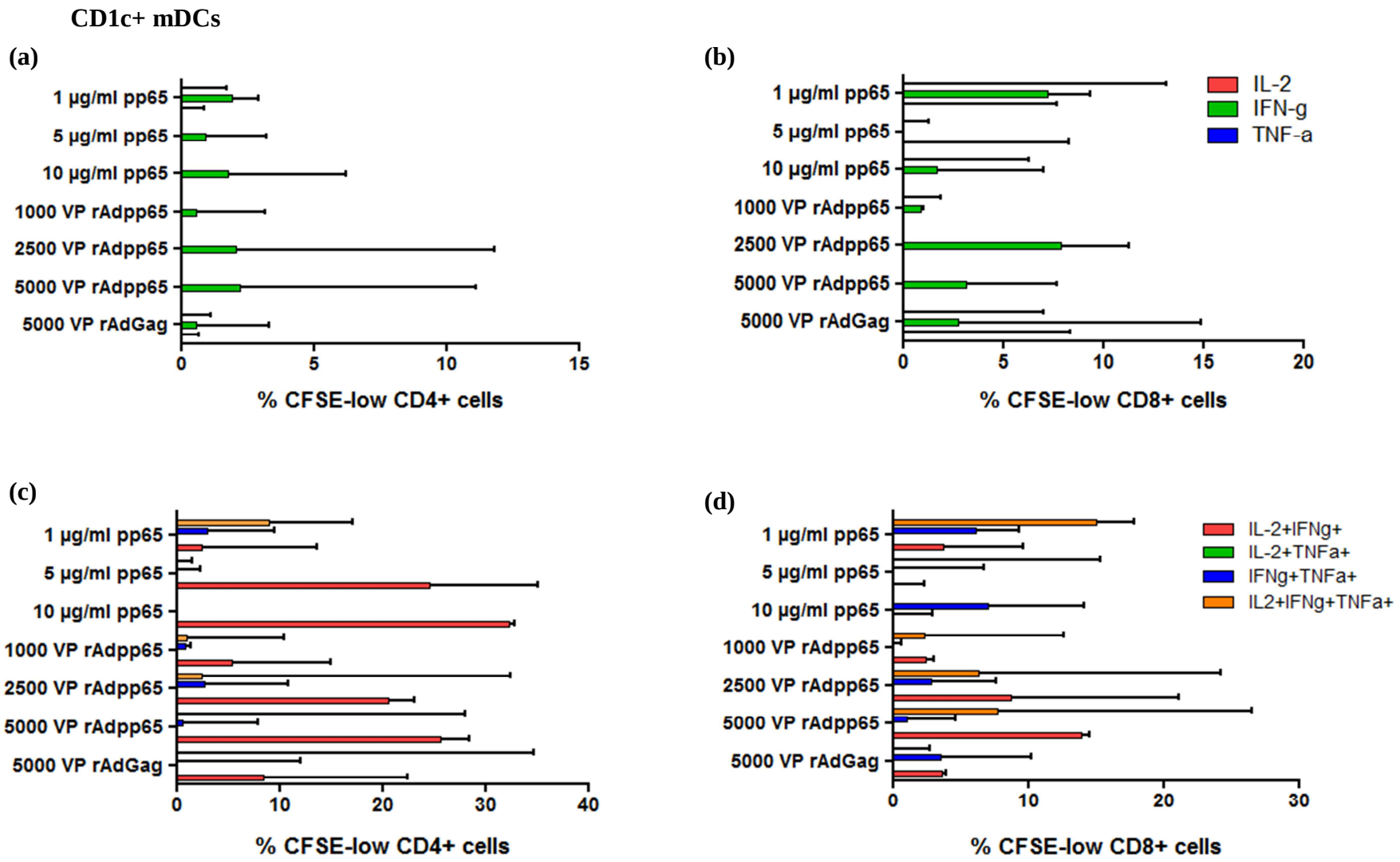


Figure 4.12 - Assessment of T-cell cytokine production after co-culture with stimulated CD1c+ mDCs, to evaluate immunogenicity of pp65 (in the form of full-length protein or via recombinant Adenovirus carrying pp65 gene). CD4+ (a and c) and CD8+ (b and d) T-cell cytokine production (IL-2, TNF-α and IFN-γ) is shown after incubation for 7 days with LPS co-stimulated CD1c+ mDCs (previously incubated with respective protein/virus for 24 hrs), followed by re-stimulation with PMA, ionomycin and BFA.. (a) and (b) depict single cytokine production, while (c) and (d) depict multiple cytokine production by individual cells. The cumulative data from 6 independent experiments is shown after correction for background responses to DC alone (negative values were designated 0). Bars depict the medians whereas error bars represent the maximum values.

4.3.4.3 CD8+ T-cell antigen-specific responses

Antigen-specific responses to CMV pp65 and MART-1 were evaluated using pentamer-staining specific to a given MHC class I pp65 and MART-1 epitope, and were detected after 7-day co-cultures as previously described. Given the low number of samples, no statistical significance was observed for antigen specificity; however the trend showed a general increase in antigen-specific responses as protein concentration increased for both pp65 and MART-1 (Figure 4.14). The responses to the virus-infected cells were less pronounced for rAdpp65 and rAdMART, with only marginal differences in antigen-specific response between the three concentrations measured. In addition, there was no apparent correlation between the levels of antigen-specific responses and the number of VP used. MART-1-specific responses were lower in magnitude, and as expected, responses to rAdGag were low. In general, antigen-specific CD8+ T-cell responses were found to be substantially lower when measured by pentamer staining compared to CFSE-staining as previously illustrated in Figures 4.9 and 4.13.

4.3.4.4 Immunogenic comparison of model antigens with their respective fusion antigens

To demonstrate that the presence of streptavidin in the fusion proteins did not negatively affect the immunogenicity of pp65 and MART-1, CD8+ T-cell proliferation was briefly examined after stimulating cells with three concentrations of model antigens, and respective streptavidin-fusion antigens (Figure 4.15). For pp65, the difference in proliferation was more pronounced at low concentrations, with pp65 inducing a four-fold lower proliferative response compared to pp65-strep at a concentration of 0.1 µg/ml (Figure 4.15a). This difference decreased as concentration of protein increased, with very little difference in immunogenicity at the higher concentrations (8.5 and 10.4 % for 1 µg/ml pp65 and pp65-strep respectively).

For MART-1, the difference in immunogenicity was less prominent at the different concentrations, with MART-streptavidin (MART-strep) demonstrating slightly better responses at the higher concentrations (11.1 and 14.5 % for MART-1 and MART-strep respectively) (Figure 4.15b). Consequently, the addition of the streptavidin core to the model antigens did not adversely affect its immunogenicity.

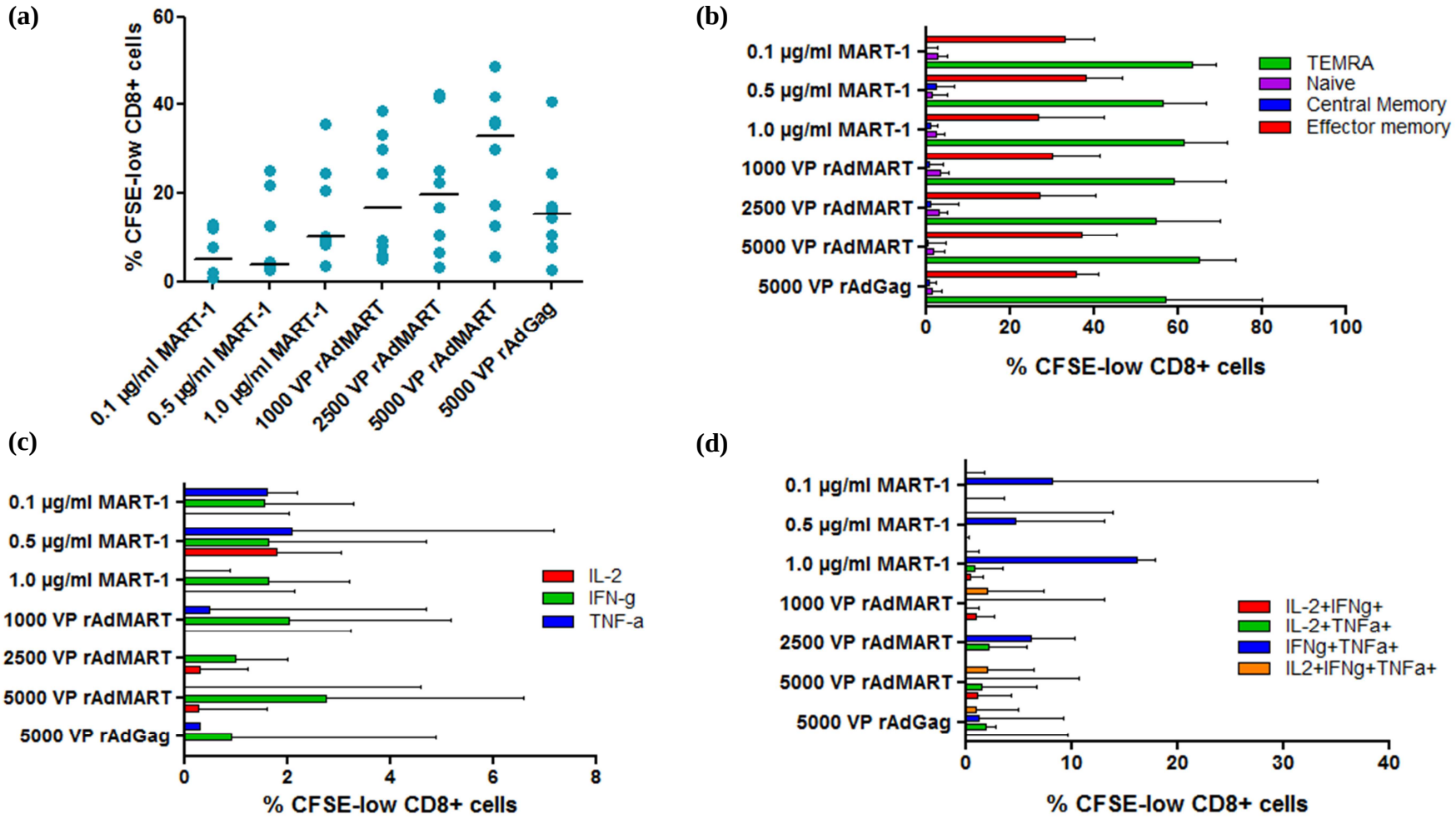


Figure 4.13 - Immunogenicity of MART-1 as presented in the form of protein and via recombinant adenovirus. CD8+ T-cell proliferation (a), CD8+ T-cell phenotypes (b), and CD8+ T-cell single and multiple cytokine production (c and d respectively) are depicted after T-cells were incubated for 7 days with LPS co-stimulated A*02:01+ moDCs (previously incubated with respective protein/virus for 24 hrs). Cytokine samples (c and d) also underwent a re-stimulation with PMA, ionomycin and BFA before being harvested. Cumulative data of 7 (a), 3 (b, c and d) independent experiments are shown after correction for background responses to DCs alone in (a, c and d). (negative values were designated 0). DC background median and range for (a): 1.3 % and 0.9-3.7 %. Horizontal lines (a) and bars (b, c, and d) depict median values while error bars show the maximum values.

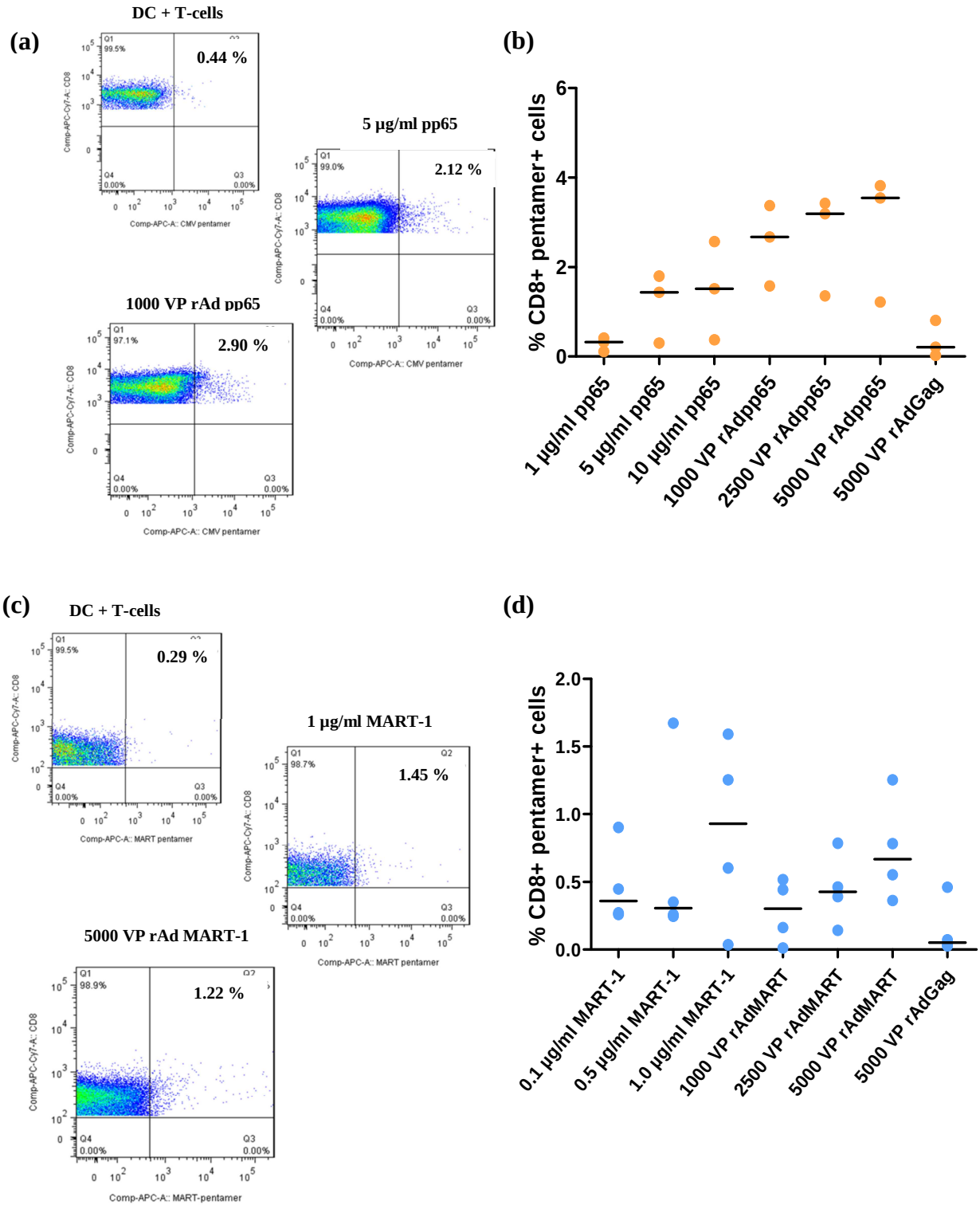


Figure 4.14 - Antigen-specific responses to pp65 and MART-1 stimuli, as evaluated by pentamer staining of proliferated T-cells after stimulation with antigen-pulsed or infected moDCs. Pentamer positive CD8+ T cells are shown for (a and b) pp65 (c and d) MART-1. (a and c) depict dot plots of the respective stimulations; (b and d) depict graphical representation of antigen-specific responses. Data shown are representative of 3 (a and c) or 4 (b and d) experiments after correction for background responses to DC alone (DC background median and range: 0.44 % and 0.15-0.67 % for (b); 0.16% and 0.09-0.29 % for (d)). In (b and d), lines depict median values whereas circles represent individual samples.

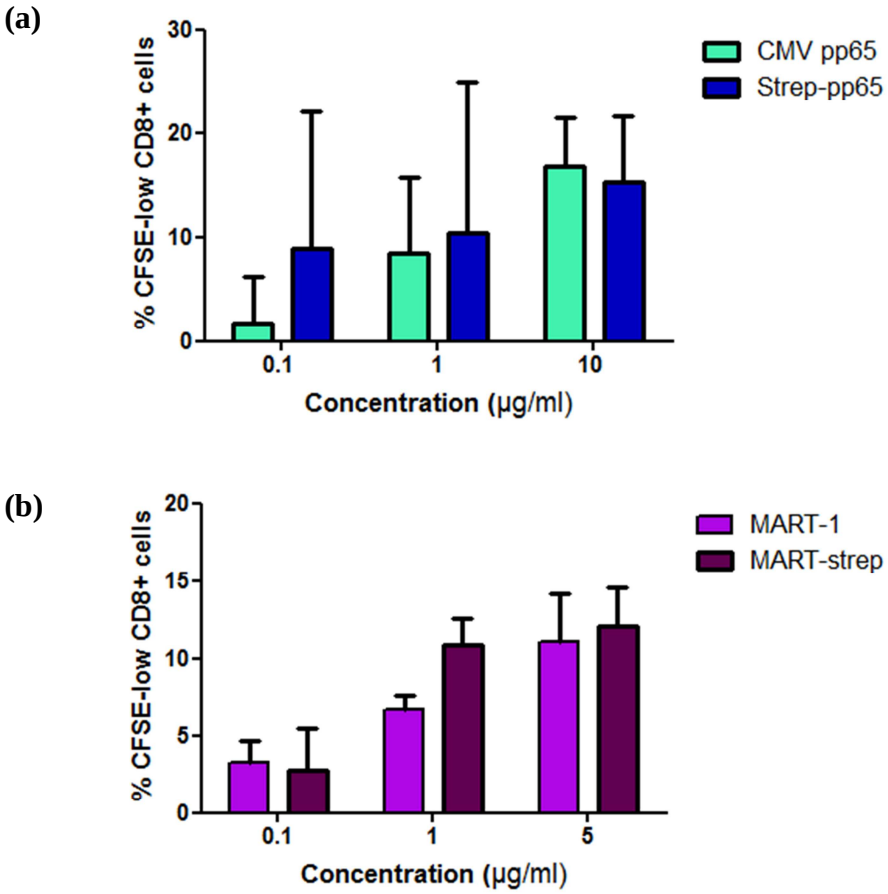


Figure 4.15 – Comparison of CD8+ T-cell proliferative responses to model antigens and streptavidin-fusion proteins as evaluated after T-cell stimulation with antigen-pulsed moDCs. (a) pp65 and streptavidin-pp65 stimuli, or (b) MART-1 and MART-strep stimuli. Cumulative data from 4 (a) or 3 (b) independent experiments are shown. Bars depict median values with error bars showing the maximum values.

4.4 Discussion

The complexity of the role DCs play in the innate and adaptive immune responses has yet to be fully elucidated. There are now at least six different human DC subsets that have been identified in blood and peripheral tissue, all of which differ in functionality. In this study we looked at the immunogenicity of our model antigens, CMV pp65 and MART-1, and compared the ability of two DC subsets to elicit T-cell responses against these antigens. The induced T-cell responses were characterised to provide a broad picture of the cell-mediated responses the antigens elicit, and were also compared to those responses observed in other studies, to verify the integrity of our produced model antigens.

Two DC subsets (moDCs and CD1c+ mDCs) were assessed as APCs in this study, evaluated with respect to their ability to activate CD4+ and CD8+ T-cells when stimulated by the model antigens, or their respective rAds. moDCs were chosen because of their common use *in vitro*, while CD1c+ mDCs were selected because they have previously demonstrated an ability to elicit better T-cell proliferative and cytokine responses than moDCs under autologous conditions, as well as influence immune reaction towards a Th1 response (Osugi et al., 2002). Precursors for both moDCs and CD1c+ mDCs were purified from leukocyte cones using immunomagnetic bead technology. Evaluation of their purity through flow cytometry confirmed that these cells were expressing the appropriate markers, and that the majority of other cell types had been successfully excluded. This was further verified by the characterisation of the cultured, immature CD1c+ mDCs and moDCs as based on their surface markers. As expected, moDCs were found to be CD1a+ CD11b+ CD11c+ DC-SIGN+ HLA-DR+, and CD1c+ mDCs showed a similar phenotype of CD1a+ CD11b+CD11c+ DC-SIGN+ HLA-DR+ in addition to being Lin- CD123-.

Once DCs had been characterised, it was important to explore the effect of various adjuvants on moDCs, to identify an appropriate adjuvant to use in *in vitro* experiments. The need for an adjuvant was two-fold. Firstly, adjuvants are able to activate DC maturation which is required to elicit immunogenic T-cell proliferation. If DCs remain immature, they induce tolerance to the stimulatory antigens (Bonifaz et al., 2002). Secondly, the presence of an adjuvant leads to an augmentation of the initial response to an antigen, hence increasing T-cell responses further. This was well demonstrated here, where the most notable adjuvants (LPS, Poly I:C,

CLO97 and CD40L) were able to induce phenotypic maturation of DCs, as well as enhance proliferative responses against pp65, MART-1 and their respective rAds. It was not entirely surprising that these four adjuvants were most effective in enhancing responses, given that they are known to encourage Th1 responses (Mazzoni and Segal, 2004). Of the four, co-stimulation with LPS in addition to stimulation with either protein or virus consistently elicited strong proliferative responses, and led to the higher expression of the co-stimulatory molecule, CD86. It was therefore favoured over the other adjuvants for use in the co-culture experiments. LPS was assumed to be a suitable adjuvant for CD1c+ mDC stimulations too, based on the similar TLR expression profile of these cells to moDCs.

The chosen model antigens have demonstrated an ability to induce strong CD8+ T-cell responses in past studies (Moss and Khan, 2004, Pittet et al., 1999). In particular, pp65 previously induced CMV-specific T cells present at high frequencies in clinical infections, with a distinct pattern of phenotypes and cytokine production (Dunn et al., 2002, Sandberg et al., 2001). We showed here that the variation in both CD4+ and CD8+ T-cell proliferative responses to pp65 was fairly high amongst donors, but responses were relatively strong, with more robust responses against rAdpp65 than pp65 protein. The rAdGag stimulations were included as a control to allow for adenovirus responses and showed prominent CD4+ and CD8+ T-cell responses against this virus; although these were always lower than the observed rAdpp65 responses. This showed that rAdpp65 was inducing a pp65-specific response in addition to the response to adenovirus.

Generally, there were stronger CD4+ and CD8+ T-cell responses to moDC-stimulated samples compared to CD1c+ mDC samples. The exception to this was CD1c+ mDC-stimulated CD8+ responses to rAdpp65, which was much stronger than the observed responses in moDC samples. This indicated that the MHC class-I presentation pathway, primarily used for endogenous antigens such as those of viral infections, is more efficiently targeted in CD1c+ mDCs compared to moDCs. Furthermore, the low CD8+ T-cell responses induced by the pp65 protein in CD1c+ mDCs suggested that access to the cross presentation pathway in CD1c+ mDCs was poor for exogenous antigen (such as the model antigen proteins). This was initially a surprising finding, given that past research had indicated otherwise for autologous reactions (Osugi et al., 2002). However, recent data has shown that it is CD141+ blood mDCs, and not CD1c+ mDCs which are able to demonstrate superior

cross presentation (Jongbloed et al., 2010). CD141+ mDCs have only recently been identified as a different blood DC subset from CD1c+ mDCs, and appear to be functionally distinct. Jongbloed et al (Jongbloed et al., 2010) showed that CD141+ mDCs elicit better T-cell responses and produce significantly higher levels of IL-12 compared to CD1c+ mDCs in the presence of poly I:C. Moreover, CD1c+ mDCs demonstrated a close correlation to CD8α- DC in mice in that they showed a limited capacity to produce IL-12 and induce Th1 responses. In particular, CD1c+ mDCs showed poor enhancement of cross presentation when a TLR agonist such as poly I:C or LPS was administered. The observations in our study are in agreement with this data, although there are also other possible explanations for the low CD8+ T-cell responses we observed. These explanations are related to the adjuvant used, DC:T-cell ratio and the type of antigen utilised, which require further investigation before any conclusions can be made.

With respect to MART-1 stimulations, T-cell proliferative studies have been looked at fairly extensively (Romero et al., 2002), showing strong CD8+ T-cell responses in response to MART-1(Casado et al., 2009). It is still unclear as to why A*02:01 positive individuals uniquely possess a naïve T-cell population that recognize the immunodominant epitope of MART-1; however the ability to activate these cells provides the opportunity to study primary T-cell responses. Data in this study showed that stimulation with MART-1 protein and rAdMART were able to elicit high responses that appeared to be greater in magnitude than those elicited by pp65, specifically the rAdMART-1 responses. This was unexpected given the strength of memory T-cell responses, specifically those demonstrated against CMV pp65. The weaker pp65 median responses could be attributed to the high levels of variation in CMV memory responses, but a closer look at the data suggested that it is also possible that some of the individuals assessed were either seronegative or displayed poor pre-existing immunity. Thus, in hind sight, it would have been beneficial to have screened individuals for CMV seropositivity before undertaking these immunogenicity experiments, especially given that myeloid DCs and monocytes are sites of CMV latency (Jahn et al., 1999) and thus CMV reactivation from DCs could have contributed to the T-cell responses observed. This should be considered more closely in future studies which deal with CMV pp65 as a model antigen.

The strong CD8+ T-cell responses to the rAds were not entirely surprising, given that the adenoviruses had access to both the classical MHC-class I presentation pathway and the cross

presentation pathway, and could therefore stimulate cumulative CD8+ T-cell responses. It was not possible to make any direct comparisons between protein and virus-induced responses because we did not have any data that quantified MART-1 or pp65 carried/produced from the respective viruses, but it was obvious from both sets of data that virus-induced responses were high compared to the protein responses, even when accounting for the response to adenovirus. Nonetheless, the protein-stimulated T-cell responses induced in MART-1 and pp65 were detectable and antigen-specific, according to the pentamer-staining data.

The specificity of the proliferative responses to pp65 and MART-1 as demonstrated using pentamer staining, was found to correspond to other studies, with broader ranges depicted for pp65 compared to MART-1 (Kern et al., 2002, Pittet et al., 1999). These responses were useful in allowing us to gauge the levels of antigen-specificity induced due to different stimuli, however, the pentamer responses appeared to be much lower than the total CD8+ T-cell proliferative responses observed. There are several reasons why this could have occurred. Firstly, as mentioned above, all the virus samples had additional responses to adenovirus that need to be accounted for. While rAdGag was used as a control for this, the presence of pp65 and adenovirus at the same time could produce an additive effect on the magnitude of the response observed. Secondly, the pentamer stain is specific for one epitope of the respective proteins, but there are more immunogenic epitopes in both pp65 and MART-1 which could have contributed to the higher total proliferative responses (Yang et al., 2008a). Furthermore, the HLA-restriction of pentamer staining does not take into consideration the HLA genetic diversity demonstrated in the human population, thus other HLA-types may have produced stronger responses than HLA*02:01 individuals.

This HLA restriction is also a limitation imposed on MART-1 experiments where donors had to be A*02:01-positive. Although this is a common HLA-type amongst Caucasian populations, it proved more difficult than expected to obtain leukocyte cone samples that were A*02:01-positive, with only 7 donors identified in the entire study. Given that the leukocyte cone donors were anonymous, it is likely that many samples were not donated by Caucasian individuals, and therefore the ethnic variation in the donor population possibly contributed to the low number of A*02:01-positive samples obtained. It is also possible that our method of detecting A*02:01 donors, while theoretically sound, may not have been

sensitive enough to identify all positive individuals. It will need to be assessed further in future related work to confirm its use for this purpose. Unfortunately, due to this limitation, the number of MART-1 samples was limited, and MART-1-stimulations of CD1c+ mDCs were not explored.

The well characterised responses to pp65 and MART-1 have provided us with information regarding many aspects related to their immunogenicity, including the T-cell phenotypes induced by these proteins. With regard to the phenotypes of the pp65 proliferating T-cells, the literature has described it as heterogeneous, but prominently made up of CD8+ terminal effector memory T-cells (TEMRA) (CD27+CD28+CD45RA+) and effector memory (EM) (CD45RA- CCR7-) T-cells (Inokuma et al., 2007, Harari et al., 2004). This was confirmed here, where T-cell proliferation responding to stimulation with both pp65 protein and virus demonstrated high percentages of the TEMRA and EM phenotype, the TEMRA phenotype being more dominant. Although we did not assess cytotoxicity in this study, several other studies have shown that TEMRA memory cells display a high capacity for cytotoxicity based on ^{51}Cr release assays and their expression of perforin and granzyme B (Tomiyama et al., 2002, Casado et al., 2009). On the other hand, EM memory T-cells have a lower cytotoxic capacity, and their lack of, or low expression of homing receptors, CCR7 and CCR5, means their potential to migrate is also low (Tomiyama et al., 2002). Given that the pp65 antigen is virus-derived, it was not surprising that it was able to induce stronger TEMRA responses, as CMV-infected cells would need to be eliminated fairly quickly to avoid the virus spreading.

Similarly, with tumour-related cells, one would expect TEMRA T-cells to dominate the response, as the destruction of these cells prevents their proliferation. Thus, MART-1 T-cell responses here correspondingly demonstrated high levels of TEMRA and EM phenotypes, as has been shown previously (Casado et al., 2009). Unusually, MART-1 T-cells also included a small percentage of naïve T-cells after stimulation. Upon closer examination, these cells appeared to be CD45RA-low. This suggested that they were more likely to be TEMRA-related rather than naïve cells, although further investigation with a greater number of samples is needed to verify the phenotype. Additionally, it would be of interest to investigate the expression of other receptors that define T-cell phenotypes, such as CD27 and CD28 (Tomiyama et al., 2002). The expression of these receptors by memory T-cells have indicated that there are several intermediate memory T-cell populations, suggesting that there is a

greater complexity to the differentiation pathways of memory T-cells than was initially thought.

In relation to cytokine production, CMV responses are usually Th1-biased, characterized by a high frequency of IFN-γ production and low IL-2 production, despite the role of pp65 in inhibiting inflammatory cytokine production (Kern et al., 2002, Harari et al., 2004). In moDC- and CD1c+ mDC-stimulated samples, production of IFN-γ was fairly prominent, with an absence of singly-produced IL-2, as has been published in the above studies. That being said, polyfunctional CD4+ T-cells producing IL-2 and IFN-γ were elicited by both cell subsets stimulated with pp65 protein. There is little in the literature describing the benefits of CMV-specific polyfunctional T-cells, however it has been noted in HIV-1 studies that the induction of T-cells producing IL-2 and IFN-γ has been correlated with protection (Boaz et al., 2002). Hence T-cell polyfunctionality is thought to contribute to T-cell efficacy.

Interestingly, the breadth of the cytokine profile elicited by MART-1 stimulations was greater than that seen with pp65, with the MART-1 protein stimulating production of all three cytokines measured, although rAdMART induced poor cytokine production comparatively. There was detectable production of IFN-γ produced by almost all MART-stimulated samples, consistent with previous data (Pittet et al., 1999), however, there was also a large percentage of cells producing IFN-γ+ TNF-α+, indicating the induction of polyfunctional T-cells by MART-1 as well. Previous studies have focussed on IFN-γ production by MART-1-specific T-cells, but given the efficacy of polyfunctional T-cells in viral infections, they are likely to be significant against tumour development too.

It is important to note that the specificity of the cytokine responses induced in this study was unknown, in view of the non-specific nature of PMA and ionomycin stimulation. Ideally, cytokine responses should have been measured after re-stimulation using pp65 or MART-1-pulsed autologous DCs, as this would have provided us with specific responses to the proteins in question. However, non-specific stimulations were deemed acceptable for the purposes of this study as in other studies (Hamann et al., 1997), because we were mainly interested in exploring basic information about the kind of cytokines that the respective model antigens could elicit. To account for the non-specificity to some degree, the appropriate negative controls were included in the experiments. These were samples that

evaluated the cytokine production of DC and T-cells alone (used to normalise stimulated samples), and cells that were exposed to BFA but not PMA and ionomycin (for gating purposes). Although it is difficult to be sure that the magnitude and breadth of the responses observed were due to antigen stimulation, the cytokine repertoire induced by the model antigens in this study agrees with data from other studies that have evaluated the immunogenicity of these antigens. However, it will be of interest to investigate the use of specific re-stimulations in future studies to validate the observations made here.

The array of cytokines assessed in this study was limited to Th1-related cytokines, based on past research, which has shown pp65 and MART-1 antigens display a bias towards Th1-induced responses (Kern et al., 2002, Butterfield et al., 2008). That being said, stimulations with these antigens could induce other cytokines such as IL-17 and IL-6, given the intertwined relations Th responses share. Moreover, data relating to the cytokine repertoire produced by the DCs upon stimulation (eg. IL-12, IL-10, TGF-β) has not been investigated, and is likely to consolidate our knowledge of the type of immune response these cells elicit. Thus, these aspects would be of interest to investigate in a more detailed study at a later stage.

For the purposes of this study, the broad evaluation of pp65 and MART-1 immunogenicity provided sufficient detail about the induced immune responses to allow for investigation into how these responses can be enhanced in the DC targeting strategies in the chapter to follow. Thus, easy comparisons can be made between free antigen immunogenicity (depicted in this chapter) and DC-targeted antigen immunogenicity (the primary focus of Chapter 5). Similarity of the pp65 and MART-1 protein responses to those of published data verifies the immunogenic integrity of the produced antigens. Further, the addition of a streptavidin core to the fusion proteins does not appear to affect the immunogenicity of the model antigens to a great extent. This data therefore confirms the produced, purified antigens are suitable for use in future experiments, where they will be targeted specifically to endocytic receptors on the surface of DCs in order to access the cross presentation pathway.

Chapter 5

In vitro assessment of T-cell responses to specific DC-receptor targeting

5.1 Background and aims

5.1.1 DC endocytic receptor targets

Research has highlighted the need to improve the induction of strong, antigen-specific CD8+ T-cell responses by HIV-1 vaccines (Boyer et al., 1999, Andrieu and Lu, 2007). Consequently, access to the cross presentation pathway has sparked the interest of vaccine researchers, because it provides a way to directly stimulate specific CD8+ T-cell responses against vaccine antigens. Certain endocytic receptors on the surface of DCs appear to preferentially direct endocytosed antigens towards the cross presentation pathway, thereby enhancing antigen-specific CD8+ T-cell responses (Bonifaz et al., 2004, Burgdorf et al., 2006). As mentioned in Chapter 1, there are a number of DC receptors that have been explored as potential targets for directing antigen towards the cross presentation pathway in mice including DEC-205, DCIR-1 and MMR amongst others (Burgdorf et al., 2006, Nchinda et al., 2008). Recently, Idoyaga et al (Idoyaga et al., 2011) demonstrated that by targeting an HIV-1 Gag p24 protein to Langerin, DEC-205 or CLEC9A receptors on CD8α+ DCs *in vivo*, Gag-specific T-cell responses could be induced and further enhanced in the presence of anti-CD40 antibody. While such mouse studies are very useful in allowing us to understand how the immune system functions and what effects certain factors have on immune responses, the information gained from mouse studies is not always directly translatable to humans. This is particularly true for DC studies, because mouse and human DC subsets differ quite significantly in functionality and phenotype (Banchereau et al., 2000, Proudfoot et al., 2007, Palucka et al., 2010). In view of this, *in vitro* human studies exploring DC receptor targeting strategies for possible use in vaccine regimens are currently of great interest. A recent study by Klechevsky et al (Klechevsky et al., 2010) indicated the success of such targeting strategies in humans, where they found targeting antigen to DCIR on the surface of skin-isolated LCs, BMDCs and pDCs mediated cross presentation and induced antigen specific T-cells. In addition, Bozzacco et al (Bozzacco et al., 2007) also demonstrated some promising

research whereby an HIV-1 Gag protein targeted to the DEC-205 receptor on moDCs stimulated proliferation and IFN-γ production by CD8+ T cells isolated from the blood of HIV-infected donors.

In this chapter, we look at targeting four selected receptors as potential targets to send antigen towards the cross presentation pathway. These include DEC-205, MMR, DC-SIGN and/or CD1a. Four different targeting strategies were investigated to discover the most efficacious option to direct antigen towards the selected receptors, and to determine which of these receptors are best able to significantly enhance CD8+ T-cell responses. There are some similarities in the four methods chosen in that they all make use of receptor-specific antibodies to target the DC receptors, and use MART-1 and/or pp65 as the antigen component. The differences lie in how the reagents are prepared for targeting purposes, and this potentially affects which processing route the antigen is targeted to, as well as how the antigen is eventually presented on the surface of DCs.

5.1.2 Aims of chapter

(i) To determine if the produced targeting reagents are functional.

(ii) To evaluate the ability of the targeting reagents (from four receptor-targeting strategies) to direct antigen towards the cross-presentation pathway.

(iii) To compare CD8+ T-cell responses (based on proliferation and cytokine production) stimulated by targeting various receptors to determine the optimal receptor to access the cross presentation pathway.

5.2 Materials and Methods

5.2.1 Assessment of targeting reagents to attach to DC surface receptors

To verify that the commercially-obtained receptor-specific biotinylated antibodies (Table 5.1) were able to attach to the intended surface receptors, flow cytometry was utilised. Immature moDCs or CD1c+ mDCs (approximately $1x10^5$ cells) were incubated with 1 µg/ml of the chosen biotinylated anti-receptor antibodies for 20 min on ice. This was followed by washing cells, and incubating with a streptavidin-fluorochrome secondary antibody for a further 20 min on ice (Table 5.1). Cells were washed once more and fixed with 2 % PFA. Respective isotype antibodies were used as controls for all the attachment experiments described here.

To confirm that the pp65-streptavidin (pp65-strep) and MART-streptavidin (MART-strep) antigens were able to bind to DCs via the above biotinylated antibodies, a similar procedure as described above was used. Briefly, immature moDCs were incubated with the biotinylated anti-receptor antibodies, cells were then washed and further incubated with the respective streptavidin-antigens (0.5 nM) for 20 min on ice. After another wash, cells were stained with a pp65-specific monoclonal antibody, followed by a final staining step with a goat anti-mouse fluorochrome secondary antibody (Table 5.1). Cells which were exposed to all the reagents except the primary antibody against the streptavidin proteins were used as a negative control, to account for any binding of the secondary antibody to the initial receptor-specific antibodies instead of the antigen-specific antibody. After a last wash, cells were fixed with 2 % PFA.

Attachment of the pp65-chemical conjugates to surface DC receptors was assessed as described for the fusion proteins, except that the first incubation step was eliminated because pp65 was already attached to the respective antibodies, and could therefore be incubated directly with cells at a concentration of 0.5 µg/ml. The final targeting strategy made use of a commercially purchased reagent that consisted of pp65 peptides, anti-biotin monoclonal antibody, and a fluorescent tag (Fluorescein isothiocyanate (FITC)) attached to a polymer scaffold (referred to as a dendrimer). The attachment of pp65 dendrimers (Miltenyi, UK) to DCs via the biotinylated antibodies was also evaluated. However, because the dendrimer was conjugated to a FITC tag, cells underwent the first incubation step mentioned above with the anti-receptor antibodies, and then a final incubation with the dendrimer (10 min on ice),

before they were fixed. Because the concentration of the dendrimers was unknown, the binding capacity of five dilutions of the reagent was evaluated, ranging from 0.1 to 1.

Table 5.1 – Antibodies used to target antigens to DC receptors and in flow cytometry staining procedures.

Antibody	Conjugation	Clone	Isotype	Supplier
Endocytic receptor-specific antibodies				
DEC-205 (CD205)	Biotin	MG32	Mouse IgG2b	eBioscience Ltd, UK
MMR (CD206)	Biotin	15-2	Mouse IgG1	BioLegend UK, Ltd
DC-SIGN (CD209)	Biotin	eB-h209	Rat IgG2a	eBioscience Ltd, UK
CD1a	Biotin	HI149	Mouse IgG1	eBioscience Ltd, UK
Staining antibodies for flow cytometry				
Streptavidin	PE	-	-	eBioscience Ltd, UK
Pp65	None	OBT0742	Mouse IgG1	AbD serotec (UK)
MART-1	None	M2-7C10	Mouse IgG2b	AbCam® (UK)
Goat anti-mouse	PE	Polyclonal	Goat Ig	BD Pharmagen^{TM}, UK

5.2.2 DC-T-cell co-culture assays with the targeting reagents

5.2.2.1 DC pulsing using biotinylated pp65 reagents

This method made use of biotinylated pp65, the biotinylated receptor-specific antibodies and anti-biotin microbeads (Miltenyi, UK). A pilot DC-T-cell co-culture assay was carried out to determine the optimal quantities to use of each reagent to obtain T-cell enhancement. Only DEC-205 targeting was examined at this stage. The quantities evaluated were based on similar molar ratios of antigen and antibodies, specifically exploring 1:1, 1:5 and 1:10 of antibody: antigen. First, biotinylated pp65 and biotinylated DEC-205 antibody were incubated with the anti-biotin micro-beads (in the varying ratios) at room temperature for 10-15 min. This allowed the reagents to form the targeting conjugate of pp65-anti-biotin bead-antibody. This was followed by the addition of 5×10^4 DCs to the mixture, which was incubated for a further 30 min on ice. DCs were then washed using serum-free media, resuspended in 10 % AB serum, added to 96-well U-bottomed plates at a concentration of 10^4 cells/well, and incubated overnight at 37 °C and 5 % CO_2. After incubation, LPS (TLR4 agonist) (Sigma-Aldrich, UK) was added to DCs at a concentration of 1 µg/ml, and cells were

incubated for a further 3-4 hrs before the addition of autologous, CFSE-stained T-cells (see section 4.2.5.3). As a positive control, SEB (500 ng/ml) was used to pulse cells in all co-culture assays, and the respective isotype control antibodies were used as negative controls. Once the optimal ratios had been decided, all the following DC-T-cell co-culture assays for this targeting strategy were set up as described above, using the optimal quantities of beads, antibodies and biotinylated pp65.

5.2.2.2 DC pulsing using chemically-conjugated reagents

An initial titration co-culture experiment was carried out to determine an appropriate concentration of the chemical conjugate to use in further experiments. Three concentrations were assessed (0.1, 0.5 and 1 µg/ml), and CD8+ T-cell proliferation was evaluated. The optimal concentration was then used for further experiments. DC-T-cell co-culture assays were set up where 5×10^4 DCs were added to sterile FACS tubes, and then pulsed for 1 hr at 37 °C with the pp65 chemical conjugates, namely, pp65-DEC-205, pp65-MMR and pp65-DC-SIGN and their respective isotype controls. Once complete, pulsed DCs were added to 96-well U-bottomed plates and the remaining steps of the co-culture experiment were carried out as described in section 5.2.2.1. An FcR blocking agent (Miltenyi, UK) was used in all experiments to eliminate non-specific binding of reagents to cells.

5.2.2.3 DC pulsing using streptavidin fusion reagents

As with the chemical conjugate experiment, an initial titration co-culture experiment was carried out to determine an appropriate concentration of pp65-strep to be used. Once identified, this concentration was used for further experiments with these reagents. DC-T-cell co-culture assays were then set up where receptor-specific antibodies (5 µg/ml) were added to sterile FACS tubes, followed by the addition of 5×10^4 DCs, and incubation on ice for 20 min. DC were washed, and further incubated on ice with pp65-strep or MART-strep. The pulsed DCs were then washed again, resuspended in 10 % human AB serum, and added to 96-well U-bottomed plates for overnight incubation at 37 °C and 5 % CO_2. The remaining steps of the co-culture experiment were carried out as described in section 5.2.2.1. All MART-1-related stimulations were done using A*02:01 cell samples. Controls for these experiments included the use of SEB-pulsed DCs, isotype antibodies for each of the respective biotinylated antibodies, as well as DCs incubated with and without the antigen alone. In addition, an FcR blocking agent (Miltenyi, UK) was used in experiments to

eliminate non-specific binding of reagents to cells. A second FcR blocking agent (BioLegend, UK) was employed for later experiments depicted in Figure 5.10.

5.2.2.4 DC pulsing using CMV pp65 dendrimer reagent

This procedure was the same as that used for the streptavidin-fusion reagents, with the exception of the second incubation step. The initial incubation involved the addition of a commercially available pp65 dendrimer to cells (used at the recommended concentration of manufacturer) (Miltenyi, UK) instead of the streptavidin-fusion reagents. In this case, the pp65 dendrimer was incubated at the recommended concentration with DCs for 15 min at 4 °C. In addition, an FcR blocking agent (Miltenyi, UK) was used in experiments to eliminate non-specific binding of reagents to cells.

5.2.3.5 CFSE staining of T-cells

Done as described in section 4.2.5.3.

5.2.3 Titration of reagents

5.2.3.1 Lymphocyte proliferation assay

These assays were performed using the pp65-strep reagent and pp65 dendrimer reagent to stimulate DCs (Miltenyi Biotec, UK). DC-T-cell co-culture assays were carried out for 5 days, and were performed as described in sections 5.2.2.3 and 5.2.2.4 respectively. After this, the cultured T-cells were pulsed for 16 hrs at 37 °C with 2.5 µC/well [^{3}H]-thymidine (PerkinElmer LAS Ltd, UK). Thymidine incorporation was halted by freezing samples at -20 °C. Cells were then thawed at 37 °C for 1 hr, and harvested onto filter mats. These were left overnight to dry, after which, mats were coated with beta-emitting scintillation liquid and sealed in plastic covers. Thymidine incorporation was read as counts per minute on a Beta-plate liquid scintillation counter (Wallac, Turku, Finland).

5.2.4 Phenotypic and functional analysis of T-cells in co-culture assays

As described in section 4.2.6

5.2.5 Data acquisition, gating strategy and statistical analysis

As described in section 4.2.7 and 4.2.8

5.3 Results

Initial assessment of the efficacy of the targeting reagents began with a functional analysis of their binding capacity to the surface DC receptors. The attachment of the commercially purchased biotinylated receptor-specific antibodies to their respective receptors on DCs was first examined (Figure 5.1 and 5.2). On moDCs, all antibodies bound to the respective receptors (Figure 5.1a), although there were variations in the expression of the chosen receptors, which is why some receptors seemed to be detected better than others (Figure 5.1b). DC-SIGN and CD1a were most prominently expressed (67.9 and 66.5 % on average respectively), while DEC-205 and MMR were expressed to a lesser extent (31.3 and 39.3 %). The $CD1c^+$ mDCs demonstrated high levels of expression of DEC-205 and CD1a (55.7 % and 78.2 % respectively), with moderate levels of DC-SIGN (35.9 %) and no detection of MMR. The lower levels of DC-SIGN on $CD1c^+$ mDCs compared to moDCs has been reported previously, and the absence of MMR on $CD1c^+$ mDCs has also been noted (Kato et al., 2000). Overall, all receptor antibodies seemed to attach as expected to the surface of the chosen DCs and proved to be adequately biotinylated to be utilised in the targeting strategies.

5.3.1 Targeting DC receptors using biotinylated pp65

The first method of directing pp65 antigen towards the chosen receptors on moDCs, was to use a mixture of biotinylated pp65 (bio-pp65) and biotinylated receptor-specific antibody with anti-biotin magnetic beads. The premise behind this strategy was that by adding different molar ratios of the antigen and antibody to the anti-biotin beads, we would maximise the binding of both reagents to individual beads (as shown in Figure 5.3a), and therefore create an antibody-pp65-bead conjugate. This would therefore allow antigen to be targeted to the selected receptors. Using varying concentrations and amounts of bio-pp65 and beads, and keeping the DEC-205 concentration constant (1 µg/ml), a pilot titration experiment was set up to determine an appropriate ratio of the three reagents that would induce strong T-cell proliferation after targeting to DEC-205 and its isotype control, IgG2b (Figure 5.3b).

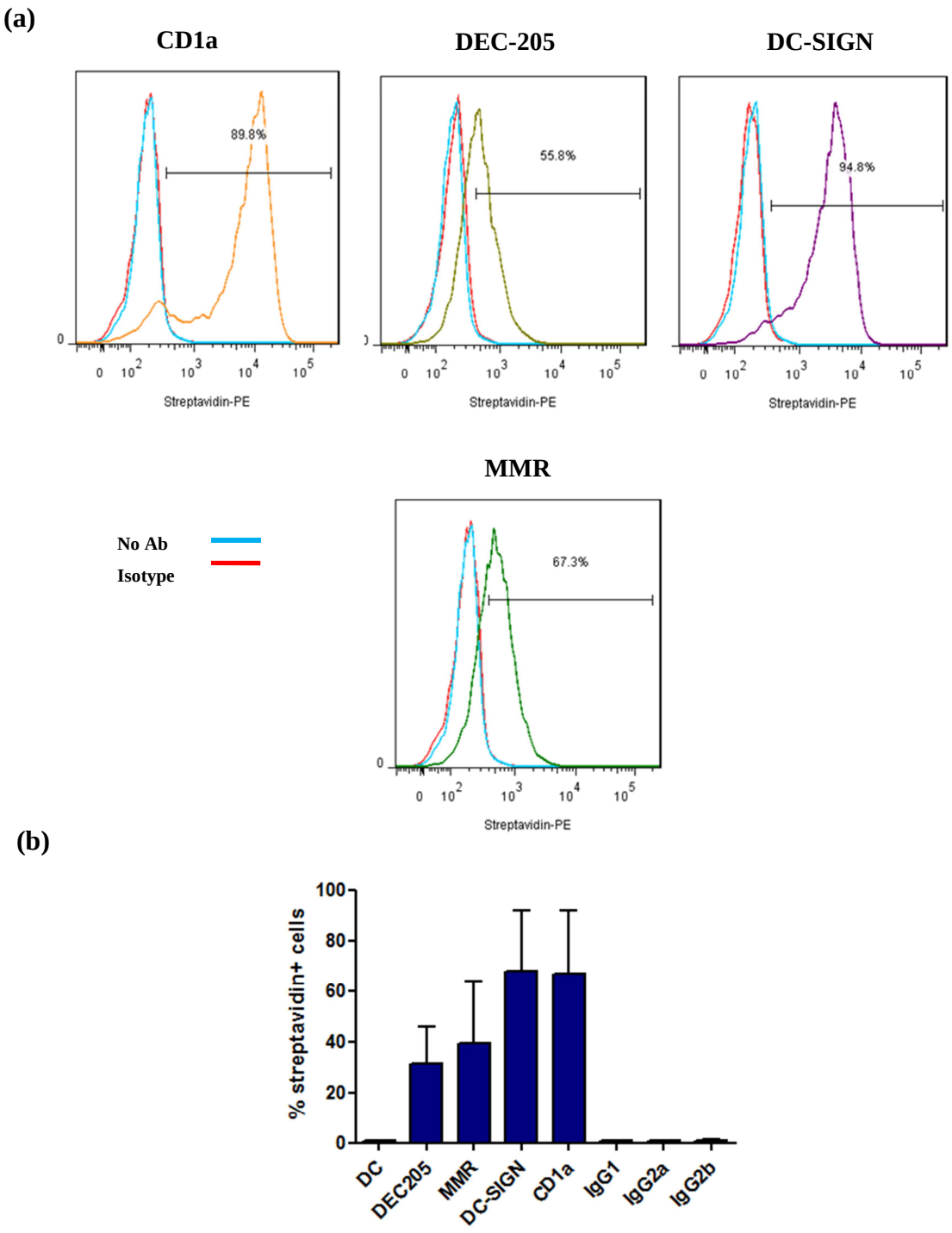
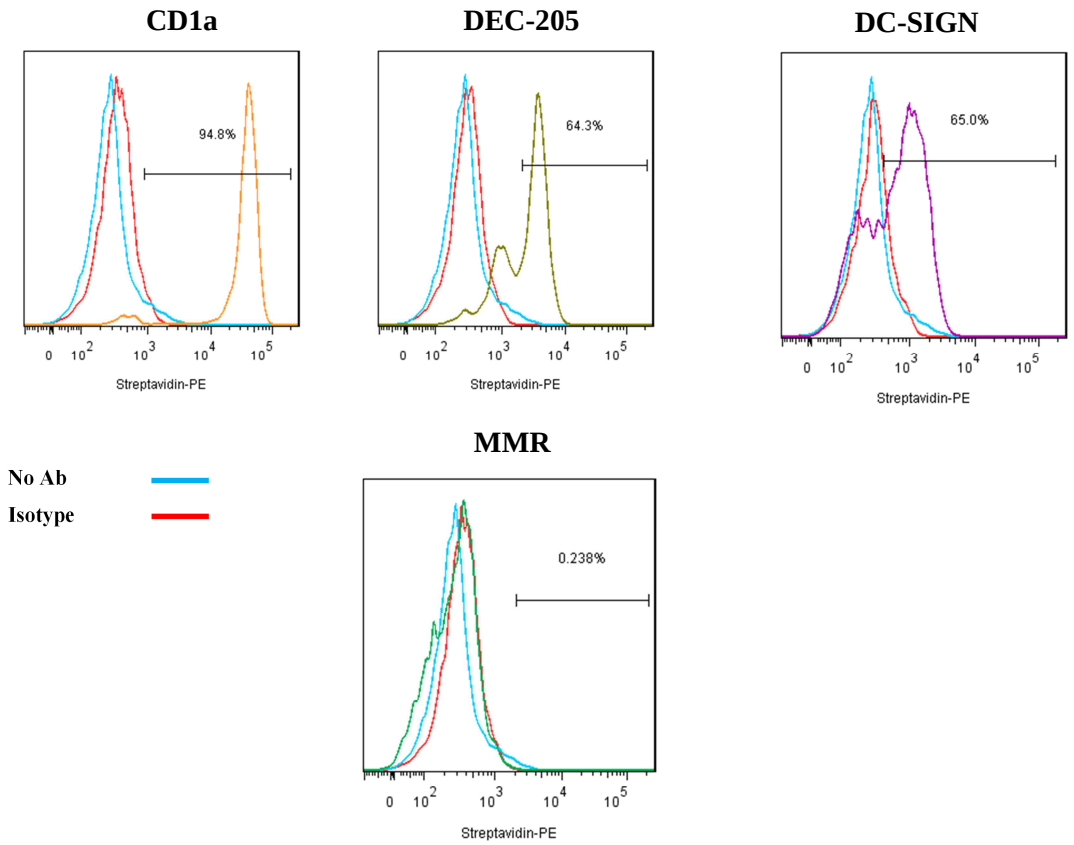


Figure 5.1 – Assessment of the binding of receptor-specific antibodies to endocytic receptors on moDC surface. (a) Attachment of biotinylated receptor-specific antibodies to the respective receptors (DEC-205, MMR, CD1a, DC-SIGN) on moDCs. Histograms are gated on respective isotypes, and moDCs alone were used as a negative control. (b) Percentage of the respective receptors detected on moDCs. Data is representative of 3 independent experiments, and the mean and SD is depicted in (b). Ab = antibody.

(a)



(b)

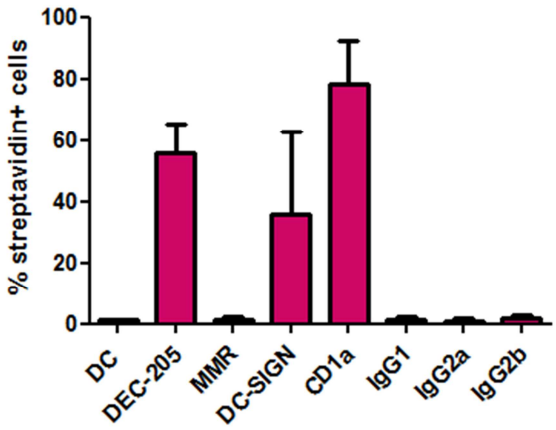


Figure 5.2 – Assessment of the binding of receptor-specific antibodies to endocytic receptors on CD1c+ mDC surface. (a) Attachment of biotinylated receptor-specific antibodies to the respective receptors (DEC-205, MMR, CD1a, DC-SIGN) on CD1c+ mDCs. Histograms are gated on respective isotypes, and CD1c+ mDCs alone was used as a negative control. (b) Percentage of the respective receptors detected on CD1c+ mDCs. Data is representative of 3 independent experiments, and the mean and S.D. is depicted in (b).

The use of 0.1 µg/ml of bio-pp65 and 30 µl of magnetic beads (unknown concentration) stimulated the best CD4+ and CD8+ T-cell proliferative responses, demonstrating values almost four times greater than using bio-pp65 alone (Figure 5.3b). This ratio (1:1 of antibody: antigen) was thus used for further experiments.

While the responses varied quite considerably, targeting receptors to induce enhanced CD8+ T-cell responses using this method was not promising, with all targeted receptors depicting similar proliferative responses to each other and their isotypes (Figure 5.3c). There were also no significant differences between these responses and bio-pp65 + beads with no antibody, or antibody + beads with no bio-pp65. Similarly, cytokine production reflected only marginal differences between targeted and non-targeted samples, despite the high percentage of cells producing IFN-γ and TNF-α (Figure 5.4a). These responses can possibly be attributed to the presence of the beads rather than pp65, as they were prominent in all samples including those that lacked antigen. Interestingly, there was a higher production of multiple cytokines by receptor-targeted bio-pp65, specifically IFN-γ-TNF-α-IL-2 production by bio-pp65 targeted to DEC-205. MMR and DC-SIGN targets also induced good polyfunctional CD8+ T-cell responses, although these did not appear to be markedly different from their isotype controls (Figure 5.4b). An Fc blocking agent was not included in these experiments, but would probably have been useful to dampen the responses we observed for the isotype controls. That being said, the similarity between targeted and non-targeted responses depicted high non-specific responses, and implied that the targeting of DC receptors with biotinylated pp65 was not effective in enhancing CD8+ T-cell proliferation. Optimisation for this targeting approach was difficult due to limited knowledge provided by the manufacturer about the anti-biotin beads. Therefore, this approach was not explored any further, and MART-1 targeting was not attempted for this strategy.

5.3.2 Targeting DC receptors using chemical conjugates

The second targeting strategy made use of pp65 chemically conjugated to receptor-specific antibodies using a stable thioether bond. The ability of the purified chemical conjugates and their isotypes to bind to the respective receptors on the surface of moDCs was tested using flow cytometry (Figure 5.5a). DEC-205-pp65 was able to bind most effectively, with pp65

being detected on the majority of cells. MMR and DC-SIGN conjugates seemed to bind less effectively, with almost three-fold lower percentages of pp65-positive cells. This was surprising considering the high expression of DC-SIGN on moDCs, however, as stated in Chapter 3, the presence of other components in the purified aliquots of these conjugates means that these could potentially affect the binding affinity of the conjugates. Thus, while all three conjugates did successfully demonstrate binding to moDC receptors compared to their isotype controls, the weaker binding affinity of the MMR and DC-SIGN conjugates indicated that a fair comparison of the ability of these receptors to direct antigen to the cross presentation pathway is difficult with this targeting strategy.

With that in mind, a titration experiment was set up to determine the optimal concentrations of the chemical conjugates to use (Figure 5.5b). Unexpectedly, the isotype control data was higher than expected, even though an FcR blocking agent was included in these experiments. DEC-205-pp65 had moderately better responses than their isotype controls at the different concentrations, with almost double the proliferative responses at low concentrations. However, it was only at 0.5 µg/ml that MMR-pp65 and DC-SIGN-pp65 stimulated a marginally better response than its isotype control. Consequently, this concentration was used for further experimentation.

DEC-205-pp65 induced significantly better CD8+ T-cell proliferation in moDC-T-cell co-culture experiments (12.1 %), with a four-fold increase in CD8+ T-cell responses compared to free pp65, and a three-fold increase compared to its isotype (Figure 5.6a). MMR-pp65 was also able to significantly enhance CD8+ proliferative responses by more than two times that elicited by its isotype control, IgG1 (7.4 % compared to 3.1 % respectively), while DC-SIGN-pp65 induced responses that were more than double of the free pp65-induced responses (6.7 % and 2.9 % respectively), but similar to its isotype.

Data from stimulations with CD1c+ mDCs was less encouraging. Although all targeting conjugates produced better responses than free pp65, the difference in responses compared to their isotypes was small, even in the presence of an FcR blocking agent (Figure 5.6b).

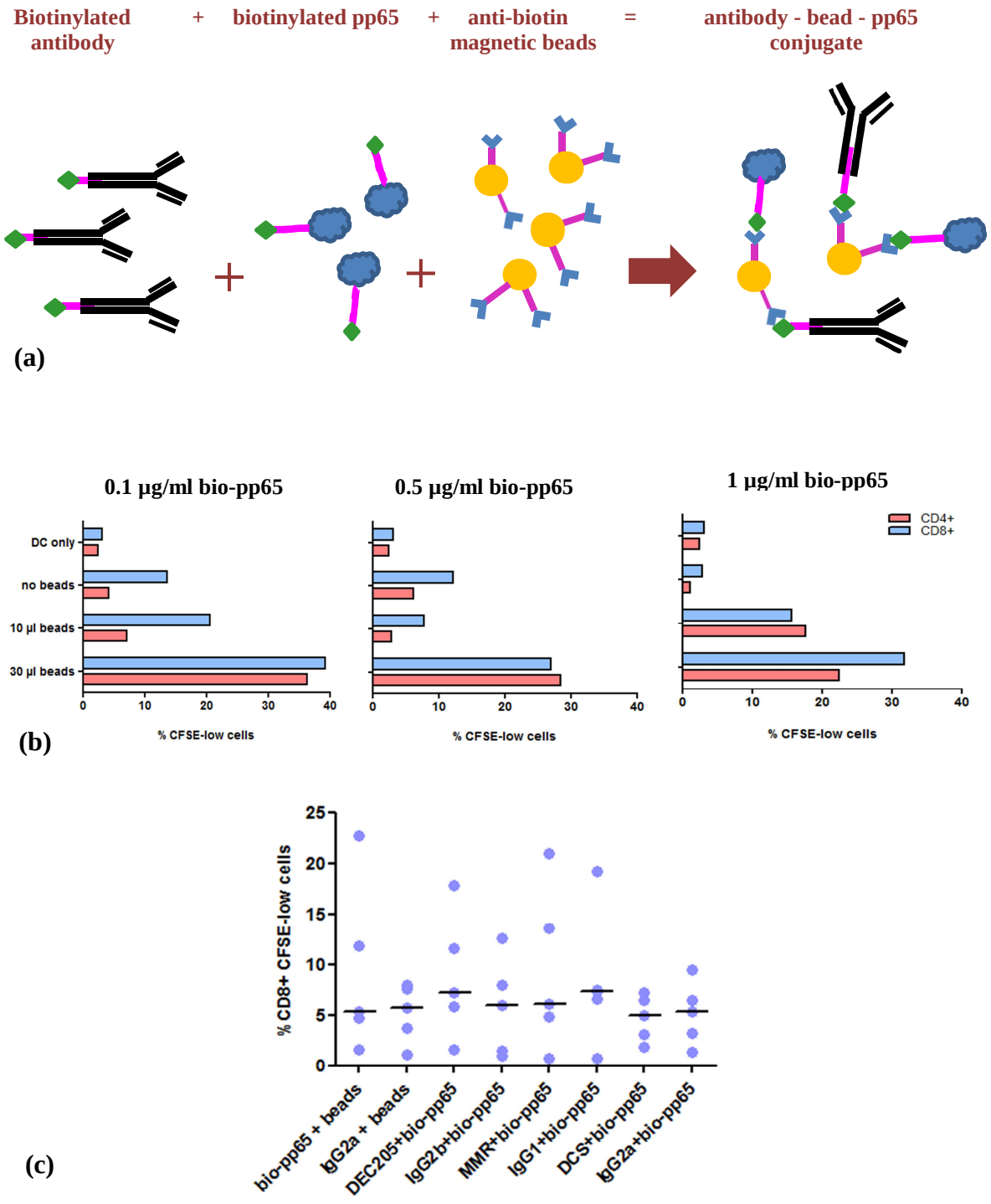
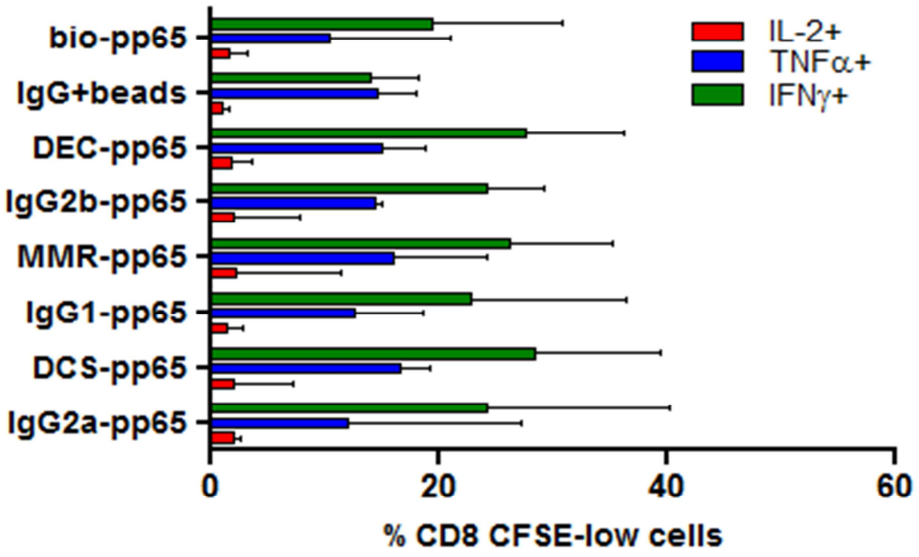


Figure 5.3 – Targeting DC receptors with biotinylated pp65 using anti-biotin magnetic beads. (a) Schematic diagram of the binding of biotinylated pp65, biotinylated antibodies and anti-biotin beads to form the targeted conjugate used in these experiments. (b) Pilot experiment targeting DEC-205 to evaluate appropriate ratio of biotinylated pp65 (bio-pp65) and anti-biotin beads to be used in further experiments. T-cell proliferation is shown after incubation for 7 days with LPS-stimulated, autologous moDCs (pulsed with respective targeting agent for 1 hr before 24 hr incubation at 37 °C). Three concentrations of bio-pp65 were evaluated, namely, 0.1, 0.5, 1.0 µg/ml. (c) Using the targeting agents at an optimal ratio (0.1 µg/ml of bio-pp65, 1 µg/ml receptor-specific antibody and 30 µl anti-biotin beads), CD8+ T-cell proliferation responses were further evaluated. The cumulative data from 2 (b) or 5 (c) independent experiments are shown, where correction for background responses to DCs alone (DC background median and range: 2.4 % and 1.2-3.6 % for (c). Bars or horizontal lines depict the median.

(a)



(b)

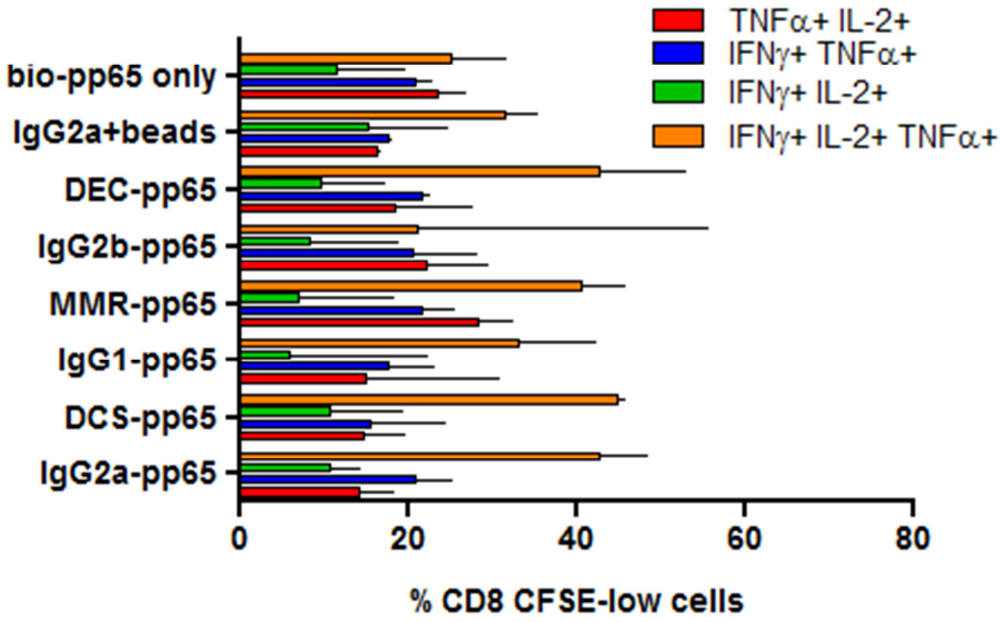


Figure 5.4 – CD8+ T-cell cytokine production after targeting endocytic receptors with biotinylated pp65 using anti-biotin magnetic beads. CD8+ T-cell cytokine production (IL-2, TNF-α and IFN-γ) is assessed, shown after incubation for 7 days with LPS-stimulated moDCs (pulsed with respective targeting agent for 1 hr before 24 hr incubation at 37 °C). (a) depicts single cytokine production, while (b) depicts multiple cytokine production by individual cells. The cumulative data from 5 independent experiments are shown after correction for background responses to DCs alone (negative values were designated 0). Bars depict the medians whereas error bars represent the maximum values.

The magnitude of moDC responses compared to CD1c+ mDC responses were alike, except for DEC-205-pp65 responses which induced almost two-fold better responses than free pp65 and its isotype (8.17 % and 4.13 % and 5.65 % respectively). Cytokine data also indicated that moDCs were better at inducing functional activation of CD8+ T-cells, with DEC-205-pp65 and MMR-pp65 producing IL-2, IFN-γ and TNF-α, and targeting to DC-SIGN producing high amounts of IFN-γ and TNF-α (Figure 5.7a). All three conjugates demonstrated better cytokine production than their isotype controls, with MMR-pp65 and DC-SIGN-pp65 also producing 2-3-fold more IFN-γ and TNF-α than pp65 alone.

IFN-γ production was most prominent in CD1c+ mDC-stimulated samples (Figure 5.7b), although DC-SIGN-pp65 also produced small amounts of IL-2 and TNF-α (1.6 and 4.7 % respectively). DC-SIGN-pp65 elicited the highest IFN-γ response in moDC and CD1c+ mDC samples (7.4 and 19.7 % respectively), with a response that was 13 times greater than free pp65 and 2-fold greater than its isotype induced in CD1c+ mDC samples. This suggests that despite the similar proliferative responses that DC-SIGN induced to its isotype, targeting to this receptor was able to successfully enhance the functional activation of CD8+ T-cell responses. This highlights the importance of assessing more than one variable when exploring the effect of a targeting strategy within the immune system.

The production of multiple cytokines from individual cells showed that CD1c+ mDC samples had a variety of responses, some of which were quite high for the isotype controls, specifically production of IL-2 and IFN-γ from the sample stimulated with the isotype control for DC-SIGN (IgG2a-pp65) (15.5 %) (Figure 5.7d). For moDCs, multiple cytokine production was most notable from samples targeted with MMR-pp65, with strong IL-2-TNF-α responses and IFN-γ-TNF-α responses (13.7 and 19.2 % respectively) (Figure 5.7c). Responses from DEC-205-pp65 were also high for IL-2-TNF-α (12.2 %), and all conjugates demonstrated greater stimulation of polyfunctional CD8+ T-cells than free pp65 and their isotype controls.

Overall, targeting pp65 to the respective receptors using the chemical conjugates showed an enhancement in both proliferative CD8+ T-cell responses and cytokine production. While the responses were not considerably higher than free pp65, use of the chemical conjugates to target pp65 to the cross presentation pathway was effective in enhancing responses.

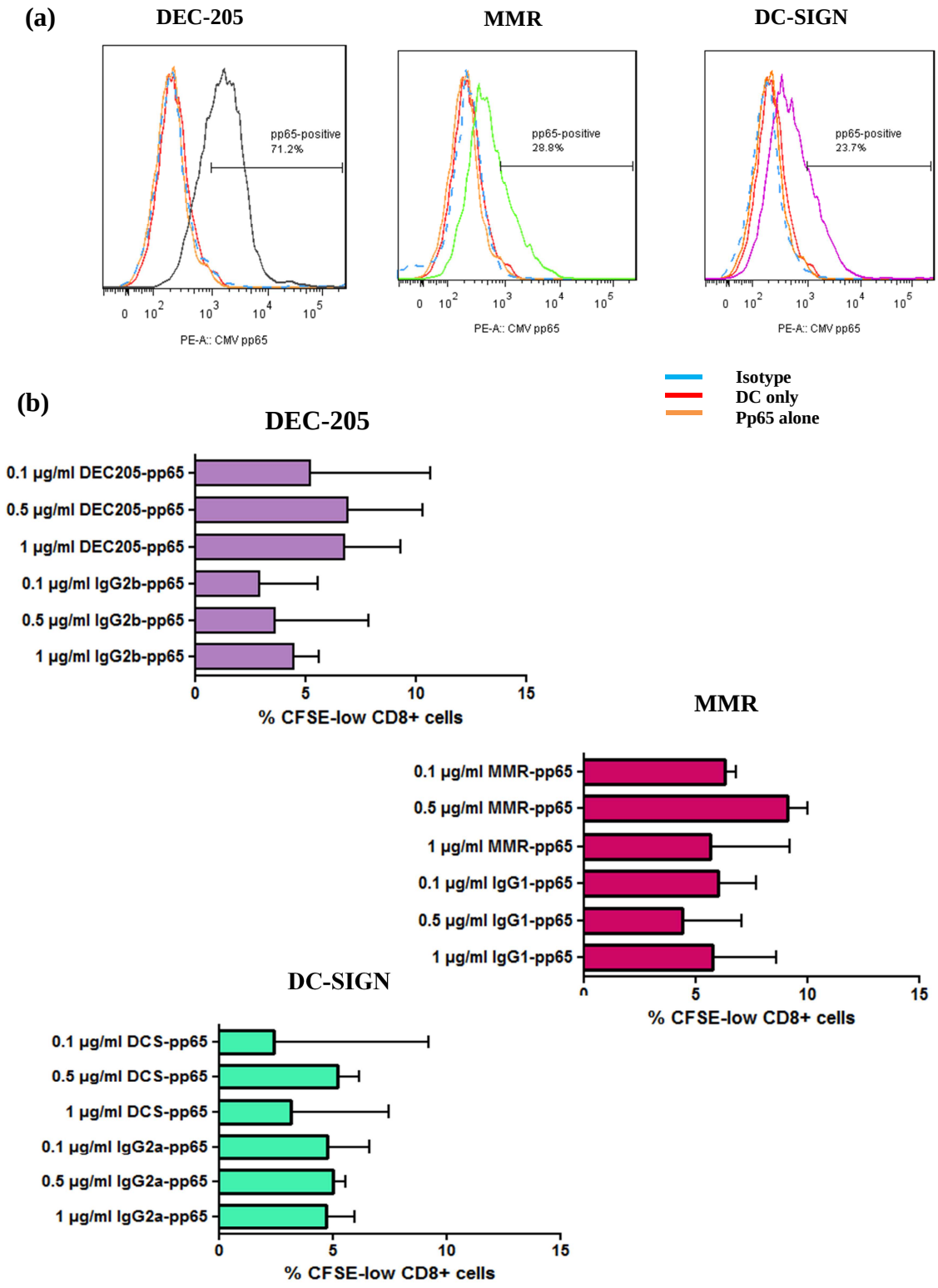
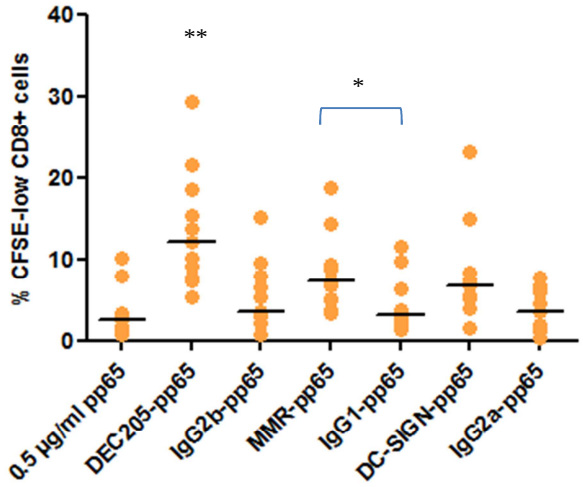


Figure 5.5 – Use of chemical conjugates to target moDC receptors. (a) Binding capacity of pp65 chemical conjugates (DEC-205-pp65, MMR-pp65 and DC-SIGN-pp65) to moDC receptors. (b) Pilot titration experiment to measure CD8+ T-cell proliferation after 7-day co-culture with LPS-stimulated moDCs pulsed with pp65 chemical conjugates (at varying concentrations). Histograms are gated on respective isotypes, and moDCs alone was used as a negative control. Data shown is representative of 3 independent experiments after correction for background responses to DCs alone (DC background median and range: 1.4 % and 0.2-1.7 %). Bars in (b) depict the median with upper range.

(a)



(b)

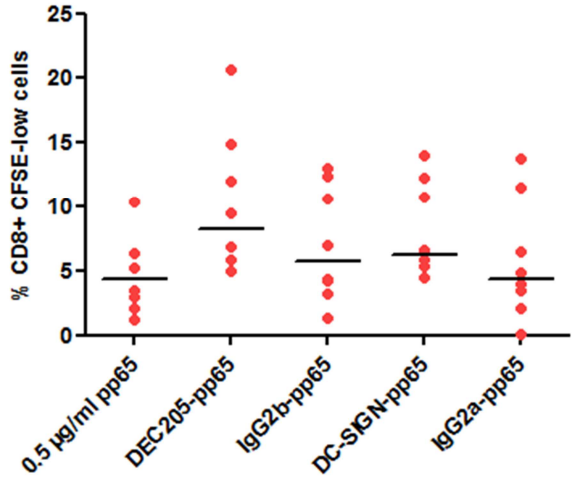


Figure 5.6 – Proliferative CD8+ T-cell responses after targeting DCs with chemical conjugates. Assessment done after a 7 day co-culture with LPS-stimulated moDCs (a) or CD1c+ mDCs (b) that were stimulated with pp65 chemical conjugates (DEC-205-pp65, MMR-pp65, and DC-SIGN-pp65). The cumulative data from 11 (a) or 7(b) independent experiments are shown after correction for background responses to DCs alone (DC background median and range: 1.5 % and 0.4-2.3 % for (a); 0.8 % and 0.1-0.9 % for (b)). Horizontal lines depict the median. * - denotes $p < 0.05$; as analysed by the non-parametric, paired Wilcoxon signed rank test, with a Bonferroni post-test.

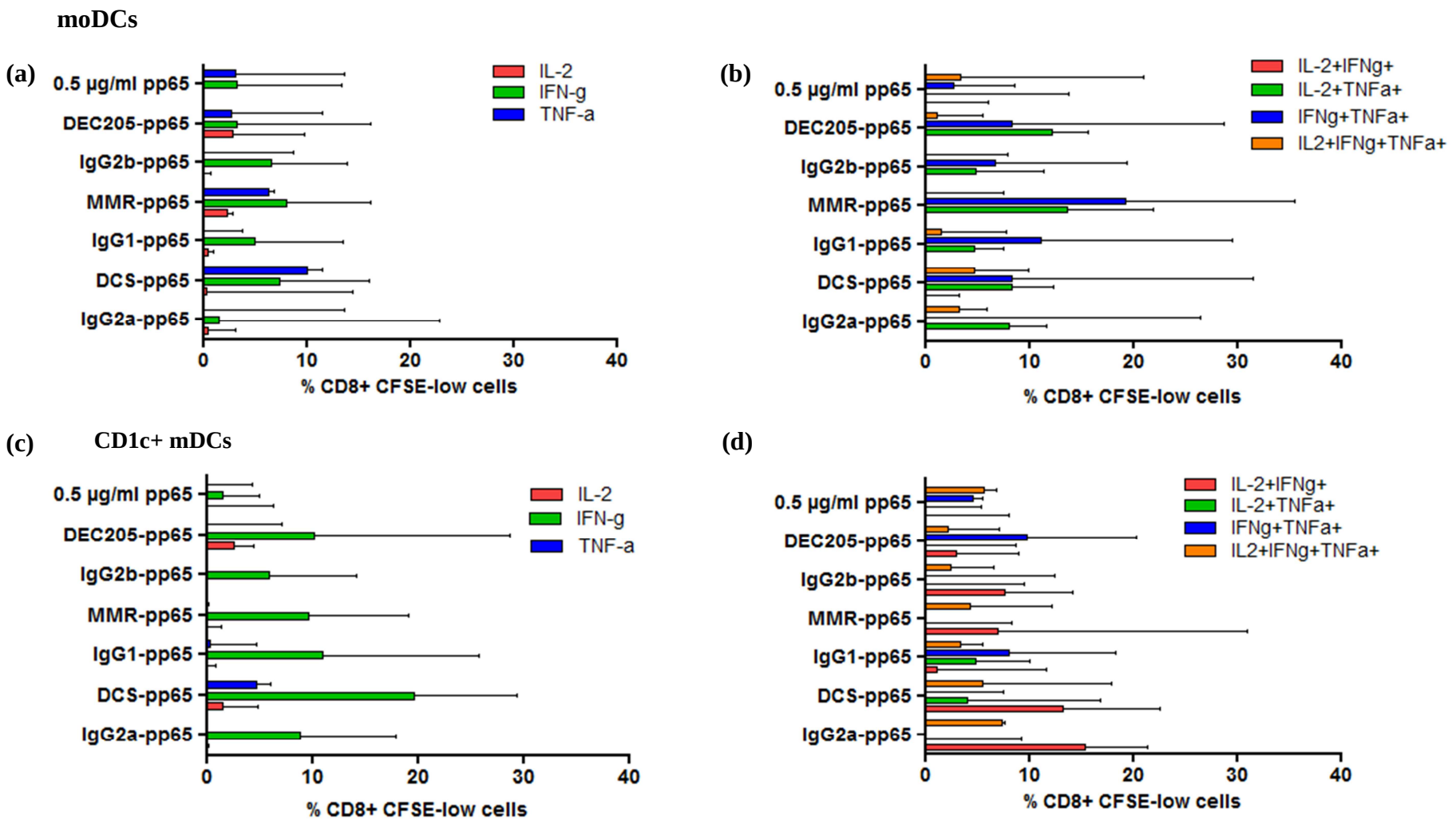


Figure 5.7 – CD8+ T-cell cytokine production (IL-2, TNF-α and IFN-γ) after targeting DCs with chemical conjugates. 7 day co-cultures were set up with T-cells and LPS-stimulated moDCs (a and b) or CD1c+ mDCs (c and d) that were stimulated with pp65 chemical conjugates (DEC-205-pp65, MMR-pp65, and DC-SIGN-pp65). (a) and (c) depict single cytokine production, while (b) and (d) depict multiple cytokine production by individual cells. The cumulative data from 7 (a and b) or 4 (c and d) independent experiments are shown after correction for background responses to DCs alone (Negative values were designated 0). Bars depict the median, and error bars indicate the maximum values.

5.3.3 Targeting DC receptors using streptavidin-fusion proteins

To demonstrate that the streptavidin proteins were functionally capable of attaching to biotinylated proteins *in vitro*, moDCs were initially incubated with the respective biotinylated receptor-specific antibodies, followed by a wash step and incubation with the streptavidin-fusion proteins. Cells were then washed and stained to detect pp65 or MART-1 on the surface of cells (Figure 5.8a). A negative control included samples that were incubated with the receptor-specific antibodies but not the primary antibody against the strep-fusion proteins. This was done to account for any residual attachment of the secondary antibody to the receptor-specific antibodies. Attachment of the secondary antibody to these cells was always under 5 % (data not shown). pp65-strep was detected most prominently on those cells that had the antigen targeted to DEC-205 and CD1a (79.7 and 87.9 % respectively). Percentages of pp65-strep directed towards MMR and DC-SIGN were similar (58.3 and 68.5 % respectively), and far better detected on the cell surface than free pp65 or any of the isotype controls. Analogous binding capacities were observed for MART-strep to MMR and DC-SIGN (54.9 and 44.7 % respectively), although DEC-205 binding capacity was lower than what was seen for pp65 (51.4 %) (Figure 5.8b). Nonetheless, this confirmed that the system of targeting receptors on the surface of DC using pp65-strep or MART-strep worked well.

A pilot titration experiment was then performed to determine an optimal concentration of pp65-strep to use in further experiments (Figure 5.8c). The lowest concentration tested (0.05 µg/ml) stimulated poor CD8+ T-cell proliferation, while a 10-fold increase in concentration seemed to increase responses by two-fold. Although there was no significant differences between targeting to the three receptors chosen, using 0.5 µg/ml pp65-strep showed DC-SIGN to induce slightly better proliferative responses. At a 10-fold higher concentration, proliferation as a result of free antigen stimulation was greater than pp65-strep targeted to DEC-205 and DC-SIGN, and only slightly less than pp65-strep when targeted to MMR. This suggests that at 5 µg/ml, the system was saturated with antigen, and the effects of targeting became negligible. Thus, a concentration of 0.5 µg/ml pp65-strep was utilised for further experiments.

Surprisingly, using the optimal concentration from the pilot titration experiment did not show a similar trend when DC-T-cell co-culture experiments were set-up to examine the effects of

targeting in more detail. As can be seen in Figure 5.9a, targeting pp65-strep to receptors on moDCs induced poorer CD8+ T-cell proliferative responses overall, than exposing moDCs to free pp65-strep. Even more unusual, was that the isotype control responses were similar if not slightly better than responses obtained by targeting pp65-strep to the endocytic receptors, with MMR showing a noticeably lower response compared to its isotype (2.89 % and 5.5 % respectively). Considering that an FcR blocking agent was used, this was unexpected.

The data was more promising with the targeting of MART-strep to receptors (using the same concentrations as pp65-strep) (Figure 5.9b), with prominent responses from both DEC-205 (8.5 %) and MMR (7.3 %), which was almost 6 and 1.6 times greater than their isotype controls, and about two-fold greater than the free antigen (4.63 %). DC-SIGN did not differ from its isotype control or the free antigen.

From this initial data, further optimisation of the targeting strategy using pp65-strep seemed necessary to improve enhancement of CD8+ T-cell responses. The first attempt at optimising these experiments was to explore mixing the reagents before adding them to DCs, instead of adding antibody and pp65-strep separately to DCs (Figure 5.10a). Although only a small number of experiments were done, the trend seemed to indicate that using the reagents separately was more effective than mixing them before the addition of cells. In theory this seemed logical, as by mixing the reagents first and then adding it to cells, there was no certainty that unbound antibodies would not bind to the DC surface receptors and block the attachment of pp65-strep-bound antibodies.

CD4+ T-cell proliferative responses were then evaluated, in the hope that the targeted reagents were enhancing CD4+ T-cell responses instead of CD8+ T-cell responses, because the chosen receptors were possibly directing antigen more effectively to the MHC class II pathway. Figure 5.10b indicated that this was not the case, as the profile of CD4+ T-cell proliferation was analogous to that of the CD8+ T-cell profile. It was also surprising to see here that the isotype control for MMR (IgG1) was stimulating almost a four-fold increased response compared to targeting towards MMR. DEC-205 and DC-SIGN targeting seemed to elicit similar responses to their isotype controls IgG2b and IgG2a respectively, despite the presence of the FcR blocking agent. All responses were once again lower than what was elicited by free pp65-strep.

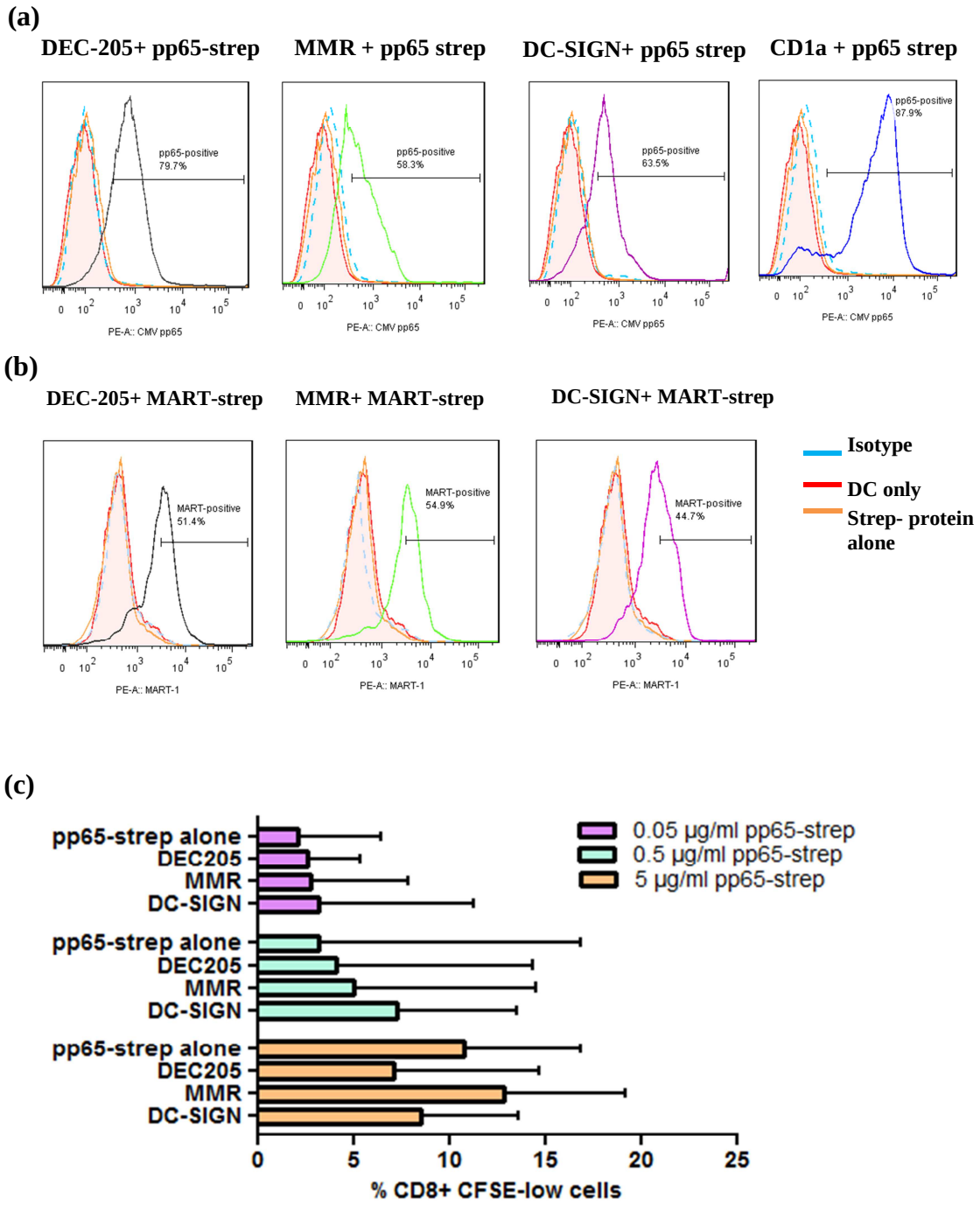
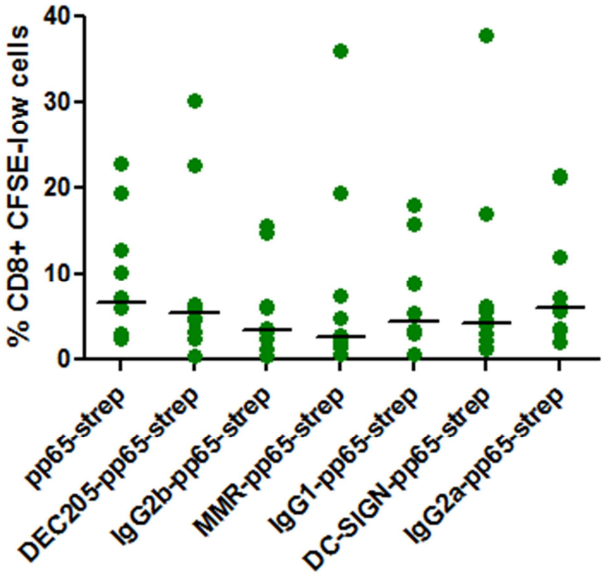


Figure 5.8 – Use of streptavidin-fusion protein to target moDC receptors. (a) Binding capacity of pp65-streptavidin (pp65-strep) to receptor-specific antibodies (DEC-205, MMR, DC-SIGN, CD1a) to moDCs. (b) Binding capacity of MART-streptavidin (MART-strep) to receptor-specific antibodies (DEC-205, MMR and DC-SIGN) to moDCs. (c) Pilot titration experiment to measure CD8+ T-cell proliferation after 7-day co-culture with LPS-stimulated moDCs pulsed with pp65-strep (at varying concentrations) and receptor-specific antibodies. Histograms are gated on respective isotypes, and moDCs alone were used as a negative control. Cumulative data from 3(a and b) or 5(c) independent experiments are shown after correction for background responses to DCs alone (DC background median and range:1.4 % and 1.3-2.2 % for (c)). Bars and error bars in (c) depict the median and maximum value respectively.

(a)



(b)

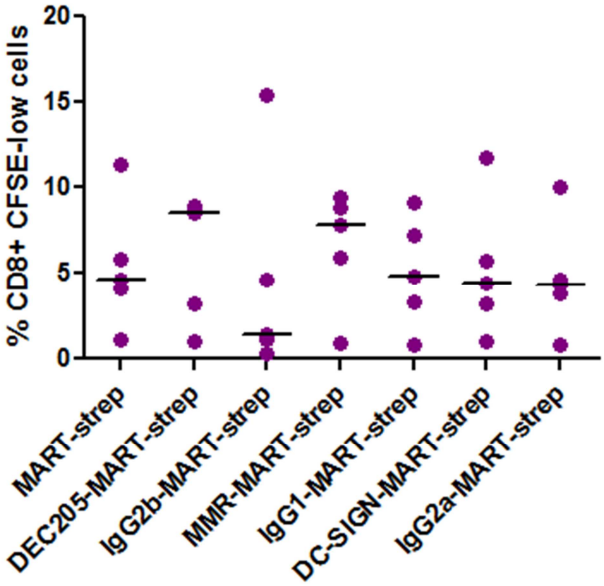
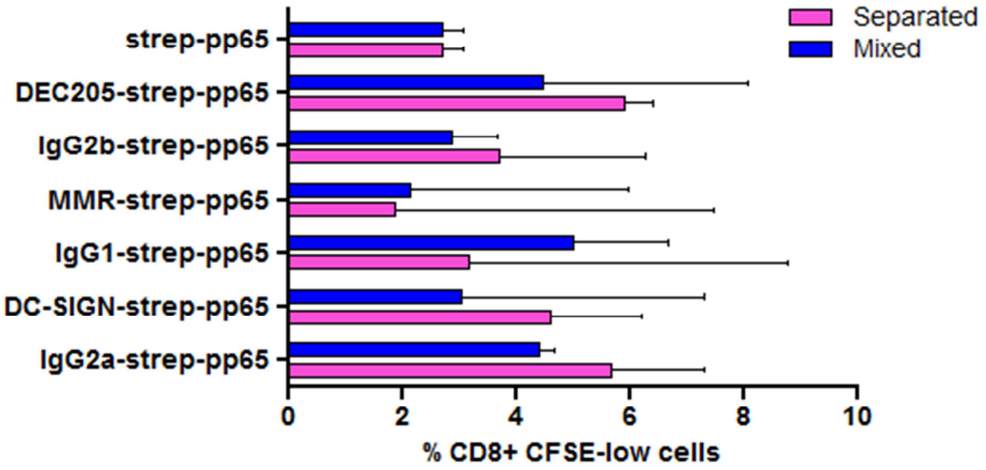


Figure 5.9 – Assessment of CD8+ T-cell proliferation after a 7 day co-culture with LPS-stimulated moDCs that underwent a receptor-targeting strategy with pp65-strep (a) or MART-strep (b), and antibodies specific for DEC-205, MMR, and DC-SIGN. Cumulative data from 10 (a) or 5 (b) independent experiments are shown after correction for background responses to DCs alone (DC background median and range: 2.1 % and 1.2-4.6 % for (a); 1.7 % and 0.7-1.8 % for (b)). Horizontal lines depict the median.

(a)



(b)

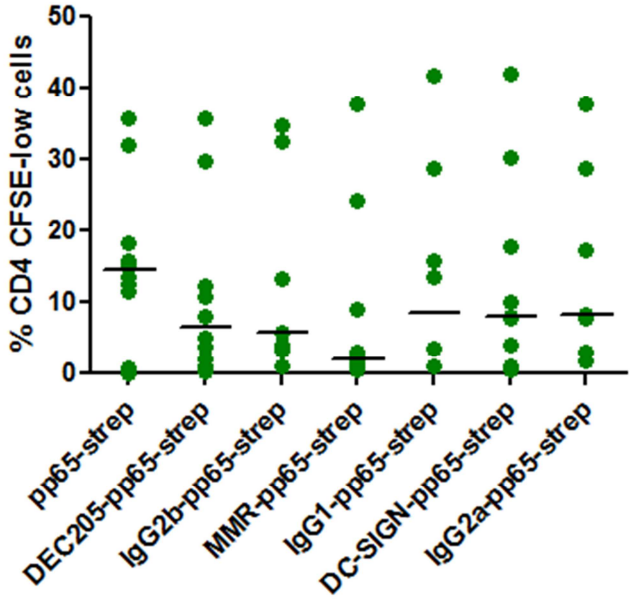


Figure 5.10 – Troubleshooting pp65-strep targeting. (a) CD8+ T-cell responses after stimulation with targeted moDCs pulsed with receptor-specific antibodies and pp65-streptavidin that were either mixed before the addition of cells (blue bars), or separately added to cells as done before (pink bars). (b) CD4+ T-cell proliferation responses to complement the CD8+ T-cell proliferative responses observed in Figure 5.9. Cumulative data from 3 (a) or 10 (b) independent experiments are shown after correction for background responses to DCs alone (DC background median and range: 1.7 % and 1.2-3.4 % for (a);4.7 % and 2.4-9.6 % for (b)). Bars and horizontal lines depict the median, while error bars depict maximum values.

The last aspect that was examined in some detail was the concentration of antigen and antibody used. A more extensive titration experiment was set up using ^{3}H-Thymidine incorporation assay to determine the optimal antigen and antibody concentration to stimulate enhanced T-cell proliferation (Figure 5.11 a and b). DC-T-cell co-culture experiments were set up with pp65-strep targeted to DEC-205 and its isotype control, IgG2b, using various concentrations of pp65-strep and the respective antibodies. DEC-205 was chosen over the other receptors given its moderately better proliferative responses. The results of the titration assay indicated that as concentration of pp65-strep was increased, the T-cell proliferation increased proportionally, as depicted for targeting to both DEC-205 and IgG2b (Figure 5.11a and b). Although the highest concentration of pp65-strep (2500 pM or 207.5 µg/ml) induced the best proliferative responses, 500 pM responses were moderate and demonstrated more of a difference in response between DEC-205 and its isotype, specifically at 0.5 µg/ml of antibody (47444.8 CPM and 36546.5 CPM respectively). However, the most striking observation of this assay was the general similarity in responses elicited by targeting DEC-205 and IgG2b in the absence of an FcR blocking agent. It suggested that the majority of the responses observed for DEC-205 targeting were non-specific. Given that the isotype controls shown in Figure 5.1 and 5.2 did not attach to the surface of moDCs, or encourage the attachment of pp65-strep to the surface, the high proliferative responses to IgG2b are difficult to explain.

It was interesting to note the effect of antibody concentration on the proliferative responses, as this was not initially considered as an influencing factor. The results indicated that, while there were no marked effects of antibody concentration at low antigen concentrations, there was an obvious increase in proliferative responses for an antigen concentration of 2500 pM, where antibody concentration increased to 2.5 µg/ml, and proliferation increased to a maximum. Proliferation then decreased at higher antibody concentrations, implying that that 2.5 µg/ml of antibody is optimal to stimulate high T-cell responses.

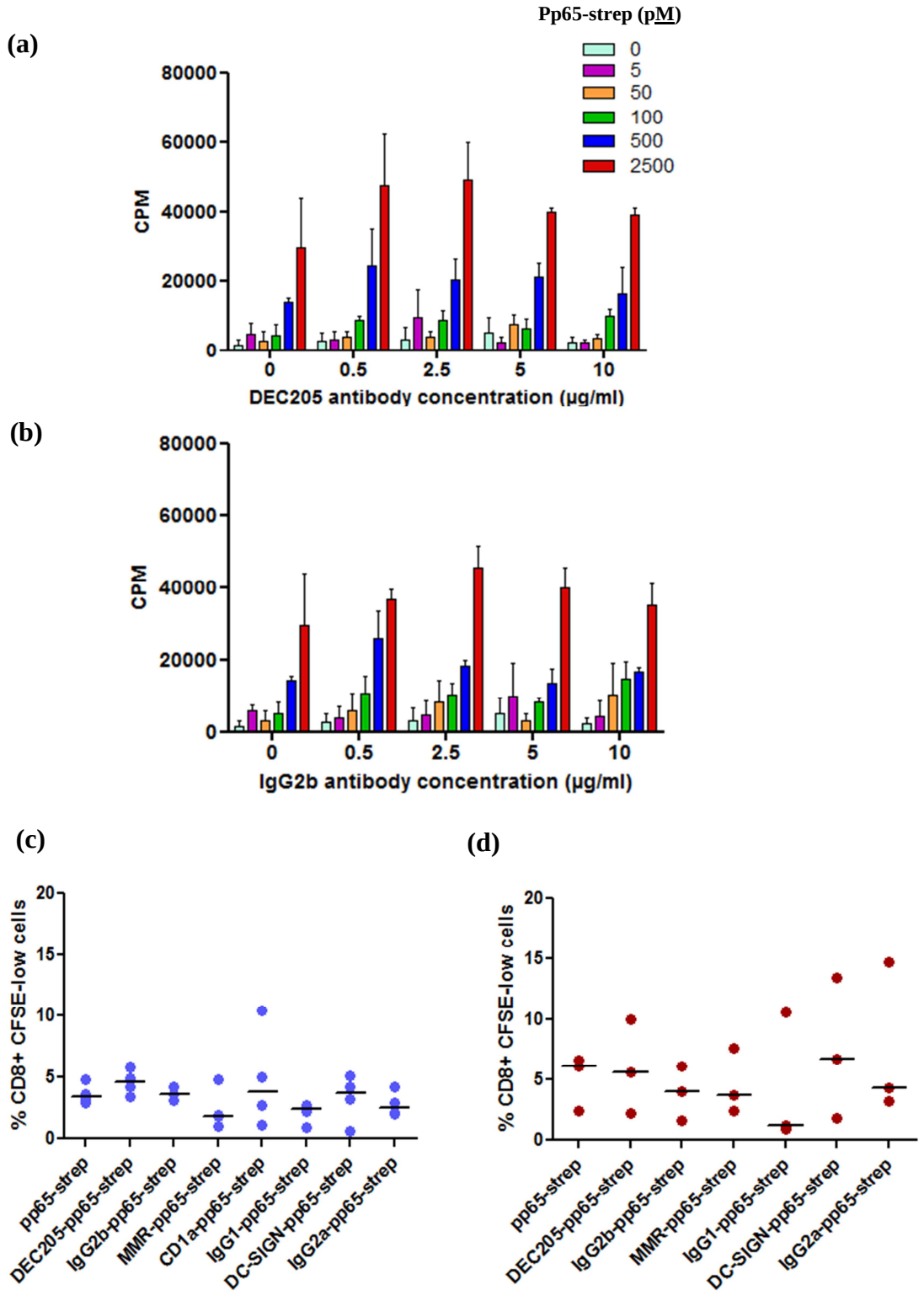


Figure 5.11 – Optimisation of pp65-streptavidin targeting strategy. (a) Pilot titration DC-T-cell co-culture experiment using ^{3}H-Thymidine incorporation assay to assess the effect of antibody concentration and pp65-streptavidin concentration on T-cell proliferation. The DEC-205 receptor was targeted (a), and its complementary isotype antibody, IgG2b was used as a control (b). After 5-day co-culture incubation, ^{3}H was added to cells overnight, and a β-cell counter was used to measure counts per minute (CPM). (c) and (d) represent T-cell proliferation from co-culture experiments using optimized amounts of pp65-streptavidin and antibodies to stimulate moDC (c) or CD1c+ mDC (d). Data shown is from 3(a, b, and d) or 4(c) independent experiments. Data depicts the mean with standard deviation (a and b) or the median (c and d). Data in (c) and (d) have been corrected for background responses to DCs alone (DC background median and range for (c): 1.4 % and 0.8-2.7 %; for (d): 1.6 % and 0.8-1.8 %).

The difference between the responses at 0.5 and 2.5 µg/ml for the DEC-205 antibody samples was quite small, and there was more of a distinction in response between the isotype and DEC-205 samples at 0.5 µg/ml. In view of this, preference was given to using 500 pM of pp65-strep and 0.5 µg/ml of the respective antibodies for further experiments. An assumption was made that these optimal concentrations were adequate for use in the targeting of the two other receptors as well, given that targeting induced similar responses in the last set of experiments.

In addition to using the optimal concentrations, a different FcR blocking agent was included in the optimised assays, as it appeared as though the previous agent was not functioning efficiently. Also, one other receptor (CD1a) was targeted which had not been included in past experiments. CD1a is not an endocytic receptor like the other targeted receptors, and is rather recognized as having a similar role on the surface of APCs as MHC class I molecules (La Rocca et al., 2004). However, we chose to include it in these experiments as an additional surface receptor of interest, because of its wide distribution on DCs and its role in antigen presentation. Unfortunately, even with the optimized concentrations and new FcR blocking agent, the pp65-strep targeting strategy was still unable to induce strong CD8+ T-cell responses (Figure 5.11c and d). Receptor targeting to moDCs (Figure 5.11c) displayed poor responses overall, with only slight increases in targeted responses, compared to their respective isotypes and pp65-strep. The response to targeting the MMR was particularly low as seen before (1.9 %), while DEC-205 and CD1a displayed a moderately better response compared to other responses (4.6 and 3.9 %). Similar to moDC data, targeting to CD1c+ mDCs did not improve the targeting strategy (Figure 5.11d). Free pp65-strep appeared to induce marginally better responses than the targeted pp65-strep, except for targeting to DC-SIGN, which was slightly better (6.7 % versus 6.0 % for free pp65-strep). Isotype control responses were still too similar to the targeted receptor responses, indicating that the targeting in this strategy was not enhancing responses as was expected.

With regard to the production of cytokines by targeted cells, moDCs targeted with pp65-strep produced an array of cytokines, where IFN-γ was produced to a greater extent than IL-2 and TNF-α (Figure 5.12a). As with the proliferative data, responses were quite similar for the different targeting agents, including the isotype controls.

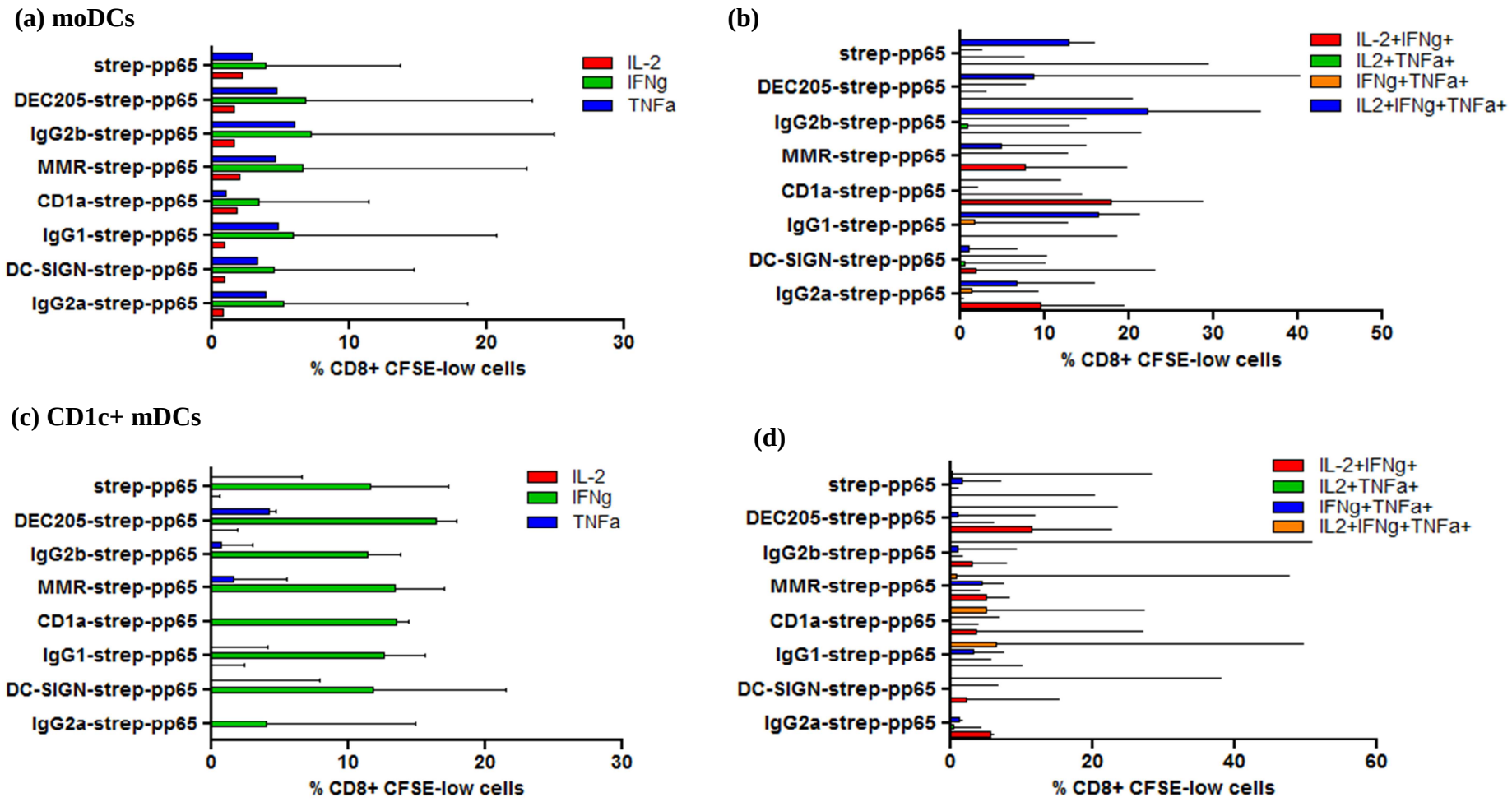


Figure 5.12 – CD8+ T-cell cytokine production (IL-2, TNF-α and IFN-γ) after pp65-strep targeting optimisation. 7 day co-cultures were set up with T-cells and LPS-stimulated moDCs (a and c) or CD1c+ mDCs (b and d) that underwent a receptor-targeting strategy with receptor-specific antibodies (DEC-205, MMR, DC-SIGN) and the pp65-streptavidin fusion protein. (a) and (b) depict single cytokine production, while (c) and (d) depict multiple cytokine production. The cumulative data from 4 (a and c) or 3 (b and d) independent experiments is shown after correction for background responses to DC alone (negative values were designated 0). Bars depict the medians whereas error bars represent the maximum values.

This was true for stimulated CD1c+ mDCs as well, where DEC-205 IFN-γ and TNF-α responses were higher than the other responses, but only marginally better than free pp65-strep (Figure 5.12b). Multiple cytokine production indicated that production of IFN-γ and TNF-α from single cells was quite prominent from the moDCs but not CD1c+ mDCs (Figure 5.12c and d). Cytokine production from CD1c+ mDCs stimulated with pp65-strep was low for multiple cytokine production.

Attempts to further optimise this targeting strategy included using rAdpp65-pre-stimulated PBMCs instead of mixed T-cells in the co-culture, use of different FcR blocking agents (including heat-aggregated human AB serum), and increasing incubation of culture from 7 to 10 days (Data not shown). Unfortunately, none of the above changes were able to enhance the T-cell proliferation of the targeted pp65-strep compared to free pp65-strep and its isotype control.

5.3.4 Targeting DC receptors using a commercial pp65 dendrimer

The final method to target antigen to the cross presentation pathway made use of a commercially available pp65 dendrimer. This dendrimer is a scaffold for covalently-coupled pp65 peptides and a monoclonal, anti-biotin-FITC conjugate. Using a biotinylated primary antibody, the dendrimer specifically targets any surface molecule on the selected cell-type. In this case, it was used in a similar way as pp65-strep to target selected receptors on the surface of moDCs, and was applied to experiments as advised by the manufacturer's instructions.

Initially, the ability of the dendrimer to attach to biotinylated antibodies on the surface of moDCs was assessed at different dilutions, as done with reagents before (Figure 5.13). Attachment of the pp65 dendrimer to all selected receptors was observed, with DC- SIGN and MMR depicting as much as 95 % attachment at low concentrations of the dendrimer (Figure 5.13b). CD1a and DEC-205 demonstrated better attachment at the higher concentrations, and all isotype controls showed negligible attachment of the dendrimer to the cell surface. As before, co-culture experiments were set up to evaluate the ability of targeted pp65 dendrimer to elicit CD8+ T-cell proliferative and cytokine responses. When moDCs were stimulated with the dendrimer, responses were generally much lower than seen with

other targeting strategies, despite the use of LPS to mature DCs before the addition of the T-cells (Figure 5.14a). Also, targeted responses were similar to free pp65 dendrimer and the respective isotypes, with only CD1a displaying a 2-fold increase in response compared to free dendrimer and its isotype, IgG1 (3.2 % and 1.3 % respectively). Analogous data was observed for the stimulation of CD1c+ mDCs, where responses were also low but targeting to CD1a and DC-SIGN elicited moderately better responses (Figure 5.14b). Initially, it was assumed that perhaps responses to the dendrimer itself may be masking the responses to pp65, and that perhaps if pp65-specific responses were explored, a more distinct difference between samples could be determined. Thus, pentamer staining was done on a set of co-culture samples (Figure 5.14c), only to reveal that while CD1a did seem to have better responses compared to its isotype, all elicited responses were lower than stimulating with free pp65 dendrimer alone. Additionally, the antigen-specific responses were generally much lower than what was observed in Chapter 4, but this is possibly because the dendrimer is attached to a range of pp65 peptides, the collective composition of which may not include the epitope that the pentamer is selective for, on all dendrimer molecules.

Cytokine data revealed CD1a-targeted moDC samples did have better IFN-γ (15.5 %) and TNF-α responses (12.6 %), and IFN-γ-TNF-α-IL-2 responses (10.7 %) compared to its isotype control (0.05, 0.2 and 1.4 % respectively) and free pp65 dendrimer (0.2, 0 and 0.2 % respectively) (Figure 5.15a and c), while other samples were not considerably different. The cytokine data from CD1c+ mDC samples displayed negligible differences in cytokine production between samples, although DEC-205-targeting induced moderate levels of IFN-γ, TNF-α and IL-2, while CD1a-targeting was able to elicit good polyfunctional responses (Figure 5.15b and d).

It was suspected that LPS may not have been an adequate adjuvant for these experiments, given the generally low responses. The absence of adjuvant or the use of two other adjuvants was therefore assessed, namely poly I:C (TLR3 ligand) and CLO97 (TLR7/8 ligand). This was done in the hope that these adjuvants would demonstrate better enhancement of responses compared to LPS responses. The data indicated that without any adjuvant, all targeted samples had 3-6 fold greater responses than free pp65 dendrimer alone (CD1a being the best targeted receptor with a response of 1.85 % compared to 0.3 %), but that these responses were not significantly different from the isotype controls (Figure 5.16a).

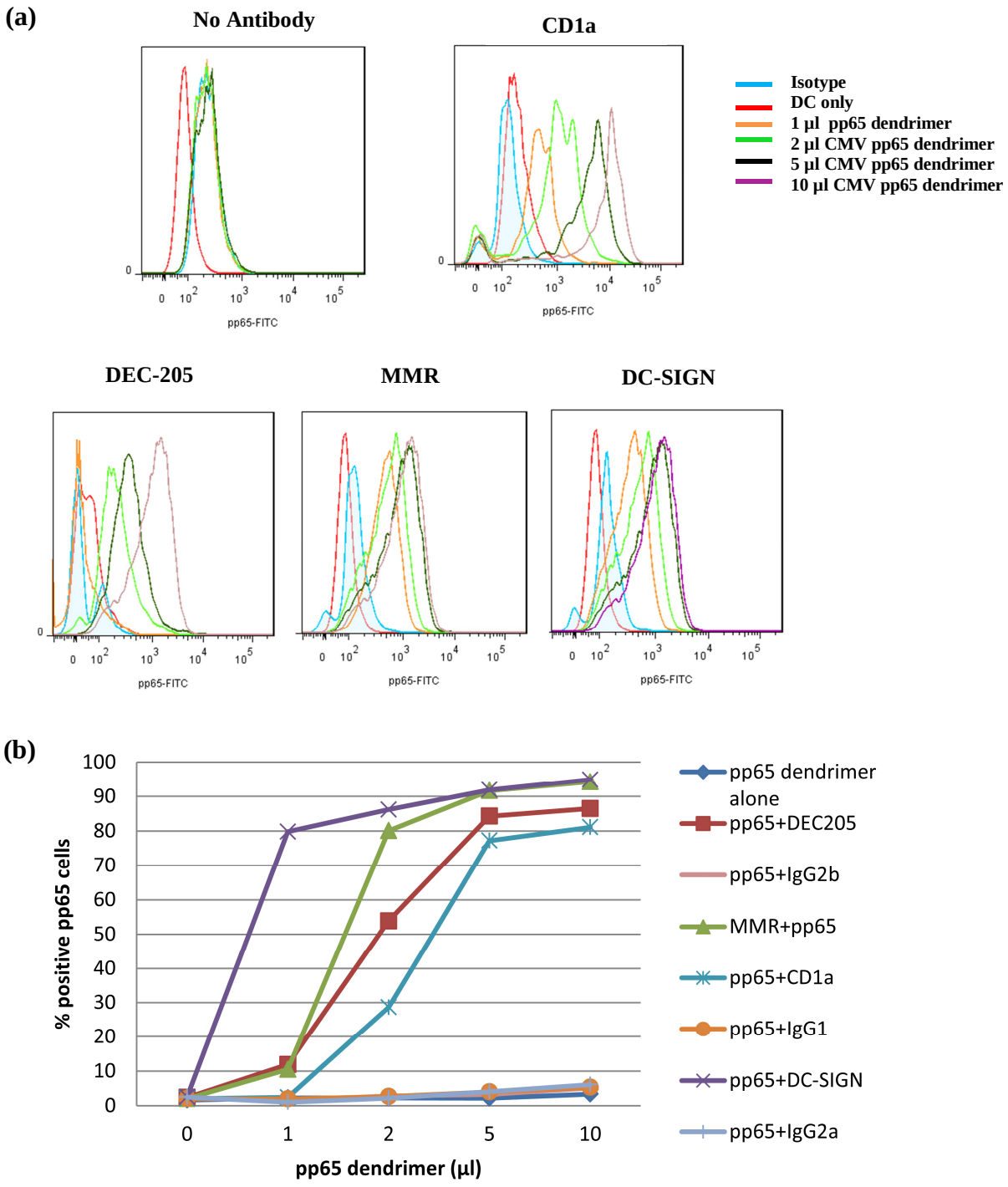


Figure 5.13 – Binding capacity of pp65-conjugated dendrimer to biotinylated receptor-specific antibodies attached to moDCs. (a) Binding of pp65-conjugated dendrimer (at different concentrations) to biotinylated receptor-specific antibodies that were attached to the respective receptors (DEC-205, MMR, CD1a, DC-SIGN) on moDCs. Histograms are gated on respective isotypes, and moDCs alone were used as a negative control. (b) Trend of binding capacity (proportional to increasing concentration) of pp65 dendrimer to receptor-specific antibodies on moDCs, as shown by percentage of pp65-positive cells. Data is representative of 3 independent experiments.

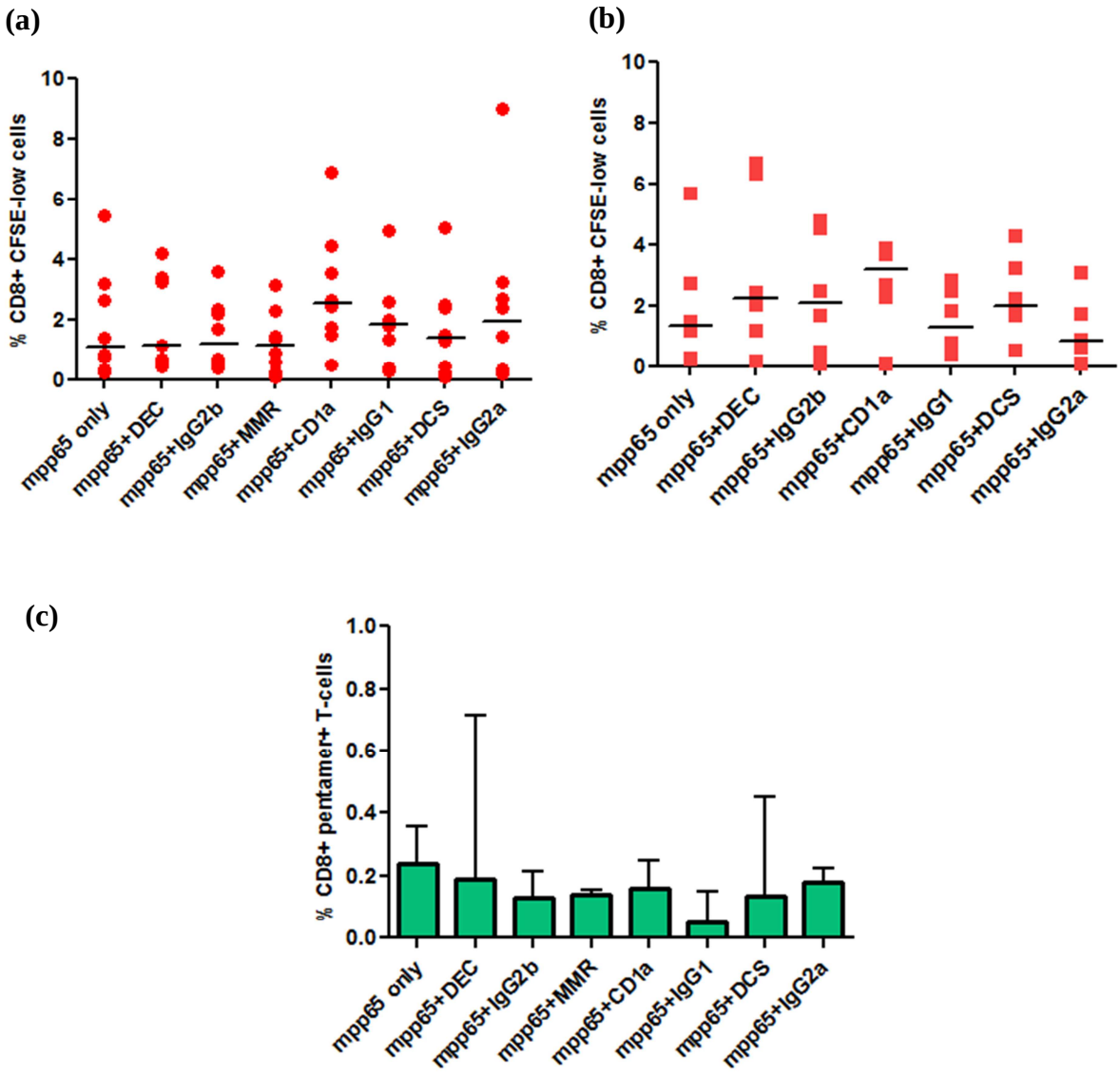


Figure 5.14 – Assessment of T-cell proliferation after targeting DCs with pp65 dendrimers. A 7 day co-culture was set up with T-cells and LPS-stimulated DC that underwent a receptor-targeting strategy with receptor-specific antibodies (DEC-205, MMR, DC-SIGN and CD1a) and the pp65 dendrimer (mpp65). CD8+ T-cell proliferative responses were measured after stimulation with targeted moDCs (a) or CD1c+ mDCs (b). (c) pp65-specific CD8+ T-cell responses after stimulation with targeted moDCs determined by pentamer staining. The cumulative data 6 (a and b) or 3(c) independent experiments are shown after correction for background responses to DC alone (DC background median and range: 1.7 % and 0.9-2.1 % in (a); 1.9 % and 1.1-2.9 % in (b); 0.3% and 0-0.8 % in (c)). Bars and horizontal lines depict the medians whereas error bars represent the maximum values.

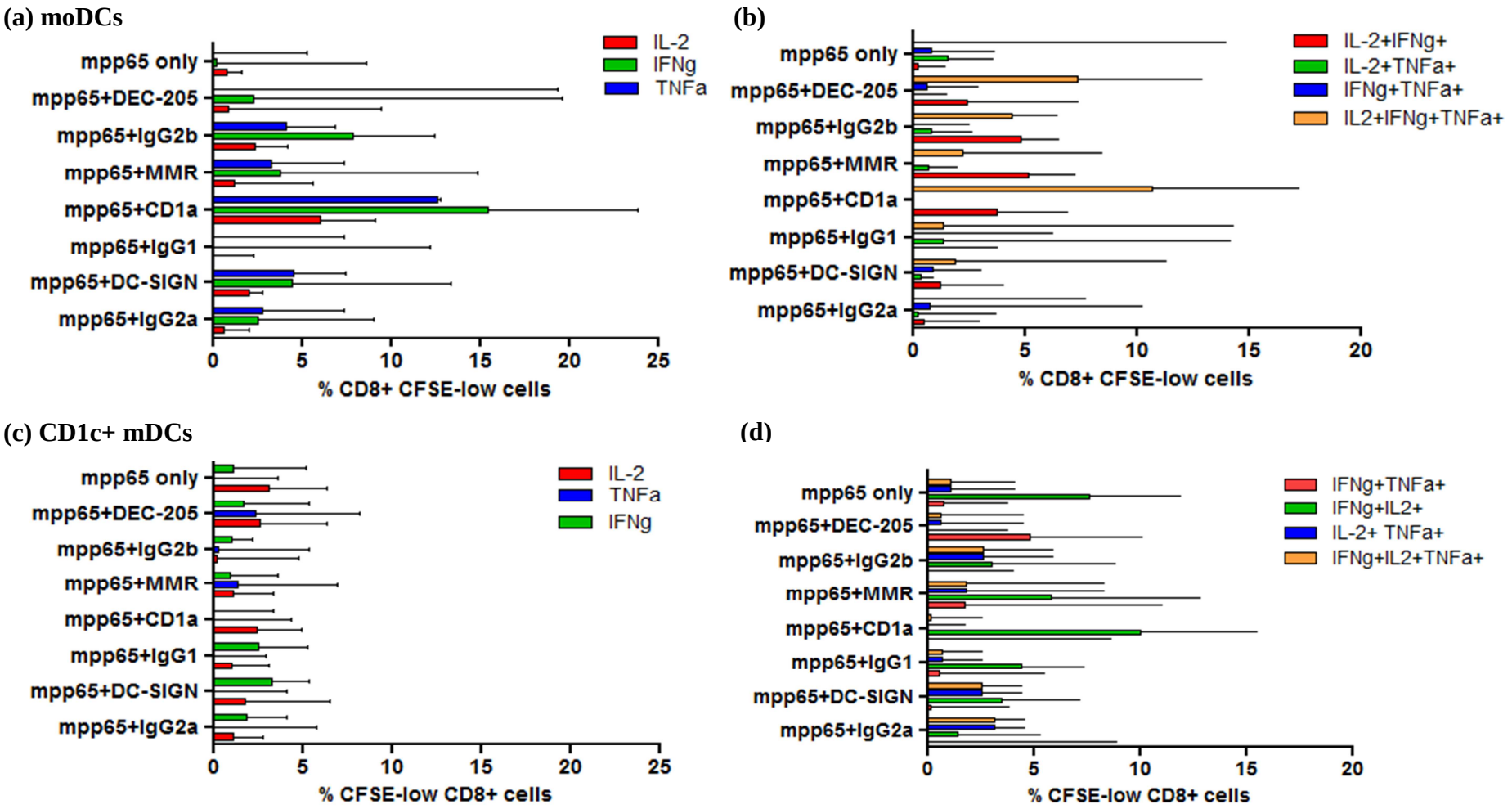


Figure 5.15 – CD8 T-cell cytokine production (IL-2, TNF-α and IFN-γ) after targeting DCs with pp65 dendrimers. A 7 day co-culture was set up with T-cells a LPS-stimulated moDC (a and c) or CD1c+ mDC (b and d) that underwent a receptor-targeting strategy with receptor-specific antibodies (DEC-205, MMR, DC-SIGN and CD1a) and the pp65 dendrimer (mpp65). (a) and (b) depict single cytokine production, while (c) and (d) depict multiple cytokine production by individual cells. The cumulative data from 6 (a and c) or 4 (b and d) independent experiments is shown after correction for background responses to DC alone (negative values were designated 0). Bars depict the medians whereas error bars represent the maximum values.

With Poly I:C stimulation, isotype responses increased further, while targeted responses remained low, except in the case of MMR and CD1a, which demonstrated more than a two-fold increase in response compared to the IgG1 proliferative response (2.9 and 2.6 % respectively, compared to 1.1 %) (Figure 5.16b). Similar data was observed for stimulation with CLO97, where CD1a displayed a response six times greater than its isotype (Figure 5.16c). Although the magnitude of responses was slightly better with these adjuvants, responses were still low, and the difference in targeted responses compared to their isotypes was minimal (aside from CD1a).

Thus, as a final attempt to optimize this targeting strategy, a ^{3}H-Thymidine incorporation assay was performed to evaluate the effect of varying the concentrations of pp65 dendrimer and antibody (Figure 5.17). A moDC-T-cell co-culture assay was set up as done before, but only exploring targeting to DEC-205 and IgG2b at differing concentrations. The data suggested that although there was some variation in response at different antibody concentrations, it was not significant or consistent. The best responses were for the highest concentration of pp65 dendrimer (which was used in all above assays). Unexpectedly, and similarly to what was seen with the pp65-strep data, the IgG2b data was only marginally lower in magnitude than the DEC-205 data.

Although an FcR agent was not included in these experiments, they were included in all the above dendrimer experiments, suggesting that while some of the isotype control responses could be accounted for by non-specific endocytosis, it seems unlikely that it was all due to this. In view of the data here, more extensive research needs to go into the molecular basis of this targeting strategy to determine what is behind the trend of high isotype responses amongst all the targeting strategies explored.

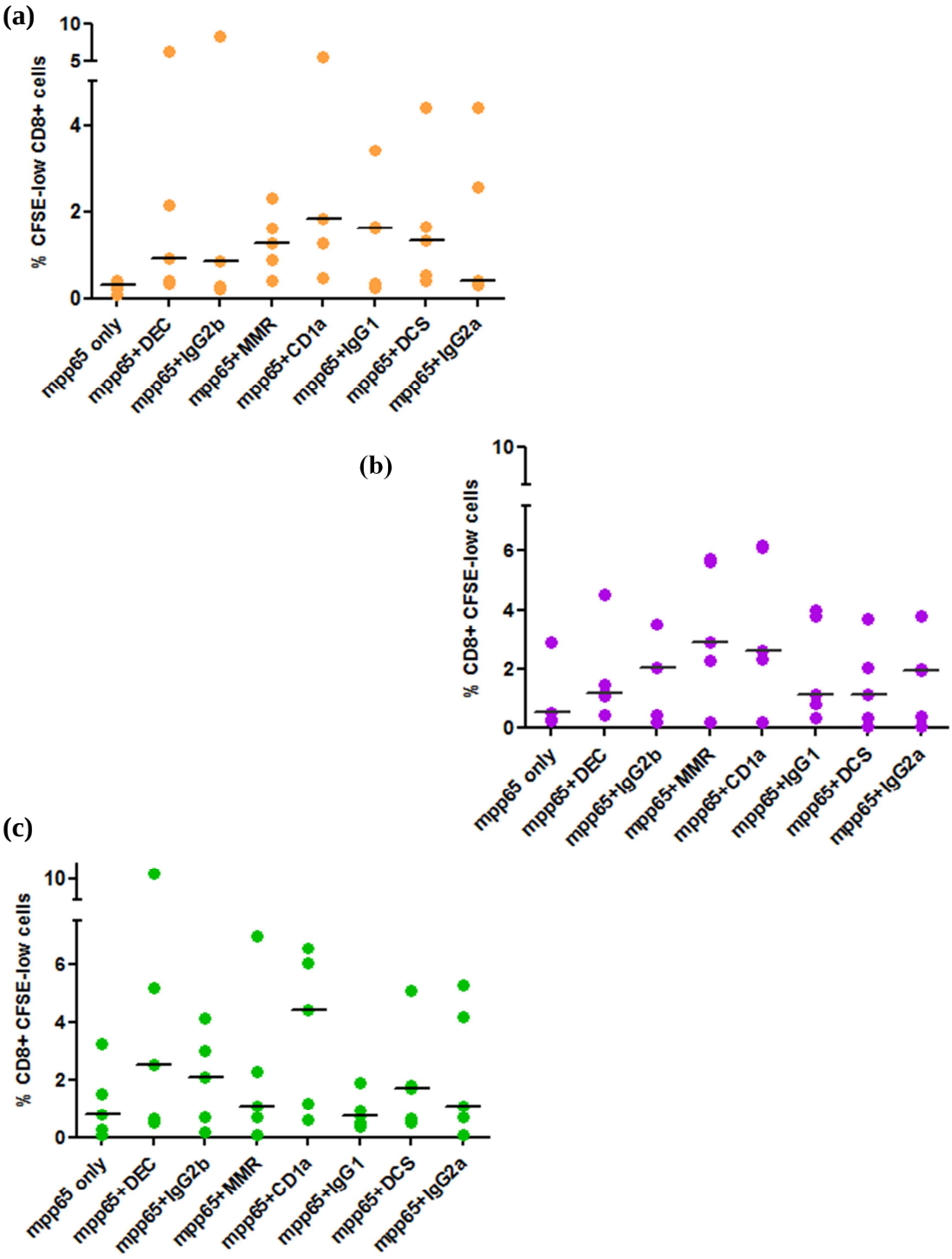


Figure 5.16 – Evaluation of the effect of different TLR agonists on T-cell proliferation after targeting DCs with pp65 dendrimers. A 7 day co-culture was set up with T-cells with moDCs that underwent a receptor-targeting strategy with receptor-specific antibodies (DEC-205, MMR, DC-SIGN and CD1a) and the pp65 dendrimer (mpp65). CD8 T-cell responses after stimulation with targeted moDC that were not exposed to any agonists (a), or were activated with poly I:C (TLR 3 agonist) (b), or activated with CLO97 (TLR 7/8 agonist) (c). Cumulative data from 5 independent experiments are shown after correction for background responses to DC alone (DC background median and range: 1.6 % and 0.5-3.1 %). Horizontal lines depict the median.

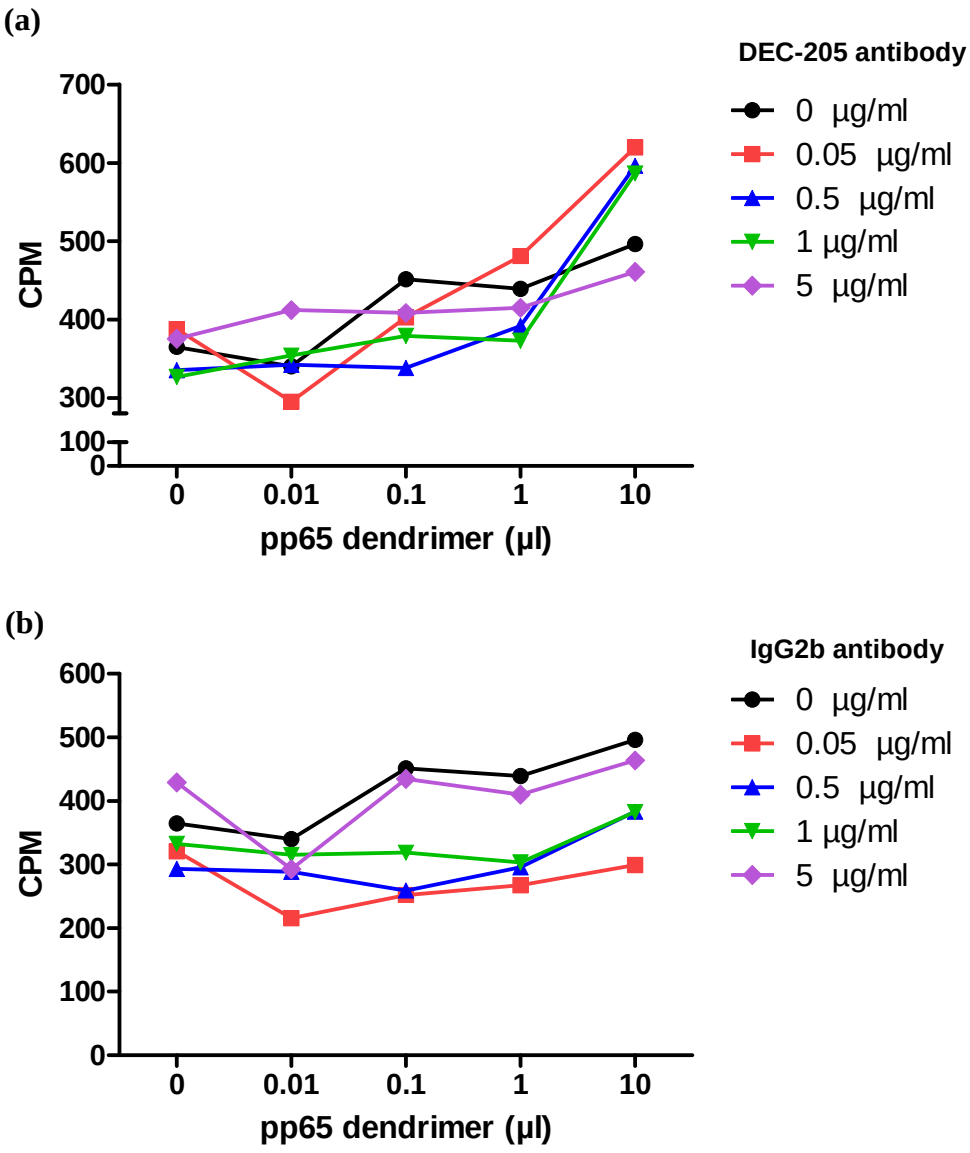


Figure 5.17 – Pilot titration experiment using ^{3}H-Thymidine incorporation assay to assess the effect of antibody concentration and pp65 dendrimer concentration on T-cell proliferation. Co-culture experiments were set up as described before, using moDCs stimulated with different amounts of pp65 dendrimer that had been pre-incubated for 15 min at room temperature with varying concentrations of DEC-205antibody (a), or its isotype control, IgG2b (b). After 5-day co-culture incubation, ^{3}H was added to cells overnight, and a β-cell counter was used to measure counts per minute (CPM). Data shown is from 2 independent experiments, where each point depicts the mean for the given stimuli.

5.4 Discussion

Directing antigens to specific receptors on the surface of DCs in order to target the cross presentation pathway has emerged as a novel way to enhance CD8+ T-cell responses, which is particularly useful in HIV-1 and tumour vaccine strategies. In this study we explored four ways to target selected model antigens to a number of DC surface receptors in the hope of amplifying CD8+ T-cell responses, and specifically looking at targeting two human DC subsets.

In Chapter 4 myeloid blood DCs (CD1c+ mDCs) were selected as a good comparative DC subset to moDCs because they are easily isolated in adequate quantities from blood samples, and have demonstrated better migratory (Luft et al., 2002) and CTL–inducing capacity *in vitro* than moDCs (Osugi et al., 2002). In the present study, mDCs were found to elicit similar if not slightly lower CD8+ T-cell responses than moDCs, and this is consistent with previous work conducted by Radford et al (Radford et al., 2006), who showed that mDCs induced allogeneic CD8+ T-cell responses comparable to that of moDCs, but not significantly better. Additionally, a recent study by Jongbloed et al (Jongbloed et al., 2010) has clearly shown that it is CD141+ mDCs which are more potent stimulators of CD8+ T-cell responses, and not CD1c+ mDCs in the blood. In view of the observations here, moDCs were a better option for targeting purposes in this study, although the superior cross presentation capacity of CD141+ mDCs suggests that future work should evaluate this subset as a potential target.

Of the targeting approaches examined, targeting the chosen receptors using antibody-antigen chemical conjugates demonstrated the most promising means of enhancing CD8+ T-cell responses. This method was inspired by studies which made use of receptor-specific antibodies chemically bound to an antigen of interest to target specific receptors on the cell surface (Bonifaz et al., 2004, Tacken et al., 2005). In particular, Bonifaz et al (Bonifaz et al., 2004) demonstrated that antigen targeting to the DEC-205 receptor was able to enhance T-cell responses by almost 100-fold in mice. Consistent with these data, we also observed better proliferative responses when antigen was targeted to DEC-205 compared to the other

receptors, although the augmentation in response was not as pronounced as seen in mouse studies. A possible reason for this is the distinct differences between mouse and human DEC-205 distribution on immune cells, where DEC-205 is prominently and primarily produced on DCs in mice, while in humans it is more sparsely expressed on DCs, with a broader distribution on other immune cells, such as macrophages (Proudfoot et al., 2007). This disparity in distribution suggests a prominent and specific DC receptor such as CLEC9A, may be a more promising target for these strategies, and is a receptor to consider for further studies.

Another possible explanation for the lower enhancement of responses in this study compared to *in vivo* studies is related to the heterogeneous nature of the chemical conjugates used (as depicted in Chapter 3). Even though we attempted to remove unconjugated antibody in the purification process, traces of it remained in the purified samples. These antibodies could have attached to the respective receptors, blocking entry of the chemical conjugates as has been implied in previous research (Sapinoro et al., 2007, Molnar et al., 2003). In further agreement with this explanation is the poorer binding capacity of the chemical conjugates to DCs compared to free antibody. DC-SIGN-pp65 did not seem to bind optimally to cells compared to the DC-SIGN antibody alone, which was detected at much higher levels on the surface of cells. This suggests that there was some interference or blocking of the conjugate binding to the receptor, possibly affecting the endocytosis of the antigen. Confocal microscopy using fluorescent markers for the antibody as well as the antigen could be used to verify this, however little can be done with the current conjugate samples to prevent this interference, because of the difficulty involved in removing the contaminating antibodies.

It is therefore necessary to consider alternative ways to create the antigen-antibody conjugate, as has been proposed in other DC targeting strategies (Bozzacco et al., 2007, Idoyaga et al., 2011, Klechevsky et al., 2010). Our reagent was a chemical conjugate of a fully, intact antibody and antigen, while other more successful strategies have used genetically-fused conjugates between single chain Fv (ScFv) antibodies and antigens of interest. Although it requires a somewhat drastic change to use of ScFv-pp65 conjugates instead of chemically-linked conjugates, it may improve current responses even further. The ScFv antibodies are

genetically engineered molecules that consist of the light and heavy-chain variable region of the antibody, joined by a linker sequence (Molnar et al., 2003). Although they appear to have a slightly lower affinity than intact antibody, they lack the Fc component, making them more compact (which possibly aids in more efficient endocytosis), and allows the avoidance of non-specific binding to cells. Additionally, use of genetically-fused antibody-antigen conjugates would mean that simpler purification procedures could be used that would result in lower loss of yield, and eliminate the problem of contaminating unbound antibody in the final preparations of the conjugates. Finally, utilising ScFv reagents instead of chemically conjugated reagents means we could make several reagents fairly inexpensively and simply, by creating genetic clones that each contains a different targeting antibody component or differing antigen component. The economic benefit of this allows us to explore the use of MART-1 candidates in the future, and determine whether the antigen itself has an effect on which pathway a given receptor will direct the antigen to for processing and presentation.

On the opposite end of the spectrum, the targeting method that seemed least promising was the use of biotinylated pp65 and anti-biotin beads to direct antigen to the cross presentation pathway, with no obvious differences amongst targeted and non-targeted samples. In theory, this method, while slightly convoluted, seemed to be an interesting concept for a targeting method. It is very likely that unbound antibody also interfered with the binding of conjugates to the specific receptors in this approach, given the analogous responses we observed in all samples. In addition, the lack of Fc blocking agent in these experiments possibly contributed to the higher isotype control responses observed. That being said, attempts to further optimise this strategy were problematic because we could not confirm to what extent the biotinylated antibody and biotinylated antigen was attaching to the beads, and were not provided with any quantitative data from the manufacturer about the concentration or size of the beads being used. In addition, the anti-biotin beads alone appeared to be quite immunogenic, initiating proliferative CD8+ T-cell responses as well as detectable cytokine production in the absence of antigen. While this non-specific activation of DCs may have had an adjuvant-like effect, it could also have been masking the antigen-specific responses to the targeted pp65. In view of these limitations, this approach was not pursued further, nor was MART-1 targeting evaluated using this approach.

The use of streptavidin-fusion proteins to direct antigen to the selected receptors was expected to be the most efficacious method evaluated to augment T-cell responses because of its flexibility and ease of production. Unfortunately, the data from moDC and CD1c+ mDC stimulations depicted isotype and targeted responses to be alike, and both lower than responses to free antigen. This was highly unexpected, indicative of a flaw in the approach, but it was difficult to ascertain why.

One explanation for the similar isotype and receptor-targeted responses is that the isotype controls were targeting the antigen to Fc receptors on the surface. The selected receptors for targeting were all endocytic receptors, and should have ideally focussed antigen uptake, thereby enhancing antigen processing and presentation to a much greater extent than non-specific antigen uptake. However, it has been shown that low affinity Fcγ receptors preferentially bind IgG in immunocomplexes, enhancing phagocytosis (Molnar et al., 2003). Moreover, past research has explored directing antigens to Fc receptors on moDCs, depicting favourable induction of CD8+ T-cell responses, and indicating that these receptors are able to target antigen to the cross presentation pathway fairly efficiently (Kawamura et al., 2006, Wallace et al., 2001). Nevertheless, if this was a major occurrence, we would have expected to see that all proliferative responses were higher than that of free antigen, which was contradictory to what we observed. Thus, the similar or higher free antigen responses in the biotinylated pp65-, streptavidin fusion protein-, and pp65 dendrimer experiments imply that no antigen was being specifically targeted to the cross presentation pathway by the chosen receptors, when these modes of targeting were employed.

Other studies involving the use of streptavidin-fused antigens to target receptors showed successful attachment of the reagents to the cells of interest, as well as an ability to functionally stimulate the expected cellular or humoral responses. In addition to being used to target DC with biotinylated vaccine antigens *in vivo* (Wang et al., 2009), ScFv-streptavidin antibodies have also been used efficiently in pre-targeted radio immunotherapy, where ScFv-anti-CD20-streptavidin antibodies directed radionuclide-chelate/biotin molecules towards B-cell lymphomas (Pagel et al., 2006). As with the reagents in the above studies, both fusion proteins in this study contained streptavidin core components that successfully bound to

biotin in ELISAs (Chapter 3) and to DCs via the receptor-specific antibodies. This confirmed that the streptavidin-fused antigens were functional, and should theoretically deliver the antigen to the receptors of interest without problem. However, steric hindrance may have prevented endocytosis from happening efficiently at the cell surface. Perhaps too many streptavidin-pp65 molecules bound to a single receptor-specific antibody on the surface of DCs, and the resulting conjugate was too large to be endocytosed efficiently. This explanation seems likely, given that the nature of the biotinylation process is non-specific, and usually results in more than one biotin molecule binding to the protein, which in this case was the receptor-specific antibody. Hence, if there was more than one site for the streptavidin core to bind to on the antibody, it is possible that more than one streptavidin-pp65 molecule attached to the antibodies, given the strong affinity between biotin and streptavidin. This reasoning would agree with the higher than expected responses elicited by free antigen and the isotype controls, because these samples would not have had large structures blocking entry of the antigen into the cell via the endocytic receptors, and could therefore afford to take up more antigen, be it non-specifically. If this is indeed the cause of the lack of enhancement by the streptavidin-targeting strategy, it could be verified using confocal microscopy, which would allow us to visualise what was occurring at the cell surface. This requires further investigation in future studies.

The enhanced response that was demonstrated when MART-strep was directed towards DEC-205 suggests that using a smaller targeted antigen in this strategy may overcome the possible steric hindrance issue. MART-strep was significantly smaller than pp65-strep according to the western blot analysis in Chapter 3, so even with multiple attachments of this antigen onto a receptor-specific antibody, it seems to have been small enough to be endocytosed efficiently. This implies that not only was the targeting strategy successful when a different, smaller antigen was used, but that targeting to the DEC-205 receptor directed antigen more efficiently to the cross presentation pathway than the other two receptors. This is consistent with data from the study conducted by Bozzacco et al (Bozzacco et al., 2007) and the data from our chemical conjugate targeting experiments above, where targeting to DEC-205 was found to be more potent at enhancing CD8+ T-cell responses compared to MMR and DC-SIGN. Unfortunately, given our limited access to A*02:01 samples during this

study and the problematic nature of this strategy using streptavidin-pp65, we did not evaluate the induced cytokine production by MART-strep-stimulated cells, nor did we assess the effect of targeting MART-strep towards the CD1a receptor. However, these are potential areas of interest for further development in future studies.

The use of the pp65 dendrimer as a targeting agent was a similar strategy to using streptavidin-pp65 fusion proteins, but differed in three ways. The first was that the pp65 antigens used were peptide-based and not intact protein. The use of peptides instead of intact protein can be limiting because of restrictions of HLA-types in humans, and is one of the reasons that proteins were chosen as the source of antigen in our other methods. Secondly, the targeting reagent was produced industrially and therefore, any potential problems that we observed with the other strategies relating to their production and purification were eliminated in this strategy (unbound antibody contaminations). Thirdly, pp65 and the anti-biotin components in this reagent were attached to a macromolecular structure referred to as a dendrimer. Dendrimers have been used quite extensively in chemistry and biochemistry as an alternative to polymers, in addition to being used in biomedical applications such as tissue engineering and drug delivery (Mintzer and Grinstaff, 2011). However, the size of these molecules can potentially render them too large for efficient endocytosis when they are attached to other components. Thus, the steric hindrance issue that we believe to have been the problem with the streptavidin-fusion protein strategy is applicable here as well, and may explain the low/negligible enhancement in CD8+ T-cell responses after stimulation with the dendrimer and LPS, with the exception of CD1a, which did display a 2-fold enhancement in both moDCs and CD1c+ mDCs. Alternatively, the disappointing results from both the pp65-streptavidin and pp65 dendrimer suggest that it is not the strategy, and perhaps the antigen itself which may be hindering an enhanced CD8+ T-cell response. Pp65 has a known function of interfering with the production of pro-inflammatory cytokines at a transcriptional level (Abate et al., 2004). This would functionally affect T-cells to produce cytokines, and potentially affect their ability to proliferate. This is another factor to consider in future studies when choosing the model antigen.

The inclusion of CD1a as a targeted receptor in the final two strategies was decided upon for two reasons. Firstly, the final two strategies allowed more flexibility in terms of the number of receptors that could be targeted. Secondly, the high level of expression of CD1a on DCs and its role in antigen presentation made it an interesting and novel target, specifically because there is currently no literature exploring it as a potential targeting option. Dickgreber et al (Dickgreber et al., 2009) detailed the targeting of MHC class II molecules with some success in eliciting CD8+ T-cell responses. In view of the similar functionality of CD1a to MHC class I, it was of interest to determine if receptors other than those with endocytic functions have the ability to target antigen towards the cross presentation pathway. Targeting antigen to CD1a induced relatively high CD8+ T-cell responses compared to targeting of the other receptors, specifically when the pp65 dendrimer was used. This data suggests that if CD1a was targeted using a more successful approach (such as the use of a chemical conjugate) it may elicit more promising CD8+ T-cell responses, which is something to explore in the future.

Interestingly, changing the adjuvant used in conjunction with the dendrimer appeared to strongly influence the ability of CD1a as well as the other receptors to induce CD8+ T-cell responses. The use of no adjuvant, Poly I:C or CLO97 yielded quite different data, with DC-SIGN-targeting enhancing responses in the absence of adjuvant, MMR-targeting demonstrating enhanced responses with poly I:C co-stimulation, and strong CD8+ T-cell proliferation observed after targeting CD1a in the presence of CLO97. Also of interest was data that showed that, even in the presence of FcR blocking agents, there were strong responses induced by the isotype controls when DCs were co-stimulated with polyI:C and CLO97, specifically IgG2b. This alludes to the idea of the isotype controls targeting the Fc receptors unintentionally, and could possibly be eliminated in future experiments by using specific anti-Fc (anti-CD16, CD32 and CD64) antibodies prior to pulsing, as has been done in some studies (Idoyaga et al., 2008).

The TLR agonist data for dendrimer targeting is strong evidence towards the varying effects that TLR agonists have on the induction of immune responses, and suggests that further analysis into the choice of adjuvant to use with the other targeting methods may affect the

outcome. Studies have described a close relationship between TLRs and CLRs in terms of their roles in T-cell activation and instruction (van Kooyk, 2008). This indicates that optimizing the combination of targeting strategy and TLR agonist could potentially be the key to improving CD8+ T-cell responses even further. Thus, future work will need to empirically determine the best combination to use for induction of an optimally enhanced pro-inflammatory response.

In general, the cytokine data from the different approaches prominently showed the induction of IFN-γ, produced singularly or in addition to other cytokines from individual cells. This confirms what has been seen in other pp65 and MART-1 studies and what we observed in Chapter 4, where pro-inflammatory cytokines are strongly induced by these antigens (Butterfield et al., 2008, Kern et al., 2002). The elicitation of broader cytokine production by the biotinylated pp65 and pp65 dendrimer strategy is most likely due to the presence of an additional component in the targeting reagent, which could be beneficial, but also be potentially masking the true response to the antigen. This is something to keep in mind when designing targeting strategies in the future. Additionally, if antigen-specific re-stimulations of the T-cells were administered before cytokines production was measured (as has been suggested in Chapter 4), this would provide a better picture of the level of cytokine production enhancement when antigens are targeted specifically to endocytic receptors. Nonetheless, from the data of the targeting strategy using chemical conjugates, there is a marked increase in cytokine production induced by targeted antigen, specifically in the production of IFN-γ. The other strategies do not appear to display significant differences amongst samples, although a limited number of cytokines were evaluated in this study, and it is unknown to what extent these targeting strategies affected production of other cytokines such as IL-4, IL-10 and IL-17.

On that note, it is important to acknowledge that the assumption behind this study was that the targeting strategies would enhance Th1-type responses, specifically targeting the antigen of interest to the cross presentation pathway and thereby eliciting enhanced CD8+ T-cell responses along with Th1-biased cytokines. In view of this, the effect of the targeting strategies on other immune cells such as CD4+ T-cells, NK cells and B cells, were not

assessed. Thus, although many of the targeting strategies did not render the expected enhancement of proliferative CD8+ T-cell responses, we do not know if they had an enhancing or inhibitory effect on other cells, or if the effects that it had on the CD8+ T-cell activation were not evaluated here. The pp65-DC-SIGN cytokine data suggests the latter is possible, given that this conjugate induced poor CD8+ T-cell proliferation but higher levels of cytokine production compared to the other chemical conjugates. Furthermore, the MMR and DC-SIGN receptors have shown an involvement in enhanced CD4+ T-cell responses and Th2 bias under certain circumstances (Aarnoudse et al., 2008, Royer et al., 2010), suggesting that perhaps targeting to MMR and DC-SIGN may have been more efficient at directing antigen to the MHC class II pathway, and thus induced CD4+ T-cells, which were not evaluated here.

From this study, we do know that at least two methods tested in this study were moderately effective at augmenting CD8+ T-cell responses (via the cross presentation pathway), and have highlighted ways in which we can perhaps improve these methods in future work. The DEC-205 receptor was identified as the best candidate of those evaluated in terms of its ability to target antigen to the cross presentation pathway, although data from the pp65 dendrimer targeting approach does loosely suggest that the targeting of an antigen to the cross presentation pathway can be manipulated by the choice of adjuvant, irrespective of the targeted receptor. Collectively, these studies represent preliminary work and require further investigation and optimisation in future studies in order to be able to successfully utilise the favoured approaches for more substantial research, but they have provided useful insight into different ways in which dendritic cell receptors can be targeted, and the polarising effects TLR agonists can have on the induction of CD8+ T-cells.

Chapter 6

Final discussion and future work

HIV-1vaccine research has primarily emphasised the importance of eliciting CD8+ T-cell responses in order to combat an infection. In particular, several HIV-1 vaccines have been designed to attempt to induce strong, broad, polyfunctional CD8+ T-cells systemically as well as at the mucosal level, as this has been identified as a correlate of protection against the virus (Kim et al., 2010, Makedonas and Betts, 2011). Consequently, there is a growing interest in strategies that are able to enhance CD8+ T-cell responses. Such strategies have included the utilisation of adjuvants, design of chimaeric vaccines that consist of several immunogenic viral proteins, and the use of prime-boost vaccine regimens. A promising approach that has emerged in the last decade is the targeting of vaccines towards specific receptors on DCs. This approach is able to augment antigen-specific CD8+ T-cell responses by providing vaccine antigens with direct access to the cross presentation pathway. Several mouse studies have documented the efficacy of this strategy; however there has been limited research regarding which receptors on human DCs most efficiently target the cross presentation pathway, and if their capabilities differ amongst DC subsets.

Thus, the primary aim of this study was to investigate which of four DC receptors optimally targeted antigens to the cross presentation pathway, and to evaluate their targeting abilities in two human DC subsets. To do this, model antigens were produced and purified in large quantities, and were used in four DC-receptor targeting strategies. DC-T-cell co-culture assays were then performed to assess the induced CD8+ T-cell proliferative responses and cytokine production.

6.1 Production and purification of reagents

Large scale production of the model antigens, pp65 and MART-1, was performed using an adenovirus expression system (AES) instead of a stably-expressing cell line, as this system

produced superior yields. The AES was optimised by monitoring the effects of the influential factors, MOI and time post infection, on recombinant protein production. Optimal conditions differed for each of the proteins expressed, but more than adequate quantities of the model antigens and their respective streptavidin-fusion proteins were produced. Even after optimisation, there was also significant variation in yields of the recombinant proteins, probably due to the nature of the different antigens. These differences in yields and optimal production conditions underscore the importance of empirical research in determining the best conditions for recombinant protein production, and highlight the significance of identifying factors that influence the recombinant protein production within a given expression system, before one attempts large scale protein production.

His-tag purification of the recombinant proteins proved to be an efficient means to purify proteins, resulting in the isolation of relatively pure protein samples with yields of between 2.9-8.2 mg in total. There did appear to be a lower efficiency of purification detected with the smaller proteins, MART-1 and MART-strep, but whether this is a size-related issue or due to protein-folding blocking accessibility to the His tag remains unclear. Additionally, the issue of His tag accessibility may have also contributed to the lower yields obtained for chemical conjugate purifications. It will be necessary in the future to further optimise the purification process for the chemical conjugates, and perhaps perform two purification steps to ensure that the final product is not a heterogeneous mixture as was observed in this study. This will, however, probably be at the expense of yields, and should be taken into consideration when producing these chemical conjugates in the future.

6.2 DC targeting strategies

Of the chosen DC targeting strategies, the most promising strategy was the use of chemically conjugated antigen-antibodies. This method was able to significantly enhance CD8+ T-cell responses, specifically when targeted to DEC-205 and MMR. Nevertheless, this targeting strategy can possibly be further improved by replacing the chemical conjugates with genetically-fused, single-chained antibody-antigen proteins. Such conjugates would be a

better means to target the DC receptors in a similar way as the chemical conjugates, but without the disadvantage of contaminating unbound antibody and yield limitations.

With respect to the streptavidin-fusion protein strategy, the results of the MART-strep experiments indicate that this method is an advantageous way to direct antigen towards the receptors, but it requires further optimisation before it can be useful. The pp65-strep targeting did not appear to enhance CD8+ T-cell responses, possibly due to steric hindrance preventing effective targeting. A study that used a similar targeting strategy to direct drugs towards tumour cells, fused streptavidin to the receptor-specific antibody and biotinylated the drug to be targeted (Wang et al., 2007). Biotinylating the antigen instead of the antibody in future work could potentially eliminate the steric hindrance issue that is suspected to have hindered targeting in this study, as this allows the number of antigen molecules that attach to the receptor-specific antibody to be limited.

The anti-biotin-bead-biotinylated-pp65 approach was a risky strategy, as there were numerous factors affecting the success of targeting the antigen to the receptor that was not accounted for. It was unfortunately unsuccessful in enhancing CD8+ T-cell responses, and could not be optimised due to lack of information about the anti-biotin bead reagent. Similarly with the pp65 dendrimer, optimisation of the approach was limited by the lack of information provided to us by the manufacturer. Nonetheless, both strategies provided an interesting means to target pp65 to the receptors of interest. Although CD8+ T-cell responses were not augmented using these targeting approaches, they could potentially have enhanced aspects of the immune response that were not analysed, such as CD4+ T-cell responses, and IL-4 and IL-5 production. Thus, it is important to note that while these targeting strategies were not successful in eliciting enhanced CD8+ T-cell responses and are therefore not suitable for the purpose of this study, we cannot dismiss the possibility that these approaches may have affected other immune responses.

6.3 Differences observed between DC subsets

There are currently four blood DC subsets, including three distinct populations of mDCs (MacDonald et al., 2002). Of the three mDC populations, the BDCA-3+ (CD141+) mDCs demonstrate a superior ability to direct antigens towards the cross-presentation pathway in the presence of poly I:C, and thus activate CD8+ T-cell responses (Jongbloed et al., 2010). Thus, while CD1c+ mDCs display a moderate ability to induce CD8+ T-cells, it has recently been found to be the less favoured DC subset for cross presentation. This is consistent with the observations of this study, where the induction of CD8+ T-cell responses by moDCs was stronger compared to CD1c+ mDCs in all experiments performed. However, this contradicts older studies such as those of Osugi et al (Osugi et al., 2002), which demonstrated the induction of stronger CD8+ T-cell responses by stimulated CD1c+ mDCs compared to moDCs. This difference may be attributed to the unclear distinction between CD1c+ mDCs and CD141+ mDCs at the time of Osugi's study, and the probable inclusion of CD141+ mDCs in the preparation of BMDCs used. Alternatively, the use of a different TLR agonist in our experiments may have contributed to the poorer cross presentation capabilities of the CD1c+ mDCs. Many mDC studies, including the above mentioned, appear to favour the use of poly I:C as an adjuvant (Radford et al., 2006, Jongbloed et al., 2010), however we used LPS, as it was determined to be the optimal TLR agonist in moDC stimulations. In hindsight, the assumption in our study that the preferred moDC TLR agonist would also be the preferred CD1c+ mDC adjuvant was perhaps too presumptuous, given the variable distributions of TLRs on different DC subsets. Thus, it is possible that the CD1c+ mDCs may have responded differently to the range of TLR agonists that were investigated with moDC stimulations and this should be considered in future studies.

Future work should also explore the use of CD141+ mDCs as potential vaccine targets, given the evidence of their superior capability to induce CD8+ T-cells via the cross presentation pathway, and the specificity of CLEC9A expression by these cells (Caminschi et al., 2008). In addition, it will be of interest to investigate the targeting of skin DC subsets with the chemical conjugate strategy, as this would be a practical and effective approach to maximise DC utilization at the mucosa. Lisziewicz et al (Lisziewicz et al., 2005) explored applying a

HIV-1 DNA vaccine to the skin, and showed that it targeted the superficial LCs and deeper dDCs to induce strong viral-specific $CD4^+$ and $CD8^+$ memory T cells. Furthermore, it is reported that LCs induce a more potent autologous CTL response to foreign antigen compared to other DC subsets (Ratzinger et al., 2004). Thus, these DC subsets are potentially useful targets for the activation of HIV-specific mucosal immune responses.

6.4 Use of TLR agonists

TLRs are integrally involved in the initiation and sustainability of immune responses, taking part in several stages of the induction and regulatory processes. As was shown in Chapters 4 and 5, TLR agonists have varying abilities to enhance cellular immune responses. LPS was determined to be the preferred agonist for moDC-pp65 stimulations, however, the pp65 dendrimer data strongly suggest that the type and magnitude of the cellular immune responses elicited is a result of a collective effect of several factors including the receptor targeted, the TLR agonist used, and the nature of the antigen. Thus, future work should consider utilising different TLR agonists with the targeting strategy of choice, as this could further improve CD8+ T-cell responses. Moreover, previous research has demonstrated the potential advantage of the synergistic effects that result from using multiple TLR agonists (Napolitani et al., 2005, Raman et al., 2010). Thus, it might be of interest to investigate the augmentation of CD8+ T-cell responses when synergistic agonists are used in conjunction with a targeting strategy.

6.5 Favoured receptor for cross presentation

A number of DC endocytic receptors have been studied to investigate their potential use as vaccine targets, although many of these studies have been done in mice. The differences in distribution and the phenotypic and functional aspects of mouse and human DCs indicate that while these studies are useful in providing insight into the interactions of DCs with their natural environment and other immune cells, it is difficult to directly infer similar outcomes in human studies without empirical evidence. Thus, *in vitro* human studies such as ours provide the opportunity to explore how human DCs react to receptor targeting strategies, be it

in an artificial environment. Interestingly, the chemical conjugate and MART-strep targeting data concluded that targeting antigen to DEC-205 stimulated the strongest proliferative CD8+ T-cell responses compared to MMR and DC-SIGN, which was in agreement with other studies that showed DEC-205 as the endocytic receptor most likely to target antigens to the cross-presentation pathway (Bonifaz et al., 2004, Bozzacco et al., 2007, Flacher et al., 2010). This is not to say that the other receptors failed to target the antigen for presentation, as it is possible that the antigens targeted to the other receptors were targeted to the MHC class II pathway, and enhanced CD4+ T-cell responses. In particular, DC-SIGN preferably target antigen towards late, acidic endosomes/lysosomes for presentation on MHC class II molecules (Burgdorf and Kurts, 2008), suggesting that even though murine studies have shown targeting to DC-SIGN can enhance CD8+ T-cell responses (Singh et al., 2009), this does not appear to be the case in humans.

Interestingly, targeting pp65 to CD1a using the dendrimer yielded some promising proliferative CD8+ T-cell responses, indicating that DC receptors other than endocytic receptors have the potential to direct antigen towards the cross presentation pathway. This opens the door to the exploration of other DC receptors as potential targeting options, some of which are more specific to DCs and expressed to a greater extent on the surface than DEC-205. Thus, despite the promising potential of DEC-205 to elicit enhanced CD8+ T-cell responses, other potential receptors that might be more useful in a human setting include receptors such as CLEC9A and langerin. Future work should therefore explore these receptors as vaccine targets, once the targeting strategies have been further optimised.

In summary, this study has detailed the successful design and production of targeting reagents that directed antigens towards specific endocytic DC receptors, in the hope of eliciting enhanced CD8+ T-cell responses. Of the four targeting strategies evaluated, two strategies showed promise, namely the chemical conjugate strategy and the MART-strep strategy. However, both strategies can be further improved in order to enhance CD8+ T-cell responses, as well as eliminate the current drawbacks. This research has highlighted the complexity of influencing a cellular immune response by demonstrating that a number of factors can affect to what extent a CD8+ T-cell response is elicited, including DC subset, receptor targeted,

adjuvant utilised and the nature of the antigen. Consequently, this study provides a sound foundation for future work involving DC receptor targeting, which can potentially explore several avenues, examining each of these influencing factors more extensively.

References

AARNOUDSE, C. A., BAX, M., SANCHEZ-HERNANDEZ, M., GARCIA-VALLEJO, J. J. & VAN KOOYK, Y. 2008. Glycan modification of the tumor antigen gp100 targets DC-SIGN to enhance dendritic cell induced antigen presentation to T cells. *International journal of cancer. Journal international du cancer,* 122**,** 839-46.

ABATE, D. A., WATANABE, S. & MOCARSKI, E. S. 2004. Major human cytomegalovirus structural protein pp65 (ppUL83) prevents interferon response factor 3 activation in the interferon response. *Journal of Virology,* 78**,** 10995-1006.

ACKERMAN, A. L., KYRITSIS, C., TAMPE, R. & CRESSWELL, P. 2005. Access of soluble antigens to the endoplasmic reticulum can explain cross-presentation by dendritic cells. *Nat Immunol,* 6**,** 107-13.

ACOSTA-RODRIGUEZ, E. V., RIVINO, L., GEGINAT, J., JARROSSAY, D., GATTORNO, M., LANZAVECCHIA, A., SALLUSTO, F. & NAPOLITANI, G. 2007. Surface phenotype and antigenic specificity of human interleukin 17-producing T helper memory cells. *Nature immunology,* 8**,** 639-46.

ADAMS, E. W., RATNER, D. M., SEEBERGER, P. H. & HACOHEN, N. 2008. Carbohydrate-mediated targeting of antigen to dendritic cells leads to enhanced presentation of antigen to T cells. *Chembiochem,* 9**,** 294-303.

AGARWAL, S. & RAO, A. 1998. Modulation of chromatin structure regulates cytokine gene expression during T cell differentiation. *Immunity,* 9**,** 765-75.

AHONEN, C. L., DOXSEE, C. L., MCGURRAN, S. M., RITER, T. R., WADE, W. F., BARTH, R. J., VASILAKOS, J. P., NOELLE, R. J. & KEDL, R. M. 2004. Combined TLR and CD40 triggering induces potent CD8+ T cell expansion with variable dependence on type I IFN. *The Journal of experimental medicine,* 199**,** 775-84.

ALINE, F., BRAND, D., PIERRE, J., ROINGEARD, P., SEVERINE, M., VERRIER, B. & DIMIER-POISSON, I. 2009. Dendritic cells loaded with HIV-1 p24 proteins adsorbed on surfactant-free anionic PLA nanoparticles induce enhanced cellular immune responses against HIV-1 after vaccination. *Vaccine,* 27**,** 5284-91.

ALLARD, S. D., PLETINCKX, K., BRECKPOT, K., HEIRMAN, C., BONEHILL, A., MICHIELS, A., VAN BAALEN, C. A., GRUTERS, R. A., OSTERHAUS, A. D., LACOR, P., THIELEMANS, K. & AERTS, J. L. 2008. Functional T-cell responses generated by dendritic cells expressing the early HIV-1 proteins Tat, Rev and Nef. *Vaccine,* 26**,** 3735-41.

ANDERSON, K. V., BOKLA, L. & NUSSLEIN-VOLHARD, C. 1985. Establishment of dorsal-ventral polarity in the Drosophila embryo: the induction of polarity by the Toll gene product. *Cell,* 42**,** 791-8.

ANDRIEU, J. M. & LU, W. 2007. A dendritic cell-based vaccine for treating HIV infection: background and preliminary results. *J Intern Med,* 261**,** 123-31.

APPLEQUIST, S. E., ROLLMAN, E., WAREING, M. D., LIDEN, M., ROZELL, B., HINKULA, J. & LJUNGGREN, H. G. 2005. Activation of innate immunity, inflammation, and

potentiation of DNA vaccination through mammalian expression of the TLR5 agonist flagellin. *Journal of immunology,* 175**,** 3882-91.

BADIEE, A., DAVIES, N., MCDONALD, K., RADFORD, K., MICHIUE, H., HART, D. & KATO, M. 2007. Enhanced delivery of immunoliposomes to human dendritic cells by targeting the multilectin receptor DEC-205. *Vaccine,* 25**,** 4757-66.

BANCHEREAU, J., BRIERE, F., CAUX, C., DAVOUST, J., LEBECQUE, S., LIU, Y. J., PULENDRAN, B. & PALUCKA, K. 2000. Immunobiology of dendritic cells. *Annu Rev Immunol,* 18**,** 767-811.

BANCHEREAU, J. & STEINMAN, R. M. 1998. Dendritic cells and the control of immunity. *Nature,* 392**,** 245-52.

BARNES, L. M. & DICKSON, A. J. 2006. Mammalian cell factories for efficient and stable protein expression. *Curr Opin Biotechnol,* 17**,** 381-6.

BATES, E. E., FOURNIER, N., GARCIA, E., VALLADEAU, J., DURAND, I., PIN, J. J., ZURAWSKI, S. M., PATEL, S., ABRAMS, J. S., LEBECQUE, S., GARRONE, P. & SAELAND, S. 1999. APCs express DCIR, a novel C-type lectin surface receptor containing an immunoreceptor tyrosine-based inhibitory motif. *Journal of immunology,* 163**,** 1973-83.

BENKO, S., MAGYARICS, Z., SZABO, A. & RAJNAVOLGYI, E. 2008. Dendritic cell subtypes as primary targets of vaccines: the emerging role and cross-talk of pattern recognition receptors. *Biol Chem,* 389**,** pp. 469–485.

BENLAHRECH, A., HARRIS, J., MEISER, A., PAPAGATSIAS, T., HORNIG, J., HAYES, P., LIEBER, A., ATHANASOPOULOS, T., BACHY, V., CSOMOR, E., DANIELS, R., FISHER, K., GOTCH, F., SEYMOUR, L., LOGAN, K., BARBAGALLO, R., KLAVINSKIS, L., DICKSON, G. & PATTERSON, S. 2009. Adenovirus vector vaccination induces expansion of memory CD4 T cells with a mucosal homing phenotype that are readily susceptible to HIV-1. *Proceedings of the National Academy of Sciences of the United States of America,* 106**,** 19940-5.

BENNEKOV, T., SPECTOR, D. & LANGHOFF, E. 2004. Induction of immunity against human cytomegalovirus. *The Mount Sinai journal of medicine, New York,* 71**,** 86-93.

BEVAN, M. J. 1976. Minor H antigens introduced on H-2 different stimulating cells cross-react at the cytotoxic T cell level during in vivo priming. *J Immunol,* 117**,** 2233-8.

BEVAN, M. J. 2006. Cross-priming. *Nat Immunol,* 7**,** 363-5.

BINDER, R. J. & SRIVASTAVA, P. K. 2005. Peptides chaperoned by heat-shock proteins are a necessary and sufficient source of antigen in the cross-priming of CD8+ T cells. *Nat Immunol,* 6**,** 593-9.

BIRKHOLZ, K., SCHWENKERT, M., KELLNER, C., GROSS, S., FEY, G., SCHULER-THURNER, B., SCHULER, G., SCHAFT, N. & DORRIE, J. 2010. Targeting of DEC-205 on human dendritic cells results in efficient MHC class II-restricted antigen presentation. *Blood,* 116**,** 2277-85.

BLANDER, J. M. 2008. Phagocytosis and antigen presentation: a partnership initiated by Toll-like receptors. *Ann Rheum Dis,* 67 Suppl 3**,** iii44-9.

BLANDER, J. M. & MEDZHITOV, R. 2006. Toll-dependent selection of microbial antigens for presentation by dendritic cells. *Nature,* 440**,** 808-12.

BOAZ, M. J., WATERS, A., MURAD, S., EASTERBROOK, P. J. & VYAKARNAM, A. 2002. Presence of HIV-1 Gag-specific IFN-gamma+IL-2+ and CD28+IL-2+ CD4 T cell responses is associated with nonprogression in HIV-1 infection. *J Immunol,* 169**,** 6376-85.

BONIFACINO, J. S. & WEISSMAN, A. M. 1998. Ubiquitin and the control of protein fate in the secretory and endocytic pathways. *Annual review of cell and developmental biology,* 14**,** 19-57.

BONIFAZ, L., BONNYAY, D., MAHNKE, K., RIVERA, M., NUSSENZWEIG, M. C. & STEINMAN, R. M. 2002. Efficient targeting of protein antigen to the dendritic cell receptor DEC-205 in the steady state leads to antigen presentation on major histocompatibility complex class I products and peripheral CD8+ T cell tolerance. *J Exp Med,* 196**,** 1627-38.

BONIFAZ, L. C., BONNYAY, D. P., CHARALAMBOUS, A., DARGUSTE, D. I., FUJII, S., SOARES, H., BRIMNES, M. K., MOLTEDO, B., MORAN, T. M. & STEINMAN, R. M. 2004. In vivo targeting of antigens to maturing dendritic cells via the DEC-205 receptor improves T cell vaccination. *J Exp Med,* 199**,** 815-24.

BORROW, P., LEWICKI, H., WEI, X., HORWITZ, M. S., PEFFER, N., MEYERS, H., NELSON, J. A., GAIRIN, J. E., HAHN, B. H., OLDSTONE, M. B. & SHAW, G. M. 1997. Antiviral pressure exerted by HIV-1-specific cytotoxic T lymphocytes (CTLs) during primary infection demonstrated by rapid selection of CTL escape virus. *Nature medicine,* 3**,** 205-11.

BOYER, J. D., CHATTERGOON, M. A., UGEN, K. E., SHAH, A., BENNETT, M., COHEN, A., NYLAND, S., LACY, K. E., BAGARAZZI, M. L., HIGGINS, T. J., BAINE, Y., CICCARELLI, R. B., GINSBERG, R. S., MACGREGOR, R. R. & WEINER, D. B. 1999. Enhancement of cellular immune response in HIV-1 seropositive individuals: A DNA-based trial. *Clinical immunology,* 90**,** 100-7.

BOZZACCO, L., TRUMPFHELLER, C., SIEGAL, F. P., MEHANDRU, S., MARKOWITZ, M., CARRINGTON, M., NUSSENZWEIG, M. C., PIPERNO, A. G. & STEINMAN, R. M. 2007. DEC-205 receptor on dendritic cells mediates presentation of HIV gag protein to CD8+ T cells in a spectrum of human MHC I haplotypes. *Proc Natl Acad Sci U S A,* 104**,** 1289-94.

BROWN, G. D. 2006. Dectin-1: a signalling non-TLR pattern-recognition receptor. *Nature reviews. Immunology,* 6**,** 33-43.

BROWNE, S. M. & AL-RUBEAI, M. 2007. Selection methods for high-producing mammalian cell lines. *Trends Biotechnol,* 25**,** 425-32.

BUCHBINDER, S. P., MEHROTRA, D. V., DUERR, A., FITZGERALD, D. W., MOGG, R., LI, D., GILBERT, P. B., LAMA, J. R., MARMOR, M., DEL RIO, C., MCELRATH, M. J., CASIMIRO, D. R., GOTTESDIENER, K. M., CHODAKEWITZ, J. A., COREY, L. & ROBERTSON, M. N. 2008. Efficacy assessment of a cell-mediated immunity HIV-1 vaccine (the Step Study): a double-blind, randomised, placebo-controlled, test-of-concept trial. *Lancet,* 372**,** 1881-93.

BURGDORF, S., KAUTZ, A., BOHNERT, V., KNOLLE, P. A. & KURTS, C. 2007. Distinct pathways of antigen uptake and intracellular routing in CD4 and CD8 T cell activation. *Science,* 316**,** 612-6.

BURGDORF, S. & KURTS, C. 2008. Endocytosis mechanisms and the cell biology of antigen presentation. *Current opinion in immunology,* 20**,** 89-95.

BURGDORF, S., LUKACS-KORNEK, V. & KURTS, C. 2006. The mannose receptor mediates uptake of soluble but not of cell-associated antigen for cross-presentation. *J Immunol,* 176**,** 6770-6.

BUTTERFIELD, L. H., COMIN-ANDUIX, B., VUJANOVIC, L., LEE, Y., DISSETTE, V. B., YANG, J. Q., VU, H. T., SEJA, E., OSEGUERA, D. K., POTTER, D. M., GLASPY, J. A., ECONOMOU, J. S. & RIBAS, A. 2008. Adenovirus MART-1-engineered autologous dendritic cell vaccine for metastatic melanoma. *Journal of immunotherapy,* 31**,** 294-309.

CAMINSCHI, I., PROIETTO, A. I., AHMET, F., KITSOULIS, S., SHIN TEH, J., LO, J. C., RIZZITELLI, A., WU, L., VREMEC, D., VAN DOMMELEN, S. L., CAMPBELL, I. K., MARASKOVSKY, E., BRALEY, H., DAVEY, G. M., MOTTRAM, P., VAN DE VELDE, N., JENSEN, K., LEW, A. M., WRIGHT, M. D., HEATH, W. R., SHORTMAN, K. & LAHOUD, M. H. 2008. The dendritic cell subtype-restricted C-type lectin Clec9A is a target for vaccine enhancement. *Blood,* 112**,** 3264-73.

CARLSSON, J., DREVIN, H. & AXEN, R. 1978. Protein thiolation and reversible protein-protein conjugation. N-Succinimidyl 3-(2-pyridyldithio)propionate, a new heterobifunctional reagent. *The Biochemical journal,* 173**,** 723-37.

CASADO, J. G., DELAROSA, O., PAWELEC, G., PERALBO, E., DURAN, E., BARAHONA, F., SOLANA, R. & TARAZONA, R. 2009. Correlation of effector function with phenotype and cell division after in vitro differentiation of naive MART-1-specific CD8+ T cells. *International immunology,* 21**,** 53-62.

CASELLA, C. R. & MITCHELL, T. C. 2008. Putting endotoxin to work for us: monophosphoryl lipid A as a safe and effective vaccine adjuvant. *Cellular and molecular life sciences : CMLS,* 65**,** 3231-40.

CAUX, C., MASSACRIER, C., DUBOIS, B., VALLADEAU, J., DEZUTTER-DAMBUYANT, C., DURAND, I., SCHMITT, D. & SAELAND, S. 1999. Respective involvement of TGF-beta and IL-4 in the development of Langerhans cells and non-Langerhans dendritic cells from CD34+ progenitors. *Journal of leukocyte biology,* 66**,** 781-91.

CHEN, W., JIN, W., HARDEGEN, N., LEI, K. J., LI, L., MARINOS, N., MCGRADY, G. & WAHL, S. M. 2003. Conversion of peripheral CD4+CD25- naive T cells to CD4+CD25+ regulatory T cells by TGF-beta induction of transcription factor Foxp3. *The Journal of experimental medicine,* 198**,** 1875-86.

CHUSAINOW, J., YANG, Y. S., YEO, J. H., TOH, P. C., ASVADI, P., WONG, N. S. & YAP, M. G. 2009. A study of monoclonal antibody-producing CHO cell lines: what makes a stable high producer? *Biotechnol Bioeng,* 102**,** 1182-96.

CLIMENT, N., GUERRA, S., GARCIA, F., ROVIRA, C., MIRALLES, L., GOMEZ, C. E., PIQUE, N., GIL, C., GATELL, J. M., ESTEBAN, M. & GALLART, T. 2011. Dendritic cells exposed to MVA-based HIV-1 vaccine induce highly functional HIV-1-specific CD8(+) T cell responses in HIV-1-infected individuals. *PLoS ONE,* 6**,** e19644.

COFFMAN, R. L., SHER, A. & SEDER, R. A. 2010. Vaccine adjuvants: putting innate immunity to work. *Immunity,* 33**,** 492-503.

COLONNA, M., TRINCHIERI, G. & LIU, Y. J. 2004. Plasmacytoid dendritic cells in immunity. *Nature immunology,* 5**,** 1219-26.

CONSTANT, S. L., LEE, K. S. & BOTTOMLY, K. 2000. Site of antigen delivery can influence T cell priming: pulmonary environment promotes preferential Th2-type differentiation. *European journal of immunology,* 30**,** 840-7.

CRESSWELL, P. 1994. Assembly, transport, and function of MHC class II molecules. *Annual review of immunology,* 12**,** 259-93.

CRESSWELL, P., ACKERMAN, A. L., GIODINI, A., PEAPER, D. R. & WEARSCH, P. A. 2005. Mechanisms of MHC class I-restricted antigen processing and cross-presentation. *Immunol Rev,* 207**,** 145-57.

CROTTY, S. 2011. Follicular helper CD4 T cells (TFH). *Annual review of immunology,* 29**,** 621-63.

CURRIER, J. R., NGAUY, V., DE SOUZA, M. S., RATTO-KIM, S., COX, J. H., POLONIS, V. R., EARL, P., MOSS, B., PEEL, S., SLIKE, B., SRIPLIENCHAN, S., THONGCHAROEN, P., PARIS, R. M., ROBB, M. L., KIM, J., MICHAEL, N. L. & MAROVICH, M. A. 2010. Phase I safety and immunogenicity evaluation of MVA-CMDR, a multigenic, recombinant modified vaccinia Ankara-HIV-1 vaccine candidate. *PLoS ONE,* 5**,** e13983.

DABBAGH, K. & LEWIS, D. B. 2003. Toll-like receptors and T-helper-1/T-helper-2 responses. *Current opinion in infectious diseases,* 16**,** 199-204.

DEE, K. U. & SHULER, M. L. 1997. Optimization of an assay for baculovirus titer and design of regimens for the synchronous infection of insect cells. *Biotechnol Prog,* 13**,** 14-24.

DELNESTE, Y., MAGISTRELLI, G., GAUCHAT, J., HAEUW, J., AUBRY, J., NAKAMURA, K., KAWAKAMI-HONDA, N., GOETSCH, L., SAWAMURA, T., BONNEFOY, J. & JEANNIN, P. 2002. Involvement of LOX-1 in dendritic cell-mediated antigen cross-presentation. *Immunity,* 17**,** 353-62.

DEMAIN, A. L. & VAISHNAV, P. 2009. Production of recombinant proteins by microbes and higher organisms. *Biotechnol Adv,* 27**,** 297-306.

DEMEURE, C. E., WU, C. Y., SHU, U., SCHNEIDER, P. V., HEUSSER, C., YSSEL, H. & DELESPESSE, G. 1994. In vitro maturation of human neonatal CD4 T lymphocytes. II. Cytokines present at priming modulate the development of lymphokine production. *Journal of immunology,* 152**,** 4775-82.

DI PUCCHIO, T., CHATTERJEE, B., SMED-SORENSEN, A., CLAYTON, S., PALAZZO, A., MONTES, M., XUE, Y., MELLMAN, I., BANCHEREAU, J. & CONNOLLY, J. E. 2008. Direct proteasome-independent cross-presentation of viral antigen by plasmacytoid dendritic cells on major histocompatibility complex class I. *Nature immunology,* 9**,** 551-7.

DICKGREBER, N., STOITZNER, P., BAI, Y., PRICE, K. M., FARRAND, K. J., MANNING, K., ANGEL, C. E., DUNBAR, P. R., RONCHESE, F., FRASER, J. D., BACKSTROM, B. T. & HERMANS, I. F. 2009. Targeting antigen to MHC class II molecules promotes efficient cross-presentation and enhances immunotherapy. *Journal of immunology,* 182**,** 1260-9.

DIEBOLD, S. S. 2008. Determination of T-cell fate by dendritic cells. *Immunology and cell biology,* 86**,** 389-97.

DOAN, L. X., LI, M., CHEN, C. & YAO, Q. 2005. Virus-like particles as HIV-1 vaccines. *Rev Med Virol,* 15**,** 75-88.

DUBSKY, P., UENO, H., PIQUERAS, B., CONNOLLY, J., BANCHEREAU, J. & PALUCKA, A. K. 2005. Human dendritic cell subsets for vaccination. *Journal of clinical immunology,* 25**,** 551-72.

DUDZIAK, D., KAMPHORST, A. O., HEIDKAMP, G. F., BUCHHOLZ, V. R., TRUMPFHELLER, C., YAMAZAKI, S., CHEONG, C., LIU, K., LEE, H. W., PARK, C. G., STEINMAN, R. M. & NUSSENZWEIG, M. C. 2007. Differential antigen processing by dendritic cell subsets in vivo. *Science,* 315**,** 107-11.

DUERR, A., WASSERHEIT, J. N. & COREY, L. 2006. HIV vaccines: new frontiers in vaccine development. *Clinical infectious diseases : an official publication of the Infectious Diseases Society of America,* 43**,** 500-11.

DUNN, H. S., HANEY, D. J., GHANEKAR, S. A., STEPICK-BIEK, P., LEWIS, D. B. & MAECKER, H. T. 2002. Dynamics of CD4 and CD8 T cell responses to cytomegalovirus in healthy human donors. *The Journal of infectious diseases,* 186**,** 15-22.

DURAISINGHAM, S. S., HORNIG, J., GOTCH, F. & PATTERSON, S. 2009. TLR-stimulated CD34 stem cell-derived human skin-like and monocyte-derived dendritic cells fail to induce Th17 polarization of naive T cells but do stimulate Th1 and Th17 memory responses. *Journal of immunology,* 183**,** 2242-51.

DUTHIE, M. S., WINDISH, H. P., FOX, C. B. & REED, S. G. 2011. Use of defined TLR ligands as adjuvants within human vaccines. *Immunological reviews,* 239**,** 178-96.

EISENBARTH, S. C., PIGGOTT, D. A., HULEATT, J. W., VISINTIN, I., HERRICK, C. A. & BOTTOMLY, K. 2002. Lipopolysaccharide-enhanced, toll-like receptor 4-dependent T helper cell type 2 responses to inhaled antigen. *The Journal of experimental medicine,* 196**,** 1645-51.

ENGERING, A., GEIJTENBEEK, T. B., VAN VLIET, S. J., WIJERS, M., VAN LIEMPT, E., DEMAUREX, N., LANZAVECCHIA, A., FRANSEN, J., FIGDOR, C. G., PIGUET, V. & VAN KOOYK, Y. 2002. The dendritic cell-specific adhesion receptor DC-SIGN internalizes antigen for presentation to T cells. *J Immunol,* 168**,** 2118-26.

FAHRER, J., RIEGER, J., VAN ZANDBERGEN, G. & BARTH, H. 2010. The C2-streptavidin delivery system promotes the uptake of biotinylated molecules in macrophages and T-leukemia cells. *Biological chemistry,* 391**,** 1315-25.

FAJARDO-MOSER, M., BERZEL, S. & MOLL, H. 2008. Mechanisms of dendritic cell-based vaccination against infection. *Int J Med Microbiol,* 298**,** 11-20.

FAURE, F., MANTEGAZZA, A., SADAKA, C., SEDLIK, C., JOTEREAU, F. & AMIGORENA, S. 2009. Long-lasting cross-presentation of tumor antigen in human DC. *European journal of immunology,* 39**,** 380-90.

FIGDOR, C. G., VAN KOOYK, Y. & ADEMA, G. J. 2002. C-type lectin receptors on dendritic cells and Langerhans cells. *Nat Rev Immunol,* 2**,** 77-84.

FLACHER, V., SPARBER, F., TRIPP, C. H., ROMANI, N. & STOITZNER, P. 2009. Targeting of epidermal Langerhans cells with antigenic proteins: attempts to harness their properties for immunotherapy. *Cancer immunology, immunotherapy : CII,* 58**,** 1137-47.

FLACHER, V., TRIPP, C. H., STOITZNER, P., HAID, B., EBNER, S., DEL FRARI, B., KOCH, F., PARK, C. G., STEINMAN, R. M., IDOYAGA, J. & ROMANI, N. 2010. Epidermal Langerhans cells rapidly capture and present antigens from C-type lectin-targeting antibodies deposited in the dermis. *The Journal of investigative dermatology,* 130**,** 755-62.

FLINT, S. J., SKALKA, A. M., ENQUIST, L. W., KRUG, R. M. & RACANIELLO., V. R. (eds.) 1999. *Principle of Virology: Molecular Biology, Pathogenesis and Control,* Washington D.C.: ASM Press.

FRISON, N., TAYLOR, M. E., SOILLEUX, E., BOUSSER, M. T., MAYER, R., MONSIGNY, M., DRICKAMER, K. & ROCHE, A. C. 2003. Oligolysine-based oligosaccharide clusters: selective recognition and endocytosis by the mannose receptor and dendritic cell-specific intercellular adhesion molecule 3 (ICAM-3)-grabbing nonintegrin. *The Journal of biological chemistry,* 278**,** 23922-9.

GAILLET, B., GILBERT, R., AMZIANI, R., GUILBAULT, C., GADOURY, C., CARON, A. W., MULLICK, A., GARNIER, A. & MASSIE, B. 2007. High-level recombinant protein production in CHO cells using an adenoviral vector and the cumate gene-switch. *Biotechnol Prog,* 23**,** 200-9.

GALLORINI, S., BERTI, F., MANCUSO, G., COZZI, R., TORTOLI, M., VOLPINI, G., TELFORD, J. L., BENINATI, C., MAIONE, D. & WACK, A. 2009. Toll-like receptor 2 dependent immunogenicity of glycoconjugate vaccines containing chemically derived zwitterionic polysaccharides. *Proceedings of the National Academy of Sciences of the United States of America,* 106**,** 17481-6.

GANTNER, B. N., SIMMONS, R. M., CANAVERA, S. J., AKIRA, S. & UNDERHILL, D. M. 2003. Collaborative induction of inflammatory responses by dectin-1 and Toll-like receptor 2. *The Journal of experimental medicine,* 197**,** 1107-17.

GARNIER, A., COTE, J., NADEAU, I., KAMEN, A. & MASSIE, B. 1994. Scale-up of the adenovirus expression system for the production of recombinant protein in human 293S cells. *Cytotechnology,* 15**,** 145-55.

GEIJTENBEEK, T. B. & GRINGHUIS, S. I. 2009. Signalling through C-type lectin receptors: shaping immune responses. *Nat Rev Immunol,* 9**,** 465-79.

GEIJTENBEEK, T. B., VAN VLIET, S. J., ENGERING, A., T HART, B. A. & VAN KOOYK, Y. 2004. Self- and nonself-recognition by C-type lectins on dendritic cells. *Annu Rev Immunol,* 22**,** 33-54.

GEISSE, S., GRAM, H., KLEUSER, B. & KOCHER, H. P. 1996. Eukaryotic expression systems: a comparison. *Protein Expr Purif,* 8**,** 271-82.

GEISSMANN, F., PROST, C., MONNET, J. P., DY, M., BROUSSE, N. & HERMINE, O. 1998. Transforming growth factor beta1, in the presence of granulocyte/macrophage colony-stimulating factor and interleukin 4, induces differentiation of human peripheral blood monocytes into dendritic Langerhans cells. *The Journal of experimental medicine,* 187**,** 961-6.

GNJATIC, S., SAWHNEY, N. B. & BHARDWAJ, N. 2010. Toll-like receptor agonists: are they good adjuvants? *Cancer journal,* 16**,** 382-91.

GOLDBERG, A. L. & ROCK, K. L. 1992. Proteolysis, proteasomes and antigen presentation. *Nature,* 357**,** 375-9.

GONZALEZ, M., BAGATOLLI, L. A., ECHABE, I., ARRONDO, J. L., ARGARANA, C. E., CANTOR, C. R. & FIDELIO, G. D. 1997. Interaction of biotin with streptavidin. Thermostability and conformational changes upon binding. *The Journal of biological chemistry,* 272**,** 11288-94.

GUAN, Y., RANOA, D. R., JIANG, S., MUTHA, S. K., LI, X., BAUDRY, J. & TAPPING, R. I. 2010. Human TLRs 10 and 1 share common mechanisms of innate immune sensing but not signaling. *Journal of immunology,* 184**,** 5094-103.

GURER, C., STROWIG, T., BRILOT, F., PACK, M., TRUMPFHELLER, C., ARREY, F., PARK, C. G., STEINMAN, R. M. & MUNZ, C. 2008. Targeting the nuclear antigen 1 of Epstein-Barr virus to the human endocytic receptor DEC-205 stimulates protective T-cell responses. *Blood,* 112**,** 1231-9.

HAMANN, D., BAARS, P. A., REP, M. H., HOOIBRINK, B., KERKHOF-GARDE, S. R., KLEIN, M. R. & VAN LIER, R. A. 1997. Phenotypic and functional separation of memory and effector human CD8+ T cells. *The Journal of experimental medicine,* 186**,** 1407-18.

HARARI, A., ZIMMERLI, S. C. & PANTALEO, G. 2004. Cytomegalovirus (CMV)-specific cellular immune responses. *Hum Immunol,* 65**,** 500-6.

HARRINGTON, L. E., HATTON, R. D., MANGAN, P. R., TURNER, H., MURPHY, T. L., MURPHY, K. M. & WEAVER, C. T. 2005. Interleukin 17-producing CD4+ effector T cells develop via a lineage distinct from the T helper type 1 and 2 lineages. *Nature immunology,* 6**,** 1123-32.

HATTORI, Y., KAWAKAMI, S., SUZUKI, S., YAMASHITA, F. & HASHIDA, M. 2004. Enhancement of immune responses by DNA vaccination through targeted gene delivery using mannosylated cationic liposome formulations following intravenous administration in mice. *Biochemical and biophysical research communications,* 317**,** 992-9.

HAVENGA, M. J., HOLTERMAN, L., MELIS, I., SMITS, S., KASPERS, J., HEEMSKERK, E., VAN DER VLUGT, R., KOLDIJK, M., SCHOUTEN, G. J., HATEBOER, G., BROUWER, K., VOGELS, R. & GOUDSMIT, J. 2008. Serum-free transient protein production system based on adenoviral vector and PER.C6 technology: high yield and preserved bioactivity. *Biotechnol Bioeng,* 100**,** 273-83.

HAWIGER, D., INABA, K., DORSETT, Y., GUO, M., MAHNKE, K., RIVERA, M., RAVETCH, J. V., STEINMAN, R. M. & NUSSENZWEIG, M. C. 2001. Dendritic cells induce peripheral T cell unresponsiveness under steady state conditions in vivo. *J Exp Med,* 194**,** 769-79.

HEL, Z., JOHNSON, J. M., TRYNISZEWSKA, E., TSAI, W. P., HARROD, R., FULLEN, J., TARTAGLIA, J. & FRANCHINI, G. 2002. A novel chimeric Rev, Tat, and Nef (Retanef) antigen as a component of an SIV/HIV vaccine. *Vaccine,* 20**,** 3171-86.

HOLMES, B. J., MACARY, P. A., NOBLE, A. & KEMENY, D. M. 1997. Antigen-specific CD8+ T cells inhibit IgE responses and interleukin-4 production by CD4+ T cells. *European journal of immunology,* 27**,** 2657-65.

HORTON, R. M., HUNT, H. D., HO, S. N., PULLEN, J. K. & PEASE, L. R. 1989. Engineering hybrid genes without the use of restriction enzymes: gene splicing by overlap extension. *Gene,* 77**,** 61-8.

HU, Z. B., WU, C. T., WANG, H., ZHANG, Q. W., WANG, L., WANG, R. L., LU, Z. Z. & WANG, L. S. 2008. A simplified system for generating oncolytic adenovirus vector carrying one or two transgenes. *Cancer Gene Ther,* 15**,** 173-82.

HULEATT, J. W., JACOBS, A. R., TANG, J., DESAI, P., KOPP, E. B., HUANG, Y., SONG, L., NAKAAR, V. & POWELL, T. J. 2007. Vaccination with recombinant fusion proteins incorporating Toll-like receptor ligands induces rapid cellular and humoral immunity. *Vaccine,* 25**,** 763-75.

IDOYAGA, J., CHEONG, C., SUDA, K., SUDA, N., KIM, J. Y., LEE, H., PARK, C. G. & STEINMAN, R. M. 2008. Cutting edge: langerin/CD207 receptor on dendritic cells mediates efficient antigen presentation on MHC I and II products in vivo. *J Immunol,* 180**,** 3647-50.

IDOYAGA, J., LUBKIN, A., FIORESE, C., LAHOUD, M. H., CAMINSCHI, I., HUANG, Y., RODRIGUEZ, A., CLAUSEN, B. E., PARK, C. G., TRUMPFHELLER, C. & STEINMAN, R. M. 2011. Comparable T helper 1 (Th1) and CD8 T-cell immunity by targeting HIV gag p24 to CD8 dendritic cells within antibodies to Langerin, DEC205, and Clec9A. *Proceedings of the National Academy of Sciences of the United States of America,* 108**,** 2384-9.

IEZZI, G., KARJALAINEN, K. & LANZAVECCHIA, A. 1998. The duration of antigenic stimulation determines the fate of naive and effector T cells. *Immunity,* 8**,** 89-95.

IMAI, J., HASEGAWA, H., MARUYA, M., KOYASU, S. & YAHARA, I. 2005. Exogenous antigens are processed through the endoplasmic reticulum-associated degradation (ERAD) in cross-presentation by dendritic cells. *Int Immunol,* 17**,** 45-53.

INOKUMA, M., DELA ROSA, C., SCHMITT, C., HAALAND, P., SIEBERT, J., PETRY, D., TANG, M., SUNI, M. A., GHANEKAR, S. A., GLADDING, D., DUNNE, J. F., MAINO, V. C., DISIS, M. L. & MAECKER, H. T. 2007. Functional T cell responses to tumor antigens in breast cancer patients have a distinct phenotype and cytokine signature. *Journal of immunology,* 179**,** 2627-33.

IVANOV, II, MCKENZIE, B. S., ZHOU, L., TADOKORO, C. E., LEPELLEY, A., LAFAILLE, J. J., CUA, D. J. & LITTMAN, D. R. 2006. The orphan nuclear receptor RORgammat directs the differentiation program of proinflammatory IL-17+ T helper cells. *Cell,* 126**,** 1121-33.

JAHN, G., STENGLEIN, S., RIEGLER, S., EINSELE, H. & SINZGER, C. 1999. Human cytomegalovirus infection of immature dendritic cells and macrophages. *Intervirology,* 42**,** 365-72.

JANEWAY, C. 2005. *Immunobiology : the immune system in health and disease,* New York ; London, Garland Science/Churchill Livingstone.

JARROSSAY, D., NAPOLITANI, G., COLONNA, M., SALLUSTO, F. & LANZAVECCHIA, A. 2001. Specialization and complementarity in microbial molecule recognition by human myeloid and plasmacytoid dendritic cells. *European journal of immunology,* 31**,** 3388-93.

JONGBLOED, S. L., KASSIANOS, A. J., MCDONALD, K. J., CLARK, G. J., JU, X., ANGEL, C. E., CHEN, C. J., DUNBAR, P. R., WADLEY, R. B., JEET, V., VULINK, A. J., HART, D. N.

& RADFORD, K. J. 2010. Human CD141+ (BDCA-3)+ dendritic cells (DCs) represent a unique myeloid DC subset that cross-presents necrotic cell antigens. *The Journal of experimental medicine,* 207**,** 1247-60.

JUSFORGUES-SAKLANI, H., UHL, M., BLACHERE, N., LEMAITRE, F., LANTZ, O., BOUSSO, P., BRAUN, D., MOON, J. J. & ALBERT, M. L. 2008. Antigen persistence is required for dendritic cell licensing and CD8+ T cell cross-priming. *Journal of immunology,* 181**,** 3067-76.

KAIKO, G. E., HORVAT, J. C., BEAGLEY, K. W. & HANSBRO, P. M. 2008. Immunological decision-making: how does the immune system decide to mount a helper T-cell response? *Immunology,* 123**,** 326-38.

KANAZAWA, N. 2007. Dendritic cell immunoreceptors: C-type lectin receptors for pattern-recognition and signaling on antigen-presenting cells. *Journal of dermatological science,* 45**,** 77-86.

KATO, M., NEIL, T. K., FEARNLEY, D. B., MCLELLAN, A. D., VUCKOVIC, S. & HART, D. N. 2000. Expression of multilectin receptors and comparative FITC-dextran uptake by human dendritic cells. *International immunology,* 12**,** 1511-9.

KAWAMURA, K., KADOWAKI, N., SUZUKI, R., UDAGAWA, S., KASAOKA, S., UTOGUCHI, N., KITAWAKI, T., SUGIMOTO, N., OKADA, N., MARUYAMA, K. & UCHIYAMA, T. 2006. Dendritic cells that endocytosed antigen-containing IgG-liposomes elicit effective antitumor immunity. *Journal of immunotherapy,* 29**,** 165-74.

KERN, F., BUNDE, T., FAULHABER, N., KIECKER, F., KHATAMZAS, E., RUDAWSKI, I. M., PRUSS, A., GRATAMA, J. W., VOLKMER-ENGERT, R., EWERT, R., REINKE, P., VOLK, H. D. & PICKER, L. J. 2002. Cytomegalovirus (CMV) phosphoprotein 65 makes a large contribution to shaping the T cell repertoire in CMV-exposed individuals. *The Journal of infectious diseases,* 185**,** 1709-16.

KIEPIELA, P., NGUMBELA, K., THOBAKGALE, C., RAMDUTH, D., HONEYBORNE, I., MOODLEY, E., REDDY, S., DE PIERRES, C., MNCUBE, Z., MKHWANAZI, N., BISHOP, K., VAN DER STOK, M., NAIR, K., KHAN, N., CRAWFORD, H., PAYNE, R., LESLIE, A., PRADO, J., PRENDERGAST, A., FRATER, J., MCCARTHY, N., BRANDER, C., LEARN, G. H., NICKLE, D., ROUSSEAU, C., COOVADIA, H., MULLINS, J. I., HECKERMAN, D., WALKER, B. D. & GOULDER, P. 2007. CD8+ T-cell responses to different HIV proteins have discordant associations with viral load. *Nat Med,* 13**,** 46-53.

KIM, J. H., RERKS-NGARM, S., EXCLER, J. L. & MICHAEL, N. L. 2010. HIV vaccines: lessons learned and the way forward. *Current opinion in HIV and AIDS,* 5**,** 428-34.

KIMURA, A. & KISHIMOTO, T. 2010. IL-6: regulator of Treg/Th17 balance. *European journal of immunology,* 40**,** 1830-5.

KIMURA, A. & KISHIMOTO, T. 2011. Th17 cells in inflammation. *International immunopharmacology,* 11**,** 319-22.

KINDT, T. J., GOLDSBY, R. A. & OSBORNE, B. A. 2007. *Kuby Immunology, 6th ed.,* New York, W.H. Freeman and Company.

KLECHEVSKY, E., FLAMAR, A. L., CAO, Y., BLANCK, J. P., LIU, M., O'BAR, A., AGOUNA-DECIAT, O., KLUCAR, P., THOMPSON-SNIPES, L., ZURAWSKI, S., REITER, Y., PALUCKA, A. K., ZURAWSKI, G. & BANCHEREAU, J. 2010. Cross-priming CD8+ T cells by targeting antigens to human dendritic cells through DCIR. *Blood,* 116**,** 1685-97.

KLUGER, R., FOOT, J. S. & VANDERSTEEN, A. A. 2010. Protein-protein coupling and its application to functional red cell substitutes. *Chemical communications,* 46**,** 1194-202.

KONDO, E., AKATSUKA, Y., KUZUSHIMA, K., TSUJIMURA, K., ASAKURA, S., TAJIMA, K., KAGAMI, Y., KODERA, Y., TANIMOTO, M., MORISHIMA, Y. & TAKAHASHI, T. 2004. Identification of novel CTL epitopes of CMV-pp65 presented by a variety of HLA alleles. *Blood,* 103**,** 630-8.

KOSHIOL, J., SCHROEDER, J., JAMIESON, D. J., MARSHALL, S. W., DUERR, A., HEILIG, C. M., SHAH, K. V., KLEIN, R. S., CU-UVIN, S., SCHUMAN, P., CELENTANO, D. & SMITH, J. S. 2006. Smoking and time to clearance of human papillomavirus infection in HIV-seropositive and HIV-seronegative women. *American journal of epidemiology,* 164**,** 176-83.

KOUP, R. A., SAFRIT, J. T., CAO, Y., ANDREWS, C. A., MCLEOD, G., BORKOWSKY, W., FARTHING, C. & HO, D. D. 1994. Temporal association of cellular immune responses with the initial control of viremia in primary human immunodeficiency virus type 1 syndrome. *Journal of Virology,* 68**,** 4650-5.

KRETZ-ROMMEL, A., QIN, F., DAKAPPAGARI, N., TORENSMA, R., FAAS, S., WU, D. & BOWDISH, K. S. 2007. In vivo targeting of antigens to human dendritic cells through DC-SIGN elicits stimulatory immune responses and inhibits tumor growth in grafted mouse models. *Journal of immunotherapy,* 30**,** 715-26.

KROMENAKER, S. J. & SRIENC, F. 1994. Stability of producer hybridoma cell lines after cell sorting: a case study. *Biotechnol Prog,* 10**,** 299-307.

KWAKS, T. H., BARNETT, P., HEMRIKA, W., SIERSMA, T., SEWALT, R. G., SATIJN, D. P., BRONS, J. F., VAN BLOKLAND, R., KWAKMAN, P., KRUCKEBERG, A. L., KELDER, A. & OTTE, A. P. 2003. Identification of anti-repressor elements that confer high and stable protein production in mammalian cells. *Nat Biotechnol,* 21**,** 553-8.

LA ROCCA, G., ANZALONE, R., BUCCHIERI, F., FARINA, F., CAPPELLO, F. & ZUMMO, G. 2004. CD1a and antitumour immune response. *Immunology letters,* 95**,** 1-4.

LANZAVECCHIA, A. & SALLUSTO, F. 2005. Understanding the generation and function of memory T cell subsets. *Curr Opin Immunol,* 17**,** 326-32.

LAURENCE, A., TATO, C. M., DAVIDSON, T. S., KANNO, Y., CHEN, Z., YAO, Z., BLANK, R. B., MEYLAN, F., SIEGEL, R., HENNIGHAUSEN, L., SHEVACH, E. M. & O'SHEA J, J. 2007. Interleukin-2 signaling via STAT5 constrains T helper 17 cell generation. *Immunity,* 26**,** 371-81.

LE BON, A., ETCHART, N., ROSSMANN, C., ASHTON, M., HOU, S., GEWERT, D., BORROW, P. & TOUGH, D. F. 2003. Cross-priming of CD8+ T cells stimulated by virus-induced type I interferon. *Nature immunology,* 4**,** 1009-15.

LEON, B., LOPEZ-BRAVO, M. & ARDAVIN, C. 2007. Monocyte-derived dendritic cells formed at the infection site control the induction of protective T helper 1 responses against Leishmania. *Immunity,* 26**,** 519-31.

LICHTY, J. J., MALECKI, J. L., AGNEW, H. D., MICHELSON-HOROWITZ, D. J. & TAN, S. 2005. Comparison of affinity tags for protein purification. *Protein Expr Purif,* 41**,** 98-105.

LIN, M. L., ZHAN, Y., VILLADANGOS, J. A. & LEW, A. M. 2008. The cell biology of cross-presentation and the role of dendritic cell subsets. *Immunol Cell Biol,* 86**,** 353-62.

LIN, Y., PAGEL, J. M., AXWORTHY, D., PANTELIAS, A., HEDIN, N. & PRESS, O. W. 2006. A genetically engineered anti-CD45 single-chain antibody-streptavidin fusion protein for pretargeted radioimmunotherapy of hematologic malignancies. *Cancer research,* 66**,** 3884-92.

LISZIEWICZ, J., TROCIO, J., WHITMAN, L., VARGA, G., XU, J., BAKARE, N., ERBACHER, P., FOX, C., WOODWARD, R., MARKHAM, P., ARYA, S., BEHR, J. P. & LORI, F. 2005. DermaVir: a novel topical vaccine for HIV/AIDS. *J Invest Dermatol,* 124**,** 160-9.

LIU, J., YU, Q., STONE, G. W., YUE, F. Y., NGAI, N., JONES, R. B., KORNBLUTH, R. S. & OSTROWSKI, M. A. 2008. CD40L expressed from the canarypox vector, ALVAC, can boost immunogenicity of HIV-1 canarypox vaccine in mice and enhance the in vitro expansion of viral specific CD8+ T cell memory responses from HIV-1-infected and HIV-1-uninfected individuals. *Vaccine,* 26**,** 4062-72.

LUCIW, P. A. 1996. Fields Virology. *In:* B.N. FIELDS, D. M. K., P.M. HOWLEY ET AL. (ed.) third edition ed. Philadelphia: Lippincott - Raven publishers.

MACDONALD, K. P., MUNSTER, D. J., CLARK, G. J., DZIONEK, A., SCHMITZ, J. & HART, D. N. 2002. Characterization of human blood dendritic cell subsets. *Blood,* 100**,** 4512-20.

MAHNKE, K., GUO, M., LEE, S., SEPULVEDA, H., SWAIN, S. L., NUSSENZWEIG, M. & STEINMAN, R. M. 2000. The dendritic cell receptor for endocytosis, DEC-205, can recycle and enhance antigen presentation via major histocompatibility complex class II-positive lysosomal compartments. *The Journal of cell biology,* 151**,** 673-84.

MAIZEL, J. V., JR., WHITE, D. O. & SCHARFF, M. D. 1968. The polypeptides of adenovirus. I. Evidence for multiple protein components in the virion and a comparison of types 2, 7A, and 12. *Virology,* 36**,** 115-25.

MAKEDONAS, G. & BETTS, M. R. 2011. Living in a house of cards: re-evaluating CD8+ T-cell immune correlates against HIV. *Immunological reviews,* 239**,** 109-24.

MASATO KATO, KYLIE J MCDONALD, SEEMA KHAN, IAN L ROSS, SLAVICA VUCKOVIC, KE CHEN, DAVID MUNSTER, MACDONALD, K. P. & HART, D. N. 2006. Expression of human DEC-205 (CD205) multilectin receptor on leukocytes. *International Immunology,* 18**,** Pp. 857-869.

MASCOLA, J. R., SNYDER, S. W., WEISLOW, O. S., BELAY, S. M., BELSHE, R. B., SCHWARTZ, D. H., CLEMENTS, M. L., DOLIN, R., GRAHAM, B. S., GORSE, G. J., KEEFER, M. C., MCELRATH, M. J., WALKER, M. C., WAGNER, K. F., MCNEIL, J. G., MCCUTCHAN, F. E. & BURKE, D. S. 1996. Immunization with envelope subunit vaccine products elicits neutralizing antibodies against laboratory-adapted but not primary isolates of

human immunodeficiency virus type 1. The National Institute of Allergy and Infectious Diseases AIDS Vaccine Evaluation Group. *The Journal of infectious diseases,* 173**,** 340-8.

MASOPUST, D., HA, S. J., VEZYS, V. & AHMED, R. 2006. Stimulation history dictates memory CD8 T cell phenotype: implications for prime-boost vaccination. *Journal of immunology,* 177**,** 831-9.

MASSIE, B., COUTURE, F., LAMOUREUX, L., MOSSER, D. D., GUILBAULT, C., JOLICOEUR, P., BELANGER, F. & LANGELIER, Y. 1998a. Inducible overexpression of a toxic protein by an adenovirus vector with a tetracycline-regulatable expression cassette. *Journal of Virology,* 72**,** 2289-96.

MASSIE, B., MOSSER, D. D., KOUTROUMANIS, M., VITTE-MONY, I., LAMOUREUX, L., COUTURE, F., PAQUET, L., GUILBAULT, C., DIONNE, J., CHAHLA, D., JOLICOEUR, P. & LANGELIER, Y. 1998b. New adenovirus vectors for protein production and gene transfer. *Cytotechnology,* 28**,** 53-64.

MATSUI, T., CONNOLLY, J. E., MICHNEVITZ, M., CHAUSSABEL, D., YU, C. I., GLASER, C., TINDLE, S., PYPAERT, M., FREITAS, H., PIQUERAS, B., BANCHEREAU, J. & PALUCKA, A. K. 2009. CD2 distinguishes two subsets of human plasmacytoid dendritic cells with distinct phenotype and functions. *Journal of immunology,* 182**,** 6815-23.

MATSUMOTO, T., SAWAMOTO, S., SAKAMOTO, T., TANAKA, T., FUKUDA, H. & KONDO, A. 2011. Site-specific tetrameric streptavidin-protein conjugation using sortase A. *Journal of biotechnology,* 152**,** 37-42.

MAZOUZ, N., OOMS, A., MOULIN, V., VAN MEIRVENNE, S., UYTTENHOVE, C., DEGIOVANNI, G. 2002. CD40 triggering increases the efficiency of dendritic cells for antitumoral immunization. *Cancer Immunity,* 2.

MAZZONI, A. & SEGAL, D. M. 2004. Controlling the Toll road to dendritic cell polarization. *J Leukoc Biol,* 75**,** 721-30.

MCGREAL, E. P., MILLER, J. L. & GORDON, S. 2005. Ligand recognition by antigen-presenting cell C-type lectin receptors. *Curr Opin Immunol,* 17**,** 18-24.

MENDELSON, M., MONARD, S., SISSONS, P. & SINCLAIR, J. 1996. Detection of endogenous human cytomegalovirus in CD34+ bone marrow progenitors. *The Journal of general virology,* 77 (Pt 12)**,** 3099-102.

MERAD, M., GINHOUX, F. & COLLIN, M. 2008. Origin, homeostasis and function of Langerhans cells and other langerin-expressing dendritic cells. *Nature reviews. Immunology,* 8**,** 935-47.

MICONNET, I., PANTALEO, G. 2008. A soluble hexameric form of CD40 ligand activates human dendritic cells and augments memory T cell response. *Vaccine,* 26**,** 4006-4014.

MINTZER, M. A. & GRINSTAFF, M. W. 2011. Biomedical applications of dendrimers: a tutorial. *Chemical Society reviews,* 40**,** 173-90.

MOLNAR, E., PRECHL, J., ISAAK, A. & ERDEI, A. 2003. Targeting with scFv: immune modulation by complement receptor specific constructs. *Journal of molecular recognition : JMR,* 16**,** 318-23.

MOSMANN, T. R., LI, L. & SAD, S. 1997. Functions of CD8 T-cell subsets secreting different cytokine patterns. *Seminars in immunology,* 9**,** 87-92.

MOSS, P. & KHAN, N. 2004. CD8(+) T-cell immunity to cytomegalovirus. *Human immunology,* 65**,** 456-64.

MOURIES, J., MORON, G., SCHLECHT, G., ESCRIOU, N., DADAGLIO, G. & LECLERC, C. 2008. Plasmacytoid dendritic cells efficiently cross-prime naive T cells in vivo after TLR activation. *Blood,* 112**,** 3713-22.

MUKHOPADHAYA, A., HANAFUSA, T., JARCHUM, I., CHEN, Y. G., IWAI, Y., SERREZE, D. V., STEINMAN, R. M., TARBELL, K. V. & DILORENZO, T. P. 2008. Selective delivery of beta cell antigen to dendritic cells in vivo leads to deletion and tolerance of autoreactive CD8+ T cells in NOD mice. *Proceedings of the National Academy of Sciences of the United States of America,* 105**,** 6374-9.

NABEL, G. J. 2002. HIV vaccine strategies. *Vaccine,* 20**,** 1945-7.

NADEAU, I., GARNIER, A., COTE, J., MASSIE, B., CHAVARIE, C. & KAMEN, A. 1996. Improvement of recombinant protein production with the human adenovirus/293S expression system using fed-batch strategies. *Biotechnol Bioeng,* 51**,** 613-23.

NAIK, S. H., METCALF, D., VAN NIEUWENHUIJZE, A., WICKS, I., WU, L., O'KEEFFE, M. & SHORTMAN, K. 2006. Intrasplenic steady-state dendritic cell precursors that are distinct from monocytes. *Nature immunology,* 7**,** 663-71.

NAPOLITANI, G., RINALDI, A., BERTONI, F., SALLUSTO, F. & LANZAVECCHIA, A. 2005. Selected Toll-like receptor agonist combinations synergistically trigger a T helper type 1-polarizing program in dendritic cells. *Nature immunology,* 6**,** 769-76.

NCHINDA, G., KUROIWA, J., OKS, M., TRUMPFHELLER, C., PARK, C. G., HUANG, Y., HANNAMAN, D., SCHLESINGER, S. J., MIZENINA, O., NUSSENZWEIG, M. C., UBERLA, K. & STEINMAN, R. M. 2008. The efficacy of DNA vaccination is enhanced in mice by targeting the encoded protein to dendritic cells. *J Clin Invest,* 118**,** 1427-36.

NESTLE, F. O., ZHENG, X. G., THOMPSON, C. B., TURKA, L. A. & NICKOLOFF, B. J. 1993. Characterization of dermal dendritic cells obtained from normal human skin reveals phenotypic and functionally distinctive subsets. *Journal of immunology,* 151**,** 6535-45.

NI, L., GAYET, I., ZURAWSKI, S., DULUC, D., FLAMAR, A. L., LI, X. H., O'BAR, A., CLAYTON, S., PALUCKA, A. K., ZURAWSKI, G., BANCHEREAU, J. & OH, S. 2010. Concomitant activation and antigen uptake via human dectin-1 results in potent antigen-specific CD8+ T cell responses. *Journal of immunology,* 185**,** 3504-13.

O'NEILL, L. A. & BOWIE, A. G. 2007. The family of five: TIR-domain-containing adaptors in Toll-like receptor signalling. *Nature reviews. Immunology,* 7**,** 353-64.

O'REILLY, D. R., MILLER, L.K., LUCKNOW, V.A. 1994. *Baculovirus Expression Vectors: A Laboratory Manual,* New York, Oxford University Press, Inc.

OSUGI, Y., VUCKOVIC, S. & HART, D. N. 2002. Myeloid blood CD11c(+) dendritic cells and monocyte-derived dendritic cells differ in their ability to stimulate T lymphocytes. *Blood,* 100**,** 2858-66.

OZINSKY, A., UNDERHILL, D. M., FONTENOT, J. D., HAJJAR, A. M., SMITH, K. D., WILSON, C. B., SCHROEDER, L. & ADEREM, A. 2000. The repertoire for pattern recognition of pathogens by the innate immune system is defined by cooperation between toll-like receptors. *Proceedings of the National Academy of Sciences of the United States of America,* 97**,** 13766-71.

PAGEL, J. M., LIN, Y., HEDIN, N., PANTELIAS, A., AXWORTHY, D., STONE, D., HAMLIN, D. K., WILBUR, D. S. & PRESS, O. W. 2006. Comparison of a tetravalent single-chain antibody-streptavidin fusion protein and an antibody-streptavidin chemical conjugate for pretargeted anti-CD20 radioimmunotherapy of B-cell lymphomas. *Blood,* 108**,** 328-36.

PALUCKA, K., BANCHEREAU, J. & MELLMAN, I. 2010. Designing vaccines based on biology of human dendritic cell subsets. *Immunity,* 33**,** 464-78.

PANTALEO, G. & KOUP, R. A. 2004. Correlates of immune protection in HIV-1 infection: what we know, what we don't know, what we should know. *Nat Med,* 10**,** 806-10.

PATTERSON, S., DONAGHY, H., AMJADI, P., GAZZARD, B., GOTCH, F. & KELLEHER, P. 2005. Human BDCA-1-positive blood dendritic cells differentiate into phenotypically distinct immature and mature populations in the absence of exogenous maturational stimuli: differentiation failure in HIV infection. *J Immunol,* 174**,** 8200-9.

PIGUET, V. & BLAUVELT, A. 2002. Essential roles for dendritic cells in the pathogenesis and potential treatment of HIV disease. *J Invest Dermatol,* 119**,** 365-9.

PILLAY, S., SHEPHARD, E. G., MEYERS, A. E., WILLIAMSON, A. L. & RYBICKI, E. P. 2010. HIV-1 sub-type C chimaeric VLPs boost cellular immune responses in mice. *Journal of immune based therapies and vaccines,* 8**,** 7.

PITTET, M. J., VALMORI, D., DUNBAR, P. R., SPEISER, D. E., LIENARD, D., LEJEUNE, F., FLEISCHHAUER, K., CERUNDOLO, V., CEROTTINI, J. C. & ROMERO, P. 1999. High frequencies of naive Melan-A/MART-1-specific CD8(+) T cells in a large proportion of human histocompatibility leukocyte antigen (HLA)-A2 individuals. *J Exp Med,* 190**,** 705-15.

PITTET, M. J., ZIPPELIUS, A., VALMORI, D., SPEISER, D. E., CEROTTINI, J. C. & ROMERO, P. 2002. Melan-A/MART-1-specific CD8 T cells: from thymus to tumor. *Trends Immunol,* 23**,** 325-8.

POLLACK, H., ZHAN, M. X., SAFRIT, J. T., CHEN, S. H., ROCHFORD, G., TAO, P. Z., KOUP, R., KRASINSKI, K. & BORKOWSKY, W. 1997. CD8+ T-cell-mediated suppression of HIV replication in the first year of life: association with lower viral load and favorable early survival. *Aids,* 11**,** F9-13.

POOLEY, J. L., HEATH, W. R. & SHORTMAN, K. 2001. Cutting edge: intravenous soluble antigen is presented to CD4 T cells by CD8- dendritic cells, but cross-presented to CD8 T cells by CD8+ dendritic cells. *Journal of immunology,* 166**,** 5327-30.

POULIN, L. F., SALIO, M., GRIESSINGER, E., ANJOS-AFONSO, F., CRACIUN, L., CHEN, J. L., KELLER, A. M., JOFFRE, O., ZELENAY, S., NYE, E., LE MOINE, A., FAURE, F., DONCKIER, V., SANCHO, D., CERUNDOLO, V., BONNET, D. & REIS E SOUSA, C. 2010. Characterization of human DNGR-1+ BDCA3+ leukocytes as putative equivalents of mouse CD8alpha+ dendritic cells. *The Journal of experimental medicine,* 207**,** 1261-71.

PROIMMUNE 2011. http://www.proimmune.com/ecommerce/page.php?page=pentamer_info. *ProImmune Inc.*

PROMEGA 1996-1999. pGem-T and pGem-T Easy vector systems: Instructions for use of products. Wisconsin, USA: Promega Corporation.

PROUDFOOT, O., APOSTOLOPOULOS, V. & PIETERSZ, G. A. 2007. Receptor-mediated delivery of antigens to dendritic cells: anticancer applications. *Mol Pharm,* 4**,** 58-72.

PULENDRAN, B., BANCHEREAU, J., BURKEHOLDER, S., KRAUS, E., GUINET, E., CHALOUNI, C., CARON, D., MALISZEWSKI, C., DAVOUST, J., FAY, J. & PALUCKA, K. 2000. Flt3-ligand and granulocyte colony-stimulating factor mobilize distinct human dendritic cell subsets in vivo. *Journal of immunology,* 165**,** 566-72.

RADFORD, K. J., TURTLE, C. J., KASSIANOS, A. J. & HART, D. N. 2006. CD11c+ blood dendritic cells induce antigen-specific cytotoxic T lymphocytes with similar efficiency compared to monocyte-derived dendritic cells despite higher levels of MHC class I expression. *Journal of immunotherapy,* 29**,** 596-605.

RAMAKRISHNA, V., VASILAKOS, J. P., TARIO, J. D., JR., BERGER, M. A., WALLACE, P. K. & KELER, T. 2007. Toll-like receptor activation enhances cell-mediated immunity induced by an antibody vaccine targeting human dendritic cells. *J Transl Med,* 5**,** 5.

RAMAN, V. S., BHATIA, A., PICONE, A., WHITTLE, J., BAILOR, H. R., O'DONNELL, J., PATTABHI, S., GUDERIAN, J. A., MOHAMATH, R., DUTHIE, M. S. & REED, S. G. 2010. Applying TLR synergy in immunotherapy: implications in cutaneous leishmaniasis. *Journal of immunology,* 185**,** 1701-10.

RASMUSSEN, L. 1999. Molecular pathogenesis of human cytomegalovirus infection. *Transplant infectious disease : an official journal of the Transplantation Society,* 1**,** 127-34.

RATZINGER, G., BAGGERS, J., DE COS, M. A., YUAN, J., DAO, T., REAGAN, J. L., MUNZ, C., HELLER, G. & YOUNG, J. W. 2004. Mature human Langerhans cells derived from CD34+ hematopoietic progenitors stimulate greater cytolytic T lymphocyte activity in the absence of bioactive IL-12p70, by either single peptide presentation or cross-priming, than do dermal-interstitial or monocyte-derived dendritic cells. *J Immunol,* 173**,** 2780-91.

REIS E SOUSA, C. 2004. Toll-like receptors and dendritic cells: for whom the bug tolls. *Seminars in immunology,* 16**,** 27-34.

REIS E SOUSA, C. & GERMAIN, R. N. 1995. Major histocompatibility complex class I presentation of peptides derived from soluble exogenous antigen by a subset of cells engaged in phagocytosis. *J Exp Med,* 182**,** 841-51.

ROBERTS, A. D., ELY, K. H. & WOODLAND, D. L. 2005. Differential contributions of central and effector memory T cells to recall responses. *The Journal of experimental medicine,* 202**,** 123-33.

ROBSON, N. C., BEACOCK-SHARP, H., DONACHIE, A. M. & MOWAT, A. M. 2003. Dendritic cell maturation enhances CD8+ T-cell responses to exogenous antigen via a proteasome-independent mechanism of major histocompatibility complex class I loading. *Immunology,* 109**,** 374-83.

ROCK, K. L. & SHEN, L. 2005. Cross-presentation: underlying mechanisms and role in immune surveillance. *Immunol Rev,* 207**,** 166-83.

ROLLIER, C., VERSCHOOR, E. J., PARANHOS-BACCALA, G., DREXHAGE, J. A., VERSTREPEN, B. E., BERLAND, J. L., HIMOUDI, N., BARNFIELD, C., LILJESTROM, P., LASARTE, J. J., RUIZ, J., INCHAUSPE, G. & HEENEY, J. L. 2005. Modulation of vaccine-induced immune responses to hepatitis C virus in rhesus macaques by altering priming before adenovirus boosting. *The Journal of infectious diseases,* 192**,** 920-9.

ROMERO, P., VALMORI, D., PITTET, M. J., ZIPPELIUS, A., RIMOLDI, D., LEVY, F., DUTOIT, V., AYYOUB, M., RUBIO-GODOY, V., MICHIELIN, O., GUILLAUME, P., BATARD, P., LUESCHER, I. F., LEJEUNE, F., LIENARD, D., RUFER, N., DIETRICH, P. Y., SPEISER, D. E. & CEROTTINI, J. C. 2002. Antigenicity and immunogenicity of Melan-A/MART-1 derived peptides as targets for tumor reactive CTL in human melanoma. *Immunol Rev,* 188**,** 81-96.

ROYER, P. J., EMARA, M., YANG, C., AL-GHOULEH, A., TIGHE, P., JONES, N., SEWELL, H. F., SHAKIB, F., MARTINEZ-POMARES, L. & GHAEMMAGHAMI, A. M. 2010. The mannose receptor mediates the uptake of diverse native allergens by dendritic cells and determines allergen-induced T cell polarization through modulation of IDO activity. *Journal of immunology,* 185**,** 1522-31.

SADAGOPAL, S., AMARA, R. R., MONTEFIORI, D. C., WYATT, L. S., STAPRANS, S. I., KOZYR, N. L., MCCLURE, H. M., MOSS, B. & ROBINSON, H. L. 2005. Signature for long-term vaccine-mediated control of a Simian and human immunodeficiency virus 89.6P challenge: stable low-breadth and low-frequency T-cell response capable of coproducing gamma interferon and interleukin-2. *J Virol,* 79**,** 3243-53.

SALLUSTO, F. & LANZAVECCHIA, A. 1994. Efficient presentation of soluble antigen by cultured human dendritic cells is maintained by granulocyte/macrophage colony-stimulating factor plus interleukin 4 and downregulated by tumor necrosis factor alpha. *The Journal of experimental medicine,* 179**,** 1109-18.

SALLUSTO, F. & LANZAVECCHIA, A. 2002. The instructive role of dendritic cells on T-cell responses. *Arthritis research,* 4 Suppl 3**,** S127-32.

SALLUSTO, F. & LANZAVECCHIA, A. 2009. Heterogeneity of CD4+ memory T cells: functional modules for tailored immunity. *European journal of immunology,* 39**,** 2076-82.

SANCHO, D., MOURAO-SA, D., JOFFRE, O. P., SCHULZ, O., ROGERS, N. C., PENNINGTON, D. J., CARLYLE, J. R. & REIS E SOUSA, C. 2008. Tumor therapy in mice via antigen targeting to a novel, DC-restricted C-type lectin. *The Journal of clinical investigation,* 118**,** 2098-110.

SANDBERG, J. K., FAST, N. M. & NIXON, D. F. 2001. Functional heterogeneity of cytokines and cytolytic effector molecules in human CD8+ T lymphocytes. *Journal of immunology,* 167**,** 181-7.

SANTEGOETS, S. J., GIBBS, S., KROEZE, K., VAN DE VEN, R., SCHEPER, R. J., BORREBAECK, C. A., DE GRUIJL, T. D. & LINDSTEDT, M. 2008. Transcriptional profiling of human skin-resident Langerhans cells and CD1a+ dermal dendritic cells: differential activation states suggest distinct functions. *Journal of leukocyte biology,* 84**,** 143-51.

SAPINORO, R., MAGUIRE, C. A., BURGESS, A. & DEWHURST, S. 2007. Enhanced transduction of dendritic cells by FcgammaRI-targeted adenovirus vectors. *The journal of gene medicine,* 9**,** 1033-45.

SARIC, T., CHANG, S. C., HATTORI, A., YORK, I. A., MARKANT, S., ROCK, K. L., TSUJIMOTO, M. & GOLDBERG, A. L. 2002. An IFN-gamma-induced aminopeptidase in the ER, ERAP1, trims precursors to MHC class I-presented peptides. *Nat Immunol,* 3**,** 1169-76.

SATO, T., TERAI, M., YASUDA, R., WATANABE, R., BERD, D., MASTRANGELO, M.J., HASUMI, K. 2004. Combination of monocyte-derived dendritic cells and activated T cells which express CD40 ligand: a new approach to cancer immunotherapy. *Cancer Immunol Immunother,* 53**,** 53–61.

SCHAACK, J. 2005. Adenovirus vectors deleted for genes essential for viral DNA replication. *Front Biosci,* 10**,** 1146-55.

SCHREIBELT, G., TEL, J., SLIEPEN, K. H., BENITEZ-RIBAS, D., FIGDOR, C. G., ADEMA, G. J. & DE VRIES, I. J. 2010. Toll-like receptor expression and function in human dendritic cell subsets: implications for dendritic cell-based anti-cancer immunotherapy. *Cancer immunology, immunotherapy : CII,* 59**,** 1573-82.

SCHULZ, O., DIEBOLD, S. S., CHEN, M., NASLUND, T. I., NOLTE, M. A., ALEXOPOULOU, L., AZUMA, Y. T., FLAVELL, R. A., LILJESTROM, P. & REIS E SOUSA, C. 2005. Toll-like receptor 3 promotes cross-priming to virus-infected cells. *Nature,* 433**,** 887-92.

SCHUMACHER, R., ADAMINA, M., ZURBRIGGEN, R., BOLLI, M., PADOVAN, E., ZAJAC, P., HEBERER, M. & SPAGNOLI, G. C. 2004. Influenza virosomes enhance class I restricted CTL induction through CD4+ T cell activation. *Vaccine,* 22**,** 714-23.

SCHWARZ, K., STORNI, T., MANOLOVA, V., DIDIERLAURENT, A., SIRARD, J. C., ROTHLISBERGER, P. & BACHMANN, M. F. 2003. Role of Toll-like receptors in costimulating cytotoxic T cell responses. *European journal of immunology,* 33**,** 1465-70.

SEDER, R. A., GAZZINELLI, R., SHER, A. & PAUL, W. E. 1993. Interleukin 12 acts directly on CD4+ T cells to enhance priming for interferon gamma production and diminishes interleukin 4 inhibition of such priming. *Proceedings of the National Academy of Sciences of the United States of America,* 90**,** 10188-92.

SEKALY, R. P. 2008. The failed HIV Merck vaccine study: a step back or a launching point for future vaccine development? *J Exp Med,* 205**,** 7-12.

SHIVER, J. W., FU, T. M., CHEN, L., CASIMIRO, D. R., DAVIES, M. E., EVANS, R. K., ZHANG, Z. Q., SIMON, A. J., TRIGONA, W. L., DUBEY, S. A., HUANG, L., HARRIS, V. A., LONG, R. S., LIANG, X., HANDT, L., SCHLEIF, W. A., ZHU, L., FREED, D. C., PERSAUD, N. V., GUAN, L., PUNT, K. S., TANG, A., CHEN, M., WILSON, K. A., COLLINS, K. B., HEIDECKER, G. J., FERNANDEZ, V. R., PERRY, H. C., JOYCE, J. G., GRIMM, K. M., COOK, J. C., KELLER, P. M., KRESOCK, D. S., MACH, H., TROUTMAN, R. D., ISOPI, L. A., WILLIAMS, D. M., XU, Z., BOHANNON, K. E., VOLKIN, D. B., MONTEFIORI, D. C., MIURA, A., KRIVULKA, G. R., LIFTON, M. A., KURODA, M. J., SCHMITZ, J. E., LETVIN, N. L., CAULFIELD, M. J., BETT, A. J., YOUIL, R., KASLOW, D. C. & EMINI, E. A. 2002. Replication-incompetent adenoviral vaccine vector elicits effective anti-immunodeficiency-virus immunity. *Nature,* 415**,** 331-5.

SHORTMAN, K., LAHOUD, M. H. & CAMINSCHI, I. 2009. Improving vaccines by targeting antigens to dendritic cells. *Exp Mol Med,* 41**,** 61-6.

SILVER, M. L., GUO, H. C., STROMINGER, J. L. & WILEY, D. C. 1992. Atomic structure of a human MHC molecule presenting an influenza virus peptide. *Nature,* 360**,** 367-9.

SINGH, S. K., STEPHANI, J., SCHAEFER, M., KALAY, H., GARCIA-VALLEJO, J. J., DEN HAAN, J., SAELAND, E., SPARWASSER, T. & VAN KOOYK, Y. 2009. Targeting glycan modified OVA to murine DC-SIGN transgenic dendritic cells enhances MHC class I and II presentation. *Mol Immunol,* 47**,** 164-74.

SOARES, C. R., MORGANTI, L., MILOUX, B., LUPKER, J. H., FERRARA, P. & BARTOLINI, P. 2000. High-level synthesis of human prolactin in Chinese-Hamster ovary cells. *Biotechnol Appl Biochem,* 32 (Pt 2)**,** 127-35.

SPAETE, R. R., GEHRZ, R. C. & LANDINI, M. P. 1994. Human cytomegalovirus structural proteins. *The Journal of general virology,* 75 (Pt 12)**,** 3287-308.

SPELLBERG, B. & EDWARDS, J. E., JR. 2001. Type 1/Type 2 immunity in infectious diseases. *Clinical infectious diseases : an official publication of the Infectious Diseases Society of America,* 32**,** 76-102.

SRINIVAS, O., LARRIEU, P., DUVERGER, E., BOCCACCIO, C., BOUSSER, M. T., MONSIGNY, M., FONTENEAU, J. F., JOTEREAU, F. & ROCHE, A. C. 2007. Synthesis of glycocluster-tumor antigenic peptide conjugates for dendritic cell targeting. *Bioconjugate chemistry,* 18**,** 1547-54.

STEINHAGEN, F., KINJO, T., BODE, C. & KLINMAN, D. M. 2011. TLR-based immune adjuvants. *Vaccine,* 29**,** 3341-55.

STEINMAN, R. M. 2001. Dendritic cells and the control of immunity: enhancing the efficiency of antigen presentation. *Mt Sinai J Med,* 68**,** 160-6.

STRATAGENE 2008. AdEasy™ Adenoviral Vector System Instruction Manual.

SU, S. V., GURNEY, K. B. & LEE, B. 2003. Sugar and spice: viral envelope-DC-SIGN interactions in HIV pathogenesis. *Curr HIV Res,* 1**,** 87-99.

SZABO, S. J., KIM, S. T., COSTA, G. L., ZHANG, X., FATHMAN, C. G. & GLIMCHER, L. H. 2000. A novel transcription factor, T-bet, directs Th1 lineage commitment. *Cell,* 100**,** 655-69.

TACKEN, P. J., DE VRIES, I. J., GIJZEN, K., JOOSTEN, B., WU, D., ROTHER, R. P., FAAS, S. J., PUNT, C. J., TORENSMA, R., ADEMA, G. J. & FIGDOR, C. G. 2005. Effective induction of naive and recall T-cell responses by targeting antigen to human dendritic cells via a humanized anti-DC-SIGN antibody. *Blood,* 106**,** 1278-85.

TACKEN, P. J., DE VRIES, I. J., TORENSMA, R. & FIGDOR, C. G. 2007. Dendritic-cell immunotherapy: from ex vivo loading to in vivo targeting. *Nat Rev Immunol,* 7**,** 790-802.

TACKEN, P. J., TORENSMA, R. & FIGDOR, C. G. 2006. Targeting antigens to dendritic cells in vivo. *Immunobiology,* 211**,** 599-608.

TILLMAN, B. W., HAYES, T. L., DEGRUIJL, T. D., DOUGLAS, J. T. & CURIEL, D. T. 2000. Adenoviral vectors targeted to CD40 enhance the efficacy of dendritic cell-based vaccination

against human papillomavirus 16-induced tumor cells in a murine model. *Cancer Res,* 60**,** 5456-63.

TOMIYAMA, H., MATSUDA, T. & TAKIGUCHI, M. 2002. Differentiation of human CD8(+) T cells from a memory to memory/effector phenotype. *Journal of immunology,* 168**,** 5538-50.

UENO, H., SCHMITT, N., KLECHEVSKY, E., PEDROZA-GONZALEZ, A., MATSUI, T., ZURAWSKI, G., OH, S., FAY, J., PASCUAL, V., BANCHEREAU, J. & PALUCKA, K. 2010. Harnessing human dendritic cell subsets for medicine. *Immunological reviews,* 234**,** 199-212.

UNGER, W. W. & VAN KOOYK, Y. 2011. 'Dressed for success' C-type lectin receptors for the delivery of glyco-vaccines to dendritic cells. *Current opinion in immunology,* 23**,** 131-7.

VALLADEAU, J. & SAELAND, S. 2005. Cutaneous dendritic cells. *Seminars in immunology,* 17**,** 273-83.

VAN KOOYK, Y. 2008. C-type lectins on dendritic cells: key modulators for the induction of immune responses. *Biochemical Society transactions,* 36**,** 1478-81.

VAN MONTFOORT, N., CAMPS, M. G., KHAN, S., FILIPPOV, D. V., WETERINGS, J. J., GRIFFITH, J. M., GEUZE, H. J., VAN HALL, T., VERBEEK, J. S., MELIEF, C. J. & OSSENDORP, F. 2009. Antigen storage compartments in mature dendritic cells facilitate prolonged cytotoxic T lymphocyte cross-priming capacity. *Proc Natl Acad Sci U S A,* 106**,** 6730-5.

VERDIJK, R. M., MUTIS, T., ESENDAM, B., KAMP, J., MELIEF, C. J., BRAND, A. & GOULMY, E. 1999. Polyriboinosinic polyribocytidylic acid (poly(I:C)) induces stable maturation of functionally active human dendritic cells. *J Immunol,* 163**,** 57-61.

VIEIRA, H. L., CUNHA, L., GOLDMACHER, V. S. & ALVES, P. M. 2009. The effect of the cell death suppressor vMIA on the production of a recombinant protein in the adenovirus-293 expression system. *Protein Expr Purif,* 64**,** 179-84.

VUKMANOVIC-STEJIC, M., VYAS, B., GORAK-STOLINSKA, P., NOBLE, A. & KEMENY, D. M. 2000. Human Tc1 and Tc2/Tc0 CD8 T-cell clones display distinct cell surface and functional phenotypes. *Blood,* 95**,** 231-40.

VYAS, J. M., VAN DER VEEN, A. G. & PLOEGH, H. L. 2008. The known unknowns of antigen processing and presentation. *Nature reviews. Immunology,* 8**,** 607-18.

WALLACE, P. K., TSANG, K. Y., GOLDSTEIN, J., CORREALE, P., JARRY, T. M., SCHLOM, J., GUYRE, P. M., ERNSTOFF, M. S. & FANGER, M. W. 2001. Exogenous antigen targeted to FcgammaRI on myeloid cells is presented in association with MHC class I. *Journal of immunological methods,* 248**,** 183-94.

WANG, W. W., DAS, D., MCQUARRIE, S. A. & SURESH, M. R. 2007. Design of a bifunctional fusion protein for ovarian cancer drug delivery: single-chain anti-CA125 core-streptavidin fusion protein. *Eur J Pharm Biopharm,* 65**,** 398-405.

WANG, W. W., DAS, D. & SURESH, M. R. 2009. A versatile bifunctional dendritic cell targeting vaccine vector. *Molecular pharmaceutics,* 6**,** 158-72.

WILLE-REECE, U., FLYNN, B. J., LORE, K., KOUP, R. A., KEDL, R. M., MATTAPALLIL, J. J., WEISS, W. R., ROEDERER, M. & SEDER, R. A. 2005. HIV Gag protein conjugated to a

Toll-like receptor 7/8 agonist improves the magnitude and quality of Th1 and CD8+ T cell responses in nonhuman primates. *Proc Natl Acad Sci U S A,* 102**,** 15190-4.

WOLD, W. S. M. 1999. *Adenovirus methods and protocols,* Totowa, Humana.

WOODLAND, D. L. 2004. Jump-starting the immune system: prime-boosting comes of age. *Trends Immunol,* 25**,** 98-104.

WORGALL, S., BUSCH, A., RIVARA, M., BONNYAY, D., LEOPOLD, P. L., MERRITT, R., HACKETT, N. R., ROVELINK, P. W., BRUDER, J. T., WICKHAM, T. J., KOVESDI, I. & CRYSTAL, R. G. 2004. Modification to the capsid of the adenovirus vector that enhances dendritic cell infection and transgene-specific cellular immune responses. *J Virol,* 78**,** 2572-80.

WURM, F. & BERNARD, A. 1999. Large-scale transient expression in mammalian cells for recombinant protein production. *Current Opinion in Biotechnology,* 10**,** 156-9.

YAN, M., PENG, J., JABBAR,I.A., LIU, X., FILGUEIRA, L., FRAZER, I.H., THOMASA, R. 2004. Despite differences between dendritic cells and Langerhans cells in the mechanism of papillomavirus-like particle antigen uptake, both cells cross-prime T cells. *Virology,* 324**,** 297-310.

YANG, R., XIA, T., XU, G., LI, Z., YING, Z. & XU, X. 2008a. Human cytomegalovirus specific CD8(+) T lymphocytes display interferon-gamma secretion impairment in kidney transplant recipients with pp65 antigenemia. *Transplantation proceedings,* 40**,** 3500-4.

YANG, X. O., PAPPU, B. P., NURIEVA, R., AKIMZHANOV, A., KANG, H. S., CHUNG, Y., MA, L., SHAH, B., PANOPOULOS, A. D., SCHLUNS, K. S., WATOWICH, S. S., TIAN, Q., JETTEN, A. M. & DONG, C. 2008b. T helper 17 lineage differentiation is programmed by orphan nuclear receptors ROR alpha and ROR gamma. *Immunity,* 28**,** 29-39.

YUAN, J., LATOUCHE, J. B., HODGES, J., HOUGHTON, A. N., HELLER, G., SADELAIN, M., RIVIERE, I. & YOUNG, J. W. 2006. Langerhans-type dendritic cells genetically modified to express full-length antigen optimally stimulate CTLs in a CD4-dependent manner. *J Immunol,* 176**,** 2357-65.

ZANONI, I. & GRANUCCI, F. 2010. Regulation of antigen uptake, migration, and lifespan of dendritic cell by Toll-like receptors. *Journal of molecular medicine,* 88**,** 873-80.

ZHONG, F., ZHONG, Z. Y., LIANG, S. & LI, X. J. 2006. High expression level of soluble SARS spike protein mediated by adenovirus in HEK293 cells. *World J Gastroenterol,* 12**,** 1452-7.